

Philipps



Universität
Marburg

Charakterisierung der an der Biosynthese des Cofaktors der [Fe]-Hydrogenase Hmd beteiligten Hcg-Proteine

DISSERTATION

zur

Erlangung des Doktorgrades

der Naturwissenschaften

(Dr. rer. nat.)

dem Fachbereich Biologie

der Philipps-Universität Marburg

Vorgelegt von

Liping Bai

aus Sichuan, China

Marburg/Lahn, 2017

Die Untersuchungen zur vorliegenden Arbeit wurden in der Zeit von September 2013 bis August 2017 am Max-Planck-Institut für Terrestrische Mikrobiologie in Marburg/Lahn unter der Leitung von Dr. Seigo Shima durchgeführt.

Vom Fachbereich Biologie der Philipps-Universität in Marburg/Lahn als Dissertation angenommen am:

Erstgutachter: Dr. Seigo Shima

Zweitgutachter: Prof. Dr. Johann Heider

Tag der mündlichen Prüfung:

ERKLÄRUNG

Hiermit versichere ich, dass ich meine Dissertation mit dem Titel

"Charakterisierung der an der Biosynthese des Cofaktors der [Fe]-Hydrogenase Hmd beteiligten Hcg-Proteine"

selbständig und ohne unerlaubte Unterstützung angefertigt und mich dabei keiner anderen als der von mir ausdrücklich bezeichneten Quellen und Hilfen bedient habe.

Die Dissertation wurde weder in der jetzigen noch in einer ähnlichen Form bei einer anderen Hochschule eingereicht und hat keinen sonstigen Prüfungszwecken gedient

Marburg, den 05.2017

Liping Bai

A part of this PhD thesis was published as original papers in the journal as described below.

Fujishiro, T.* , Bai, L.* , Xu, T., Xie, X., Schick, M. Kahnt, J., Rother, M., Hu, X., Ermler, U. and Shima, S. (2016) Identification of HcgC as SAM-dependent pyridinol methyltransferase in [Fe]-hydrogenase cofactor biosynthesis. *Angew. Chem. Int. Ed.* 55, 9648-9651.

Bai, L., Fujishiro, T., Huang, G., Koch, J., Takabayashi, A., Yokono, M., Tanaka, A., Xu, T., Hu, X., Ermler, U. and Shima, S. (2017) Towards artificial methanogenesis: biosynthesis of the [Fe]-hydrogenase cofactor and characterization of the semisynthetic hydrogenase. *Faraday Discussion*, doi: 10.1039/c6fd00209a. [Epub ahead of print]

Bai, L.* , Wagner, T.* , Xu, T., Hu, X., Ermler, U. and Shima, S. Water-bridged H-bonding network contributes to the catalysis of a SAM-dependent C-methyltransferase HcgC. Submitted.

* These authors contributed equally to these works.

CONTENT

ABBREVIATIONS	1
ABSTRACT	2
ZUSAMMENFASSUNG.....	3
INTRODUCTION.....	5
MATERIALS AND METHODS.....	17
1. Materials.....	17
2. Cultivation of microorganisms	18
2.1 <i>Methanothermobacter marburgensis</i>	18
2.2 <i>Methanococcus maripaludis</i>	18
2.3 <i>Escherichia coli</i>	19
3. Gene mutation of <i>M. maripaludis</i>	20
4. Extraction and purification of coenzymes and the FeGP cofactor	20
4.1 Tetrahydromethanopterin	20
4.2 The FeGP cofactor	21
4.3 Preparation of the guanylylpyridinol moiety of the FeGP cofactor	22
5. Purification of [Fe]-hydrogenase from <i>M. marburgensis</i>	22
6. Purification of HcgB and HcgC produced in <i>E. coli</i>	23
7. Production and purification of HcgA and HcgG in <i>E. coli</i>	24
8. Enzyme activity assay	25
8.1 [Fe]-hydrogenase activity	25
8.2 HcgB activity.....	25
8.3 HcgC activity	26
9. Crystallization and structural analysis.....	26
RESULTS/PUBLICATIONS.....	28
1. Identification of HcgC as a SAM-dependent pyridinol methyltransferase in [Fe]-hydrogenase cofactor biosynthesis.....	29
2. Towards artificial methanogenesis: biosynthesis of the [Fe]-hydrogenase cofactor and characterization of the semisynthetic hydrogenase.....	63
3. Water-bridged H-bonding network contributes to the catalysis of a SAM-dependent C-methyltransferase HcgC	85
4. The growth phenotype of the Δhcg mutants of <i>M. maripaludis</i>	96

5. Over-expression of HcgA and HcgG in <i>E. coli</i>	100
6. The FeGP cofactor from <i>M. maripaludis</i> and its precursors.....	104
DISCUSSION	109
REFERENCES	121
APPENDIX	131
ACKNOWLEDGEMENTS	139

ABBREVIATIONS

ABBREVIATIONS

Hmd	H ₂ -forming methylene-tetrahydromethanopterin dehydrogenase or [Fe]-hydrogenase
FeGP cofactor	Iron-guanylylpyridinol cofactor
TosMIC	Toluenesulfonylmethyl isocyanide
GP	Guanylylpyridinol
SAM	S-Adenosylmethionine
SAH	S-Adenosyl-L-homocysteine
Pyridinol substrate	6-Carboxymethyl-5-methyl-4-hydroxy-2-pyridinol
Pyridinol product	6-Carboxymethyl-3,5-dimethyl-4-hydroxy-2-pyridinol
H ₄ MPT	Tetrahydromethanopterin
Methenyl-H ₄ MPT ⁺	Methenyl-tetrahydromethanopterin
Methylene-H ₄ MPT	Methylene-tetrahydromethanopterin
MPD	2-Methyl-2,4-pentanediol
MALDI-TOF-MS	Matrix-assisted laser-desorption/ionization time-of-flight mass spectrometry
LC-MS	Liquid-chromatography-mass-spectrometry

ABSTRACT

ABSTRACT

[Fe]-hydrogenase (Hmd) catalyzes the reduction of methenyl-H₄MPT⁺ to methylene-H₄MPT using H₂ as electron donor in the hydrogenotrophic methanogenic pathway. The production of Hmd was upregulated when the cell was grown under Ni-limiting environment. Hmd is composed of homodimer; the active sites are located at the cleft formed by the N-terminal domain and central domain. The N-terminal domain binds an iron-guanylylpyridinol (FeGP) cofactor, which is prosthetic group of this enzyme. The FeGP cofactor is composed of a low spin Fe^{II} ligated with two CO, an acyl-C and pyridinol-N; in addition, Cys-S and a solvent are bound to the iron site in the enzyme. The pyridinol ring is substituted with GMP moiety and two methyl groups. Genome analysis indicated that there are seven conserved genes which is named *hcg* gene cluster containing *hcgA–G* and *hmd* genes. Therefore, it was predicted that the *hcg* cluster is responsible for biosynthesis of the FeGP cofactor. From the *hcg* genes sequences, we could not deduce the function of the proteins. However, using the “structure to function” strategy and biochemical assays, we could identify the function of some Hcg proteins. In this thesis, I describe the function of HcgC based on crystal structure and biochemical analyses. The isotope-labeling experiment indicated that the C3 methyl group comes from methionine, probably via S-adenosylmethionine (SAM). Structure comparisons of HcgC with other proteins suggested similarity of HcgC to SAM-dependent methyltransferases. Co-crystallization of HcgC and SAM revealed that SAM binds to the active site of HcgC. Docking simulation with a possible methyl-acceptor pyridinol suggested that the binding site of the pyridinol. The predicted substrate pyridinol was chemically synthesized and the enzyme activity was determined. The structure of the HcgC-reaction product was determined by NMR, which confirmed that HcgC transfer the methyl group from SAM to C3 of pyridinol. In order to analyze the catalytic mechanism of HcgC, co-crystallization of HcgC, pyridinol, SAM or SAH was performed. The substrate binding site structure showed that seven water molecules connected pyridinol to protein. The only interaction of pyridinol with amino acid side chain was Thr179-OH. The C3 of pyridinol was close to the sulfur of SAH. In the crystal structure, there was no amino acid, which functions as general base of the typical methyl-transfer reaction. We proposed that the water molecules stabilize the deprotonated form of pyridinol by resonance effect, which increases the nucleophilicity of C3. Mutation analysis supported the essential contribution of the water molecules.

ZUSAMMENFASSUNG

ZUSAMMENFASSUNG

Die [Fe]-Hydrogenase Hmd katalysiert die Reduktion von Methenyl-H₄MPT⁺ zu Methylen-H₄MPT unter Nutzung von H₂ als Elektronendonator in der hydrogenotrophen Methanogenese. Die Produktion der Hmd war erhöht, wenn die Zellen unter Ni-limitierten Bedingungen kultiviert wurden. Hmd ist ein homodimeres Enzym, in dem die aktiven Zentren in einer Spalte zwischen den N-terminalen Domänen und den zentralen Domänen lokalisiert sind. Die N-terminale Domäne bindet einen Eisen-Guanylylpyridinol- (FeGP-) Cofaktor als prosthetische Gruppe. Der FeGP-Cofaktor besteht aus einem low-spin Fe^{II}, ligandiert durch zwei CO, einem Acyl-C und eine Pyridinol-N. Zusätzlich ist das Eisenzentrum durch ein Cys-S und ein Wassermolekül im Enzym koordiniert. Der Pyridinol-Ring ist mit einem GMP-Rest und zwei Methylgruppen substituiert. Genom-Analysen deuteten auf einen Cluster aus sieben konservierten Genen hin, der sowohl die *hcgA–G* Gene als auch das *hmd*-Gen umfasst. Aufgrund dessen wurde angenommen, dass die *hcg*-Gene für die Biosynthese des FeGP-Cofaktors verantwortlich sind. Von den Gensequenzen selbst konnten jedoch keine Funktionen für die entsprechenden Proteine abgeleitet werden. Sowohl eine „Struktur-zu-Funktion“-Strategie, als auch biochemische Charakterisierungen wurden genutzt, um die Funktionen einiger Hcg-Proteine aufzuklären. In der vorliegenden Studie wird die Funktion von HcgC, anhand seiner Kristallstruktur und biochemischer Analysen beschrieben. Isotopenmarkierungen wiesen darauf hin, dass die C3-Methylgruppe des Pyridinol-Rings aus Methionin stammt und wahrscheinlich in einer S-Adenosylmethionin- (SAM-) abhängigen Reaktion übertragen wird. Strukturvergleiche zwischen HcgC und anderen verwandten Proteinen deuteten auf Ähnlichkeiten zu SAM-abhängigen Methyltransferasen hin. Co-Kristallisation von HcgC und SAM zeigte, dass SAM tatsächlich im aktiven Zentrum von HcgC bindet. Docking-Simulationen mit einem möglichen Methylakzeptor-Pyridinol zeigten eine wahrscheinliche Bindestelle für das Pyridinol auf. Das vorhergesagte Substrat-Pyridinolderivat wurde chemisch synthetisiert und die Enzymaktivität der HcgC wurde bestimmt. Die Struktur des Reaktionsproduktes der HcgC wurde mit NMR aufgeklärt und es wurde bestätigt, dass die Methylgruppe tatsächlich von SAM auf das C3 des Pyridinols übertragen wurde. Um den Katalysemechanismus näher zu untersuchen, wurde HcgC mit Pyridinol und SAM oder S-Adosylhomocystein (SAH) co-kristallisiert. Es zeigte sich, dass sieben Wassermoleküle an der Bindung des

ZUSAMMENFASSUNG

Pyridinols im aktiven Zentrum beteiligt waren. Die einzige direkte Interaktion des Pyridinols und einer Aminosäureseitenkette war mit der Hydroxylgruppe von Thr179. Das C3 des Pyridinols lag in Nähe zum SAH-Schwefelatom. Die Kristallstruktur wies auf keine Aminosäure hin, die als generelle Base in der Reaktion hätte dienen können. Es wird vorgeschlagen, dass die koordinierenden Wassermoleküle die deprotonierte Form des Pyridinols über einen Resonanzeffekt stabilisieren, welcher die Nucleophilie des C3 erhöht. Mutationsstudien konnten die essentielle Rolle der Wassermoleküle in der Reaktion untermauern.

INTRODUCTION

INTRODUCTION

Methane, in the earth troposphere, was steadily increasing since the last century [1]. Methane could absorb the long wavelength radiation, which emitted from the planet surface [2]. It is great concern because methane is an important greenhouse effect gas next to carbon dioxide [3]. Most of the methane are produced by microbial reaction process, more exactly, by methanogenic archaea. About 30% of methane are derived from non-microbial sources: mining, biomass combustion, fossil fuel or chemical production from plant material [4]. It is estimated that approximately 70 Gt biomass are produced per year. A small part of the biomass (2%) are anaerobically degraded into carbon dioxide and molecular hydrogen, acetate and the other organic acids by bacteria, protozoa, fungi and syntrophic bacteria [5, 6]. Methanogens utilize acetate, carbon dioxide and hydrogen, and C1 compound like methanol, methylamine and methylthiol to produce methane [7]. The total amount of methane produced was approximately 1 Gt per year. When methane was diffused to atmosphere, most of them (more than 80 %) are photo-oxidized by the reaction with OH radical [4]. The other two sinks are microbial oxidation and diffusion to stratosphere. Under the oxic condition, methane produced by methanogens is oxidized to carbon dioxide by aerobic methanotrophic bacteria. Under anaerobic condition, methane is oxidized by anaerobic methanotrophic archaea coupled with the sulfate and nitrate as electron acceptor [8, 9]. Anaerobic bacteria can also oxidized methane to carbon dioxide coupled with nitrite reduction [10].

In the three domains of life, bacteria, eukaryote and archaea, all the methanogens belong to the domain archaea. Methanogens are classified into six orders in Euryarchaeota: *Methanopyrales*, *Methanococcales*, *Methanobacteriales*, *Methanomassiliicoccales*, *Methanomicrobiales* and *Methanosarcinales* (Figure I-1). In the deepest root of evolution of methanogens, *Methanopyrales* branch off first, followed by the order of *Methanococcales* and *Methanobacteriales*. Recently, metagenomic analysis revealed two new lineages of possible methanogenic archaea, Bathyarchaeota [11] and Verstraetearchaeota [12], which are phylogenetically distant from Euryarchaeota. The last branch are *Methanomicrobiales* and *Methanosarcinales* [13]. Among the six orders of methanogens, only *Methanosarcinales* has cytochromes and utilize acetate as methanogenic substrate [14-16]. In addition, many methanogens

INTRODUCTION

belonging to *Methanosarcinales* can utilize all the methanogenic substrate such as acetate, C1 compounds, and carbon dioxide and hydrogen [17]. The members of other five orders are lack of cytochromes and reduce carbon dioxide and hydrogen to methane [18]. Some of methanogens without cytochromes produce methane from formate, and H₂ and methanol [13, 19]. *Methanoculleus thermophilus* utilize 2-propanol as electron donor for methane formation [20].

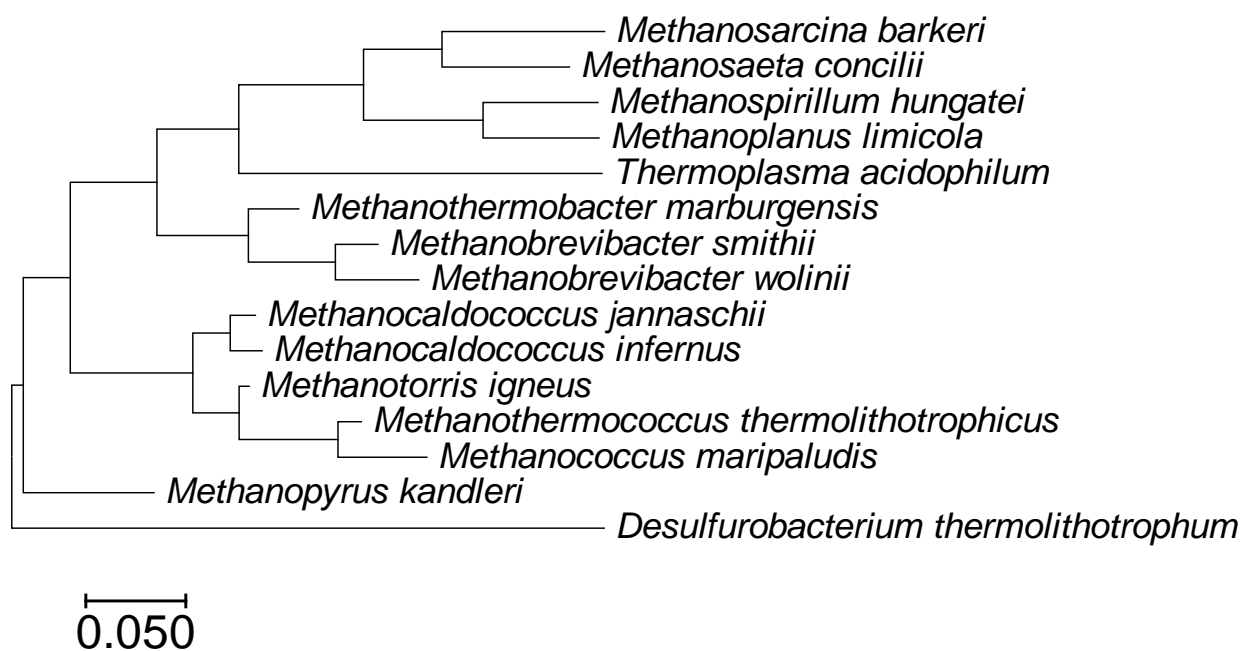


Figure I-1. Phylogenetic tree of methanogens in Euryarchaeota. Gene sequences were downloaded from the National Center for Biotechnology Information (NCBI) database. Sequence alignment and phylogeny tree construction were performed by the MEGA program. *Desulfurobacterium thermolithotrophum* as an out group.

Most of the methanogens could form methane from carbon dioxide and hydrogen, namely hydrogenotrophic methanogenic pathway (Figure I-2) [13]. In this pathway, carbon dioxide is activated and bound to a C1 carrier methanofuran (MFR) and formed formyl-MFR; this reaction is catalyzed by formyl-MFR dehydrogenase [21]. Then the formyl group is transferred to the next C1 carrier tetrahydromethanopterin (H₄MPT) to form formyl-H₄MPT [22, 23]. Methenyl-H₄MPT cyclohydrolase catalyzes the conversion of formyl-H₄MPT to methenyl-H₄MPT⁺ [24-26]. The methenyl group is reduced to methylene-H₄MPT catalyzed by two types of methylene-H₄MPT dehydrogenases: H₂-forming enzyme ([Fe]-hydrogenase or Hmd, see below) [27] and F₄₂₀-reducing enzymes (Mtd) [28, 29]. F₄₂₀ is an electron carrier of this metabolism.

INTRODUCTION

The reduced form of F_{420} is regenerated by F_{420} -reducing hydrogenase (Frh) [7]. When the cells grow under Ni-limiting condition, Frh is downregulated and Hmd and Mtd are upregulated [30]. The reduction of methylene- H_4 MPT is catalyzed by F_{420} -dependent methylene- H_4 MPT reductase (Mer), which forms methyl- H_4 MPT [31]. Next, the methyl group is transferred to coenzyme M (CoM-SH) forming methyl-S-CoM. This reaction is catalyzed by methyl- H_4 MPT: CoM-SH methyltransferase, [32, 33]. This methyltransfer reaction is coupled with sodium ion translocation [34, 35]. Finally, methyl-CoM and coenzyme B are reacted into methane and heterodisulfide (CoM-S-S-CoB), which is catalyzed by methyl-S-CoM reductase [36]. Heterodisulfide is reduced to coenzyme M and coenzyme B using electrons from H_2 ; this reaction is catalyzed by heterodisulfide-reductase/hydrogenase complex, which couples the reduction of ferredoxin and CoM-S-S-CoB by flavin-based electron-bifurcation mechanism [37-39].

Methanogens, which utilize acetate as substrate for forming methane, produce methane via acetyl-CoA in the methanogenic pathway [17]. In methanogens belonging to *Methanosarcina*, acetate is activated by acetate kinase and phosphotransacetylase [40, 41]. In the former reaction, acetate is activated by phosphorylation and in the later reaction acetyl-phosphate is ligated to acetyl-CoA. In methanogens belonging to *Methanosaeta*, acetyl-CoA synthetase ligates acetate to CoA [42-44]. Carbon monoxide dehydrogenases–acetyl-CoA synthase (CODH-ACS) complex catalyzes the cleavage of methyl group and carbon monoxide from acetyl-CoA and methyltransfer to tetrahydrosarcinapterin (H_4 SPT) forming methyl- H_4 SPT [17]. Carbon monoxide dehydrogenase part catalyzes oxidation of the CO moiety to CO_2 , from which two electrons are used for reduction of ferredoxin. In the next step, integral membrane methyltransferase catalyzes the methyl group transfer from methyl- H_4 SPT to CoM-SH. This methyltransfer reaction is coupled with sodium ion translocation [34, 35].

Methanogens utilizing C1 compounds (e.g. methanol) as the growth substrate contain methyltransferase, which catalyze methyltransfer from the C1 compound to coenzyme M [45]. One molecule of methyl-CoM is oxidized to CO_2 by the reverse reactions of hydrogenotrophic methanogenic pathway. Three molecules of methyl-CoM are converted to methane, which is catalyzed by methyl-CoM reductase. Six electrons required for the production of three molecules of methane are provided by oxidation of one methyl-S-CoM. The conversion of methylamine and methylthiol is almost same with the methanol metabolism. However, the methyltransferase reactions

INTRODUCTION

are catalyzed by different type of the enzymes, which is specific for the C1 compounds [46, 47].

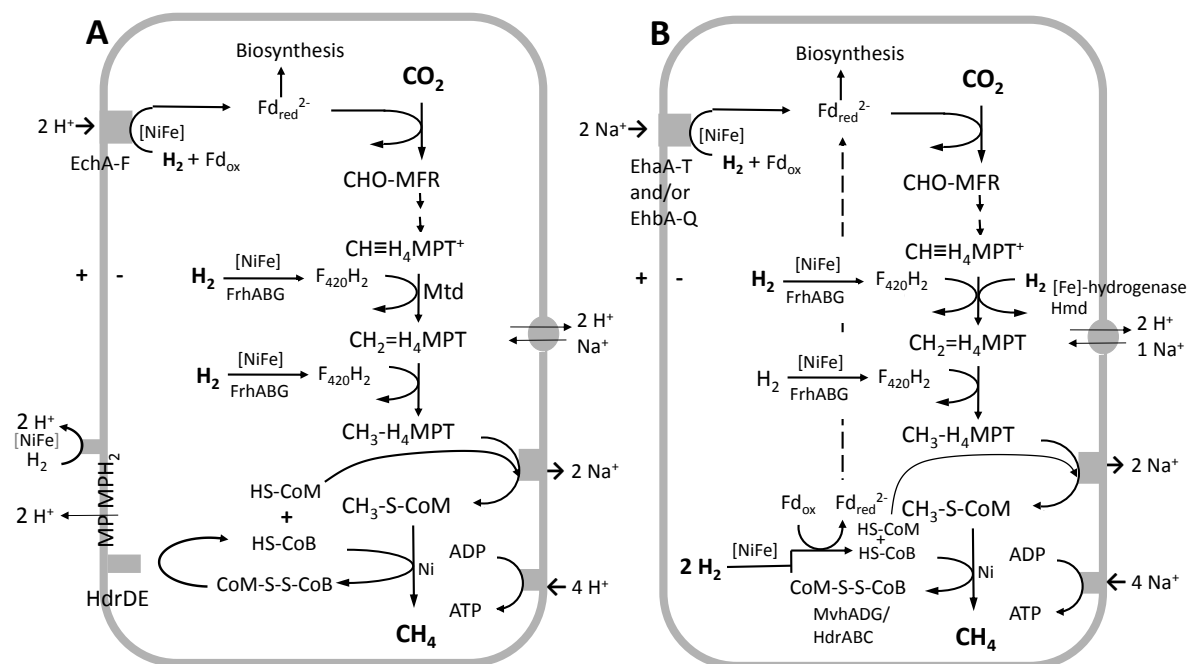


Figure I-2. Methanogenic pathway. (A) Methanogenic pathway of methanogens with cytochromes. (B) Methanogenic pathway of methanogens without cytochromes. The abbreviations are described in the text. MP/MPH₂: oxidized and reduced methanophenazine.

Methanogens with cytochromes have considerably high growth yield (up to 7 g per mole of methane) and H₂ threshold concentration (generally over 10 Pa), which are higher than the values of methanogens without cytochromes: 3 g per mole of methane and lower than 10 Pa H₂, respectively [48]. The reason of such difference is attributed to the different metabolic system involved in the energy conservation of methanogens with cytochromes and without cytochromes [5]. Energy conservation in methanogens with cytochromes involves two membrane-associated enzymes. Integral membrane methyltransferase (MtrA-H) that transfer the methyl group from H₄MPT to CoM-SH is sodium-ion pump. This chemiosmotic gradient is used for ATP synthesis catalyzed by ATP synthase [34]. Heterodisulfide is reduced by membrane-associated heterodisulfide reductase (HdrDE), which uses reduced methanophenazine as electron donor. Membrane-associated hydrogenase (VhtACG) regenerates reduced methanophenazine. This HdrDE-VhtACG system builds up an electrochemical

INTRODUCTION

potential for the ATP synthase reaction [49-51]. In methanogens without cytochromes, the integral membrane MtrA-H system is the same with that of methanogens with cytochromes. However, heterodisulfide reduction is catalyzed by soluble enzyme system other than membrane protein. The soluble heterodisulfide reductase HdrABC is complex with a hydrogenase (MvhADG) [38]. This HdrABC-MvhADG complex reduces heterodisulfide and ferredoxin with four electrons from H₂ by using electron bifurcation mechanism and the reduced ferredoxin is used for the first CO₂ reduction [39, 52].

Electron bifurcation is firstly proposed by Peter Mitchell to explain the reduction of cytochrome b, which results in the establishment of Q cycle [53]. In this cycle, the two electron from ubiquinone (QH₂) are delivered to two different energy levels acceptor [54]. Recently, the flavin-based electron bifurcation is proposed by Wolfgang Buckel and Rudolf K. Thauer [55]. In the last step of methanogenic pathway, the reduction of heterodisulfide with molecular hydrogen is associated with the reduction of ferredoxin, which catalyzed by hydrogenase-heterodisulfide reductase complex (MvhADG-HdrABC). Hdr subunits contain numerous [4Fe-4S] cluster and one FAD in the subunit HdrA, while Mvh also contain [4Fe-4S] clusters and one [2Fe-2S] cluster. The E^0 of ferredoxin pair, H₂/H⁺ and CoM-S-S-CoB/ HS-CoM and HS-CoB are -500 mV, -414 mV and -140 mV, respectively. H₂ is activated by hydrogenase and the electrons are channeled to FAD, then two electrons are used for the oxidized ferredoxin and the other two electrons are used for the reduction of heterodisulfide (Figure I-3) [39, 52].

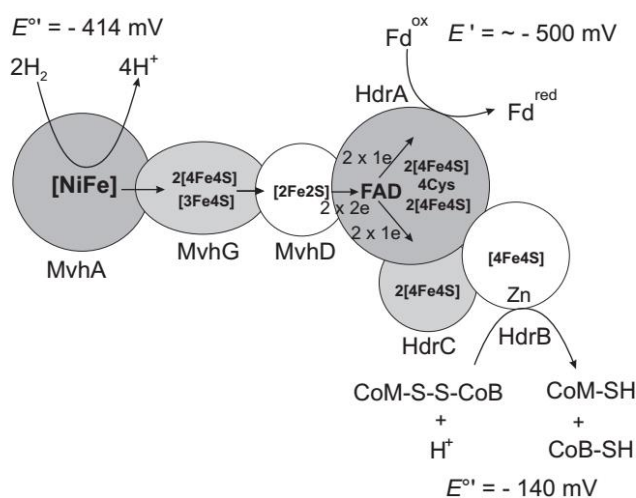


Figure I-3. Schematic presentation of electron bifurcation of MvhADG-HdrABC complex from *Methanothermobacter marburgensis* obtained from review [55, 56].

INTRODUCTION

There are three types of hydrogenases that activate molecular hydrogen: [NiFe]-hydrogenase, [FeFe]-hydrogenase and [Fe]-hydrogenase (Figure I-4). Among these three hydrogenases, [NiFe]-hydrogenase and [Fe]-hydrogenase are found in the methanogenic archaea [38, 57]. There are four different [NiFe]-hydrogenases in methanogenic archaea; F₄₂₀-reducing hydrogenase and the heterodisulfide reductase-associated hydrogenase are cytoplasmic protein, while energy converting hydrogenases and methanophenazine-reducing hydrogenase are membrane proteins. The energy converting hydrogenases are assumed to obtain energy from the proton or sodium gradient to reduce ferredoxin ($E' = -500$ mV) with H₂ ($E^{\circ} = -414$ mV). The reduced ferredoxin is used for the reduction of CO₂ [52, 58]. The F₄₂₀-reducing hydrogenases in methanogens are unique since the small subunit contains three [4Fe-4S] clusters. This cytoplasmic hydrogenase catalyzes the reversible reduction of F₄₂₀ with H₂.

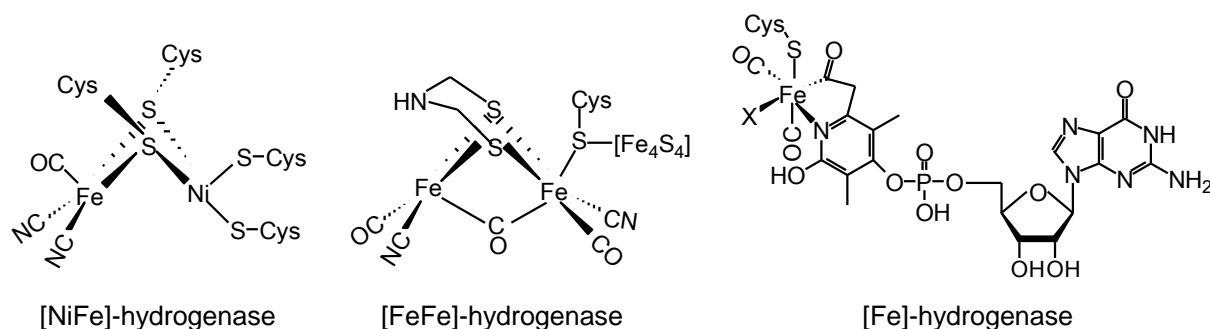


Figure I-4. The active center of the three types of hydrogenases. X: solvent-binding in the crystal structures of [Fe]-hydrogenase, which is proposed to be open for binding of hydride in the active state enzyme. In the case of [NiFe]- and [FeFe]-hydrogenases, hydride is bound between Ni and Fe, and on the iron site near the dithiomethylamine bridge nitrogen.

[NiFe]-hydrogenase maturation includes at least six proteins namely Hyp proteins (HypABCDEF) [59, 60]. In the first step, HypF catalyzes formation of HypE-thiocarboxamide at the C-terminal cysteine residue of HypE (HypE-Cys-S-CONH₂) using carbamoylphosphate and ATP [61]. Then the thiocarboxamide on HypE is dehydrated to thiocyanate by a ATP dependent reaction, releasing HypF [61, 62]. Secondly, a small iron chaperon HypC could be involved in iron-trafficking in the maturation step [63]. It is also proposed that HypC is involved in the nickel insertion step to maintain the conformation of large subunit of hydrogenase. Formation of the

INTRODUCTION

CO ligand in the active center is still not clear. Recently, mutation and isotope-labeling experiments indicated that *Ralstonia eutropha* synthesizes the CO ligands using HypX, which is a member of the *hyp* gene cluster found only in (micro) aerophilic microorganisms. The indirect evidence indicated that HypX catalyzes CO formation from formyl-tetrahydrofolate (formyl-H₄F), which is an intermediate of T₄F-based one-carbon metabolism [64]. The HypCD complex receives the cyanide ligands from HypE, which results in production of the inorganic Fe(CN)₂CO complex and HypE is released. The HypCD complex with the iron complex is bound to the large subunit, while the HypD is released [65]. In the next step, HypA and HypB are involved in the nickel insertion to the iron complex in the large subunit-HypC complex [66, 67]. Finally, the C-terminus of the large subunit is cleaved by an endopeptidase, which induces the change of protein conformation and forms the correct active site structure [68].

Different from the [NiFe]-hydrogenases, [FeFe]-hydrogenase active center (H cluster) harbors a [4Fe-4S] cluster, which connected to the binuclear [FeFe] unit [69]. [FeFe]-hydrogenase maturation requires association of three proteins HydEFG. HydE and HydG are members of the radical SAM enzyme family [70, 71]. HydE is proposed to catalyze the formation of dithiomethylamine bridge between two irons (see Figure 4) [72-74]. HydG has a high similarity with ThiH, which is involved in the thiamine pyrophosphate synthesis [75, 76] and as observed in ThiH, HydG utilizes tyrosine as substrate [77, 78]. HydG harbors two [4Fe-4S] clusters on the N- and C-terminal domains [79, 80]. The first [4Fe-4S] cluster catalyzes formation of CO and CN from tyrosine using radical SAM [79, 81, 82]. The second [4Fe-4S] cluster contributes to formation of Fe(CN)₂(CO) unit using an external Fe and cysteine [83]. HydF is an iron-sulfur cluster protein, which has GTPase activity and functions as [FeFe] center insertion into HydA. HydA is [FeFe]-hydrogenase structure protein, which contains a [4Fe-4S] cluster [71, 84].

[Fe]-hydrogenase (Hmd) is functionally important in methanogens without cytochromes when the cells grow under Ni-limiting condition [30]. Hmd catalyzes the reversible transfer of hydride from H₂ to Methenyl-H₄MPT⁺, which is reduced to methylene-H₄MPT (Figure I-5B). Facing the changing concentration of nickel in the environment, methanogens regulate the production of Hmd, F₄₂₀-dependent methylene-H₄MPT dehydrogenase (Mtd) and F₄₂₀-reducing [NiFe]-hydrogenase (Frh). Hmd and Mtd are upregulated in Ni-limiting condition, while Frh is downregulated [30,

INTRODUCTION

85]. In the Ni-limiting condition, the Frh reaction was substituted by a coupled reaction of Hmd and Mtd, which regenerates $F_{420}H_2$ using H_2 as a hydride donor.

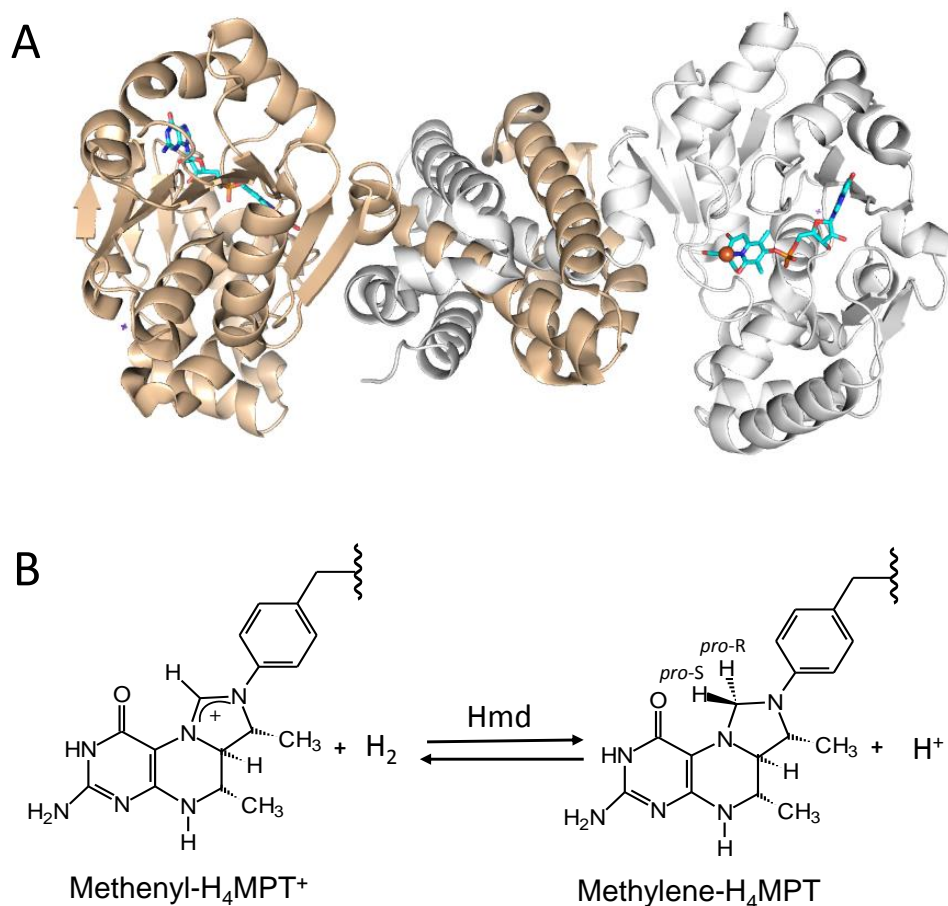


Figure I-5. (A) Structure of Hmd from *Methanocaldococcus jannaschii* binding the FeGP cofactor and (B) the stereo-specific hydride-transfer reaction catalyzed by Hmd.

Most of microorganisms including methanogens have high-affinity nickel-uptake transporters [86]. Therefore, it is long time overlooked that nickel is an essential element for most of organisms [38]. How the regulation response to the nickel concentration in environment is still unknown. Bacteria contain Ni-dependent regulators NikR and RcnR, which regulate gene expression positively and negatively. Most of methanogens harbor NikR homologs but do not have RcnR [38]. However, at least in *Methanothermobacter marburgensis*, negative nickel response regulator like RcnR should exist because Hmd production is negatively regulated in the higher concentration of nickel in the medium.

The structure of Hmd from *Methanocaldococcus jannaschii* has been reported on 2008 (Figure I-5A) [87, 88]. The homodimeric enzyme is composed of three folding

INTRODUCTION

units. The N-terminal domains consist of a Rossmann-like fold, which can be subdivided into a classical Rossmann fold and an α -helix part. The two C-terminal domains of the Hmd homodimer intertwine and form the central domain [87, 89, 90]. X-ray crystal structure indicated that the holoenzyme is in an open conformation respect to the active-site cleft between the N-terminal and central domains. On the contrary, the apoenzyme is open conformation in the crystal structure. This enzyme contains the iron-guanylylpyridinol (FeGP) cofactor as a prosthetic group. In the iron center of this cofactor, a low spin Fe(II) is coordinated with pyridinol-N, two CO ligands, an acyl group and thiolate of cysteine in the N-terminal domain. An iron coordination site is occupied with a solvent molecule (Figure I-6B). The 2-pyridinol is substituted with 3,5-methyl, 4-GMP and 6-acylmethyl groups. [90-92]. The FeGP cofactor can be isolated from Hmd in the extraction solution containing 60% methanol, 1 mM 2-mercaptoethanol and 1% ammonia. In the extracted FeGP cofactor, 2-mercaptoethanol-sulfur and -oxygen substitute the cysteine-sulfur and solvent ligand. The FeGP cofactor can also be extracted by 50% acetic acid; in this case acetate bonds to the iron-center as a bidentate ligand [91]. By mixing the extracted cofactor and Hmd apoenzyme heterologously produced in *E. coli* reconstitute the active holoenzyme.

Methanogens harboring the *hmd* gene always have *hmd*-occurring genes (*hcgA-G*) (Figure I-6A). Furthermore, in many methanogens, these seven *hcg* genes are clustered near the *hmd* gene. This observation led to a hypothesis that the seven *hcg* genes are involved in the biosynthesis of FeGP cofactor [38]. At first, biosynthesis of the FeGP cofactor in methanogens was tested using isotope labeling [93]. Methanogens were cultivated in the medium containing isotope labeled compounds (e.g. acetate, pyruvate and CO₂) and the cofactor was analyzed by NMR and Mass spectrometry [93].

To analyze the function of the *hcg* genes, a unique “structure to function strategy” method is applied in the group of Seigo Shima since there is no indication about the function based on the primary structure analysis. Firstly, the gene was over-expressed in the *Escherichia coli* strain and the protein was purified. Secondly, the purified protein was crystallized and the structure was solved. The protein structure is used as the model for the similarity search in the database. Once the similar protein in the database found, the possible enzyme function are predicted from the function of the structural homologs. Co-crystallization of the Hcg proteins with possible ligands was performed

INTRODUCTION

to check the affinity of the ligands. Finally, the enzyme activity was tested using the possible substrates which is commercially available, or synthesized chemically or biologically to confirm the predicted reaction.

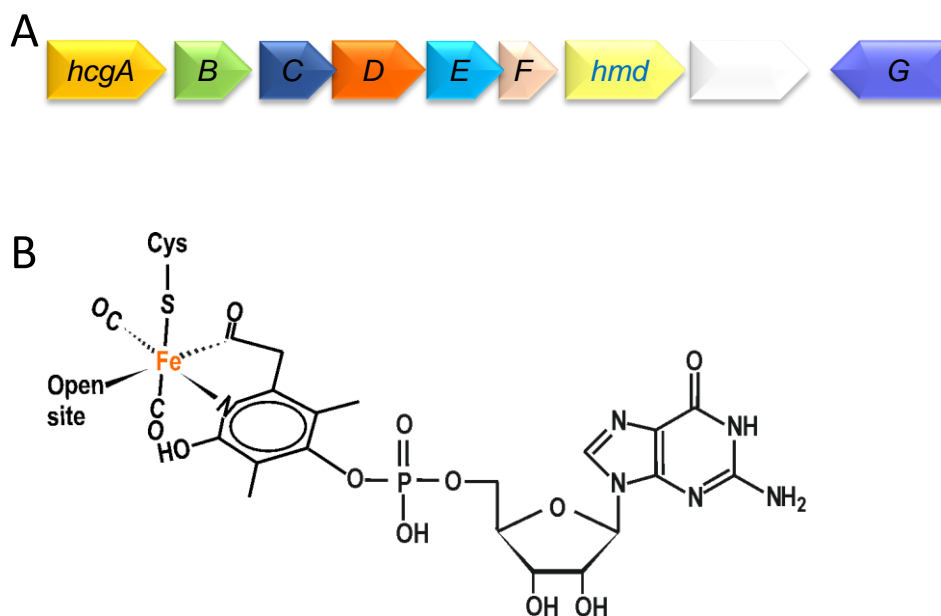


Figure I-6. (A) The *hcg* gene cluster for the FeGP cofactor biosynthesis and (B) structure of the FeGP cofactor.

By using this methods, the function of *hcgB*, *hcgD*, *hcgE* and *hcgF* has been elucidated. The structure of HcgB is similar with nucleoside triphosphatase (NTPase) that cleave off the pyrophosphate from nucleosidetriphosphates. From this information, HcgB was predicted as guanylyltransferase, which ligate the GMP moiety and pyridinol ring forming the guanylylpyridinol part. The prediction is confirmed by the enzyme reaction [94].

The structure of HcgD showed that it is a member of Nif3-like protein. A Nif3-like protein is first identified in yeast two hybrid system; this type of enzyme is involved in the transcriptional regulation and human disease but the exact physiological function is still unknown [95-97]. HcgD structure organized in the hexameric form, which is a trimer of a compact dimer. Like the other Nif3 protein, HcgD has a two iron-binding site, in which Fe1 is more easily to be washed out by chelating agent like EDTA than Fe2 site. Based on the structure and properties, HcgD is proposed to have iron trafficking function [98].

INTRODUCTION

The primary structure of HcgE shows similarity with E1-like ubiquitin-activating enzyme, which activate the C-terminal carboxy group of ubiquitin or ubiquitin like proteins [99, 100]. The crystal structure of HcgE was solved. The structure comparison indicated that the HcgE structure shares the same structure with E1 like ubiquitin enzyme including ATP binding site. However, ubiquitin-binding site was not conserved in HcgE. Based on this finding, it was predicted that HcgE catalyzes the adenylation of carboxy group of guanylylpyridinol. This hypothesis was confirmed by co-crystallization with ATP and guanylylpyridinol but lacking divalent cation like Mg^{2+} [98]. The enzyme reaction product was detected by mass spectrometry and the enzyme reaction was kinetically assayed using pyrophosphate production from ATP and guanylylpyridinol [101].

The primary structure of HcgF does not show any similarity with any known function protein. The structure of HcgF was solved and the structure was compared with that of proteins with known function [101]. This analysis indicated that HcgF is similar to nicotinamide mononucleotide (NMN) deaminase, but HcgF do not have NMN deaminase activity. As NMN has some similarities with structure of guanylylpyridinol, co-crystallization of HcgF with guanylylpyridinol was performed. In the complex structure, HcgF binds guanylylpyridinol. Interestingly, guanylylpyridinol bond to HcgF forms a covalent thioester bond between carboxyl group and protein Cys9. This observation and HcgE adenylation reaction led to the hypothesis that HcgF forms the thiol-ester bond of guanylylpyridinol using adenylated guanylylpyridinol as the substrate. The enzyme reaction is finally performed to prove this hypothesis [101].

The function of HcgA and HcgG are still not known. Blast search of the HcgA sequence shows that it belong to a radical SAM super family including HydG. HydG is a radical SAM enzyme involved in maturation of the [FeFe]-hydrogenase active site (H-cluster), which catalyzes the formation of CO and CN ligands (see above and the Discussion section) [79, 102]. However, HcgA lacks the typical sequence motif for [4Fe-4S] cluster, which is crucial for the radical SAM enzyme [103]. Blast search of HcgG shows that it belongs to a fibrillar family, but there is no further indications.

In my PhD project, I studied the structure and function of HcgC. We solved the structure of HcgC, which indicated that HcgC is similar to SAM dependent methyltransferases and NAD(P) dependent hydrogenase. To analyze the binding affinity of possible substrates, we performed co-crystallization experiments with SAM and NAD(P). This result indicated that HcgC is a SAM dependent methyltransferase.

INTRODUCTION

We successfully confirmed the prediction by enzyme activity using chemically synthesized pyridinol. The enzyme reaction product was determined by NMR, which confirmed the position of methyl transfer. Furthermore, co-crystallization of HcgC with chemically synthesized pyridinol and SAH and mutation assay indicated possible catalytic mechanism of this enzyme.

MATERIALS AND METHODS

1. Materials

The following chemicals were purchased from Roth: sodium chloride (NaCl), potassium chloride (KCl), sodium hydroxide (NaOH), hydrogen chloride (HCl), potassium dihydrogenphosphate (KH₂PO₄), dipotassium hydrogen phosphate (K₂HPO₄), potassium hydroxide (KOH), ammonium sulfate ([NH₄]₂SO₄), magnesium chloride (MgCl₂), ammonia (NH₃), calcium chloride (CaCl₂), sodium hydrogen carbonate (NaHCO₃), Iron(II) sulfate (FeSO₄), sodium acetate, casamino acid, magnesium sulfate (MgSO₄), ammonium chloride (NH₄Cl), manganese(II) sulfate (MnSO₄), zinc sulfate (ZnSO₄), copper(II) sulfate (CuSO₄), sodium dodecyl sulfate (SDS), Tris(hydroxymethyl)aminomethane, 3-(N-morpholino)propanesulfonic acid, lysogeny broth (LB) medium, ethylenediaminetetraacetic acid (EDTA), Bradford reagent (Coomassie Brilliant Blue G250), imidazole, D₂O, methanol, formaldehyde, , resazurin, cysteine-HCl,

The following chemicals were from Sigma: nickel(II) chloride (NiCl₂), cobalt(II) chloride (CoCl₂), sodium molybdate dihydrate (NaMoO₄·2H₂O), sodium selenite (Na₂SeO₃), sodium tungstate dihydrate (Na₂WO₄·2H₂O), sodium sulfide (Na₂S), dimethyl sulfoxide (DMSO), 2-mercaptoethanol, toluenesulfonylmethyl isocyanide (TosMIC), ammonium formate, ethanesulfonic acid, 2-Methyl-2,4-pentanediol (MPD), biotin, folic acid, pyridoxine-HCl, thiamine-HCl, riboflavin, nicotinic acid, D-calcium-pantothenate, Vitamin B12, *p*-aminobenzoic acid, lipoic acid.

Isopropyl β-D-1-thiogalactopyranoside (IPTG) and Dithiothreitol (DTT) were from Thermo Science.

6-Carboxymethyl-4-hydroxy-5-methyl-pyridinol was chemically synthesized by Xile Hu (Ecole polytechnique fédérale de Lausanne, EPFL). H₄MPT was extracted from *M. marburgensis* and purified [104].

Gasses used for the cultivation of methanogens and anaerobic experiments were purchased from Messer.

MATERIALS AND METHODS

2. Cultivation of microorganisms

2.1 *Methanothermobacter marburgensis*

The organism *Methanothermobacter marburgensis* (DSM2133) was purchased from Deutsche Sammlung von Mikroorganismen und Zellkulturen (DSMZ). The culture medium contained NH_4Cl 2.12 g/L, KH_2PO_4 6.8 g/L, Na_2CO_3 2.5 g/L, resazurin (0.2%) 0.3 mL/L and 1-mL trace element solution ($\text{MgCl}_2 \cdot 6\text{H}_2\text{O}$ 4 g/L, $\text{FeCl}_2 \cdot 6\text{H}_2\text{O}$ 1 g/L, $\text{CoCl}_2 \cdot 6\text{H}_2\text{O}$ 20 mg/L, $\text{NiCl}_2 \cdot 6\text{H}_2\text{O}$ 0.12 g/L, $\text{NaMo}_2\text{O}_4 \cdot 6\text{H}_2\text{O}$ 20 mg/L). In medium used for the cultivation under Ni-limiting condition, the concentration of nickel ($\text{NiCl}_2 \cdot 6\text{H}_2\text{O}$) was decreased to 0.65 μM in the pre-culture and excluded in the large-scale cultivation.

M. marburgensis cultivated under Ni-limiting condition for the Hmd purification, while it was cultivated under the normal condition for the H₄MPT purification. *M. marburgensis* was pre-cultivated in 360-mL medium in a 400-mL glass fermenter with a plastic-coated magnetic stirrer bar at 400 rpm and continuous flow of a gas mixture $\text{H}_2/\text{CO}_2/\text{H}_2\text{S}$ (80%/20%/0.1%) at 100 mL min⁻¹ at 65 °C for 16 hours. Around 100-ml fresh pre-culture was inoculated into 10 L nickel-free medium in 11 L glass fermenter. *M. marburgensis* was grown at 65 °C under the continuous gas flow described above at a flow rate of 1.5 L·min⁻¹ and the agitation speed of 1000 rpm. When the optical density (578 nm) of the culture reached to 5–6, which takes around 21 hours, the culture was cooled down to 4 °C. The cell was harvested anaerobically under H_2/CO_2 (80%/20%) by continuous-flow centrifugation. For the normal nickel concentration cultivation, the pre-culture preparation could be omit. Around 100 mL *M. marburgensis* culture stored at 4 °C was inoculated into the 11 L glass fermenter. The cultivation condition was same with that of Ni-limiting condition described above.

2.2 *Methanococcus maripaludis*

Methanococcus maripaludis Mm901 strain was obtained from John Leigh (University of Washington). The strains Mm901 Δ *hmd*, Mm901 Δ *hmdjhmd*, Mm901 Δ *hmdjhmd* Δ *hcgB* and Mm901 Δ *hmdjhmd* Δ *hcgC* were prepared by Micahel Rother (Technische Universität Dresden) and Michael Schick (PhD

MATERIALS AND METHODS

Thesis, 2012). The McA culture medium (1 L) contained 500 mL the general salts solution (KCl 0.67 g/L, MgCl₂·6H₂O 5.5 g/L, MgSO₄·7H₂O 6.9 g/L, CaCl₂·2H₂O 0.28 g/L, NH₄Cl 1.0 g/L), 5 g NaHCO₃, 10 mL K₂HPO₄ solution (14 g/L), 5 mL FeSO₄ solution (1.9 g/L in 10mM HCl), 1 mL trace element solution (MnSO₄·2H₂O 1 g/L, CoCl₂ 1 g/L, ZnSO₄ 1 g/L, CuSO₄·5H₂O 0.1 g/L, Na₂MoO₄·2H₂O 1 g/L, NiCl₂·6H₂O 0.25 g/L, Na₂SeO₃ 2 g/L, Na₂WO₄·2H₂O 1 g/L), 10 mL vitamin solution (Biotin 2.0 mg/L, folic acid 2.0 mg/L, pyridoxine-HCl 10.0 mg/L, thiamine-HCl 5.0 mg/L, riboflavin 5.0 mg/L, nicotinic acid 5.0 mg/L, D-calcium pantothenate 5.0 mg/L, vitamin B₁₂ 0.1 mg/L, p-aminobenzoic acid 5.0 mg/L, lipoic acid 5.0 mg/L), 1 ml resazurin solution, 1.4 g Na acetate, and 0.5 g cysteine·HCl. In the case of genetic experiments, 2 g casamino acid was added to the 1 L medium (McCas medium). The medium was vacuumed for 1 min and then filled with N₂ gas, which was repeated for 30 times using the gas exchanger (Siemens). Finally, the gas mixer (80% H₂/ 20% CO₂) was filled into the bottle with the pressure around +0.5 bar and 2-mM Na₂S (final concentration) was added to the medium before the inoculation. The organism was grown at 37 °C and the gas phase was exchange every 3 hours only in the day time. Optical density at 578 nm of the culture was measured to monitor the cell growth.

2.3 *Escherichia coli*

The *hcgA*, *hcgB*, *hcgC* and *hcgG* genes from several methanogenic archaea were synthesized with optimized codon usages by GenScript. The sequences are shown in the Appendix section at the end of this thesis. The DNA fragments were digested by *NdeI* and another restriction enzyme (*SalI/XhoI*) and inserted into pET24b(+). *E. coli* BL21(DE3) (Novogen) was transformed with the constructed expression vectors. The recombinant *E. coli* strains harboring each of *hcgB*, *hcgC* and *hcgG* were cultivated in LB medium supplemented with 50 µg/mL kanamycine at 37 °C on the shaker (200 rpm). After 4-6-h induction with 1.0-mM IPTG (final concentration), the *E. coli* cells were harvested. For HcgA production, the *E. coli* C41(DE3) strain, which harbors pRKISC and pCodonplus, was used. The pRKISC plasmid contains iron-sulfur cluster formation enzymes [105, 106]. The recombinant *E. coli* was cultivated in the Terrific Broth (TB)

MATERIALS AND METHODS

medium, which contained 12 g/L tryptone, 24 g/L yeast extract, 4 mL glycerol, 2.3 g/L KH_2PO_4 , 12.5 g/L K_2HPO_4 [107]; for assisting the iron-sulfur cluster formation, 1mM cysteine, 1.3 mM ferrous sulfate, 0.8 mM ferric citrate and 0.75 mM ferric ammonium citrate were supplemented and pH was adjusted to 7.3 [105]. To keep the three plasmids, 50 $\mu\text{g}/\text{mL}$ kanamycine, 25 $\mu\text{g}/\text{mL}$ chloramphenicol and 10 $\mu\text{g}/\text{mL}$ tetracycline were added to the medium for production of HcgA. The gene induction conditions are the same as the case of the other Hcg proteins.

3. Gene mutation of *M. maripaludis*

M. maripaludis is a model strain for the genetic experiments of methanogens. The complete genome sequence is available and the genetic methods are established. Moore and Leigh developed a *M. maripaludis* strain Mm901 from the S2 wildtype strain for markerless mutagenesis by deletion the *upt* gene encoding uracil phosphoribosyltransferase. The sensitivity of *M. maripaludis* to 6-azauracil (an analog of uracil) takes the advantage of negative selection for homologous recombination [108, 109]. In this method, the target gene with more than 500-bp flanking sequences is synthesized and inserted into a plasmid pCRUPTNEO. The host cell *M. maripaludis* Mm901 $\Delta hmd\Delta jhmd$ was transformed with this plasmid and the transformants were selected by antibiotic (neomycine) resistance. The transformants' colonies were picked up and cultivated on the McCas medium. Aliquots of this culture was plated on the agar medium with 6-azauracil for the second selection. Finally, incorporation of proper mutation was identified by PCR. Using this genetic manipulation, the *hcgB* and *hcgC* were deleted in *M. maripaludis* Mm901 $\Delta hmd\Delta jhmd$ (PhD Thesis, Michael Schick).

4. Extraction and purification of coenzymes and the FeGP cofactor

4.1 Tetrahydromethanopterin

Tetrahydromethanopterin (H_4MPT) was extracted from *M. marburgensis* cell. Frozen cell (140 g) stored in the brown serum bottle was resuspended in 150

MATERIALS AND METHODS

mL Mops/KOH pH7.0 and incubated in water at 60 °C for 10 min. Then in the anaerobic tent, 38-mL of 5% cetyltrimethylammoniumbromid (CTAB) solution was added. The cell extract solution was cooled on ice water after 6 min incubation at 18 °C. The cell extract was adjusted to pH 3.0 by adding 7.5-mL 100% formic acid. The acidic solution was centrifuged using JA-25.50 rotor (Beckman) at 8,000 rpm for 30 min at 4 °C and the supernatant was further ultracentrifuged with Ti45 rotor (Thermo) for 30 min at 30,000 rpm at 4 °C. The supernatant was loaded onto the column Serdolit PADII, which equilibrated with 500 mL of H₂O/HCOOH containing 10 mM mercaptoethanol at pH 3.0 adjusted by NaOH (buffer A). After washing the column using 300 mL of buffer A, the target compound was eluted with buffer with 15 % methanol. Each of 100-ml fractions was checked by UV-Vis spectrum and all H₄MPT containing fractions was pooled and lyophilized for around 15 hours. The dried powder was resuspended into 50 mL water and loaded onto the column Serdolit PAD I, which equilibrated with 500 mL buffer A. The pure H₄MPT was eluted with 100-mL buffer A containing 30 % methanol. Each fraction was checked by UV-Vis spectrum and the fractions containing H₄MPT was lyophilized for around 15 hours and stored at -80 °C.

To convert H₄MPT to methylene-H₄MPT, 40 µl of 200 mM formaldehyde solution was anaerobically added to 1 ml of 2 mM H₄MPT dissolved in 120 mM potassium phosphate buffer (pH 6.0). The mixer solution was evaporated to dry and the dried substance was re-dissolved in anaerobic water.

4.2 The FeGP cofactor

The FeGP cofactor was purified from Hmd, which was purified from *M. marburgensis* under anaerobic condition. Because of sensitivity of this cofactor to UV-A/blue light, the whole extraction and purification processes were performed under red or yellow light using amber serum bottles to keep the cofactor intact. Cofactor extraction solution, containing 60 % methanol, 1 mM mercaptoethanol, 1 % ammonia, 2 mg/mL Hmd and water, was incubated in 40 °C water for 15 min. CaCl₂ was added into the solution to the final concentration of 5 mM after the solution was cooled on the ice water. The precipitated protein aggregate in the solution was removed by centrifugation with JA-25.50

MATERIALS AND METHODS

(Beckman) at 4500 rpm for 20 min at 4 °C. Methanol was removed by short evaporation, then the rest of protein was removed using 10 kDa cut off filter (Millipore). The isolated cofactor was stored under 100 % N₂ at –80 °C.

4.3 Preparation of the guanylylpyridinol moiety of the FeGP cofactor

The guanylylpyridinol part of the FeGP cofactor, named GP, was obtained by light-induced decomposition of the FeGP cofactor. The FeGP cofactor was exposed to white light beamer (SCHOTT KL 2500, 3000 K) for 2 hours on ice. Then the decomposed cofactor solution was loaded onto the column (HiTrap Q HP, 5 mL, GE Health) equilibrated with water. GP was eluted with the linear gradient of from 0- to 500-mM NaCl. To remove salt, the eluted fraction was loaded onto the column SYNERGI Polar RP 80A (Phenomenex) equilibrated with H₂O/HCl pH 4.0. The FeGP cofactor was eluted with methanol in a linear gradient elution and flowrate 1 mL/min. Salt was washed out at the beginning of the elution, while GP was eluted at around 10 % methanol. Methanol in the pooled fraction was removed by evaporation. The concentrated GP solution was stored under –80 °C. The concentration of the GP was calculated using extinction coefficient at 300 nm ($\epsilon_{300} \sim 9.0 \text{ mM}^{-1}\text{cm}^{-1}$) [92].

5. Purification of [Fe]-hydrogenase from *M. marburgensis*

Hmd purification was performed under strictly anaerobic condition. Frozen *M. marburgensis* cell (~100 g) was resuspended in the 200 mL of 50 mM potassium phosphate pH 7.0 and disrupted by sonication using Ultrasonic Homogenizer (Bandelin HD200) with MS76 tip in the sonication vessel in ice water. Sonication was performed at 50 % cycle for 8 min; the treatment was repeated 6 times with 7 min pause. The cell extract was ultracentrifuged with Ti45 rotor at 40,000 rpm for 40 min at 4 °C. Ammonia sulfate powder was added slowly into the supernatant to the final concentration of 2.5 M (60 % saturation) and the solution mixer was incubated with gentle stirring on ice for 20 min. Precipitated proteins were removed by centrifugation with JA-25.50 rotor at 20,000 rpm for 20 min at 4 °C. Hmd was precipitated by incubation for 20 min on ice with 3.7 M ammonium sulfate (90% saturation concentration). The

MATERIALS AND METHODS

mixture solution was centrifuged at 20,000 rpm for 20 min at 4 °C. The Hmd containing pellet was resuspended in 15 mL of 50 mM Mops/KOH pH 7.0 and dialyzed against 50 mM citric acid/NaOH pH 5.0 at 4 °C for 18 hours. Then the dialyzed protein solution was centrifuged at 20,000 rpm using Ti45 rotor (Thermo) for 20 min at 4 °C. The collected supernatant was loaded onto the column SOURCE 30Q equilibrated with 50 mM citric acid/NaOH pH 5.0. The column was washed with 250 mL equilibration buffer containing 200 mM NaCl to wash the contaminated protein. Hmd was eluted with linear gradient of NaCl from 200 mM to 500 mM in 500 mL buffer with the flow rate 7 mL/min⁻¹ and 10 mL fraction were collected. All fractions eluted at a protein peak around 300 mM NaCl were combined and neutralized by adding of 10 mL 1 M MOPS/KOH pH 7.0 and 0.6 mL 1 M NaOH to avoid Hmd precipitated. Then the fraction was concentrated to 15 mL using ultrafiltration (30 KDa cut off, Millipore). To remove the salt, the concentrated protein solution was loaded onto column Sephadex G-25 (HiPrep 26 × 10) equilibrated with water. Hmd was eluted before salt and the pooled fractions was concentrated, which stored at -80 °C. Protein concentration was measured using Bradford method using a dye reagent from Bio-Rad and bovine serum albumin as a standard [110].

6. Purification of HcgB and HcgC produced in *E. coli*.

M. maripaludis *hcgB* gene (MMP1497, GenBank accession number NP_988617.1) was expressed in *E. coli*. HcgB was purified under aerobic condition. The around 5-g frozen cells harvested from LB medium was suspended in 40 mL of 50 mM potassium phosphate pH7.0 containing 0.5 M KCl, 20 mM imidazole and and disrupted by sonication using Ultrasonic Homoginizer (Bandelin HD200) with MS76 tip in the sonication vessel in ice water. Sonication was performed at 50 % cycle for 1 min; the treatment was repeated 10 times with 1 min pause. The cell extract was centrifuged JA-25.50 rotor at 18,000 rpm for 40 min at 4 °C). The supernatant was loaded on the column HisTrap HP (5 mL, GE Healthcare) equilibrated with 50 mM potassium phosphate buffer pH 7.0. The column was washed with 25 ml of the equilibration buffer. The target protein was eluted with increasing concentration of imidazole from 20 mM to 500 mM in 60 mL buffer with flowrate 3 mL/min and

MATERIALS AND METHODS

5 mL fractions were collected. All fractions of the eluted protein were pooled and the protein solution was concentrated by 10 kDa cut off filter (Millipore).

The *hcgC* gene from *M. maripaludis* (MMP1498, GenBank accession number NP_988618.1) was heterologously produced in *E. coli* and the protein was purified as described for HcgB from *M. maripaludis*.

The *hcgC* gene from *M. jannaschii* (MJ0489, GenBank accession number NP_247465) and *M. maripaludis* (MMP1498, GenBank accession number NP_988618.1) were expressed in *E. coli*. Purification of HcgC from *M. jannaschii* was performed under aerobic condition. The frozen cell was resuspended in 50 mM potassium phosphate buffer (pH 7.0) containing 0.5 M NaCl and disrupted by sonication as described above. The supernatant of cell extract was collected by centrifugation with JA-25.50 rotor at 18,000 rpm for 40 min and at 4 °C and the supernatant was incubated in water at 80 °C for 20 min. The heat-treated solution in 50-ml tube was centrifuged with Thermo Megafuge 16 at 4500 rpm for 15 min at 4 °C. Ammonia sulfate was added into the supernatant to the final concentration of 1 M. The solution was filtered using 0.45 µm filter and loaded onto column HiTrap Buty-S Fast Flow (5 ml, GE Healthcare), which equilibrated with 50 mM potassium phosphate buffer pH 7.0 containing 1 M ammonia sulfate. The column was washed with at least 10 column volumes of buffer. HcgC was eluted with a stepwise gradient of ammonium sulfate from 1 M to 0 M with the flow rate 3 mL/min and 5-mL fractions were collected. The HcgC fractions were pooled, concentrated by 10-kDa cut off filter (Millipore) and loaded onto HiPrep Sephacryl S-200 column (GE Healthcare) equilibrated with 50 mM potassium phosphate buffer pH 7.0 containing 0.3 M KCl. HcgC were eluted as two peaks; the second fraction was used for further experiments. The HcgC concentration was determined using the Bradford method.

7. Production and purification of HcgA and HcgG in *E. coli*

HcgA from different methanogens were expressed in *E. coli*. These organisms were *Methanopyrus kandleri*, *Methanotorris igneus*, *Methanocaldococcus fervens*, *Methanocaldococcus infernus* and *Desulfurobacterium thermolithotrophum*. Purification of HcgA was performed

MATERIALS AND METHODS

under the anaerobic condition. Frozen cell (~4.5 g) was resuspended in the 20 mM Tris/HCl pH 8.0, 0.5 M NaCl (buffer A) and 20 mM imidazole and disrupted by sonication as described above for the purification of HcgB and HcgC. The HcgA proteins were purified using HisTrap HP (5 mL, GE Healthcare) column equilibrated with buffer A. The HcgA proteins were eluted with increasing concentration of imidazole from 20 mM to 500 mM in 60 mL buffer with flowrate 3 mL/min and 5 mL fractions were collected. The HcgC fractions were pooled, concentrated by 10-kDa cut off filter (Millipore) and loaded onto HiPrep Sephacryl S-200 column (GE Healthcare) equilibrated with 20 mM Tris/HCL pH 8.0. The HcgA concentration was determined using the Bradford method.

The iron concentration was measured by the colorimetric method using iron chelator 3-(2-Pyridyl)-5,6-di(2-furyl)-1,2,4-triazine-5',5''-disulfonic acid disodium salt (Ferene) [111]. Purified protein (50 μ L) was acidified by 1 % HCl (final concentration) and incubated at 80 °C for 20 min. Freshly prepared 50- μ L 0.1 M ascorbic acid was added into the protein solution after cooling. The protein was treated with 25 μ L of 10 % SDS. Finally, 25- μ L of 25 mM Ferene was added into the solution. The UV-Vis spectrum analyzed.

8. Enzyme activity assay

8.1 [Fe]-hydrogenase activity

[Fe]-hydrogenase activity was determined under strictly anaerobic condition. The standard 0.7-mL reaction-solution containing 120 mM potassium phosphate pH 6.0, 1 mM EDTA and 20 μ M methylene- H_4 MPT under 100 % N_2 gas phase in 1 mL quartz cuvettes (1 cm light pass), was incubated at 40 °C for 5 min. The reaction was started by the addition of 10- μ L of Hmd enzyme solution. The rate of reaction was determined by following the increase of methenyl- H_4 MPT⁺ at absorbance of 336 nm [104].

8.2. HcgB activity

HcgB activity was determined by high-performance liquid chromatography (HPLC). The reaction solution, containing 10 mM Mops/KOH pH 7.0, 1 mM $MgCl_2$, 1 mM GTP, 1 mM pyridinol and 1 μ M HcgB, was incubated on 37 °C

MATERIALS AND METHODS

for different time. The reaction solution was filtered by 0.2 μm filter (Millipore) and then loaded onto HPLC column Synergi 4 μ Polar-RP 80A (Phenomenex) equilibrated with 5 mM ammonia formate pH 5.0. HPLC peak was monitored at 262 nm. The amount of product was calculated using the area of product based on the standard product curve which purified product. The reaction product was analyzed by Matrix-assisted laser-desorption/ionization time-of-flight mass spectrometry (MALDI-TOF-MS) using positive mode.

8.3. HcgC activity

HcgC reaction product was analyzed by HPLC. The reaction solution, containing 10 mM Mops/KOH pH 7.0, 1 mM SAM, 1mM pyridinol and 1 μM HcgC, was incubated on 37 $^{\circ}\text{C}$ for different reaction time. The product was loaded onto the column Synergi 4 μ Polar-RP 80A (Phenomenex) equilibrated with $\text{H}_2\text{O}/\text{HCl}$ pH 4.0 after filtered by 0.2 mm filter. The product was eluted with increasing linear gradient from 0–100 % methanol in 12.5 mL. The substrate and product were eluted at the 76 % and 80 % methanol concentrations, respectively. The enzyme activity was calculated based on the peak area of absorbance 288 nm.

9. Crystallization and structural analysis

Purified HcgC, which dissolved in potassium phosphate buffer, was diluted in the 10 mM MOPS/KOH pH 7.0 and concentrated. This dilution process was repeated several times to exchange the buffer. Crystallization was performed under 8 $^{\circ}\text{C}$ using Sitting Drop Vapor Diffusion method. Reservoir solution from crystal screening kit (JBScreen series and QIAGEN JCSG series) was added into the crystal plate (Jena Bioscience, 96 well or 24 well). Protein solution, containing ~ 5 mg/mL HcgC, 2 mM SAM or SAH, 2 mM pyridinol, was mixed with reservoir at the ratio of 1:1. The crystal grown under 8 $^{\circ}\text{C}$. The first hits were obtained in a reservoir solution containing 100 mM Tris/HCl pH 8.5, 40% polyethylene glycol (PEG) 400 and 200 mM lithium sulfate (LiSO_4) or 100 mM HEPES/NaOH pH 7.5, 0.2 M NaCl, and 35% MPD (2-Methyl-2,4-pentanediol) within several weeks. The cocrystallized HcgC with SAM and pyridinol crystals

MATERIALS AND METHODS

come from a crystallization solution containing 50% v/v PEG 400, 100 mM NaAcetate pH 4.5, 200 mM LiSO₄ and the cocrystallized HcgC with SAH and pyridinol crystal comes from a crystallization solution containing 40% v/v PEG 400, 100 mM Tris/HCl pH 8.5 and 200 mM LiSO₄. The freshly fished crystals (growth after 4 days and immediately fished) from a SAH and pyridinol cocrystallization appeared in 100 mM HEPES/NaOH pH 7.0, 0.1 M NaCl, and 30% MPD. The crystals of HcgC apoenzyme were obtained from a solution containing 100 mM HEPES/NaOH pH 7.5, 0.1 M NaCl, and 33% MPD. The apoenzyme crystals were soaked overnight in the same crystallization solution which contained additionally 2 mM SAH and 3 mM pyridinol.

The crystals were cryo-protected by soaking with 30 % glycerol (v/v) in the crystallization solution for 3-5 seconds. The diffraction experiments were performed at 100 K on beamline X10SA equipped with a PILATUS 6M detector at the Swiss Light Source (Villigen, Switzerland). The data was processed with XDS [112] and scaled with SCALA from the ccp4 suite [113]. The structure was solved using template of HcgC from *M. jannaschii* in complex with SAM (PDB: 2JJF) with PHASER [114]. The model was manually constructed with COOT [115] and refined by PHENIX [114]. The final model was validated by using the MolProbity server (<http://molprobity.biochem.duke.edu>) [116]. Figures for the protein structures were made using PyMOL program.

RESULTS/PUBLICATIONS

1. Identification of HcgC as a SAM-dependent pyridinol methyltransferase in [Fe]-hydrogenase cofactor biosynthesis.

Function of HcgC was elucidated by structure to function analysis. This section was published as an original paper in *Angewandte Chemie International Edition*. The paper is presented in this section.

2. Towards artificial methanogenesis: biosynthesis of the [Fe]-hydrogenase cofactor and characterization of the semi-synthetic hydrogenase.

The reaction sequence of HcgB and HcgC was determined by the HcgB-pyridinol complex structure and enzyme assay of HcgC. This section was published as an original paper in *Faraday Discussion*. The paper is presented in this section.

3. Water-bridged H-bonding network contributes to the catalysis of a SAM-dependent C-methyltransferase HcgC.

A catalytic mechanism of HcgC was proposed based on the co-crystal structure of HcgC with SAH and the pyridinol substrate, and the mutation analysis. This part was submitted for publication as an original paper.

4. The growth phenotype of the Δhcg mutants of *M. maripaludis*.

The *hcgB* and *hcgC* deletion mutants did not reveal the Hmd activity, which confirmed importance of the genes in biosynthesis of the FeGP cofactor. The growth phenotype of the Δhcg mutants are discussed.

5. Heterologous production of HcgA and HcgG genes in *E. coli*.

HcgA and HcgG were heterologously over produced in *E. coli*. HcgA was purified as soluble protein and this enzyme appeared to contain iron-sulfur cluster. Crystallization of HcgA was tested. HcgG formed inclusion body.

6. The FeGP cofactor from *M. maripaludis* and its precursors.

Structure of the FeGP cofactor from *M. maripaludis* was estimated based on the structural analysis of the FeGP cofactor from *M. jannaschii* and comparison between the crystal structures of HcgB and HcgC from *M. maripaludis* and *M. jannaschii*.

Biosynthesis

International Edition: DOI: 10.1002/anie.201604352
German Edition: DOI: 10.1002/ange.201604352

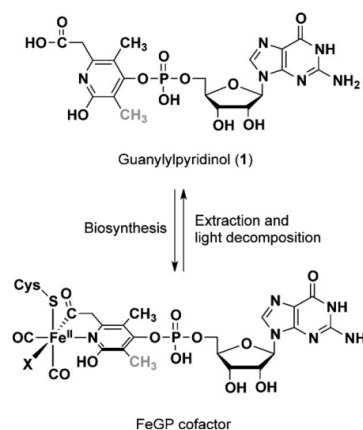
Identification of HcgC as a SAM-Dependent Pyridinol Methyltransferase in [Fe]-Hydrogenase Cofactor Biosynthesis

Takashi Fujishiro[†], Liping Bai[†], Tao Xu, Xiulan Xie, Michael Schick, Jörg Kahnt, Michael Rother, Xile Hu, Ulrich Ermler, and Seigo Shima*

Abstract: Previous retrosynthetic and isotope-labeling studies have indicated that biosynthesis of the iron guanylylpyridinol (FeGP) cofactor of [Fe]-hydrogenase requires a methyltransferase. This hypothetical enzyme covalently attaches the methyl group at the 3-position of the pyridinol ring. We describe the identification of HcgC, a gene product of the *hcgA-G* cluster responsible for FeGP cofactor biosynthesis. It acts as an *S*-adenosylmethionine (SAM)-dependent methyltransferase, based on the crystal structures of HcgC and the HcgC/SAM and HcgC/*S*-adenosylhomocysteine (SAH) complexes. The pyridinol substrate, 6-carboxymethyl-5-methyl-4-hydroxy-2-pyridinol, was predicted based on properties of the conserved binding pocket and substrate docking simulations. For verification, the assumed substrate was synthesized and used in a kinetic assay. Mass spectrometry and NMR analysis revealed 6-carboxymethyl-3,5-dimethyl-4-hydroxy-2-pyridinol as the reaction product, which confirmed the function of HcgC.

Nature has developed three major types of hydrogenases, which use unique metal-containing cofactors to cleave and/or form H₂.^[1] [Fe]-hydrogenases hydrogenate methenyltetrahydromethanopterin to methylenetetrahydromethanopterin

within the methanogenic pathway of many methanogenic archaea.^[2] This enzyme contains an iron guanylylpyridinol (FeGP) cofactor as a prosthetic group. The Fe center, which activates inert H₂, consists of a single iron atom coordinated by two CO molecules, a cysteine residue, one solvent molecule, a pyridinol nitrogen, and the acyl carbon of the 6-substituent of pyridinol (Scheme 1).^[3] The solvent-binding site is postulated to be the H₂-binding site. Owing to several



Scheme 1. Structures of guanylylpyridinol **1** and the iron guanylylpyridinol (FeGP) cofactor of [Fe]-hydrogenase (X = solvent). Compound **1** is both the decomposition product of FeGP upon irradiation and most likely a genuine intermediate of the FeGP biosynthetic pathway. The 3-methyl group (shown in gray) of the pyridinol moiety is biosynthesized through a methyltransferase reaction.^[8]

unique structural features, namely the two CO ligands, the acyl-iron bond, GMP-pyridinol conjugation, and the methyl substituents at the pyridinol ring, its biosynthesis is a chemically challenging process that is of great scientific and biotechnological interest.

The FeGP cofactor biosynthesis enzymes are encoded by at least seven conserved genes (*hcgA-G*) that co-occur with *hmd* (the gene for [Fe]-hydrogenase).^[2b] A previous analysis of the growth of *hcgA-G* knockout mutants of *Methanococcus maripaludis* indicated a relationship between these genes and biosynthesis of the FeGP cofactor.^[4] Based on recent structure-to-function studies, HcgB was annotated as a guanylyltransferase that catalyzes the reaction between GTP and 2,4-dihydroxypyridines, most likely to afford guanylylpyridinol **1** (Scheme 1).^[5] Interestingly, guanylylpyridinol **1**, an intermediate in the FeGP cofactor biosynthetic pathway, can be also obtained as a decomposition product of the FeGP

[*] Dr. T. Fujishiro,^[†] L. Bai,^[†] Dr. M. Schick, J. Kahnt, Dr. S. Shima
Max-Planck-Institut für terrestrische Mikrobiologie
Karl-von-Frisch-Straße 10, 35043 Marburg (Germany)
E-mail: shima@mpi-marburg.mpg.de

Dr. T. Xu, Prof. Dr. X. Hu
Institute of Chemical Science and Engineering
Ecole Polytechnique Fédérale de Lausanne (EPFL)
ISIC-LSCI, BCH 3305, 1015 Lausanne (Switzerland)

Dr. X. Xie
Department of Chemistry, Philipps Universität Marburg
Hans-Meerwein-Straße, 35032 Marburg (Germany)

Prof. Dr. M. Rother
Institut für Mikrobiologie, Technische Universität Dresden
01062 Dresden (Germany)

Dr. U. Ermler
Max-Planck-Institut für Biophysik
Max-von-Laue-Straße 3, 60438 Frankfurt/Main (Germany)

Dr. S. Shima
PRESTO, Japan, Science and Technology Agency, JST
Saitama 332-0012 (Japan)

Dr. T. Fujishiro^[†]
Present address: Department of Biochemistry and Molecular Biology
Graduate School of Science and Engineering, Saitama University
Shimo-ohkubo 255, Sakura-ku, Saitama, 338-8570 (Japan)

[†] These authors contributed equally to this work.

Supporting information for this article (including experimental details, sequences, structures, and PDB codes) can be found under <http://dx.doi.org/10.1002/anie.201604352>.

cofactor upon irradiation with UV-A/blue light. Through this process, its acyl group is hydrolyzed to a carboxy group (Scheme 1).^[3c,f] The activation of the carboxy group during FeGP cofactor biosynthesis is carried out by HcgE and HcgF. HcgE was identified as an adenylyltransferase that adenylylates the 6-carboxy group of **1**. A subsequent transesterification reaction is catalyzed by HcgF by using an inherent cysteine that forms a thioester bond with **1**. The thioester is proposed to be a direct precursor of acyl–iron bond biosynthesis.^[6] For HcgD, a function as an iron-trafficking protein was proposed.^[7] The functions of HcgA, HcgC, and HcgG are unknown.

Stable-isotope labeling studies of the FeGP cofactor revealed that the 5-methyl group of the pyridinol moiety originates from C2 of acetate, and the 3-methyl group from the methyl group of methionine.^[8] Therefore, we assume the 3-methylation to be catalyzed by an *S*-adenosylmethionine (SAM)-dependent methyltransferase. Several SAM-dependent methyltransferases have already been biochemically characterized and their participation in vital biological processes such as regulation and cofactor biosynthesis demonstrated.^[9]

In this report, we predicted HcgC as the SAM-binding methyltransferase, primarily based on structural data. Subsequently, the HcgC-catalyzed reaction was verified using the predicted pyridinol substrate, which was chemically synthesized.

Targeted *hcgC* and *hcgB* knockout mutants in *M. maripaludis* were constructed (see the Supporting Information) to investigate the physiological effect of their gene products. No Hmd activity was detectable in strains lacking either *hcgB* or *hcgC* (Tables S1, S2, and S3, and Figure S1 in the Supporting Information), which demonstrates their participation in the biosynthesis of the FeGP cofactor and that they cannot be substituted by other genes.

On the basis of these results, we applied a structure-to-function strategy for annotating HcgC. We started the project with the determination of the crystal structure of HcgC (MJ0489) from *Methanocaldococcus jannaschii* at 2.7 Å resolution (Figure 1, Table S4, and Figure S2). HcgC was found in the crystalline state as a homotetramer, but was dominantly found as a homodimer in solution (data not shown). The monomers are composed of a Rossmann-like coenzyme-binding domain (31–190; 256–267), made of six parallel and one peripheral antiparallel strand, which is flanked by six α -helices and a smaller α/β domain (1–30; 191–255) termed the interface domain due to its extended contact with the partner monomer (Figure 1 a). According to the Dali server,^[10] the coenzyme-binding domain is structurally most similar to those of NAD(P)H-dependent oxidoreductases^[11] (e.g., shikimate dehydrogenase AroE; PDB ID: 2HK9)^[12] and SAM-dependent methyltransferases (e.g., 5-methyluridine methyltransferase RumA, PDB ID: 2BH2;^[13] Figure S3). This relationship allows us to suggest HcgC as a binding protein for an adenosine moiety of either NAD(P)⁺ or SAM; this prediction would be impossible to obtain on the basis of a primary structure comparison although HcgC revealed partial sequence identity to genes annotated as RNA methyltransferases. To obtain further information about its

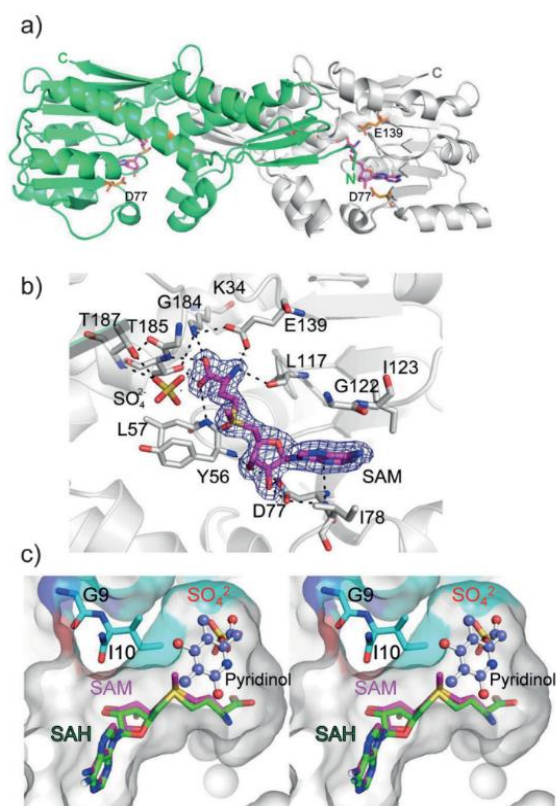


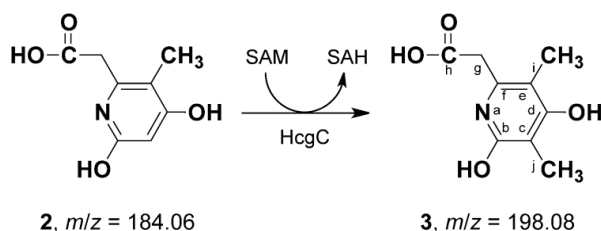
Figure 1. Structural information for HcgC. a) The overall fold of the HcgC homodimer. The monomers (green, gray) are composed of a larger coenzyme-binding domain and a smaller interface domain. Since the N-terminal residues of the partner monomers contribute to the methyl acceptor binding site, the dimer is considered as the functional unit. In the cocrystal structure, one *S*-adenosylmethionine (SAM) molecule (magenta stick model) is bound per monomer. The N and C termini and some important residues are indicated (carbon atoms shown in orange). b) The SAM-binding site. The 2F_o-F_c electron density (blue mesh) for SAM was contoured at 1 σ . Polar interactions are shown as dashed lines. c) Structure model of the HcgC/SAH/pyridinol **3** complex in stereoview. The orientation/position of pyridinol **3** (ball-and-stick model) was determined by docking calculations inside a properly sized/shaped pocket; SAH (green) and the superimposed SAM (magenta) are shown as stick models.

ligand-binding capabilities, HcgC was co-crystallized either with NAD⁺, NADP⁺, or SAM and subsequently structurally characterized. Extra electron density was only detectable for SAM, which could be reliably modeled at the expected position in front of the C-terminal loops of three parallel β -strands of the coenzyme-binding domain (Figure 1 a,b). SAM is embedded into a precisely tailored pocket and both the methionine and adenosine moieties are fixed by conserved residues, thus suggesting SAM as the natural substrate of HcgC. For example, the amino and carboxy groups of the methionine moiety are hydrogen-bonded to Lys34, Glu139, and Thr185. The two ribose-OH groups of the adenosine moiety interact with the invariant residue Asp77 (Figure 1 b and Figure S4). Furthermore, SAM binding induces specific conformational changes to encapsulate the active site. We

assume that the mentioned SAM–polypeptide interactions fix segment 79–92, which was disordered in the empty HcgC structure but is clearly visible partly as an α -helix in structure of the HcgC/SAM complex. More precisely, the flexible two-helix extension of the interface domain moves towards segment 79–92, thereby resulting in mutual stabilization by multiple mostly hydrophobic interactions and in closure of the cleft between them. As a result, SAM becomes partially shielded (Figure S2). Moreover, the absence of the cysteine-rich CX3CX2C motif that is characteristic of radical SAM enzymes that bind a [4Fe-4S] cluster^[14] rules out HcgC as a radical-SAM enzyme, which might be required in the FeGP biosynthetic pathway for formation of the CO ligand^[15] or heterocyclic ring formation.^[16] These findings strongly argue for HcgC as a SAM-dependent methyltransferase.

Methyl transfer normally proceeds through an S_N2 -type mechanism, which implies a binding site for the methyl-accepting atom in van der Waals contact with the methyl group of SAM. Indeed, a deep but solvent-exposed pocket occupied by a putative sulfate ion and several firmly bound water molecules was identified directly beside the SAM-binding site (Figure 1b). To gain information about the nature of the methyl acceptor and thus the function of the SAM-dependent methyltransferase, we also determined a crystal structure of HcgC soaked with SAH and the artificial guanylylpyridinol at 1.6 Å resolution (Figure S5 and Table S4). SAH binds equivalently into the same SAM-binding site of HcgC, and triggers the same induced-fit movement (Figure 1c and Figure S5), which supports HcgC as SAM-dependent methyltransferase. Unprecedentedly, the conserved residues 9–11 of the partner subunit, which are disordered in the previous structures, become rigid. The empty binding site for the methyl acceptor is thereby shrunk to a size which contains space for pyridinol but not for the larger guanylylpyridinol. Notably, the artificial guanylylpyridinol was partly visible at the interdimer interface of the HcgC tetramer, but this binding site is presumably not functionally relevant (Figure S5).

Docking simulations^[17] of the possible 3-methylated product **3** (Scheme 2) into the decreased methyl acceptor binding site of SAH-bound HcgC resulted in a reasonable geometry between the 3-methyl group of pyridinol **3** and the SAH sulfur atom. Their distance of 3.8 Å is in the range to realize methyl transfer between **2** and SAM by HcgC



Scheme 2. The proposed SAM-dependent methylation catalyzed by HcgC. Pyridinol **3** is subsequently conjugated to the GMP moiety in a reaction catalyzed by HcgB. The pyridinols appear to be present as pyridone and pyridinol tautomeric forms in dimethyl sulfoxide and water, respectively.

(Figure 1c). Moreover, the carboxy group of pyridinol **3** is placed onto the putative sulfate-binding site of the superimposed HcgC/SAM complex structure, thus supporting the validity of the calculation. In conclusion, the size and hydrophobic profile of the postulated binding pocket in HcgC suggests that the 3-methyl group is introduced at the pyridinol stage. Although co-crystallization experiments with SAH and **3** have so far been unsuccessful, the results of the structure-to-function approach confidently suggest HcgC as a novel SAM-dependent methyltransferase, and all of the data are consistent with pyridinol **2** as the methyl acceptor (Scheme 2).

To confirm the predicted HcgC reaction, we synthesized pyridinol **2** ($m/z = 184.06$) through carboxylation of 5,6-dimethylpyridine-2,4-diol (for details, see the Supporting Information and Figure S6). Matrix-assisted laser desorption/ionization mass spectrometry (MALDI-TOF-MS) analysis of the HcgC enzyme assay indicated conversion of substrate **2** into a 14 m/z larger species (**3**; Figure 2a). Species **3** was not formed in the absence of HcgC. The attachment of one methyl group to **2** through a catalytic reaction is thus definitively confirmed. The HcgC reaction product contained three protons that are exchangeable with deuterons according to MALDI-TOF-MS data (Figure S7), which is in agreement with the chemical structure of **3**. The HcgC product **3** was also indirectly verified by its further reaction to give guanylylpyridinol **1** in the presence of GTP and HcgB, the enzyme that catalyzes the subsequent step in the FeGP cofactor biosynthetic pathway (Figure S8). The ¹H-¹³C HMBC NMR spectrum of the HcgC product showed additional cross-peaks from the methyl protons at 1.9 ppm to C(b) (162 ppm), C(c) (105 ppm) and C(d) (163 ppm; Figure S9), which specified

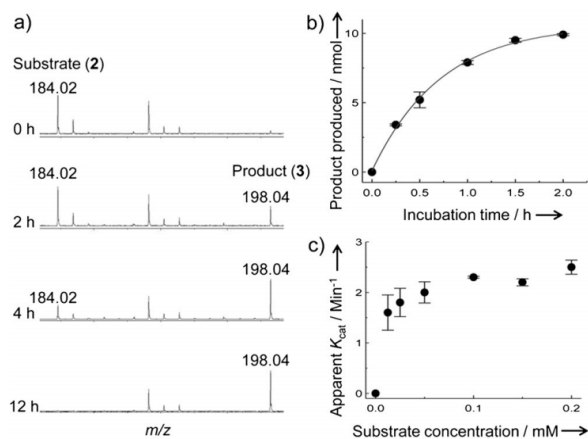


Figure 2. Kinetic analysis of the HcgC reaction. a) Conversion of the substrate (**2**, $m/z = 184$) into the methylated product (**3**, $m/z = 198$) by HcgC. The reaction mixture was incubated at 37 °C for defined periods in the presence of 0.4 mM **2** and then analyzed by MALDI-TOF-MS. Peaks from the matrix observed at the $m/z = 190$ region are not changed during the reaction. b) The time dependency of the production of **3** in the presence of 0.1 mM **2**, which was determined by HPLC. c) The dependency of the HcgC-catalyzed reaction on the substrate concentration. The error bar indicates standard deviation for duplicate measurements.

methylation in the 3-position [C(c)] of pyridinol **2**. The HcgC reaction was kinetically characterized through determination of the product concentration by HPLC (Figure 2b,c and Figure S10). The apparent k_{cat} was 2.5 min^{-1} .

In conclusion, this powerful structure-to-function approach provided us with sound information to postulate HcgC as a SAM-dependent methyltransferase and pyridinol **2** as the most likely methyl acceptor. On this basis, the assumed substrate was chemically synthesized. The predicted methyl transfer to the 3-position of pyridinol **2** as catalyzed by HcgC was demonstrated by product analysis.

Acknowledgements

We thank Prof. Dr. Rolf Thauer for discussions and helpful suggestions; Prof. Dr. Hartmut Michel for continuous support; the staff of the PXII beamline at the Swiss-Light-Source, Villigen, and the staff of the beamline proxima 1 and proxima 2A at the SOLEIL synchrotron, Paris for help during data collection; and Ulrike Demmer for technical assistance. We also thank Dr. Haruka Tamura for construction of the HcgC expression system, and Kerstin Yacoub for assistance with mutant generation. This work was supported by a grant from the Max Planck Society to R. K. Thauer, a grant from the PRESTO program of the Japan Science and Technology Agency to S.S. and a grant from the Swiss National Science Foundation to X.H. (200020_152850/1).

Keywords: cofactors · enzymes · hydrogenases · methyltransferases · protein structures

How to cite: *Angew. Chem. Int. Ed.* **2016**, *55*, 9648–9651
Angew. Chem. **2016**, *128*, 9800–9803

- [1] a) W. Lubitz, H. Ogata, O. Rüdiger, E. Reijerse, *Chem. Rev.* **2014**, *114*, 4081–4148; b) J. C. Fontecilla-Camps, A. Volbeda, C. Cavazza, Y. Nicolet, *Chem. Rev.* **2007**, *107*, 4273–4303; c) P. M. Vignais, B. Billoud, *Chem. Rev.* **2007**, *107*, 4206–4272.
- [2] a) S. Shima, U. Ermler, *Eur. J. Inorg. Chem.* **2011**, 963–972; b) R. K. Thauer, A. K. Kaster, M. Goenrich, M. Schick, T. Hiromoto, S. Shima, *Annu. Rev. Biochem.* **2010**, *79*, 507–536; c) H. Tamura, M. Salomone-Stagni, T. Fujishiro, E. Warkentin, W. Meyer-Klaucke, U. Ermler, S. Shima, *Angew. Chem. Int. Ed.* **2013**, *52*, 9656–9659; *Angew. Chem.* **2013**, *125*, 9838–9841; d) T. Hiromoto, E. Warkentin, J. Moll, U. Ermler, S. Shima, *Angew. Chem. Int. Ed.* **2009**, *48*, 6457–6460; *Angew. Chem.* **2009**, *121*, 6579–6582; e) S. Shima, S. Vogt, A. Göbels, E. Bill, *Angew. Chem. Int. Ed.* **2010**, *49*, 9917–9921; *Angew. Chem.* **2010**, *122*, 10113–10117; f) R. Hidese, K. Ataka, E. Bill, S. Shima, *ChemBioChem* **2015**, *16*, 1861–1865.
- [3] a) E. J. Lyon, S. Shima, R. Boecher, R. K. Thauer, F. W. Grevels, E. Bill, W. Roseboom, S. P. J. Albracht, *J. Am. Chem. Soc.* **2004**, *126*, 14239–14248; b) S. Shima, E. J. Lyon, R. K. Thauer, B. Mienert, E. Bill, *J. Am. Chem. Soc.* **2005**, *127*, 10430–10435; c) S. Shima, O. Pilak, S. Vogt, M. Schick, M. S. Stagni, W. Meyer-Klaucke, E. Warkentin, R. K. Thauer, U. Ermler, *Science* **2008**, *321*, 572–575; d) T. Hiromoto, K. Ataka, O. Pilak, S. Vogt, M. S. Stagni, W. Meyer-Klaucke, E. Warkentin, R. K. Thauer, S. Shima, U. Ermler, *FEBS Lett.* **2009**, *583*, 585–590; e) S. Shima, M. Schick, J. Kahnt, K. Ataka, K. Steinbach, U. Linne, *Dalton Trans.* **2012**, *41*, 767–771; f) S. Shima, E. J. Lyon, M. S. Sordel-Klippert, M. Kauss, J. Kahnt, R. K. Thauer, K. Steinbach, X. L. Xie, L. Verdier, C. Griesinger, *Angew. Chem. Int. Ed.* **2004**, *43*, 2547–2551; *Angew. Chem.* **2004**, *116*, 2601–2605.
- [4] T. J. Lie, K. C. Costa, D. Pak, V. Sakesan, J. A. Leigh, *FEMS Microbiol. Lett.* **2013**, *343*, 156–160.
- [5] T. Fujishiro, H. Tamura, M. Schick, J. Kahnt, X. L. Xie, U. Ermler, S. Shima, *Angew. Chem. Int. Ed.* **2013**, *52*, 12555–12558; *Angew. Chem.* **2013**, *125*, 12787–12790.
- [6] T. Fujishiro, J. Kahnt, U. Ermler, S. Shima, *Nat. Commun.* **2015**, *6*, 6895.
- [7] T. Fujishiro, U. Ermler, S. Shima, *FEBS Lett.* **2014**, *588*, 2789–2793.
- [8] M. Schick, X. L. Xie, K. Ataka, J. Kahnt, U. Linne, S. Shima, *J. Am. Chem. Soc.* **2012**, *134*, 3271–3280.
- [9] a) P. Z. Kozbial, A. R. Mushegian, *BMC Struct. Biol.* **2005**, *5*, 19; b) H. L. Schubert, R. M. Blumenthal, X. D. Cheng, *Trends Biochem. Sci.* **2003**, *28*, 329–335; c) A. W. Struck, M. L. Thompson, L. S. Wong, J. Micklefield, *ChemBioChem* **2012**, *13*, 2642–2655.
- [10] L. Holm, S. Kääriäinen, P. Rosenstrom, A. Schenkel, *Bioinformatics* **2008**, *24*, 2780–2781.
- [11] A. M. Lesk, *Curr. Opin. Struct. Biol.* **1995**, *5*, 775–783.
- [12] J. H. Gan, Y. Wu, P. Prabakaran, Y. Gu, Y. Li, M. Andrykovitch, H. H. Liu, Y. C. Gong, H. G. Yan, X. H. Ji, *Biochemistry* **2007**, *46*, 9513–9522.
- [13] T. T. Lee, S. Agarwalla, R. M. Stroud, *Cell* **2005**, *120*, 599–611.
- [14] P. A. Frey, A. D. Hegeman, F. J. Ruzicka, *Crit. Rev. Biochem. Mol. Biol.* **2008**, *43*, 63–88.
- [15] P. Dinis, D. L. M. Suess, S. J. Fox, J. E. Harmer, R. C. Driesener, L. De La Paz, J. R. Swartz, J. W. Essex, R. D. Britt, P. L. Roach, *Proc. Natl. Acad. Sci. USA* **2015**, *112*, 1362–1367.
- [16] A. P. Mehta, S. H. Abdelwahed, N. Mahanta, D. Fedoseyenko, B. Philmus, L. E. Cooper, Y. Liu, I. Jhulki, S. E. Ealick, T. P. Begley, *J. Biol. Chem.* **2015**, *290*, 3980–3986.
- [17] O. Trott, A. J. Olson, *J. Comput. Chem.* **2010**, *31*, 455–461.

Received: May 4, 2016

Published online: July 8, 2016



Supporting Information

Identification of HcgC as a SAM-Dependent Pyridinol Methyltransferase in [Fe]-Hydrogenase Cofactor Biosynthesis

*Takashi Fujishiro⁺, Liping Bai⁺, Tao Xu, Xiulan Xie, Michael Schick, Jörg Kahnt, Michael Rother, Xile Hu, Ulrich Ermler, and Seigo Shima**

anie_201604352_sm_miscellaneous_information.pdf

RESULTS/PUBLICATIONS

Supporting Information**Materials and methods**

Figure S1. Confirmation of the *hcgB* and *hcgC* deletions in *M. maripaludis*

Figure S2. Crystal structure of HcgC from *M. jannaschii*

Figure S3. Structural comparison between the Rossmann-like domains of HcgC with its structural homologues

Figure S4. Amino acid sequence alignments of HcgC from *Methanocaldococcus jannaschii*, *Methanothermobacter marburgensis*, *Methanopyrus kandleri*, *Methanococcus maripaludis*, *Methanobrevibacter smithii*, and *Methanocorpusculum labreanum*

Figure S5. Crystal structure of S-adenosylhomocysteine (SAH)- and (3,6-dimethyl-2-pyridinol)-GMP (artificial guanylylpyridinol)-bound HcgC

Figure S6. Chemical synthesis of pyridone **2** and product analysis by NMR data

Figure S7. D₂O exchange experiment of the HcgC product (pyridinol **3**)

Figure S8. HcgB enzyme assay using the pyridinol **3** produced by the HcgC reaction as substrate

Figure S9. Two dimensional ¹H–¹³C–HMBC correlation NMR spectrum of the substrate and product of the HcgC catalyzed reaction in dimethyl sulfoxid-d₆ at 300 K highlighting the connectivity within the pyridone ring

Figure S10. HPLC analysis of the HcgC reaction assay

Table S1. Plasmid for site-directed mutagenesis of *Methanococcus maripaludis*

Table S2. *Methanococcus maripaludis* strains used in this study

Table S3. Hmd activity of the cell extract from the *M. maripaludis* strains

Table S4. Data collection and refinement statistics of HcgC structures

References for Supplementary information

RESULTS/PUBLICATIONS

Materials and methods

Materials

All commercially available chemicals were used without further purification. PEG8000, PEG300, pentaerythritol propoxylate 5/4 PO/OH (PEP426), ethylene glycol, sodium cacodylate trihydrate, magnesium acetate tetrahydrate, sodium hydroxide, potassium hydroxide, *S*-(5'-adenosyl)-*L*-methionine (SAM) chloride dihydrochloride, *S*-(5'-adenosyl)-*L*-homocysteine (SAH) and 3,6-dimethyl-4-hydroxy-2-pyridinol were purchased from Sigma-Aldrich. Magnesium chloride, thiamine, lithium sulfate and magnesium chloride were purchased from Merck. *L*-(+)-Selenomethionine (SeMet) was purchased from Acros Organics. The following reagents were obtained from Roth: methanol, ethanol, kanamycin sulfate, 3-(*N*-morpholino)propanesulfonic acid (MOPS), 3-(Cyclohexylamino)-1-propanesulfonic acid (CAPS), 4-(2-hydroxyethyl)piperazine-1-ethanesulfonic acid (HEPES), hydrochloric acid, potassium chloride, potassium dihydrogen phosphate, dipotassium hydrogen phosphate, ammonium chloride, ammonium sulfate, *L*-(+)-methionine, sodium chloride, sodium dihydrogen phosphate, disodium hydrogen phosphate, hydrochloric acid, potassium chloride, potassium dihydrogen phosphate, dipotassium hydrogen phosphate, tris(hydroxymethyl)amino ethane (Tris), dithiothreitol (DTT), *D*-(+)-glucose, $\text{FeCl}_3 \cdot 6\text{H}_2\text{O}$. Isopropyl β -*D*-thiogalactopyranoside (IPTG) was purchased from Fermentas.

The light decomposition product **1** was prepared from the FeGP cofactor extracted from [Fe]-hydrogenase (Hmd) from *Methanothermobacter marburgensis*^[1]. For co-crystallization, pyridinol **3**, [6-Carboxymethyl-3,5-dimethyl-4-hydroxyl-2-pyridinol] was prepared by cleavage of **1** with phosphodiesterase I from *Crotalus atrox* (Sigma-Aldrich), followed by purification with a JASCO HPLC system in the same conditions as reported previously^[1]. (3,6-Dimethyl-4-hydroxy-2-pyridinol)-GMP-conjugate was prepared by HcgB-catalyzed reaction using GTP and 3,6-dimethyl-4-hydroxyl-2-pyridinol^[2]. Methenyl-tetrahydromethanopterin (methenyl- H_4MPT^+) and methylene-tetrahydromethanopterin (methylene- H_4MPT) were prepared from *M. marburgensis* as described previously^[3].

Construction of an expression system for HcgC

The *Methanocaldococcus jannaschii*hcgC gene (MJ0489, GenBank accession number NP_247465) was amplified by PCR from genomic DNA of *M. jannaschii* strain DSM2661 using as forward primer

5'GGCATATGGGGTGTGGAATTATGAAGTATGGAATAACTG-3' and as reverse primer 5'- CCCTCGAGTTAAAGCTCCTCAACAAAAGAATAGATGAG-3' to generate *Nde*I and

RESULTS/PUBLICATIONS

XhoI restriction sites (underlined). The PCR product was cloned into the pCR-Blunt vector using T4 DNA ligase (Invitrogen). The cloned *M. jannaschiihcgC* gene was inserted into expression vector pET24b(+) (Novagen) at *NdeI* and *XhoI* restriction sites and the generated expression vector was used for transformation of the *E. coli* BL21(DE3)Star strain (Invitrogen). For preparation of SeMet-labeled HcgC (SeMet-HcgC), *E. coli* B834 (DE3) (Novagen) cells were transformed by using the same expression plasmid for HcgC.

The *hcgC* gene from *Methanococcus maripaludis* S2 (MMP1498, GenBank accession number NP_988618.1), of which the codon usage was optimized, was synthesized by GenScript,

5'CATATGAACTACGGCATTACCGAAAGCGTGAAAACGACCCGCAGCAAAATCAA
AATCAAAGATATTGTGTCCGATGTGGTGGAAAAGAAAGCGAACGCCATCAAATA
TTTTCTGGAAGGCGAAGAATTTAAACAGGCAATTGTGTTTGGCGCTTACCTGTCA
GGTTCGTATATCGCGTACTCACTGCTGAAAGATTGCGAAGAAGTCATTATCGTGG
ACATTCAGCCGCATCTGAAAGATATTCTGTTCAACGACGGTATCAAATTCATGGA
TCTGAACAAACTGCAACTGGAAGTGCCTAACGGCACCAGCATCAATCCGGATCTG
GTGATTGACCTGACGGGTATCGGCGGTGTTAGTCCGGATCTGATTTCCAAATTCA
ATCCGAAAGTTCTGATCGTCGAAGATCCGAAAGGCAACCACGACAAAGGTATCT
CTAAAATCGATAACACCGACAAACGTCTGTGCGTGGGCGCGAAAAAAGGTGTTT
TGAAAACCTATCGCAGCTCTAAATTTAGCAAAACGTCTGGCACCATGACCCTGGT
GGTGGATATTATCATGGACTCATGTGCGGAAATTAACGAACTGGATTCGGTTCTG
TATACCATCCCGAATCTGAAATACTTTGAGGGTACGGTCTTCCATGAGAAAAACG
TGAAAAAATTCCTGACCGAACTGAATATGTCCGCCATTACCGTTAGTTCCATCGA
TCACGTCGAATACGAACTGGAAGAAATCCTGTCAAAAAACATCAGCCGTGTGGA
CTCGTTCGTGAAAGAATTTGTGCGAC-3', and cloned into pET24b(+) expression vector cut with *NdeI* and *Sall* to introduce C-terminal His tag. *E. coli* BL21(DE3) was transformed with the vector.

Construction of an expression system for HcgB from *M. maripaludis*

The *hcgB* gene from *Methanococcus maripaludis* S2 (MMP1497, GenBank accession number NP_988617.1), of which the codon usage was optimized, was synthesized by GenScript,

5'CATATGAACATTGAAAATACCATTAAATCCGCATACGAAGAATCGCTGAATAAC
GCTCGCTTTGGTGATAAAATCGAAGAAATTGACGCAATTCAGAGTACCATCAAAT
CCGCGAAAAACGTCACCGTGGCCACGTCAAATGAGAAAAAATTCAAAGTGGTTT
CAGATATCATCTCGCGTATTACGGACGCGAACATCAGCATGCTGGAAATTCCGAC

RESULTS/PUBLICATIONS

CAATTCTGCGGATCTGACGCGCATGCCGGCCCTGAACAAAGGCCTGATCGCAGTT
 GACAGCTCTGATGCTGACCTGATTATCACCCGTGGCCGCCTGGGTATTCCGGGCT
 CAGGTTGCTGCTGCTGATCATGGATAAAAAAGGCCGTATTCTGACGGGTAGCGT
 CTCTCCGAGTTCCATTATCCATAAAAATCCGATCGATAAAACGGTTGAACTGGAA
 CTGATTACGGCACTGGAACGCATCGGTATTGTGGTGAAAAAACTCGAG-3', and
 cloned into pET24b(+) expression vector cut with NdeI and XhoI to introduce C-terminal His
 tag. *E. coli* BL21(DE3) was transformed with the vector.

Expression and purification of HcgC

The *E. coli* cells were transformed with the expression plasmid containing the *M. jannaschiihcgC* gene and grown at 37°C in LB medium supplemented with 50 µg/mL kanamycin to an OD₆₀₀ = 0.8–1.0. After addition of 1 mM IPTG for HcgC expression the cells were grown for 4–6 h. Then the cells were harvested by centrifugation and stored at –80 °C before further use. Purification of HcgC except for heat treatment at 80 °C, were performed on ice or at 4 °C. The frozen cells were resuspended in 50 mM potassium phosphate buffer pH 7.0 containing 0.5 M potassium chloride and disrupted by sonication. The supernatant of the cell extract was collected by centrifugation and then heated at 80 °C for 20 min and then centrifuged to remove the precipitate. Subsequently, the resulting supernatant was mixed with ammonium sulfate to a concentration of 1 M. The ammonium sulfate-containing supernatant was then filtrated with a 0.45 µm filter and loaded onto a HiTrap Butyl-S FF column (GE Healthcare Life Sciences) equilibrated with 50 mM potassium phosphate buffer pH 7.0 containing 1 M ammonium sulfate (buffer A). The column was washed with at least 15 column volumes of buffer A and bound HcgC was subsequently eluted with a stepwise gradient of ammonium sulfate from 1 M to 0 M in 50 mM potassium phosphate buffer pH 7.0. The HcgC fractions were pooled, concentrated by a centrifuge 10-kDa cut off filter (Millipore) to ca. 10 mL and loaded onto a HiPrep Sephacryl S-200 column (GE Healthcare Life Sciences) equilibrated with 50 mM potassium phosphate buffer pH 7.0 containing 0.3 M KCl. Two fractions of HcgC were recorded in the gel filtration profile; the latter larger fraction corresponding to a HcgC dimer was used for further experiments. The HcgC concentration was determined using the Bradford method. For purification of SeMet-HcgC, the transformed B834(DE3) cells were grown in M9 medium supplemented with 2.5 mM MgSO₄, 2% (w/v) D-(+)-glucose, 0.01% (w/v) thiamine, 0.025 mM FeCl₃, 50 µg/mL L-selenomethionine, and 50 µg/mL kanamycin at 37 °C to an OD₆₀₀ of 0.5. SeMet-HcgC was purified as described for HcgC, except that all buffers contained 1 mM DTT.

RESULTS/PUBLICATIONS

Cell extract of HcgC from *M. maripaludis* was prepared as described for HcgC from *M. jannaschii*. The supernatant of 18,000 ×g centrifugation was loaded on HiTrap Chelating HP (GE Healthcare, 5 ml) equilibrated with 0.1 M NiCl₂. After washing the column with 20 mM potassium phosphate buffer pH 7.0 with 0.5 M KCl, proteins were eluted increasing linear gradient (20–500 mM imidazole). The flow rate was 2.0 ml/min. HcgC was eluted at approximately 500 imidazole concentration. The fractions containing HcgC were pooled and the purity was checked with SDS-PAGE. The purified HcgC protein was washed with 50 mM potassium phosphate buffer pH 7.0 and concentrated to 24 mg/ml by a centrifuge 10-kDa cut off filter (Millipore).

Expression and purification of HcgB from *M. maripaludis*

HcgB from *M. maripaludis* was purified as described above for HcgC from *M. maripaludis*. The purified HcgB protein was washed with 50 mM potassium phosphate buffer pH 7.0 and concentrated to 7.0 mg/ml by a centrifuge 10-kDa cut off filter (Millipore).

Crystallization of HcgC from *M. jannaschii*

All crystals were grown by the sitting drop vapor diffusion method. A 1 μL aliquot of HcgC (3.8 mg/mL) in 10 mM MOPS/KOH (pH 7.0) was mixed with 1 μL of a reservoir solution composed of 27 % (v/v) PEG400, 45 mM Tris-HCl pH 8.5, 45 mM sodium sulfate, 45 mM lithium sulfate and 0.2 M 2,2,2-trifluoroethanol. Crystals of HcgC in the space group P1 appeared at room temperature within 2 months. Crystals of SeMet-HcgC grew in two space groups, *P*₂₁₂₁₂₁ and *P*1. For obtaining crystal form *P*1, an aliquot of 1.6 μL of SeMet-HcgC (8.3 mg/mL) in 10 mM MOPS/KOH buffer pH 7.0 containing 1 mM DTT was mixed with 0.4 μL of 22.5 % (w/v) PEP426, 90 mM HEPES-NaOH pH 7.5, 45 mM magnesium chloride and 0.2 M 2,2,2-trifluoroethanol. Crystals were obtained at room temperature within 2 months. For crystallization of SeMet-HcgC in form *P*₂₁₂₁₂₁, a 1 μL aliquot of HcgC (8.0 mg/mL) in 50 mM MOPS/KOH pH 7.0 was mixed with 1 μL of a reservoir solution composed of 25% (w/v) PEP426 and 100 mM Tris-HCl pH 8.5. Crystals grew at 8 °C within 2 weeks. For crystallization of SAM-bound HcgC, an aliquot of 1 μL of HcgC (4.4 mg/mL) in 10 mM MOPS/KOH pH 7.0 was mixed with 0.2 μL of 50 mM SAM and 1.2 μL of 0.5 M Li₂SO₄ solution containing 2 % (w/v) PEG8000. Crystals were obtained at 8 °C within one week. For co-crystallizing HcgC with SAH- and artificial guanylylpyridinol (made by the HcgB catalyzed reaction from GTP and 3,6-dimethyl-4-hydroxy-2-pyridinol), 1 μL of HcgC (8.0 mg/mL) in 10 mM MOPS/KOH pH 7.0, 0.2 μL 10 mM SAH, 0.5 μL 5 mM artificial guanylylpyridinol(to a final concentration

RESULTS/PUBLICATIONS

of 0.73mM) was mixed with 1.7 μ L of 0.5 M Li_2SO_4 solution containing 2 % (w/v) PEG8000. Then the crystals obtained within one month were soaked inside the crystallization drop containing 2.5 mM artificial guanylylpyridinol with the aim to increase the occupancy of the artificial guanylylpyridinol in the HcgC crystals.

X-ray data collection and refinement

Crystals of HcgC, SAM-bound HcgC, SAH- and artificial guanylylpyridinol-bound HcgC and SeMet-HcgC from *M. jannaschii* were frozen under a cryo-stream of N_2 at 100 K without adding a cryoprotectant. Diffraction data were collected on beamline X10SA equipped with a PILATUS 6M detector at the Swiss-Light Source (Villigen, Switzerland) at 100 K. Data were processed using XDS^[4]. To determine the HcgC structure, multiple anomalous dispersion (MAD) data sets were measured at the selenium edge of SeMet-HcgC crystals. Selenium atom sites were detected with SHELX C/D.^[5] The selenium sites were refined and the phase was determined using the program SHARP and improved by the solvent flattening procedure of SOLOMON^[6] implemented in SHARP.^[7] Automatic model building was performed using Autosol^[8] and Buccaneer^[9]. Further modeling and refinement of form $P2_12_12_1$ SeMet-HcgC was performed using COOT,^[10] REFMAC5,^[11] and PHENIX.^[12] X-ray structures of HcgC and SeMet-HcgC in crystal form $P1$, SAM-bound HcgC and SAH-artificial guanylylpyridinol-bound HcgC were determined by molecular replacement with Molrep^[13] or Phaser^[14] using a monomer of the solved SeMet-HcgC structure of form $P2_12_12_1$ as a search model. The resulting structures were established at resolutions of 2.7 Å for HcgC (PDB: 5D5O), of 2.4 Å for SeMet-HcgC with $P1$ space group (PDB: 5D5T), of 2.9 Å for SeMet-HcgC from with $P2_12_12_1$ space group (PDB: 5D4T), of 2.0 Å for SAM-bound HcgC (PDB: 5D4U), and of 1.6 Å for SAH- and artificial guanylylpyridinol-bound HcgC (PDB: 5D4V). Data collection and refinement statistics are summarized in Table S4. All the protein figures were generated using PyMOL (Version 1.3r1, Schrödinger, LLC). All superpositions were done with the program SUPERPOSE^[15] and visualized with PyMOL.

Structural search for HcgC homologues

HcgC structural homologues were identified with the Dali server^[16] using the crystal structure of HcgC from *M. jannaschii*. In the list of the highly similar structures, NAD(P)⁺-dependent oxidoreductases like shikimate dehydrogenase or SAM-dependent methyltransferases are ranked first, which provided information about potential ligand candidates for HcgC in co-

RESULTS/PUBLICATIONS

crystallization experiments. For superposition with HcgC we have chosen shikimate dehydrogenase AroE (PDB code:2HK9)^[17] and SAM-dependent methyltransferases like RumaA (PDB code: 2BH2).^[18]

Amino acid sequence comparison of HcgC

The amino acid sequences of HcgC from *M. jannaschii*, *Methanothermobacter marburgensis*, *Methanopyrus kandleri*, *Methanococcus maripaludis*, *Methanobrevibacter smithii*, and *Methanocorpusculum labreanum* were aligned with Clustal W2.^[19] and depicted with ESPript3.^[20]

Docking simulation of potential substrates to SAM-bound HcgC

Molecular docking of pyridinol **3** to SAH-bound HcgC was performed with AutoDock Vina.^[21] Due to the limited size of the cavity besides SAH only a pyridinol compound but not guanylylpyridinol could be placed. Pyridinol **3** was initially placed. The calculation was converged in an orientation of the 3-methyl group of the guanylylpyridinol-derived pyridinol towards the sulfur of SAH. Furthermore, the pyridinol **3**-docked structure of SAH- and artificial guanylylpyridinol-bound HcgC was superimposed with the structure of SAM-bound HcgC using the SUPERPOSE program. This superposition revealed the methyl group of SAM at a proper position for the methyl transfer to the C3-carbon of the pyridinol (Figure 1c).

Chemical synthesis of pyridinol 2

Compound P1 was synthesized following the literature.^[22]

Step 1: To the mixture of compound **P1** (for structure, see Figure S6) (0.69 g, 5 mmol) in DMF (25 mL) was added NaH (60% w/w, 0.22 g, 1.1 eq) at 0°C. The solution was stirred for 1hr at 0°C and another 1hr at room temperature. Then chloromethyl methyl ether (MOMCl, 0.48 g, 1.2 eq) was added at 0°C. The mixture was stirred at room temperature for

RESULTS/PUBLICATIONS

another 8 h and again NaH (60% w/w, 0.24 g, 1.2 eq) was added at 0°C. After stirring for 1hr at 0 °C and another 1hr at room temperature, MOMCl (0.56 g, 1.4 eq) was added at 0 °C and the reaction was stirred at room temperature overnight. Water was added to quench the reaction and extracted with DCM. After purification by silica column chromatography using hexane/EtOAc (5:1, R_f 0.5) as the eluent, compound **P2** (for structure, see Figure S6) was obtained as an oil (0.86 g, 76%). [¹H NMR (400 MHz, CDCl₃, 25°C): δ 6.34 (s, 1H), 5.46 (s, 2H), 5.20 (s, 2H), 3.50 (s, 3H), 3.46 (s, 3H), 2.37 (s, 3H), 2.07 (s, 3H) ppm. ¹³C NMR (100 MHz, CDCl₃, 25°C): δ 163.6, 161.0, 154.7, 114.6, 93.9, 92.7, 91.7, 56.9, 56.3, 22.5, 10.7 ppm. HRMS: *m/z* (ESI) calculated [M+H]⁺: 228.1236, measured: 228.1236.]

Step 2: Compound **P2** (0.86 g, 3.8 mmol) was dissolved in dry THF (10 mL) and cooled to -78°C. For deprotonation of the 6-methyl group, lithium diisopropylamide (LDA) (2 M in THF, 5.5 mL, 2.9 eq) was added slowly and the mixture was stirred at this temperature for 2hrs. Then dimethyl carbonate (0.41 g, 1.2eq) in THF (3 mL) was added dropwisely. The reaction was stirred for another 25 mins following by quenching with water. After extraction with Et₂O and purification by silica column chromatography using hexane/EtOAc (5:1, R_f 0.3) as the eluent, the product **P3** (for structure, see Figure S6) was obtained as an oil (0.53 g, 49%). [¹H NMR (400 MHz, CDCl₃, 25°C): δ 6.31 (s, 1H), 5.46 (s, 2H), 5.21 (s, 2H), 3.76 (s, 2H), 3.71 (s, 3H), 3.50 (s, 3H), 3.47 (s, 3H), 2.08 (s, 3H) ppm. ¹³C NMR (100 MHz, CDCl₃, 25°C): δ 171.1, 164.0, 161.2, 150.2, 115.8, 94.0, 91.8, 57.0, 56.3, 51.9, 41.5, 10.6 ppm. HRMS: *m/z* (ESI) calculated [M+H]⁺: 286.1291, measured: 286.1290.]

Step 3: NaOH (30 mg, 5 eq) in H₂O (1 mL) was added to the solution of compound **P3** (44 mg, 0.088 mmol) in MeOH/THF (2 mL / 1 mL). The mixture was stirred at room temperature for 5h and TLC showed that the starting material disappeared. Aq. HCl (~3 N) was added until a pH of ca. 1 was reached. Then concentrated to dry in vacuo. MeOH/EtOAc (5 mL / 5 mL) was added and filtered to remove some dissolved salts. After concentration to dryness, DCM (1 mL) was added. Then CF₃COOH (1 mL) was added at 0°C and stirred for 2h. The mixture was stirred at room temperature for another 5 h and then concentrated to dryness. MeOH (0.1 mL) and Et₂O (3 mL) was added. After stirring for 30min at room temperature, the

RESULTS/PUBLICATIONS

product **P4** (for structure, see Figure S6. In Scheme 2 in the main text, its pyridinol form (**2**) is drawn.) was obtained as white solid after filtration (18 mg, 64%). [¹H NMR (400 MHz, D₆-DMSO, 25 °C): δ 12.54 (bs, 1H), 10.94 (bs, 1H), 10.63 (s, 1H), 5.56 (s, 1H), 3.51 (s, 2H), 1.77 (s, 3H) ppm. ¹³C NMR (100 MHz, D₆-DMSO, 25 °C): δ 170.3, 165.1, 163.2, 106.4, 97.2, 93.9, 56.3, 9.6 ppm. HRMS: m/z (ESI) calculated [M+H]⁺: 184.0610, measured: 184.0605].

Characterization of the SAM-dependent methyl-transfer reaction by HcgC

The standard reaction mixture contained 1 μM HcgC from *M. maripaludis*, 1 mM SAM, pyridinol compound **2** of different concentrations and 10 mM MOPS/KOH pH 7.0. The reaction was performed at 37 °C and the reaction mixtures were analyzed on the HPLC system equipped with the Polar-RP column, Synergi 4μ Polar RP 80A (250 mm × 4.6 mm (Phenomenex)). The sample passed through the column equilibrated with water pH 4.0 (HCl) by applying a liner gradient of methanol (0–100% in 12.5 ml; 0.5 ml/min flow rate). The production of the methylated pyridinol **3** was confirmed by MALDI-TOF-MS. The substrate **2** and product **3** were eluted at approximately 74% and 76% methanol, respectively (Figure S10).

Characterization of the GTP dependent guanylyltransfer reaction by HcgB

The standard reaction mixture contained 0.4 μM HcgB from *M. maripaludis*, 1 mM GTP, 1 mM MgCl₂, pyridinol compound **3** of different concentrations and 10 mM MOPS/KOH pH 7.0. The reaction was performed at 37 °C. The production of the methylated pyridinol **3** was confirmed by MALDI-TOF-MS (Figure S8). For kinetic assays, the reaction mixtures were analyzed on the HPLC system equipped with the HiTrap Q HP column (1 ml). The sample passed through the column equilibrated with 10 mM 2-(N-morpholino)ethanesulfonic acid/NaOH pH 6.0 by applying a liner gradient of NaCl (0–1 M in 12.5 ml; 0.5 ml/min flow rate). The guanylylpyridinol product was eluted at approximately 0.5 M NaCl concentration.

Mass spectrometry

Matrix-assisted laser-desorption/ionization time-of-flight mass spectrometry (MALDI-TOF-MS) was performed using a 4800 Proteomics Analyzer (Applied Biosystems/MDS Sciex) with α-cyano-4-hydroxycinnamic acid in 70% (v/v) acetonitril and 0.1% (v/v) trifluoroacetic acid as matrix.

NMR analysis

RESULTS/PUBLICATIONS

The sample was dissolved in dimethyl sulfoxid-d₆ and filled into Wilmad 3 mm NMR tubes (Rototec Spintec). ¹H–¹³C–HMBC experiments were performed on a Bruker Avance III 500 MHz spectrometer equipped with a 5 mm N₂-cryo-probe Prodigy BBO. The 1D ¹³C spectra were acquired with 65 536 data points and 32000 transients, while the 2D HMBC spectra were collected with 4096 points and 32 transients in the *F*₂ dimension and 512 increments in the *F*₁ dimension. Chemical shifts of ¹H and ¹³C spectra were referenced to the solvent signal. The spectra were processed by Bruker Topspin 3.1.

Mutation analysis of the functions the *hcgB* and *hcgC* genes in *M. maripaludis*

M. maripaludis is a hydrogenotrophic methanogen, and many strategies are available to target the mutation of specific genes.^[23] The study of the FeGP cofactor biosynthetic genes by knock-out-mutation is possible because active [Fe]-hydrogenase (Hmd) is not essential for growth under nickel-sufficient growth conditions.^[24] One disadvantage of using *M. maripaludis* is that the Hmd activity in cell extracts is not reproducibly detectable. To overcome this problem, a *M. maripaludis* strain was generated, in which the native *hmd* gene was replaced by that from the hyperthermophilic *M. jannaschii*. The resulting strain exhibited thermostable Hmd activity and was used for the deletion analysis of the *hcgB* and *hcgC* genes (Table S1 and S2, and Figure S1). The Hmd enzyme activity assay indicated that the *M. maripaludis* strains lacking either *hcgB* or *hcgC* gene did not exhibit Hmd activity (Table S3). This result together with the biochemical studies revealed that HcgB and HcgC are involved in the FeGP cofactor biosynthesis and that no other genes in the genome of *M. maripaludis* substitute the *hcgB* and *hcgC* genes.

Disruption and replacement of the *hmd* gene in *M. maripaludis*

Plasmids for knock-out mutation of the *hmd* gene of *M. maripaludis* were constructed using the pNPAC plasmid^[25] and are listed in Table S1. (The *M. maripaludis* strains used in this study are listed in Table S2.) The *hmd* gene in *M. maripaludis* Mm901 was disrupted by using pNPACΔ*hmd*, resulting in the loss of Hmd activity. The generated *M. maripaludis* strain Mm901Δ*hmd* grew to an OD₅₇₈ of 1.6, and the generation time was about 5 h, which was the same as the parental strain (data not shown). Plasmid pNPACΔ*hmdjhmd* was used to generate *M. maripaludis* Mm901Δ*hmdjhmd*, which also grew indistinguishably from the wild type (data not shown). The correct insertion of the DNA fragments in the chromosome of strain Mm901 was confirmed by PCR (data not shown). The Hmd activity in the cell extract from the Mm901Δ*hmdjhmd* strain was stable for 20 min at 70 °C.

RESULTS/PUBLICATIONS

Disruption of the putative FeGP cofactor biosynthesis genes

The knock-out constructs of the FeGP biosynthesis genes *hcgB* and *hcgC* are listed in Table S1. Markerless in-frame deletion of the *hcgB* and *hcgC* genes was accomplished using a plasmid pCRUPTNEO (Table S1)^[23]; the *M. maripaludis* mutant strains were designated as Mm901MΔ*hmdjhmd*Δ*hcgB* and Mm901Δ*hmdjhmd*Δ*hcgC*. To verify the deletion of the *hcgB* and *hcgC* genes, PCR was performed using the chromosomal DNA from the *M. maripaludis* strains as template and the oligonucleotide primers for the upstream and downstream regions of the target gene (Figure S1). The size of the PCR products derived from the strains corresponded to the expected sizes of the DNA fragments of the gene deletions.

Hmd activity assay of the mutated *M. maripaludis* strains

Cell extracts from the *M. maripaludis* strains were subjected to the Hmd activity assay under the standard assay conditions described below. Strains Mm901Δ*hmdjhmd*Δ*hcgB* and Mm901Δ*hmdjhmd*Δ*hcgC* exhibited no Hmd activity, like the mutant lacking Hmd, Mm901Δ*hmd* (Table S3).

Cultivation of *M. maripaludis* and the enzyme assay

The strains of *M. maripaludis* were cultivated in McCas medium containing 5g/l NaHCO₃, 22 g/l NaCl, 1.4 g/l Na acetate, 500 ml/l general salts solution, 5 ml/l FeSO₄ solution, 10 ml/l vitamin solution, 10 ml/l K₂HPO₄ solution (14 g/l), 1 ml/l trace elements solution, 0.5 ml 1 mM NiCl₂ solution, and 1ml/l resazurin solution (1 g/l). General salt solution contains 0.67 g/l KCl, 5.5 g/l MgCl₂·6H₂O, 6.9 g/l MgSO₄·7H₂O, 0.28 g/l CaCl₂·2H₂O, 1.0 g/l NH₄Cl. Trace elements solution contains 21 g/l Na₃ citrate·2H₂O, 5 g/l MnSO₄·2H₂O, 1 g/l CoCl₂·6H₂O, 1 g/l ZnSO₄·7H₂O, 0.1 g/l CuSO₄·5H₂O, 0.1 g/l AlK(SO₄)₂, 0.1 g/l H₃BO₃, 1 g/l Na₂MoO₄·2H₂O, 2 g/l Na₂SeO₃, 0.1 g V(III)Cl₃, and 0.033 g/l Na₂WO₄·2H₂O. FeSO₄ solution contains 1.9 g/l (10 mM HCl). Cultivation was performed in a 2-l glass bottle sealed with a rubber stopper and a plastic screw-cap at 37 °C with shaking at 120 rpm, in which 500 ml medium was contained under the gas phase of H₂/CO₂ (80/20, vol/vol). All experiments were performed in strictly anoxic conditions in an anaerobic chamber (Coy, Grasslake, Michigan) containing H₂/N₂ (5/95, vol/vol) or under N₂. Cells were harvested in late-exponential growth phase (optical density of the culture at 600 nm was approximately one). The cells (approximately 1.5 g) were harvested by centrifugation at 5,000 ×g for 30 min at 4 °C, and suspended in 5 ml of 50 mM phosphate buffer pH 7.0. The cells were disrupted on ice by ultrasonication (Sonopuls GM200, Ti73 tip, Bandelin) for 12 min with 50 % cycle and 60 % power. Intact cells and cell debris were removed

RESULTS/PUBLICATIONS

by centrifugation at $7,500 \times g$ for 20 min at 4°C . The supernatant was ultra-centrifuged to remove the membrane at $115,000 \times g$ for 30 min at 4°C . The supernatant was designated as the cell extract. Protein concentration of the cell extract was determined with Bradford method using dye solution from Bio-Rad. The protein standard was bovine serum albumin from Bio-Rad. The Hmd enzyme assay was performed as described previously;^[26] in the 0.7 ml assay mixture in 1-ml quartz cuvette (1 cm light path), which contained 120 mM potassium phosphate pH 6.0, 1 mM EDTA and methylene-tetrahydromethanopterin (methylene- H_4MPT) (final concentrations = 20 μM) under N_2 . The enzyme reaction was started by addition of 10 μl cell extract. Formation of methenyl- H_4MPT^+ from methylene- H_4MPT was monitored at 80°C by measuring the increase of absorbance at 336 nm. The Hmd enzyme activity was calculated using the extinction coefficient of methenyl- H_4MPT^+ ($\epsilon_{336\text{ nm}} = 21.6 \text{ mM}^{-1}\text{cm}^{-1}$).

RESULTS/PUBLICATIONS

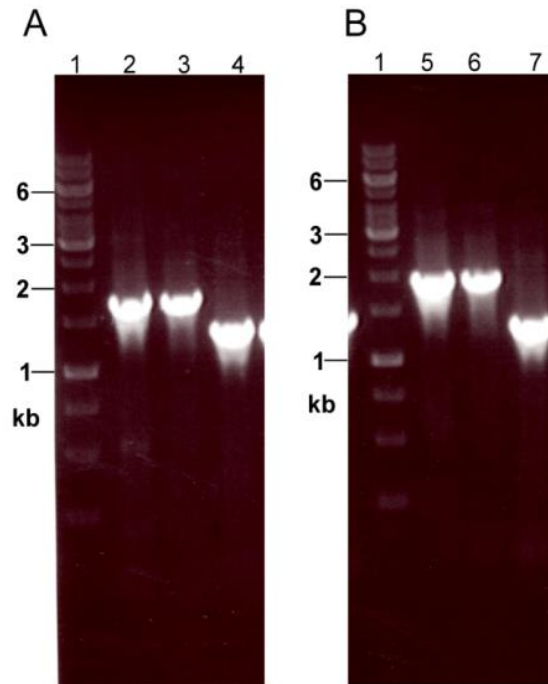


Figure S1. Confirmation of the *hcgB* and *hcgC* deletions in *M. maripaludis*.

PCR was performed using the primer pairs for the regions flanking the *hcgB* and *hcgC* genes. A) PCR products from the *hcgB* gene region. PCR primers: 1, GCGGAACTATTGATGGCG (forward); 2, CATGGTCTATCGAACTTACAG (reverse). Predicted size of the PCR products from the wild type and $\Delta hcgB$ strains are 1790 bp and 1412 bp, respectively. B) PCR products from the *hcgC* gene region. PCR primers: 1, GGAATTACAGATATCCGTG (forward); 2, CAAATTCAGCTAACCGGTC (reverse). Predicted size of the PCR products from the wild type and $\Delta hcgC$ strains are 1986 bp and 1372 bp, respectively. Chromosomal DNA from strain S2 (wild type) (lanes 2 and 5), Mm901 $\Delta hmdjhmd$ (lanes 3 and 6), Mm901 $\Delta hmdjhmd\Delta hcgB$ (lane 4), and Mm901 $\Delta hmdjhmd\Delta hcgC$ (lane 7) were used as templates. The DNA size standards are in lane 1. The size of PCR products obtained from the $\Delta hcgB$ and $\Delta hcgC$ mutants (lanes 4 and 7) corresponded to the expected sizes of the markerless *hcgB* and *hcgC* gene disruptions.

RESULTS/PUBLICATIONS

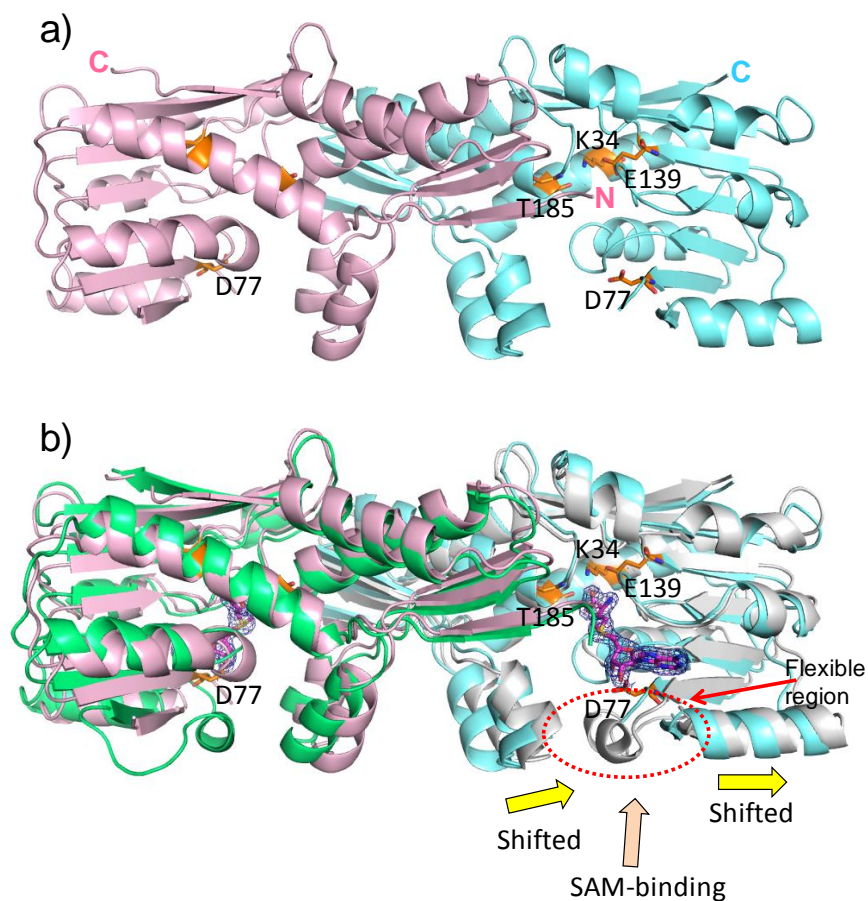


Figure S2. Crystal structure of HcgC from *M. jannaschii*. a) HcgC homodimer; two monomers are shown with pink and cyan cartoon models. The N- and C-termini and some important residues are indicated (carbon in orange). b) Superposition of HcgC with SAM-bound HcgC. HcgC homodimer was shown as pink and cyan cartoons, while SAM-bound HcgC homodimer was shown as green and white cartoons. SAM was shown as a magenta stick model. The $2F_o - F_c$ electron density map was contoured at 1σ . The α -helix indicated by a red arrow was flexible in the absence of SAM but becomes rigidified upon binding of SAM. In addition, two α -helices located at the entrance of SAM-binding are shifted towards the rigidified α -helix after binding of SAM.

RESULTS/PUBLICATIONS

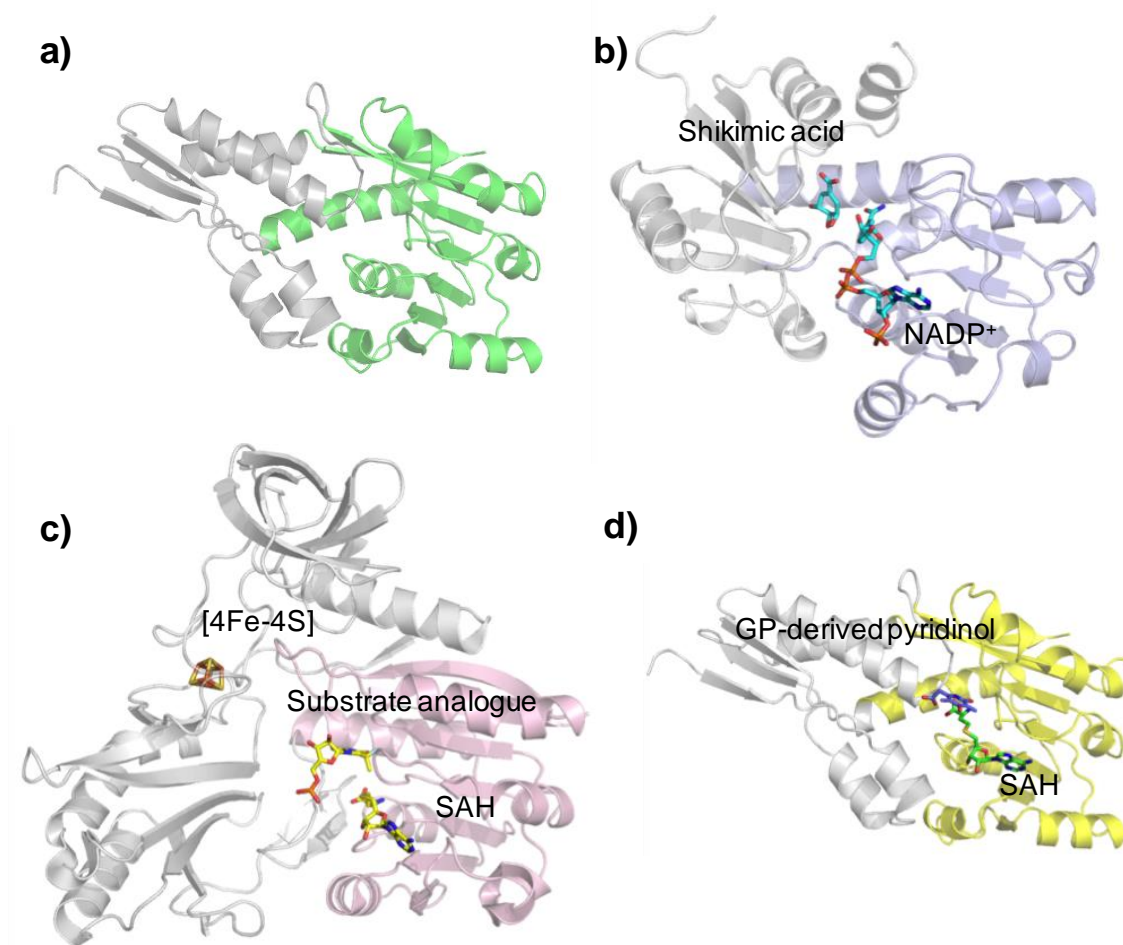


Figure S3. Structural comparison between the Rossmann-like domains of HcgC and its structural homologues. a) The monomer of SAM-bound HcgC b) Shikimate dehydrogenase AroE (PDB code: 2HK9),^[17] c) SAM-dependent methyltransferase RumA (PDB code: 2BH2)^[18] and d) Pyridinol 3-docked HcgC with SAH. The Rossmann-like domains of HcgC with SAM, AroE, RumA and pyridinol 3-docked HcgC with SAH were highlighted by green, light steel blue, pink and yellow, respectively. The ligands and the [4Fe-4S] cluster were represented as stick models. The amino acid sequence identity between HcgC and AroE and RumA are 13% and 8%, respectively. While the Rossmann-like domains exist in all three enzymes, the fold of the domains binding shikimic acid in AroE and the [4Fe-4S] cluster in RumA differ.

RESULTS/PUBLICATIONS

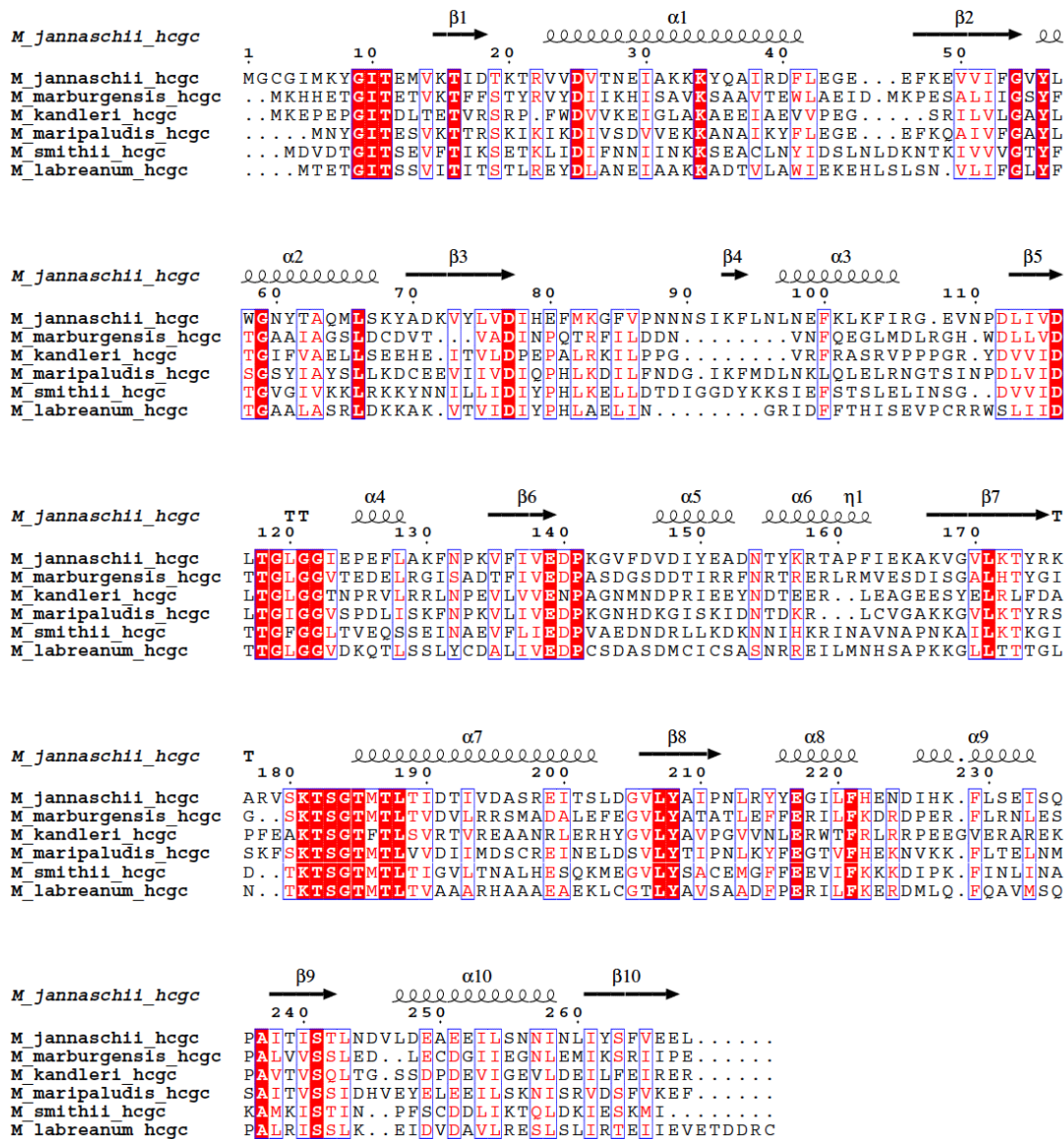


Figure S4. Amino acid sequence alignments of HcgC from *Methanocaldococcus jannaschii*, *Methanothermobacter marburgensis*, *Methanopyrus kandleri*, *Methanococcus maripaludis*, *Methanobrevibacter smithii*, and *Methanocorpusculum labreanum*. White letters on a red background indicated strictly conserved amino acid residues. Red letters in blue boxes indicated well-conserved amino acids or similar amino acids. Symbols above the blocks of sequences correspond to the secondary structures of HcgC from *M. jannaschii*: helices, strands, and turns are symbolized by spirals, arrows, and the letter T, respectively. Amino acid sequence alignments were performed using Clustal W2.^[19] The figure of the alignments was generated with ESPrpt3.^[20]

RESULTS/PUBLICATIONS

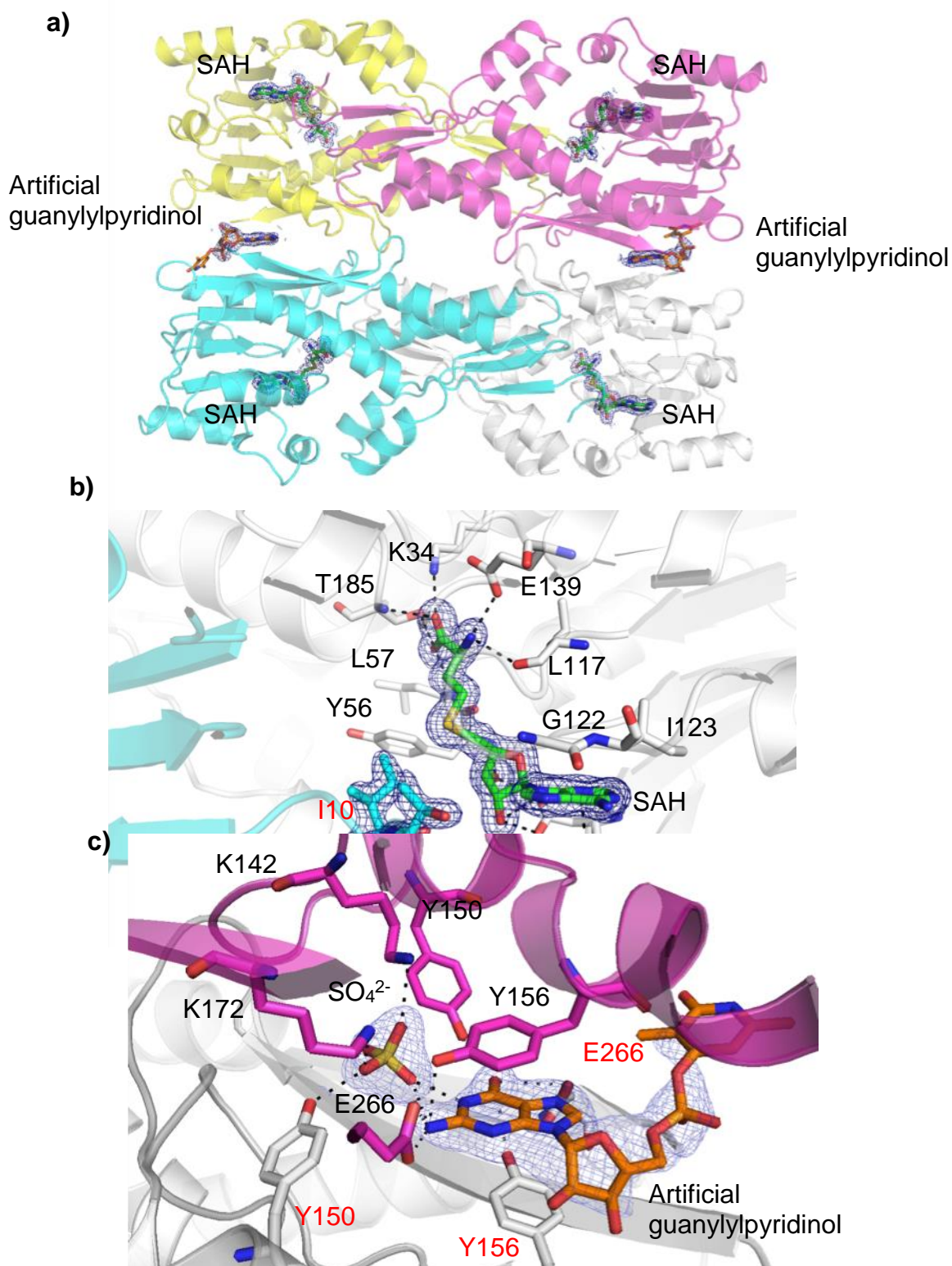


Figure S5. Crystal structure of *S*-adenosylhomocysteine (SAH)- and (3,6-dimethyl-2-pyridinol)-GMP (artificial guanylylpyridinol)-bound HcgC. To gain information about the natural methyl acceptor, co-crystallization experiments were performed between HcgC, soaked with demethylated product of SAM, *S*-adenosylhomocysteine (SAH), and pyridinol derivatives (3,6-dimethyl-4-hydroxy-2-pyridinol, 6-methyl-4-hydroxy-2-pyridinol, 4-hydroxy-2-

RESULTS/PUBLICATIONS

pyridinol and 6-carboxymethyl-3,5-dimethyl-4-hydroxy-2-pyridinol (**3**) or guanylylpyridinol synthesized from GTP and 3,6-dimethyl-4-hydroxy-2-pyridinol by the HcgB catalyzed reaction. A crystal structure at 1.6 Å resolution (Table S4) was obtained from HcgC soaked with SAH and the artificial guanylylpyridinol. a) The HcgC homotetramer in the asymmetric unit. The $2F_o - F_c$ electron density map was contoured at 1σ . SAH and the artificial guanylylpyridinol were shown as green and orange stick models, respectively. SAH is bound at the equivalent position on the Rossmann-like domain. On the other hand, the artificial guanylylpyridinol is not bound to the cavity beside SAH, but an extra electron density was visible at the interface between the dimers of the HcgC homotetramer (in the crystal), into which the artificial guanylylpyridinol was tentatively modeled. b) SAH-binding site. SAH was fixed by specific polar interactions with conserved amino acid residues such as Asp77, Lys34 and Glu139. The N-terminal conserved residues, i.e. Gly9, Ile10 and Thr11 (shown as cyan sticks), were only visible in the HcgC–SAH–artificial guanylylpyridinol complex structure, determined at 1.6 Å resolution, but not in the other HcgC structures determined at lower resolution. The rigidified residues from the partner monomer cover the largely accessible cavity beside SAH which restricts the binding site of the second substrate and therefore also their size of a potential substrate. c) The possible artificial guanylylpyridinol-binding site. Electron density at the dimer interface was observed for the GMP moiety of the artificial guanylylpyridinol (3,6-dimethyl-2-pyridinol)-GMP, but not for the pyridinol part. The guanine ring was sandwiched between two Tyr156 phenol rings from both monomers. Polar interactions are formed between the guanine base and Tyr156-OH and Glu266-COO⁻ of both monomers. Additionally, one sulfate is located in the cavity between the guanine-ring and Lys142 and Lys172. In contrast, the ribose, phosphate and the pyridinol of the artificial guanylylpyridinol are exposed to bulk solvent and showed no specific interactions to the polypeptide. The binding of the artificial guanylylpyridinol may not be functionally important because HcgC is a dimer in solution as derived from gel filtration profiles.

RESULTS/PUBLICATIONS

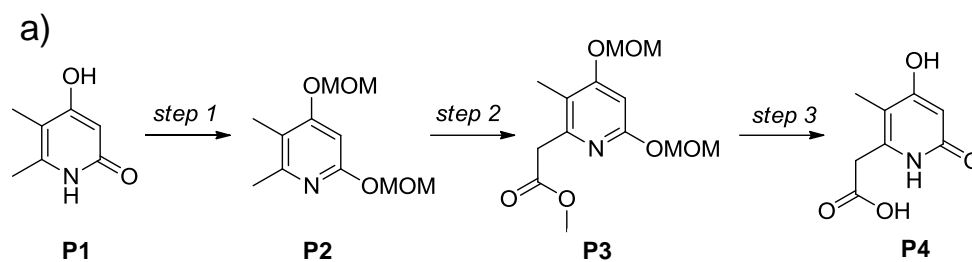
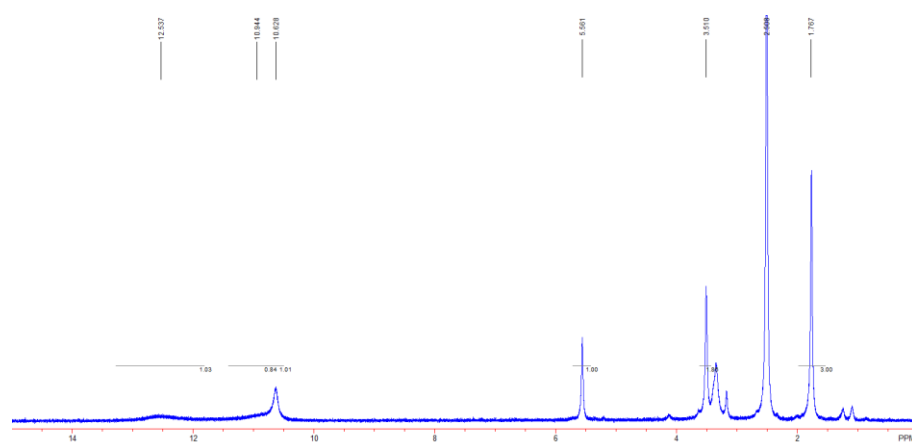
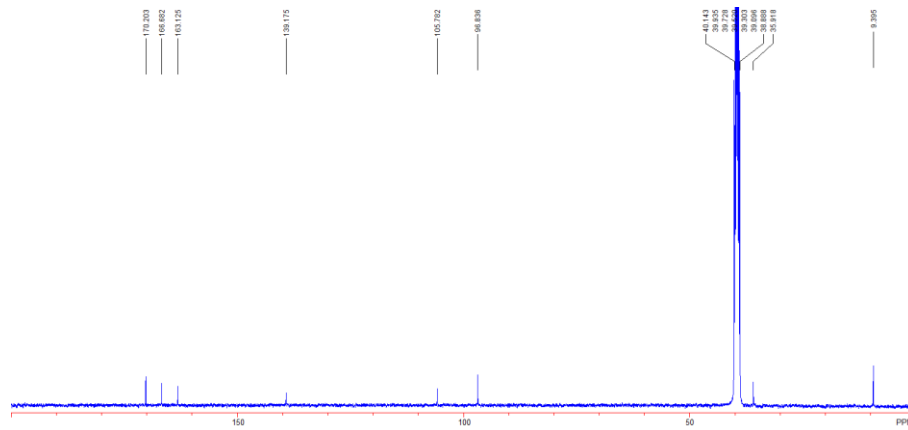
b) $^1\text{H-NMR}$ of **P4**c) $^{13}\text{C-NMR}$ of **P4**

Figure S6. Chemical synthesis of pyridone **2** and product analysis by NMR data. Method of the chemical synthesis was described in the methods section. The compounds **P4** and **2** appear to present in pyridone and pyridinol tautomeric forms in the solvents dimethyl sulfoxide and water, respectively.

RESULTS/PUBLICATIONS

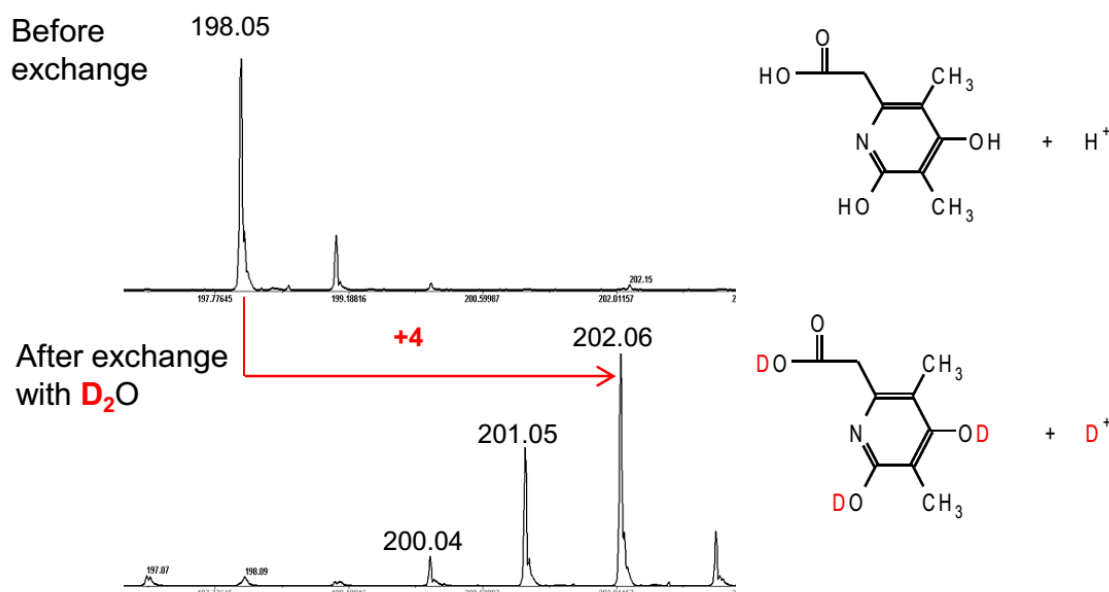


Figure S7. D_2O exchange experiment of the HcgC product (pyridinol **3**). The HcgC product was purified with HPLC described in the method section. Ten μl purified sample was mixed with 10 μl of the matrix solution and dried. The dried sample was suspended in 25 μl of D_2O and then incubated for 20 min. This treatment was repeated for three times. The final dried sample was suspended in 5 μl acetonitril and 5 μl D_2O and drastically mixed by vortex for 30 seconds and analyzed by MALDI-TOF-MS. Increase of 4 Da indicated that the HcgC product contains three exchangeable protons on account of an additional D^+ for protonation to produce positively charged species $[3 + D]^+$ (See schemes in the left panel).

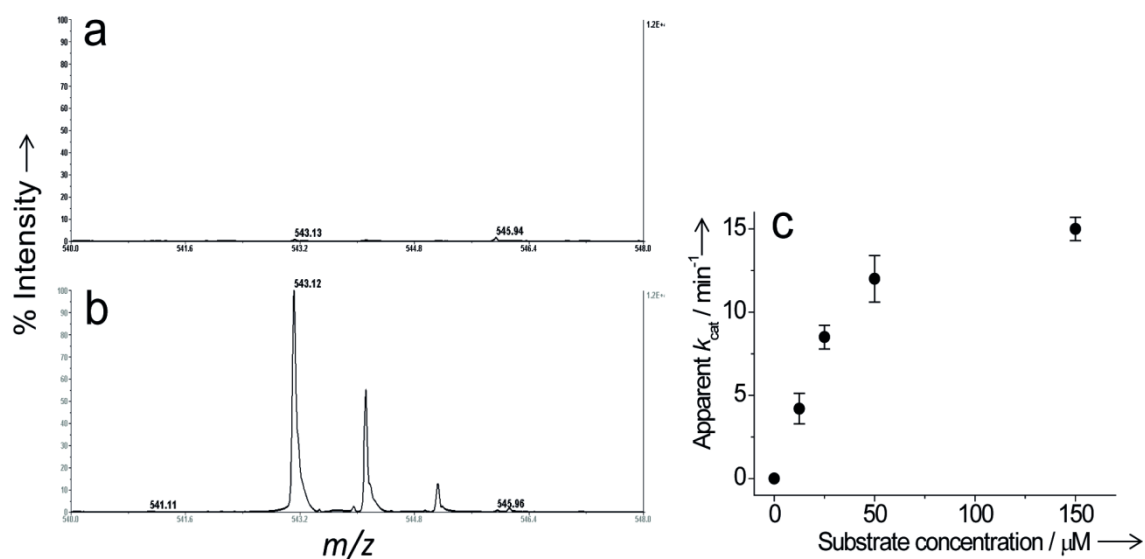


Figure S8. HcgB enzyme assay using the pyridinol **3** produced by the HcgC reaction as substrate. The 0.1 ml reaction mixture contained purified pyridinol **3**, 1 mM GTP, 1 mM $MgCl_2$,

RESULTS/PUBLICATIONS

1 μM HcgB from *M. maripaludis* and 10 mM MOPS/KOH pH 7.0. After incubation at 37 $^{\circ}\text{C}$, the reaction was finished by addition of 0.01% HCl (final concentration) and analyzed by MALDI-TOF-MS or HPLC. (a) The reaction mixture contained 0.03 mM purified pyridinol **3**. Before starting the HcgB reaction, guanylylpyridinol was not detected by MALDI-TOF-MS. (b) Most of the substrate was converted to corresponding guanylylpyridinol (**1**) (calculated $m/z = 543.124072$) within 2 h. (c) HPLC assay indicated that the apparent k_{cat} was $15 \pm 0.7 \text{ min}^{-1}$ in the presence of 150 μM of **3** and 1 mM GTP at pH 7. The error bar indicates standard deviations of duplicated measurements.

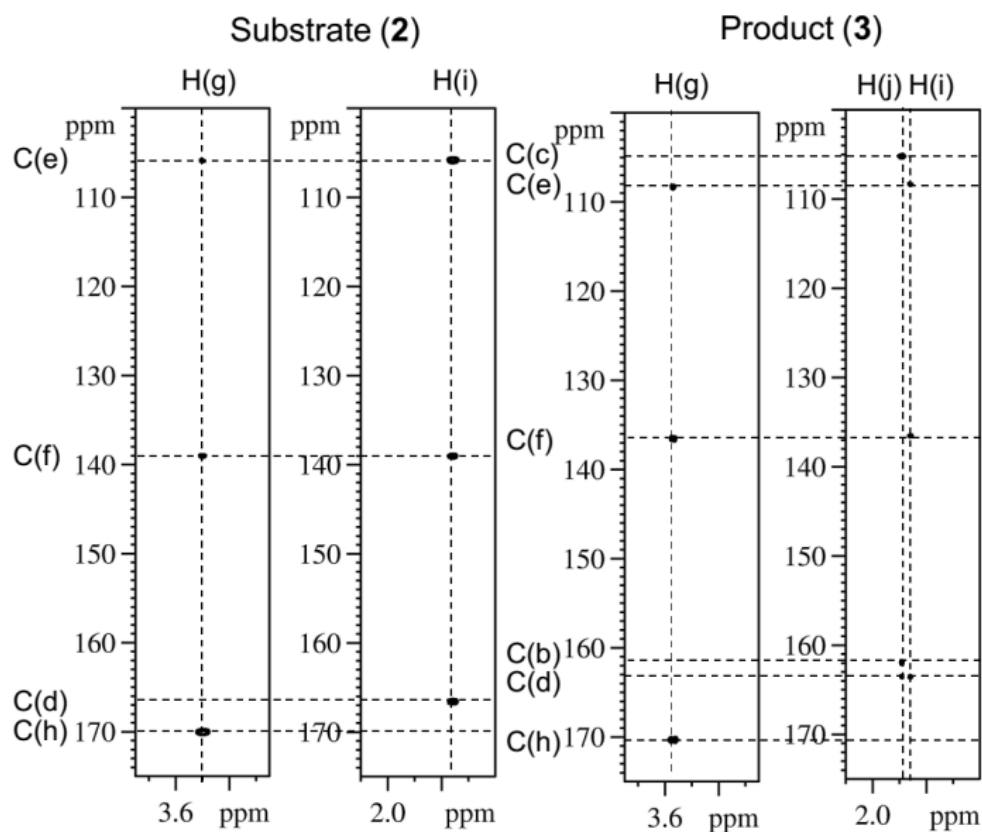


Figure S9. Two dimensional ^1H - ^{13}C -HMBC correlation NMR spectrum of the substrate and product of the HcgC catalyzed reaction in dimethyl sulfoxid- d_6 at 300 K highlighting the connectivity within the pyridone ring. The two panels of each sample show the ^1H - ^{13}C connectivity of H(g) (left) and the methyl groups (i) and/or (j) (right). For labeling of atoms of the pyridinols, see scheme 2 in the main text.

RESULTS/PUBLICATIONS

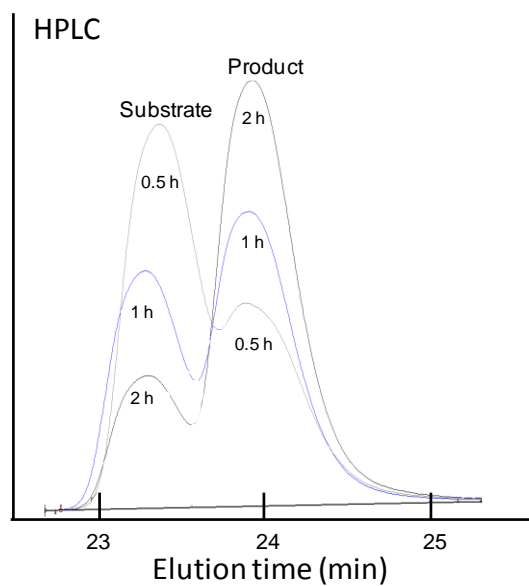


Figure S10. HPLC analysis of the HcgC reaction assay. The assay mixtures containing 0.2 mM substrate were incubated for 0.5, 1.0 and 2.0 h at 37 °C. MALDI-TOF-MS indicated that the 23.3 min peak fraction contained the substrate ($m/z = 184$) and the 24-min peak fraction the product ($m/z = 198$).

RESULTS/PUBLICATIONS

Table S1. Plasmid for site-directed mutagenesis of *Methanococcus maripaludis*.

The DNA fragments were prepared by PCR or DNA synthesis and inserted into the plasmid pNPAC or pCRUPTNEO and then used for recombination experiments.

Plasmid	PCR primers and the sequence regions of the synthesized DNA in the genome for preparation of the DNA fragments	Restriction sites	References
pNPAC			[25]
pNPAC Δ <i>hmd</i>	Up-stream of <i>hmd</i> (606 nt) 5`Forward primer: cGGATCCttctgggattcctgctcttttg 5`Reverse primer: ccGAATTCgctgttggaatagactgctgttc Down-stream of <i>hmd</i> (618 nt) 5`Forward primer: ccAAGCTTttacaaaacttctaaattggatgctg 5`Reverse primer: gACTAGTgcagacagcatgtgctttggtc	<i>Bam</i> HI <i>Eco</i> RI	This study
pNPAC Δ <i>hmdjhm</i> <i>d</i>	Up-stream of <i>hmd</i> 134690..135490 (800nt) + <i>jhmd</i> gene (1077nt)	<i>Bam</i> HI <i>Eco</i> RI	This study
	Down-stream of <i>hmd</i> : (801 nt) 5`Forward primer: ccAAGCTTgttaaacacggttttattcgtagttcaagattac 5`Reverse primer: ggACTAGTctcacagatcttagatttaatgagaaacgaaggc	<i>Hind</i> III <i>Spe</i> I	This study
pCRUPTNEO			[23]
pCRUPTNEO Δ <i>hcgB</i>	Upstream of <i>hcgB</i> : 1457980..1458579 (600nt) Downstream of <i>hcgB</i> : 1458958..1459558 (601nt)	<i>Kpn</i> I, <i>Bam</i> HI	This study
pCRUPTNEO Δ <i>hcgC</i>	Upstream of <i>hcgC</i> : 1458483..1459085 (603nt) Downstream of <i>hcgC</i> : 1459701..1460317 (617nt)	<i>Kpn</i> I, <i>Bam</i> HI	This study

Table S2. *Methanococcus maripaludis* strains used in this study

<i>M. maripaludis</i> Strains	Plasmid used for recombination in this study	Genotype	Source or reference
S2		Wild type	[24]
Mm901		S2 Δ <i>upt</i>	[23]
Mm901 Δ <i>hmd</i>	pNPAC Δ <i>hmd</i>	S2 Δ <i>upt</i> Δ <i>hmd</i>	This study
Mm901 Δ <i>hmd jhmd</i>	pNPAC Δ <i>hmdjhmd</i>	S2 Δ <i>upt</i> Δ <i>hmd</i> :: <i>jhmd</i>	This study
Mm901 Δ <i>hmd jhmd</i> Δ <i>hcgB</i>	pCRUPTNEO Δ <i>hcgB</i>	S2 Δ <i>upt</i> Δ <i>hmd</i> :: <i>jhmd</i> Δ <i>hcgB</i>	This study
Mm901 Δ <i>hmd jhmd</i> Δ <i>hcgC</i>	pCRUPTNEO Δ <i>hcgC</i>	S2 Δ <i>upt</i> Δ <i>hmd</i> :: <i>jhmd</i> Δ <i>hcgC</i>	This study

Table S3. Hmd activity of the cell extracts from the *M. maripaludis* strains.

One unit (U) of the enzyme is the amount catalyzing 1 μmol methenyl- H_4MPT^+ per minute from methylene- H_4MPT at standard assay condition. Each sample was measured at least three times.

Strains	Specific activity (U/mg)
Mm901 Δ <i>hmd</i>	< 0.01
Mm901 Δ <i>hmd jhmd</i>	3.6 \pm 0.1
Mm901 Δ <i>hmd jhmd</i> Δ <i>hcgB</i>	< 0.01
Mm901 Δ <i>hmd jhmd</i> Δ <i>hcgC</i>	< 0.01

RESULTS/PUBLICATIONS

Table S4. Data collection and refinement statistics of HcgC structures

	SeMet- HcgC (MAD peak)	SeMet- HcgC (MAD inflection)	SeMet- HcgC (MAD remote)	SeMet- HcgC in <i>P1</i> form	HcgC	SAM- bound HcgC	SAH- and artificial GP-bound HcgC
Data collection							
Temperature (K)	100	100	100	100	100	100	100
Wavelength (Å)	0.979	0.979	0.971	0.980	1.000	1.000	1.000
Space group	<i>P2</i> ₁ <i>2</i> ₁ <i>2</i> ₁	<i>P2</i> ₁ <i>2</i> ₁ <i>2</i> ₁	<i>P2</i> ₁ <i>2</i> ₁ <i>2</i> ₁	<i>P1</i>	<i>P2</i> ₁ <i>2</i> ₁ <i>2</i> ₁	<i>P2</i> ₁	<i>P2</i> ₁
Resolution (Å)	50–2.9 (3.0–2.9)	50–3.5 (3.6–3.5)	50–3.5 (3.6–3.5)	50–2.4 (2.5–2.4)	50–2.7 (2.8–2.7)	50–2.0 (2.1–2.0)	50–1.6 (1.7–1.6)
Cell dimensions							
<i>a</i> , <i>b</i> , <i>c</i> (Å)	141.4, 145.0, 150.6	141.4, 145.0, 150.6	141.4, 145.0, 150.6	52.6, 78.0, 153.7	142.3, 143.3, 148.3	86.3, 70.5, 91.2	86.1, 70.5, 91.8
α , β , γ (°)	90, 90, 90	90, 90, 90	90, 90, 90	90, 90, 90	90, 90, 90	90, 105.2, 90	90, 105.2, 90
Completeness (%) ^a	99.9 (100.0)	99.2 (96.7)	99.8 (99.8)	95.8 (94.3)	92.7 (95.7)	99.6 (99.2)	99.8 (99.7)
R_{sym} (%) ^{a, b}	13.0 (159.0)	6.6 (33.7)	9.8 (54.0)	9.4 (41.5)	12.5 (81.8)	9.8 (78.2)	4.8 (80.2)
$I/\sigma I$ ^a	11.5 (1.6)	14.2 (2.9)	12.6 (3.3)	9.5 (2.7)	7.7 (1.6)	12.7 (2.3)	16.0 (2.3)
Redundancy ^a	7.4 (7.6)	3.9 (2.4)	4.7 (4.8)	3.5 (3.2)	2.7 (2.7)	3.9 (3.8)	4.5 (4.4)
Refinement statistics							
Resolution (Å)	50.0–2.9 (2.94–2.90)			50.0–2.4 (2.46–2.40)	50.0–2.7 (2.73–2.70)	50.0–2.0 (2.03–2.00)	50.0–1.6 (1.62–1.60)
No. of monomers/ asymmetric unit	8			4	8	4	4
No. of ligands/ asymmetric unit	0			0	0	20	24
No. of waters/ asymmetric unit	11			373	34	438	934
$R_{\text{work}}/R_{\text{free}}$ (%) ^{c, d}	22.7/25.6 (35.7/38.3)			20.5/25.1 (28.3/34.2)	21.7/26.3 (33.9/39.9)	19.8/22.8 (32.5/36.0)	17.1/20.8 (29.8/32.7)
rmsd bond length (Å) ^e	0.015			0.004	0.008	0.003	0.013
rmsd bond angle (°) ^e	1.663			0.840	1.254	0.797	1.446

^aThe values in parentheses are for the highest resolution shell.

^b $R_{\text{sym}} = \frac{\sum \sum |I - \langle I \rangle|}{\sum I}$, where *I* is the intensity of each reflection.

RESULTS/PUBLICATIONS

^c $R_{\text{work}} = \sum ||F_o| - k|F_c|| / \sum |F_o|$, where F_o and F_c are the observed and calculated structure factor amplitudes, respectively.

^d R_{free} was calculated as the R_{work} for 5% of the reflections that were not included in the refinement.

^ermsd, root mean square deviation.

References for Supplementary Information

- [1] S. Shima, E. J. Lyon, M. S. Sordel-Klippert, M. Kauss, J. Kahnt, R. K. Thauer, K. Steinbach, X. L. Xie, L. Verdier, C. Griesinger, *Angew. Chem. Int. Ed.* **2004**, *43*, 2547-2551.
- [2] T. Fujishiro, H. Tamura, M. Schick, J. Kahnt, X. L. Xie, U. Ermler, S. Shima, *Angew. Chem. Int. Ed.* **2013**, *52*, 12555-12558.
- [3] J. Breitung, G. Borner, S. Scholz, D. Linder, K. O. Stetter, R. K. Thauer, *Eur. J. Biochem.* **1992**, *210*, 971-981.
- [4] W. Kabsch, *Acta Crystallogr. D* **2010**, *66*, 125-132.
- [5] G. M. Sheldrick, *Acta Crystallogr. A* **2008**, *64*, 112-122.
- [6] J. P. Abrahams, A. G. Leslie, *Acta Crystallogr. D* **1996**, *52*, 30-42.
- [7] E. delaFortelle, G. Bricogne, *Methods Enzymol.* **1997**, *276*, 472-494.
- [8] T. C. Terwilliger, P. D. Adams, R. J. Read, A. J. McCoy, N. W. Moriarty, R. W. Grosse-Kunstleve, P. V. Afonine, P. H. Zwart, L. W. Hung, *Acta Crystallogr. D* **2009**, *65*, 582-601.
- [9] K. Cowtan, *Acta Crystallogr. D* **2006**, *62*, 1002-1011.
- [10] P. Emsley, K. Cowtan, *Acta Crystallogr. D* **2004**, *60*, 2126-2132.
- [11] G. N. Murshudov, A. A. Vagin, E. J. Dodson, *Acta Crystallogr. D* **1997**, *53*, 240-255.
- [12] P. V. Afonine, R. W. Grosse-Kunstleve, V. B. Chen, J. J. Headd, N. W. Moriarty, J. S. Richardson, D. C. Richardson, A. Urzhumtsev, P. H. Zwart, P. D. Adams, *J. Appl. Crystallogr.* **2010**, *43*, 669-676.
- [13] A. Vagin, A. Teplyakov, *J. Appl. Crystallogr.* **1997**, *30*, 1022-1025.
- [14] A. J. McCoy, R. W. Grosse-Kunstleve, P. D. Adams, M. D. Winn, L. C. Storoni, R. J. Read, *J. Appl. Crystallogr.* **2007**, *40*, 658-674.
- [15] E. Krissinel, K. Henrick, *Acta Crystallogr. D* **2004**, *60*, 2256-2268.
- [16] L. Holm, P. Rosenstrom, *Nucleic Acids Research* **2010**, *38*, W545-W549.
- [17] J. H. Gan, Y. Wu, P. Prabakaran, Y. Gu, Y. Li, M. Andrykovitch, H. H. Liu, Y. C. Gong, H. G. Yan, X. H. Ji, *Biochemistry* **2007**, *46*, 9513-9522.
- [18] T. T. Lee, S. Agarwalla, R. M. Stroud, *Cell* **2005**, *120*, 599-611.

RESULTS/PUBLICATIONS

- [19] M. A. Larkin, G. Blackshields, N. P. Brown, R. Chenna, P. A. McGettigan, H. McWilliam, F. Valentin, I. M. Wallace, A. Wilm, R. Lopez, J. D. Thompson, T. J. Gibson, D. G. Higgins, *Bioinformatics* **2007**, *23*, 2947-2948.
- [20] X. Robert, P. Gouet, *Nucleic Acids Research* **2014**, *42*, W320-W324.
- [21] O. Trott, A. J. Olson, *J. Comput. Chem.* **2010**, *31*, 455-461.
- [22] W. T. McElroy, P. DeShong, *Org. Lett.* **2003**, *5*, 4779-4782.
- [23] B. F. Sarmiento, J. A. Leigh, W. B. Whitman, *Methods Enzymol.* **2011**, *494*, 43-73.
- [24] E. L. Hendrickson, J. A. Leigh, *J. Bacteriol.* **2008**, *190*, 4818-4821.
- [25] J. Sun, A. Klein, *Mol. Microbiol.* **2004**, *52*, 563-571.
- [26] C. Zirngibl, W. van Dongen, B. Schwörer, R. von Büнау, M. Richter, A. Klein, R. K. Thauer, *Eur. J. Biochem.* **1992**, *208*, 511-520.



Towards artificial methanogenesis: biosynthesis of the [Fe]-hydrogenase cofactor and characterization of the semi-synthetic hydrogenase

Liping Bai,^a Takashi Fujishiro,^a Gangfeng Huang,^a Jürgen Koch,^a Atsushi Takabayashi,^b Makio Yokono,^b Ayumi Tanaka,^b Tao Xu,^c Xile Hu,^c Ulrich Ermler^d and Seigo Shima^{*ae}

Received 7th October 2016, Accepted 18th October 2016

DOI: 10.1039/c6fd00209a

The greenhouse gas and energy carrier methane is produced on Earth mainly by methanogenic archaea. In the hydrogenotrophic methanogenic pathway the reduction of one CO₂ to one methane molecule requires four molecules of H₂ containing eight electrons. Four of the electrons from two H₂ are supplied for reduction of an electron carrier F₄₂₀, which is catalyzed by F₄₂₀-reducing [NiFe]-hydrogenase under nickel-sufficient conditions. The same reaction is catalysed under nickel-limiting conditions by [Fe]-hydrogenase coupled with a reaction catalyzed by F₄₂₀-dependent methylene tetrahydromethanopterin dehydrogenase. [Fe]-hydrogenase contains an iron-guanilylpyridinol (FeGP) cofactor for H₂ activation at the active site. Fe^{II} of FeGP is coordinated to a pyridinol-nitrogen, an acyl-carbon, two CO and a cysteine-thiolate. We report here on comparative genomic analyses of biosynthetic genes of the FeGP cofactor, which are primarily located in a hmd-co-occurring (*hcg*) gene cluster. One of the gene products is HcgB which transfers the guanosine monophosphate (GMP) moiety from guanosine triphosphate (GTP) to a pyridinol precursor. Crystal structure analysis of HcgB from *Methanococcus maripaludis* and its complex with 6-carboxymethyl-3,5-dimethyl-4-hydroxy-2-pyridinol confirmed the physiological guanylyltransferase reaction. Furthermore, we tested the properties of semi-synthetic [Fe]-hydrogenases using the [Fe]-hydrogenase apoenzyme from several methanogenic archaea and a mimic of the FeGP cofactor. On the basis of the enzymatic reactions involved in the methanogenic pathway, we came up with an idea how the

^aMax-Planck-Institut für terrestrische Mikrobiologie, 35043 Marburg, Germany. E-mail: shima@mpi-marburg.mpg.de

^bThe Institute of Low Temperature Science, Hokkaido University, Sapporo 060-0819, Japan

^cInstitute of Chemical Science and Engineering, Ecole Polytechnique Fédérale de Lausanne (EPFL), 1015 Lausanne, Switzerland

^dMax-Planck-Institut für Biophysik, Max-von-Laue-Straße 3, 60438 Frankfurt/Main, Germany

^ePRESTO, Japan, Science and Technology Agency (JST), 332-0012 Saitama, Japan

Faraday Discussions

methanogenic pathway could be simplified to develop an artificial methanogenesis system.

Introduction

Most methanogenic archaea are able to produce methane from CO_2 and H_2 (ref. 1) achieved by an eight-electron reduction process (Fig. 1).² The four H_2 molecules required are activated by hydrogenases and the electrons are stepwise supplied to CO_2 and coenzyme-bound C1-intermediates.³ The methane-forming pathway is used for energy conservation, for which specific enzymes containing tungsten, molybdenum, cobalt, nickel, zinc and iron were developed.

The active site of the methanogenic enzymes frequently contains metal-containing cofactors, which are enzymatically synthesized in the cells. Many

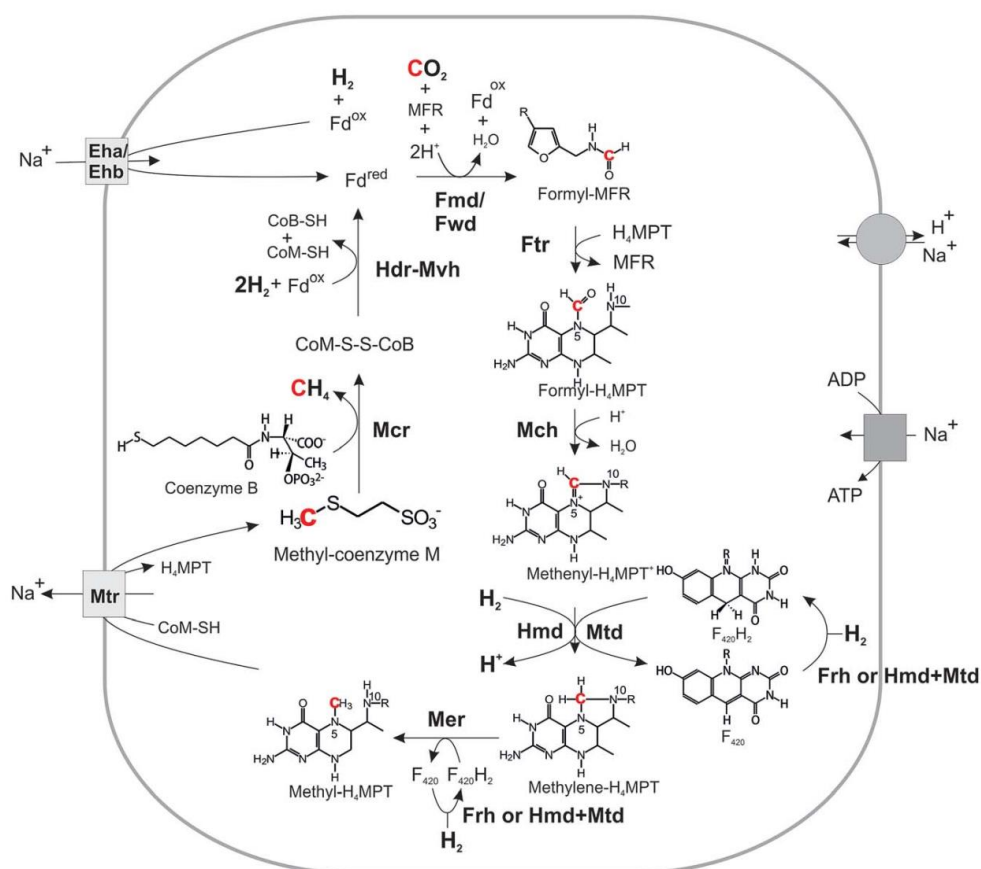


Fig. 1 Methanogenic pathway from H_2 and CO_2 in methanogens without cytochromes. Abbreviations: methanofuran (MFR), tetrahydromethanopterin (H_4MPT), coenzyme M (CoM-SH), coenzyme B (CoB-SH), ferredoxin (Fd), formylmethanofuran dehydrogenase (Fmd/Fwd), formylmethanofuran: H_4MPT formyltransferase (Ftr), methenyl- H_4MPT cyclohydrolase (Mch), F_{420} -dependent methylene- H_4MPT dehydrogenase (Mtd), H_2 -forming methylene- H_4MPT dehydrogenase ([Fe]-hydrogenase, Hmd), F_{420} -reducing [NiFe]-hydrogenase (Frh), methylene- H_4MPT reductase (Mer), methylene- H_4MPT :coenzyme M methyltransferase (Mtr), methyl-coenzyme M reductase (Mcr), heterodisulfide reductase-[NiFe]-hydrogenase complex (Hdr-Mvh), energy-converting [NiFe]-hydrogenases (Eha/Ehb). F_{420} is reduced with H_2 using Frh under nickel-sufficient conditions and a coupled reaction of Hmd and Mtd under nickel-limiting conditions.

Paper

hydrogenotrophic methanogenic archaea, for example *Methanothermobacter marburgensis*, grow in synthetic media without vitamins and organic materials (*i.e.* yeast extracts and peptone).⁴ The chemically complicated cofactors and coenzymes are synthesized from CO_2 , NH_4^+ , S^{2-} , PO_4^{3-} , Mg^{2+} , Fe^{2+} , Ni^{2+} , Co^{2+} , W^{6+} , Mo^{6+} and Zn^{2+} . It is of great scientific interest to understand their biosynthesis. This knowledge about biosynthetic precursors, enzymes and their catalytic mechanism is potentially usable to develop methods for biosynthesizing modified coenzymes and cofactors, which improve the biological pathway (*i.e.* methanogenesis and CO_2 fixation pathways). Moreover, information about their biosynthesis might support us in developing new chemical methods to synthesize biological materials and mimic compounds.^{5,6}

Artificial photosynthesis, which is the central topic of this issue, aims to construct chemical systems, which reduce CO_2 with electrons from light-driven reactions. For that, we have to develop novel catalysts, which reduce CO_2 to the desired reduced chemical compounds (carbon monoxide, formate, methane *etc.*). The hydrogenotrophic methanogenic pathway contains enzymes catalyzing the nine reaction steps from CO_2 to CH_4 . These enzymes are biochemically characterized, most of their crystal structures are established and a catalytic mechanism proposed. These data may pave the way to develop new catalysts, which are applicable for artificial biosynthesis systems.

In this report, we describe firstly the overviews of the methanogenic pathway from CO_2 , the biosynthesis of the [Fe]-hydrogenase cofactor, and the reconstitution of the semi-synthetic [Fe]-hydrogenase. In addition, we report on the analysis of genomic regions involved in the biosynthesis of the [Fe]-hydrogenase cofactor and on the characterization of one of the cofactor biosynthesis enzymes, HcgB. Finally, we will present activity and stability studies on semi-synthetic [Fe]-hydrogenases.

Methanogenesis from CO_2

Hydrogenotrophic methanogenic enzymes can be classified into two groups. One group of enzymes catalyzes reduction of CO_2 to methane *via* C1-carrier coupled C1 intermediates of different oxidation states. The C1 carriers are methanofuran (MFR), tetrahydromethanopterin (H_4MPT) and coenzyme M (HS-CoM). The second group of enzymes catalyzes the reproduction of reduced electron carriers, *i.e.* F_{420} , ferredoxin, and coenzyme B by using electrons from H_2 .

In the CO_2 reduction pathway (Fig. 1), CO_2 is reductively joined to the amino group of MFR to form formyl-MFR; this reaction is catalyzed by formyl-MFR dehydrogenase.⁷ Two types of formyl-MFR dehydrogenases are known: a tungsten-containing iron-sulfur enzyme (Fwd) and a molybdenum-containing iron-sulfur enzyme (Fmd). In the next step, a formyltransferase (Ftr) catalyzes the transfer of the formyl group of formyl-MFR to the second C1 carrier, H_4MPT to form formyl- H_4MPT .⁸⁻¹⁰ This formyl group is converted to a methenyl group by a condensation reaction, which is catalyzed by a cyclohydrolase (Mch).¹¹ The formed methenyl group is reduced to methylene- H_4MPT by F_{420} -dependent methylene- H_4MPT dehydrogenase (Mtd)^{12,13} and further to methyl- H_4MPT by F_{420} -dependent methylene- H_4MPT reductase (Mer).^{14,15} The reducing equivalents are supplied from the reduced form of F_{420} , which is a deazaflavin derivative.¹⁶ The mid-point redox potential of F_{420} is -360 mV, which is similar to that of NAD(P).¹⁷

The methyl group is transferred to the third C1 carrier HS-CoM to form methyl-S-CoM, which is catalyzed by a membrane-spanning methyltransferase complex (MtrA-H). This enzyme complex contains a cobalamin (a cobalt-containing cofactor) to mediate methyl transfer.¹⁸ The exergonic methyl-transfer reaction ($\Delta G^{\circ'} = -30 \text{ kJ mol}^{-1}$) is coupled with an endergonic sodium-ion translocation across the cytoplasmic membrane, which is the only energy-conserving reaction in hydrogenotrophic methanogens.¹⁹ Methyl-S-CoM is reduced to methane and the reductant coenzyme B (7-mercaptoheptanoylthreoninephosphate, HS-CoB) and HS-CoM are oxidized to the heterodisulfide CoM-S-S-CoB catalyzed by methyl-S-CoM reductase (Mcr) ($\Delta G^{\circ'} = -30 \text{ kJ mol}^{-1}$).²⁰⁻²⁵ Mcr contains the nickel-porphinoid F_{430} in the active site. The heterodisulfide is an important oxidant ($E^{\circ'} = -140 \text{ mV}$) in the methanogenic energy metabolism, and is used as a high potential electron acceptor in the following FAD-based electron bifurcation reaction.²⁶⁻²⁸ The electron-bifurcating heterodisulfide reductase hydrogenase complex (HdrABC-MvhAGD) catalyzes the reduction of heterodisulfide and ferredoxin by oxidizing H_2 (see below).^{1,29,30} The reduced ferredoxin is used as an electron donor for the first reductive CO_2 -fixation reaction catalyzed by Fwd or Fmd.⁷

In the hydrogenotrophic methanogenic pathway, two of four H_2 molecules are oxidized by the heterodisulfide reductase-associated [NiFe]-hydrogenase complex (MvhAGD).¹ The four electrons are transferred from the [NiFe] hydrogenase to the heterodisulfide reductase module and split there at the bifurcating FAD to two different energy levels resulting in two electrons of higher energy (strong electron donor) and two electrons of lower energy (weak electron donor). The electrons of higher energy reduce ferredoxin ($E^{\circ'} = \sim -500 \text{ mV}$) and those of lower energy CoM-S-S-CoB heterodisulfide ($E^{\circ'} = \sim -140 \text{ mV}$). The active site of the [NiFe]-hydrogenase part hosts a dinuclear Ni-Fe metal complex, at which H_2 is heterolytically cleaved to a proton and a hydride ion. The latter splits into a proton and two electrons that are shuttled to the bifurcating FAD.

In nickel-sufficient environments (nickel concentration, $\sim 5 \mu\text{M}$), reduction of F_{420} is catalyzed by F_{420} -reducing [NiFe]-hydrogenase (Frh). In nickel-limiting environments (nickel concentration, $\sim 50 \text{ nM}$), Frh is substituted by [Fe]-hydrogenase (Hmd) which reduces F_{420} (see below) together with F_{420} -dependent methylene- H_4 MPT dehydrogenase (Mtd) in an indirect manner.³¹⁻³³ In addition, membrane-spanning [NiFe]-hydrogenases (Eha and Ehb) catalyze chemiosmotically the endergonic reduction of ferredoxin by using most probably a sodium ion potential. The Eha and Ehb hydrogenases complement the reduced ferredoxin, which was consumed in anabolic reactions.

Thermodynamics

The Gibbs free energy change for each methanogenic reaction is plotted in Fig. 2. The free energy changes for the reaction steps from CO_2 to methyl- H_4 MPT (Fwd/Fmd, Ftr, Mch, Mtd and Mer reactions) are relatively small and do not allow coupling with ion gradient forming processes. The last three reactions (Mtr, Mcr, Hdr/Mvh reactions) are sufficiently exergonic to be used for energy coupling. The methyl-transfer reaction from methyl- H_4 MPT ($\Delta G^{\circ'} = -30 \text{ kJ mol}^{-1}$) to HS-CoM, catalyzed by MtrA-H, is coupled with sodium-ion translocation, which is the only energy conservation reaction of this metabolism. Methane and heterodisulfide

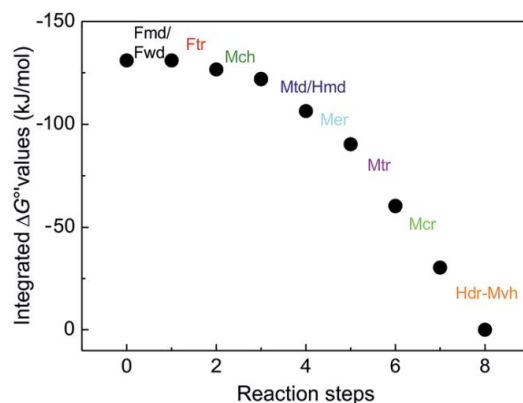


Fig. 2 Free energy change of the single reactions involved in the methanogenic pathway from H_2 and CO_2 . The total Gibbs free energy change of methane formation from H_2 and CO_2 is -131 kJ mol^{-1} . The change of free energy is shown cumulatively. For abbreviation of the enzyme names, see Fig. 1.

CoM-S-S-CoB formation from methyl-S-CoM and HS-CoB have a similar free energy ($\Delta G^\circ = -30 \text{ kJ mol}^{-1}$). Even though the Mcr reaction is not directly involved in energy coupling, it forms CoM-S-S-CoB, which is a substrate for the electron bifurcating HdrABC/MvhAGD. Reduced ferredoxin is required for reductive CO_2 fixation in the first step of the methanogenic pathway.

[Fe]-hydrogenase

[Fe]-hydrogenase (Hmd) reversibly catalyzes H_2 activation and the hydride transfer to methenyl- H_4MPT^+ (Fig. 3A). As mentioned, Mtd together with [Fe]-hydrogenase reduces F_{420} (Fig. 3B)³¹ that serves as electron-donor (F_{420}H_2) in the methanogenic pathway.^{13,15,34,35} [Fe]-hydrogenase, only found in methanogenic archaea, contains a mono-nuclear iron center as the catalytic active part of

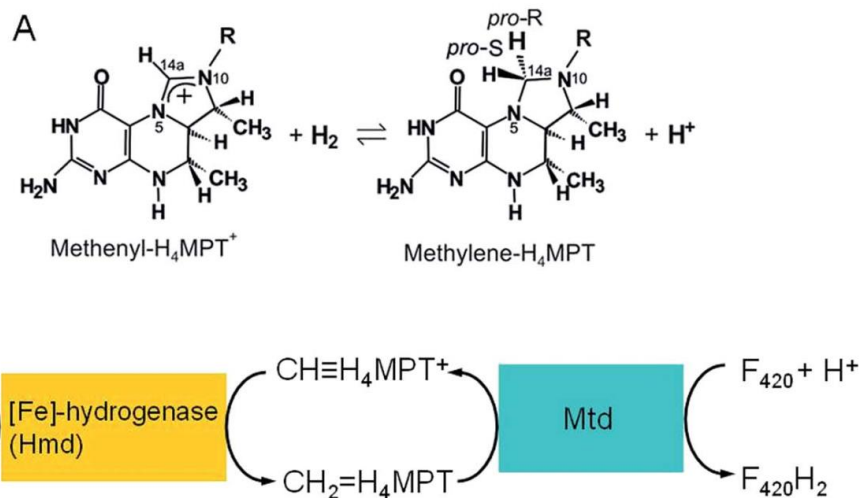


Fig. 3 Reaction catalyzed by [Fe]-hydrogenase (Hmd). (A) Hmd reversibly catalyzes the activation of H_2 and the hydride transfer to methenyl- H_4MPT^+ . (B) Hmd catalyzes the reduction of F_{420} by coupling with methenyl- H_4MPT^+ dehydrogenase (Mtd).

Faraday Discussions

the iron-guanylylpyridinol (FeGP) cofactor.³⁶ Fe^{II} is ligated to the nitrogen of the pyridinol ring and the acyl-carbon of its acylmethyl substituent (Fig. 4 right).^{37–39} In addition, Fe^{II} is coordinated to two CO and one cysteine-thiolate ligand^{40–42} that covalently connects the FeGP cofactor to the protein. The pyridinol ring becomes bulky by the presence of one GMP moiety and two methyl substituents in addition to the acylmethyl group.⁴³ The GMP part is non-covalently bound to the protein.^{37,38} The FeGP cofactor is only found in [Fe]-hydrogenase, and the acyl-carbon ligand and the highly substituted pyridinol are also only found in this cofactor. When exposed to UV-A/blue light, this cofactor decomposes to guanylylpyridinol with a 6-carboxymethyl group (Fig. 4 left), Fe²⁺ and CO. The light-sensitive FeGP cofactor can be isolated from [Fe]-hydrogenase under red light in the presence of 1 mM 2-mercaptoethanol, 60% methanol and 1% NH₃.^{44,45} The [Fe]-hydrogenase can also be reconstituted by mixing the isolated FeGP cofactor and the [Fe]-hydrogenase apoenzyme that was heterologously over-produced in *Escherichia coli*.^{44,45} Its extraction/reconstitution ability allows one to study the characteristics of the cofactor. Using a similar method, semi-synthetic [Fe]-hydrogenase was reconstituted with chemical mimics of the FeGP cofactor (see below).⁴⁶

Biosynthesis of [Fe]-hydrogenase cofactor

Stable isotope-labelling experiments using the culture of methanogenic archaea indicated that the pyridinol part of the FeGP cofactor is synthesized from CO₂ via acetate and pyruvate, the methyl group from methionine, and the CO and acyl ligands directly from CO₂.⁴⁷ The GMP part is synthesized using the common GMP biosynthesis pathway, which suggested the presence of a guanylyltransferase that transfers the GMP moiety to the pyridinol (or its precursor).⁴⁷

Studies of the pathway of FeGP cofactor biosynthesis were mainly based on the analysis of hmd-co-occurring (*hcg*) genes.² In some methanogenic archaea, the [Fe]-hydrogenase-encoding gene (*hmd*) was clustered with seven genes, termed *hcg* genes. As these genes were found in the genomes of all methanogenic archaea containing [Fe]-hydrogenase it was hypothesized that their gene products catalyse reaction steps of the FeGP cofactor biosynthetic pathway.² Use of genetic techniques was difficult for functional studies of the *hcg* genes because of the low expression level of *hcg* and *hmd* in *Methanococcus maripaludis*, the model methanogen for genetic study. To elucidate the functions of the *hcg* gene products (HcgA–G proteins), the heterologously produced Hcg proteins were crystallized and their structures determined. Based on a three-dimensional structure similarity search and co-crystallization with possible substrates, the function of the

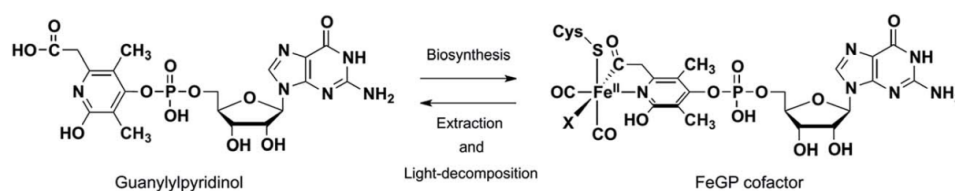


Fig. 4 Structure of the FeGP cofactor and the guanylylpyridinol precursor **3** (see Fig. 5). The guanylylpyridinol (precursor **3**) is a precursor for biosynthesizing the iron centre of the FeGP cofactor. By UV-A/blue light irradiation, the FeGP cofactor is decomposed to the guanylylpyridinol, 2CO and Fe²⁺.

Paper

Hcg proteins were predicted. Finally, the predicted functions were confirmed by enzyme assays.^{48–51}

The proposed biosynthetic pathway of the FeGP cofactor is shown in Fig. 5. In summary, HcgC is a methyltransferase, which transfers a methyl group from *S*-adenosylmethionine (SAM) to 6-carboxymethyl-3,5-dimethyl-4-hydroxy-2-pyridinol (precursor 1 in Fig. 5) to form the 3-methylated product (precursor 2).⁴⁸ HcgB is a guanylyltransferase, which catalyzes the cleavage of guanosine triphosphate (GTP) and the bonding between the GMP moiety and precursor 2 forming a guanylylpyridinol (precursor 3), which is the same compound obtained by light-decomposition of the FeGP cofactor (see Fig. 4).⁵¹ The carboxy group of precursor 3 is activated by binding an adenosine monophosphate (AMP) moiety (precursor 4). The ATP dependent reaction is catalyzed by HcgE.⁵⁰ The AMP-activated guanylylpyridinol reacts with HcgF, by which the guanylylpyridinol is bound to HcgC at the Cys9 residue to form a thioester bond.⁵⁰ It was proposed that the thioester bond could be the precursor of the acyl-ligand formation; however the enzymatic reaction(s) are not known.⁵⁰ HcgD is proposed to be an iron chaperone, which guides incorporation of an iron or iron-carbonyl precursor for acyl ligand formation.⁴⁹ The functions of HcgA and HcgG are not known yet. These two enzymes might be involved in the formation of the CO ligands or pyridinol (precursor 1).

Reconstitution of active [Fe]-hydrogenase with a mimic compound

Mimics of the FeGP cofactor have been already synthesized.^{5,52–62} However, they did not exhibit any H₂ cleavage activity except for a recent report.⁶ There are two plausible reasons for this finding. The first is the absence of the protein and the second the lack of the substrate, methenyl-H₄MPT⁺ or methylene-H₄MPT, which was required for the H₂ activation reaction in the protein. If the assumptions are correct, the mimics have to be built into the protein for activity. For the reconstitution experiments, a mimic has to be dissolved in methanol containing 1% acetic acid (Fig. 6). Infrared spectra of the dissolved compound indicated that one CO ligand was dissociated from the mimic and one acetate ligand bound. The mimic with the potential acetate ligand was bound to the apoenzyme by exchanging the acetate ligand with a cysteine thiol. The reconstituted enzyme was catalytically competent although the specific activity was ~1% of the native

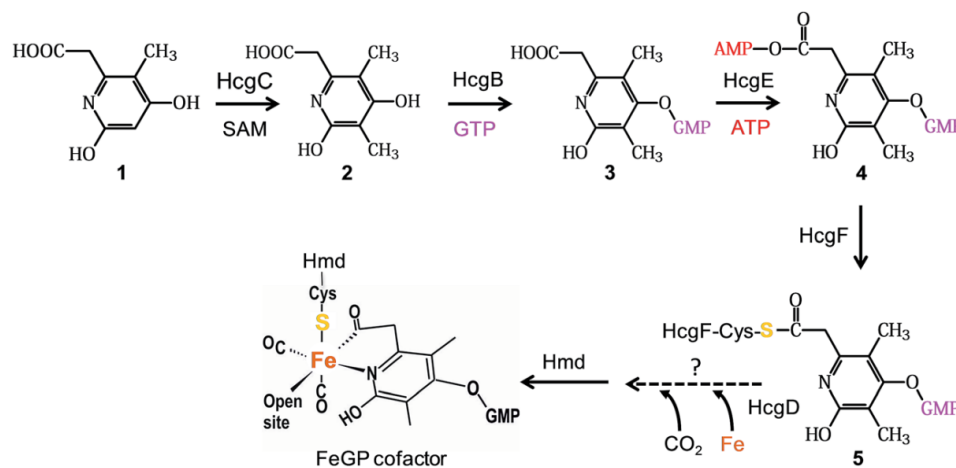


Fig. 5 Biosynthetic pathway of the FeGP cofactor.⁵⁰

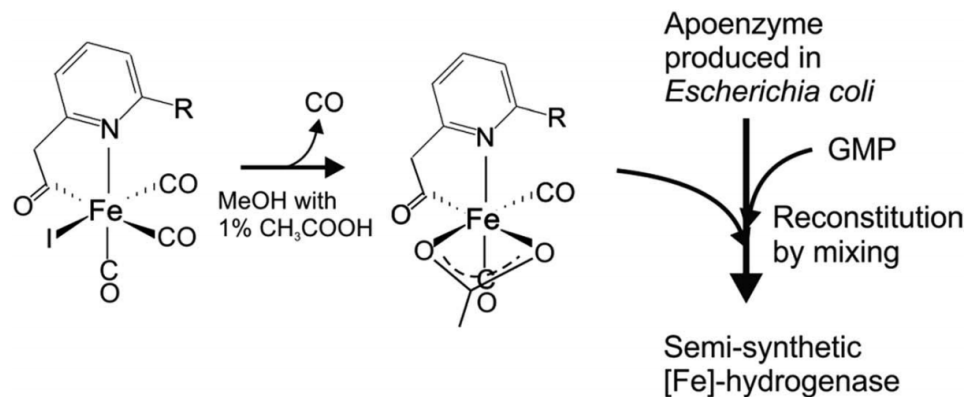


Fig. 6 Reconstitution procedure to form a semi-synthetic [Fe]-hydrogenase.⁴⁶

enzyme. To explore the function of the 2-hydroxy group as the base of the heterolytic cleavage of H₂, a mimic compound, in which the 2 position of the pyridinol was substituted with a methoxy group, was used for the reconstitution. The obtained holoenzyme did not show enzymatic activity which supported the postulated function of the 2-hydroxy group of the FeGP cofactor as the base of the catalytic reaction.

Methods

Mass-spectroscopic identification using blue-native polyacrylamide gel electrophoresis

Methanothermobacter marburgensis (DSM 2133) was obtained from the Deutsche Sammlung von Mikroorganismen und Zellkulturen (DSMZ) and was routinely grown at 65 °C in two 10 liter fermenters containing 10 liter medium. The growth conditions including medium composition were described previously by Schönheit *et al.*^{4,63} In the nickel-limiting conditions, nickel was omitted from the trace element solution (traces of nickel are still eluted from the metal part of the fermenter). Cultures were gassed with 80% H₂/20% CO₂/0.01% H₂S and stirred at 1000 rpm. The cells were harvested by centrifugation under anoxic conditions at 4 °C. Cell pellets were stored at –75 °C before enzyme purification.

The frozen cells were homogenized with mortar and pestle, and were subsequently suspended in a 200 µl ice-cold buffer containing 50 mM imidazole-HCl (pH 7.0), 20% glycerol, 5 mM 6-aminocaproic acid, and 1 mM EDTA-2Na. After supplementing with 2 mM MgCl₂, the suspensions were treated with Benzonase® nuclease (Merck, Darmstadt, Germany) for 30 min on ice for the removal of genomic DNA. The samples were solubilized with 1% (w/v) *n*-dodecyl- α -D-maltese on ice for 10 min, and were centrifuged at 15 000 rpm for 20 min. The supernatants were used for blue-native polyacrylamide gel electrophoresis as described previously⁶⁴ using 4–14% polyacrylamide gradient gels with cathode buffer containing 0.02% Coomassie Brilliant Blue-G250 (Serva, Germany). The polyacrylamide gel was sliced manually to fractionate the proteins. All gel pieces were subjected to in-gel digestion of the proteins by trypsin as described previously.⁶⁴ The peptides in the digested samples were analyzed by liquid chromatography–mass spectrometry (LC-MS). Protein identification was performed with Mascot v2.2 (Matrix Science) using the genome sequence of *M. marburgensis*.

Paper

Purification, catalytic activity assay and crystallization of HcgB

E. coli BL21(DE3) cells (Invitrogen) were transformed with pET24b harbouring *hcgB* from *M. maripaludis*. Expression and purification of HcgB from *M. maripaludis* were carried out in the same way as reported for *M. jannaschii*.⁵¹ Concentration of HcgB was determined by the Bradford method. For crystallization of HcgB from *M. maripaludis*, 1 μl aliquot of 11 mg ml⁻¹ HcgB in 10 mM 3-(*N*-morpholino)propanesulfonic acid (MOPS)/KOH (pH 7.0) was mixed with 1 μl of the reservoir solution composed of 0.1 M CAPS (pH 10.5), 0.2 M NaCl and 20% (w/v) PEG8000. The crystals of HcgB from *M. maripaludis* were grown at 8 °C by the sitting drop vapor diffusion method and obtained within one week. The catalytic activity (turnover rate of product formation = 0.165 min⁻¹) of HcgB from *M. maripaludis* was characterized at 37 °C by guanylylpyridinol formation using the reaction mixture of 1 mM GTP, 1 mM precursor 1 (Fig. 5), 1 mM MgCl₂ and 1 μM HcgB from *M. maripaludis* in 10 mM MOPS/KOH buffer (pH 7.0).⁵¹

HcgB from *M. jannaschii* was purified as reported previously.⁵¹ Co-crystals of HcgB from *M. jannaschii* and precursor 2 were obtained from the mixture of 0.5 μl of 17 mg ml⁻¹ HcgB from *M. jannaschii* in 10 mM MOPS/KOH (pH 7.0), 0.2 μl of 1.6 mM GP-derived pyridinol in H₂O and 1.0 μl of the reservoir solution containing 0.1 M sodium cacodylate (pH 6.5), 20% (w/v) PEG8000 and 0.2 M magnesium acetate. The crystals were grown at 8 °C by the sitting drop vapor diffusion method and obtained within two weeks.

Activity assay of HcgC

The reaction mixture contained 1 μM HcgC from *M. maripaludis*, 1 mM SAM, 1 mM pyridinol precursor 1 (Fig. 5) or 0.2 mM guanylylpyridinol produced by the HcgB reaction from precursor 2 and 10 mM MOPS/KOH pH 7.0. The production of the methylated guanylylpyridinol (precursor 3) was determined by matrix-assisted laser desorption/ionization time of flight mass spectrometry (MALDI-TOF-MS).

X-ray data collection and refinement

The crystals of HcgB from *M. maripaludis* and the precursor 2-bound HcgB from *M. jannaschii* were frozen under a cryo-stream of N₂ at 100 K without adding a cryoprotectant. Diffraction data were collected on beamline X10SA equipped with a PILATUS 6M detector at the Swiss-Light Source (Villigen, Switzerland) at 100 K. Data were processed using XDS.⁶⁵ Both HcgB structures were solved by molecular replacement using Phaser⁶⁶ and further refined using COOT,⁶⁷ REFMAC5 (ref. 68) and PHENIX.⁶⁹ PHENIX Xtriage⁶⁹ indicated that the data set of HcgB with the GP-derived pyridinol as pseudo-merohedral twinned with the twin fraction of 0.4 and the twin operator of $l, -k, h$. Thus, twin refinement was performed for HcgB with the GP-derived pyridinol using PHENIX refine.⁶⁹ A model of precursor 2 was created by the Dundee PRODRG server.⁷⁰ TLS (translation, libration, screw-rotation) refinement was performed in the final stage of the refinement.⁷¹ The final models were validated using MolProbity.⁷² The resulting structures were established at resolutions of 1.7 Å for HcgB from *M. maripaludis* (PDB code: 5D5P), and of 1.9 Å for GP-derived pyridinol-bound HcgB from *M. jannaschii* (PDB code: 5D5Q). All the protein figures were generated using PyMOL (Version 1.3r1, Schrödinger, LLC).

Reconstitution of [Fe]-hydrogenase with the mimic compound

The mimic with three CO ligands and an iodine ligand was dissolved in methanol containing 1% acetic acid to convert to the mimic compound with two CO ligands and one acetate ligand. For reconstitution of the semi-synthetic enzyme, 0.5 mM [Fe]-hydrogenase apoenzyme (final concentration) was mixed with 0.5 mM mimic compound and incubated for 1 h on ice under 100% N₂ atmosphere. The enzyme activity of the semi-synthetic [Fe]-hydrogenase was measured photometrically.⁴⁶ The assay solution contained 20 μM methylene-H₄MPT and 120 mM potassium phosphate buffer (pH 6.0). The reaction was started by addition of 10 μl of the reconstituted enzyme solution at 40 °C.

Results and discussion

Analysis of the genes responsible for biosynthesis of the FeGP cofactor

Previous studies indicated that the seven Hcg proteins are responsible for the biosynthesis of the FeGP cofactor. However, it cannot be excluded that other genes that are not part of the *hcg* gene cluster are required for cofactor biosynthesis. To find out the other possible biosynthetic genes, we employed a comparative genomics approach using the correlation coefficient calculation tool (CCCT) program.⁷³ This comparative genomics program identifies the genes, which coexist in the genomes with the target gene. The results shown in Table 1 indicated that the genes encoding HcgA, HcgG, HcgB and HcgE were detected with a high correlation coefficient confirming their coexistence in methanogens containing [Fe]-hydrogenase. Surprisingly, the genes encoding HcgC, HcgD and HcgF were not detected. We found that some of the methanogens, which belongs to Methanomicrobiales contain the genes encoding HcgC, HcgD and HcgF although the function of these three Hcg proteins in Methanomicrobiales is not known. Moreover, this comparative genomic analysis indicated that the genes encoding EhaF, EhaB, EhaH, EhaN, EhaJ and EhaO also revealed high correlation coefficient with the [Fe]-hydrogenase gene. The Eha proteins are subunits of an energy-conserving membrane-spanning hydrogenase, which occurs in methanogenic archaea of the methanogens without cytochromes. Many of them also contain a [Fe]-hydrogenase.

To complete the biosynthesis pathway of the FeGP cofactor, the enzymes, which catalyze formation of precursor 1 (Fig. 5), acyl- and CO-ligands are required. HcgA and HcgG could be involved in the biosynthetic reaction but proteins other than Hcg appear to be necessary. The comparative genomics analysis indicated the other two genes coexist with [Fe]-hydrogenase. The genes (YP_001324386.1 and YP_001324447.1) are annotated as cofactor-independent phosphoglycerate mutase and succinate dehydrogenase flavoprotein subunit, respectively, but their real physiological function is not known. These genes might encode additional enzymes involved in biosynthesis of the FeGP cofactor.

Identification of Hcg proteins in *M. marburgensis*

As described above, the structure to function analysis confirmed the participation of Hcg proteins in the biosynthesis of the FeGP cofactor. However, expression of the *hcg* genes and production of the Hcg proteins in the methanogen cells are not reported yet. To analyze the Hcg proteins produced in *Methanothermobacter*

Paper

Table 1 Results of comparative genomics analysis using the correlation coefficient calculation tool (CCCT).⁷³ We used the genome data of *Methanococcus aeolicus* Nankai-3, *Methanobrevibacter smithii* ATCC35061, *Methanocaldococcus jannaschii* DSM2661, *Methanococcus maripaludis* strains C5, C6, C7, and S2, *Methanococcus vannielii* SB, *Methanocorpusculum labreanum* Z, *Methanopyrus kandleri* AV19, *Methanothermobacter thermautotrophicus* ΔH. All of them contain a [Fe]-hydrogenase. As species devoid of [Fe]-hydrogenase, the genome data of *Methanococcoides burtonii* DSM6242, *Methanoculleus marisnigri* JR1, *Methanosaeta thermophila* PT, *Methanosarcina acetivorans* C2A, *Methanosarcina barkeri* Fusaro, *Methanosarcina mazei* Go1, *Methanosphaera stadtmanae* DSM3091, *Methanospirillum hungatei* JF1 were used

Gene number	Correlation coefficient	Protein name	Annotated functions
YP_001325216.1	0.92	HcgA	[FeFe]-hydrogenase maturation protein HydE homologue
YP_001325218.1	0.90	HcgG	Fibrillar protein-like protein
YP_001325479.1	0.85	HcgB	Guanylyl transfer to pyridinol
YP_001324561.1	0.85	EhaF	Energy conserving hydrogenase A, F subunit
YP_001324557.1	0.85	EhaB	Energy conserving hydrogenase A, B subunit
YP_001324815.1	0.84		Methionyl-tRNA synthetase
YP_001324563.1	0.83	EhaH	Energy conserving hydrogenase A, H subunit
YP_001324569.1	0.82	EhaN	Energy conserving hydrogenase A, N subunit
YP_001324744.1	0.82	HcgE	Adenylation of carboxymethyl group of guanylylpyridinol
YP_001324565.1	0.82	EhaJ	Energy conserving hydrogenase A, J subunit
YP_001324386.1	0.81		Cofactor-independent phosphoglycerate mutase
YP_001324447.1	0.81		Succinate dehydrogenase flavoprotein subunit: thiol:fumarate reductase, subunit A
YP_001324889.1	0.80	HmdII	H ₂ -forming methylene tetrahydromethanopterin dehydrogenase-related protein
YP_001324574.1	0.80		CBS domain-containing protein: this gene locates nearby the Eha gene cluster in <i>Methanothermobacter marburgensis</i>
YP_001324570.1	0.80	EhaO	Energy conserving hydrogenase A, O subunit

marburgensis, the cell extracts were prepared from the methanogen cells, which were cultivated under nickel-limiting and nickel-sufficient conditions, and disrupted. The proteins contained in the cell extract were fractionated by blue-native gel electrophoresis and digested with trypsin in the gel pieces. The digested peptides were analyzed by electrospray-ionization-mass-spectrometry to determine the amino-acid sequence of the peptides.⁶⁴ The stained blue-native polyacrylamide gel and the position of the gel-pieces are shown in Fig. 7. The value of the exponentially modified protein abundance index (emPAI) are a measure for the quantity of the peptides (Table 2). Production of [Fe]-hydrogenase (Hmd) and

Frh subunit A (FrhA) is known to be up-regulated and down-regulated under the nickel-limiting conditions, respectively. The empAI values of Hmd and FrhA under nickel-limiting condition were 4-fold higher and 7-fold lower than those under nickel-sufficient condition, respectively, which was consistent with previous findings. The empAI values of the Hmd paralogues (HmdII and HmdIII) and other methanogenic enzymes were almost identical under both conditions, which was also in accordance with former observations. These results indicated that we can quantify the proteins produced in the cell extract using the empAI values.

All Hcg proteins were identified in the cell extracts although the empAI values were relatively low compared to those of the methanogenic enzymes. The low empAI values could be due to the lower concentration of the proteins in the cells because the concentration of the biosynthetic proteins is generally lower than that of proteins involved in the energy metabolism. The Hcg proteins except for HcgF were detected in the sample from the nickel-limiting culture, whereas in the sample from the nickel-sufficient culture, only HcgE, HcgF and HcgG were present. These results indicated that the Hcg proteins are produced in *M. marburgensis* and the production of the Hcg proteins increased in the nickel-limiting culture conditions.

Binding of the Coomassie Brilliant Blue dye can stabilize protein-protein interaction and therefore it is possible to detect associated proteins in the blue native polyacrylamide gel electrophoresis. As shown in Table 2, some of the Hcg proteins were detected in several gel pieces, which are distantly located. This observation might be interpreted that the Hcg proteins are associated with different proteins in the cell.

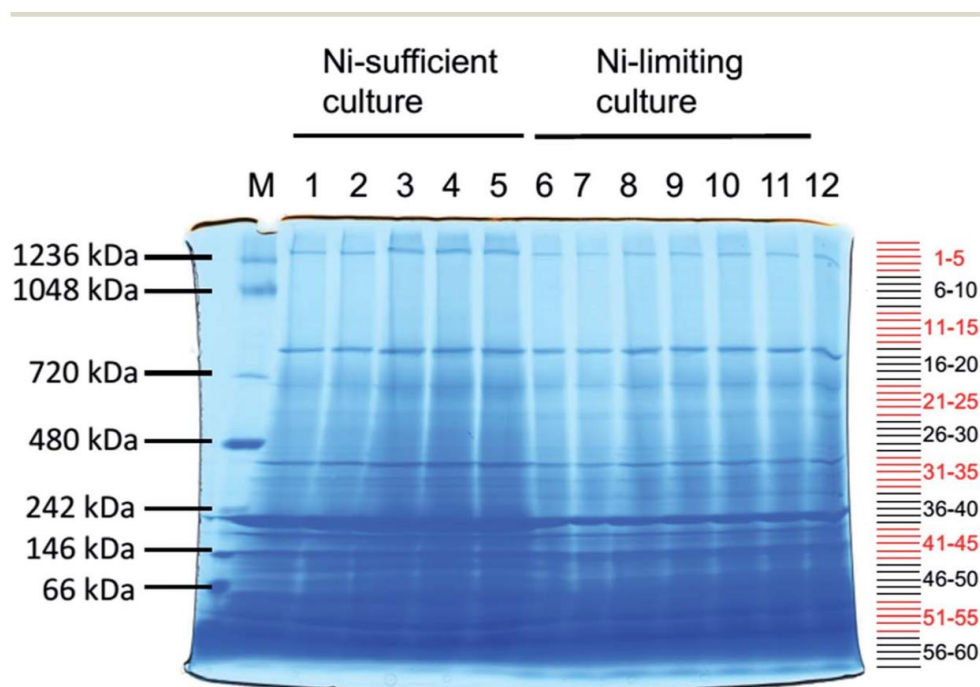


Fig. 7 Blue-native-polyacrylamide-gel-electrophoresis. (M) marker of the protein size. The size of the standard proteins are described (left). Cell extracts from the cells cultivated under nickel-sufficient conditions (lane 1–5) and nickel-limiting conditions (6–12). The positions of gel pieces cut from the gel are indicated (right). Because the gel was manually sliced, the position of the gel pieces is not exactly as indicated.

Paper

Table 2 Identification of the Hcg proteins and the methanogenic enzymes by LC-MS/MS of the fractions from blue-native-PAGE⁶⁴ of the cell extracts from *M. marburgensis* cultivated under nickel-limiting and nickel-sufficient conditions^a

Enzyme	Nickel-limiting culture		Nickel-sufficient culture	
	Gel number	emPAI	Gel number	emPAI
Hmd	56	21	56	5.5
HmdII	55	7.8	53	5.2
HmdIII	51/54/56	0.34/0.21/0.34	20/53/56	0.1/0.48/0.2
HcgA	7	0.1	ND	ND
HcgB	49	0.49	ND	ND
HcgC	58	0.13	ND	ND
HcgD	39/52	0.17/0.17	ND	ND
HcgE	19/50	0.22/0.22	41/54/55	0.17/0.17/0.17
HcgF	ND	ND	4/57	0.22/0.22
HcgG	49	0.07	16/39/45	0.07/0.07/0.07
Ftr	ND	ND	51/52	1.7/1.7
Mch	51/58	2.5/1.5	53	2.2
Mtd	45	280	48	310
Mer	55	1100	56	650
McrA (isoenzyme I)	38/39	20/22	43/44/45	13/18/8
McrA (isoenzyme II)	40	2.2	44/45	4.5/4.2
FrhA	12	7.5	15	50

^a ND, not detected. emPAI, exponentially modified protein abundance index.

The physiological substrate of HcgB

HcgB can use a relatively broad range of derivatives of 4-hydroxy-2-pyridinol as substrate.⁵¹ What is the physiological substrate of HcgB? Precursor 2, which is a methylated product of HcgC, is the most probable physiological substrate (see Fig. 5). However, it cannot be excluded that HcgC reacts with the guanylylpyridinol (precursor 3) analogue, which lacks the 3-methyl group. To test this possibility, we synthesized this guanylylpyridinol compound (precursor 3 lacking the 3-methyl group, $m/z = 529$) by the HcgB reaction using precursor 1 and GTP as the substrates (Fig. 8) and subjected it an HcgC enzyme assay. However, we did not detect the methylated product ($m/z = 543$) by mass spectrometric analysis. This result confirmed the proposed reaction sequence indicated in Fig. 5; the physiological substrate of HcgB is precursor 2.

To further corroborate the physiological substrate of HcgB, the crystal structure of HcgB from *M. jannaschii* complexed with precursor 2 was solved at 2.5 Å resolution (Fig. 9, Table 3) (PDB code 5D5Q). The structure revealed precursor 2 embedded into the same binding pocket with the same orientation as the corresponding pyridinol moiety of the guanylylpyridinol (precursor 3 in Fig. 5) in the previously reported HcgB-precursor 3-bound structure (Fig. 9D).⁵¹ The 3-methyl group of pyridinol forms van der Waals contacts to Asp77, Arg20 and Arg104 (Fig. 9C) and might play a role to adjust precursor 2 in the most productive orientation together with the other pyridinols' substituents. This crystal structure of HcgB with precursor 2 also supported precursor 2 as the physiological substrate of HcgB. In addition, we also solved the crystal structure of HcgB from

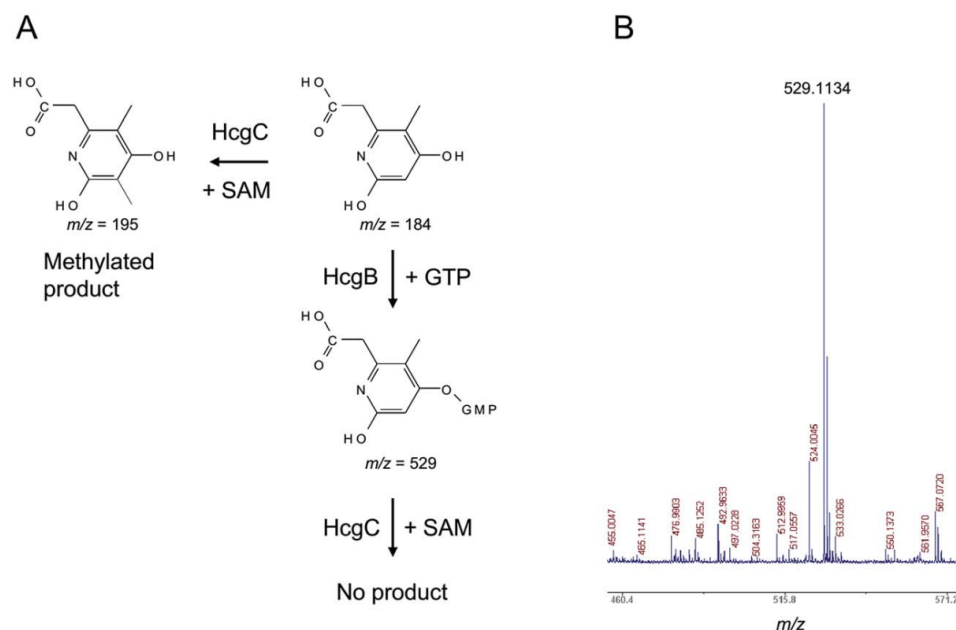


Fig. 8 The substrate of HcgC. (A) Reaction scheme, in which precursor 1 either reacts with SAM to give the product catalysed by HcgC or reacts with GTP to give guanylylpyridinol (precursor 3 lacking the 3-methyl group) by HcgB. The HcgB product was used as the methyl acceptor of the HcgC reaction. (B) Mass spectrum of the product of the HcgB reaction using precursor 1 as the substrate ($m/z = 529$). The former reaction worked but product of the latter methylation reaction was not detected.

a mesophilic methanogen, *M. maripaludis*. The crystal structure was almost identical to that of *M. jannaschii* (PDB code 5D5P, Table 3).

Preparation of the guanylylpyridinol (precursor 3)

Precursor 3 can be used as the starting material for the *in vitro* biosynthesis of the FeGP cofactor. Previously, precursor 3 could only be prepared by light decomposition of the FeGP cofactor isolated from [Fe]-hydrogenase, which has been purified from *M. marburgensis*. The preparation procedure is time-consuming and the yield of the purified precursor 3 was very low. Now, chemical synthesis of precursor 1 and the finding of the reactions of HcgC and HcgB make it possible to easily prepare a large amount of precursor 3. In routine biosynthesis experiments, we used the 5 ml reaction mixture containing 0.1 mM precursor 1, 1 mM SAM, 1 μ M HcgC from *M. maripaludis* and 10 mM MOPS/KOH pH 7.0. The HcgC reaction mixture was incubated at 37 $^{\circ}$ C for 2 h and then 1 μ M HcgB from *M. maripaludis*, 1 mM GTP and 1 mM $MgCl_2$ (final concentrations) were added and further incubated at 37 $^{\circ}$ C for 2 h. Most of the substrates were converted to the product. The guanylylpyridinol (precursor 3) in the reaction mixture was purified using a Q Sepharose HP HiTrap column (1 ml volume), which was equilibrated with 10 mM 2-(*N*-morpholino)ethanesulfonic acid (MES)/NaOH. The compound was eluted at \sim 0.4 M NaCl in the linear gradient of NaCl from 0 to 1 M. The sample was desalted with Polar RP 80A (Phenomenex) equilibrated with water at pH 4.0 (HCl) and elution was performed by a linear gradient of methanol from 0 to 100%. The target compound was eluted at 87% methanol. In this procedure, we could purify 0.12 μ mol of precursor 3 (Fig. 10).

Paper

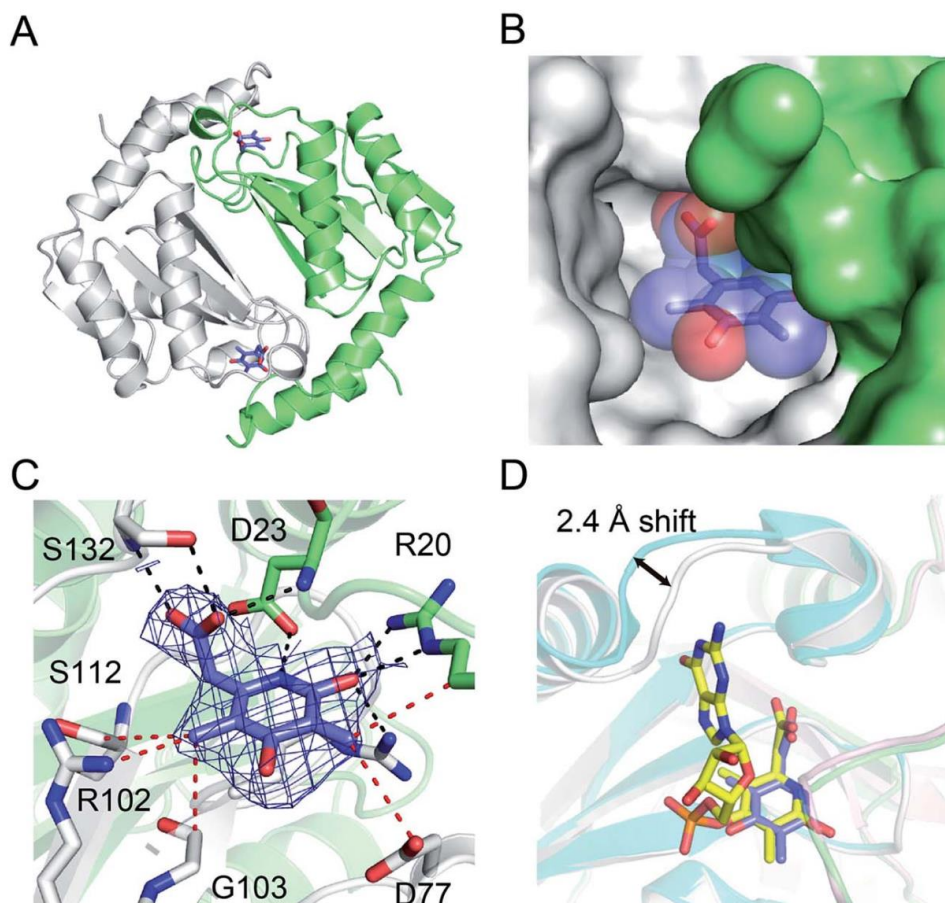


Fig. 9 Crystal structure of HcgB in complex with precursor **3**. (A) Overall structure in an HcgB homodimer with precursor **3** (Fig. 5). The precursor was represented as a blue stick model. (B) Surface representation of the active site cleft of HcgB. The precursor **3** was shown as a stick model (carbons in blue) with transparent spheres. (C) The active site structure. The $2F_o - F_c$ electron density map was contoured at 1σ (blue mesh). The pyridinol is bound to the polypeptide (6-carboxymethyl to Ser132, pyridinol-NH to Asp23 and 2-hydroxylate to Arg20). Close contacts (3.4–3.9 Å) between the 3- or 5-methyl groups of the pyridinol and surrounding amino acids are shown as red dashed lines. (D) Superimposition of pyridinol-bound HcgB (white and green) and guanylylpyridinol (precursor **3**)-bound HcgB (PDB code: 3WB0, cyan and pink). The guanylylpyridinol (precursor **3**) is represented as a stick model (carbon in yellow). The pyridinol moieties in both structures are located at equivalent positions. The flexible loop is shifted outwards upon binding of GMP part.

Characterization of semi-synthetic [Fe]-hydrogenase

The specific activity of the semi-synthetic [Fe]-hydrogenase was reported to be ~ 1 U mg^{-1} , which is $\sim 1\%$ of the specific activity of the native enzyme. We reconstituted [Fe]-hydrogenase using several different [Fe]-hydrogenase apoenzymes (enzymes without the cofactor) from *M. jannaschii* (optimum growth temperature, 85 °C), *Methanoterris igneus* (85 °C), *Methanocaldococcus infernus* (85 °C), *Methanococcus aeolicus* (37 °C), *Methanolacina paynteri* (37 °C) and *Methanoregula formicica* (30 °C) as shown in Fig. 11. The apoenzymes from hyperthermophilic methanogens (optimum growth temperature > 80 °C) revealed higher specific activity than those from mesophilic ones (20–45 °C). This finding indicated that

Table 3 Data collection and refinement statistics of HcgB structures

	Precursor 2-bound HcgB from <i>M. jannaschii</i>	HcgB from <i>M. maripaludis</i>
Data collection		
Temperature (K)	100	100
Wavelength (Å)	1.000	1.000
Space group	<i>P2</i> ₁	<i>P2</i> ₁
Resolution (Å)	50–2.5 (2.6–2.5)	50–1.7 (2.0–1.7)
Cell dimensions		
<i>a</i> , <i>b</i> , <i>c</i> (Å)	64.9, 76.5, 65.1	64.1, 72.5, 71.0
α , β , γ (°)	90, 106.8, 90	90, 99.1, 90
Completeness (%) ^a	98.3 (99.7)	99.6 (99.6)
<i>R</i> _{sym} (%) ^{a,b}	4.8 (33.8)	4.5 (73.0)
<i>I</i> / σ _{<i>I</i>} ^a	16.6 (3.9)	18.1 (2.6)
Redundancy ^a	3.3 (3.4)	3.9 (3.9)
Refinement statistics		
Resolution (Å)	43.1–2.5 (2.63–2.50)	43.7–1.7 (1.72–1.70)
No. of monomers/asymmetric unit	4	4
No. of ligands/asymmetric unit	4	0
No. of waters/asymmetric unit	56	367
<i>R</i> _{work} / <i>R</i> _{free} (%) ^{c,d}	20.6/23.2 (29.8/30.7)	18.5/21.5 (30.2/30.8)
rmsd bond length (Å) ^e	0.006	0.011
rmsd bond angle (°) ^e	1.128	1.351

^a The values in parentheses are for the highest resolution shell. ^b $R_{\text{sym}} = \frac{\sum \sum |I - \langle I \rangle|}{\sum I}$, where *I* is the intensity of each reflection. ^c $R_{\text{work}} = \frac{\sum ||F_{\text{o}}| - k|F_{\text{c}}||}{\sum |F_{\text{o}}|}$, where *F*_o and *F*_c are the observed and calculated structure factor amplitudes, respectively. ^d *R*_{free} was calculated as *R*_{work}; 5% of the reflections were excluded in refinement. ^e rmsd, root mean square deviation.

reconstitution efficiency is dependent on the nature of the apoenzyme which include its overall conformational state and the micro-structure of the active site.

It was found out that the reconstituted [Fe]-hydrogenase with the mimic lost activity quicker than the apoenzyme loaded with the FeGP cofactor. Fig. 12 indicated that the reconstituted enzyme with the FeGP cofactor was not inactivated in 36 h under oxic and anoxic conditions; however, the [Fe]-hydrogenase-mimic complex was substantially inactivated within this time period and the inactivation was even accelerated under air. The instability of the reconstituted enzyme might be due to the instability of the mimic compound bound to the protein. Under air, the iron centre, particularly the Cys176–S–Fe bond, might be damaged.

Towards the construction of artificial methanogenesis

Reconstitution of semi-synthetic hydrogenases with the mimic compound may motivate us to design other semi-synthetic methanogenic enzymes. However, other methanogenic enzymes with metallocofactors (Fwd/Fmd, MtrA–H, Mcr and Hdr–Mvh) have very complicated structures. It might be too difficult to construct

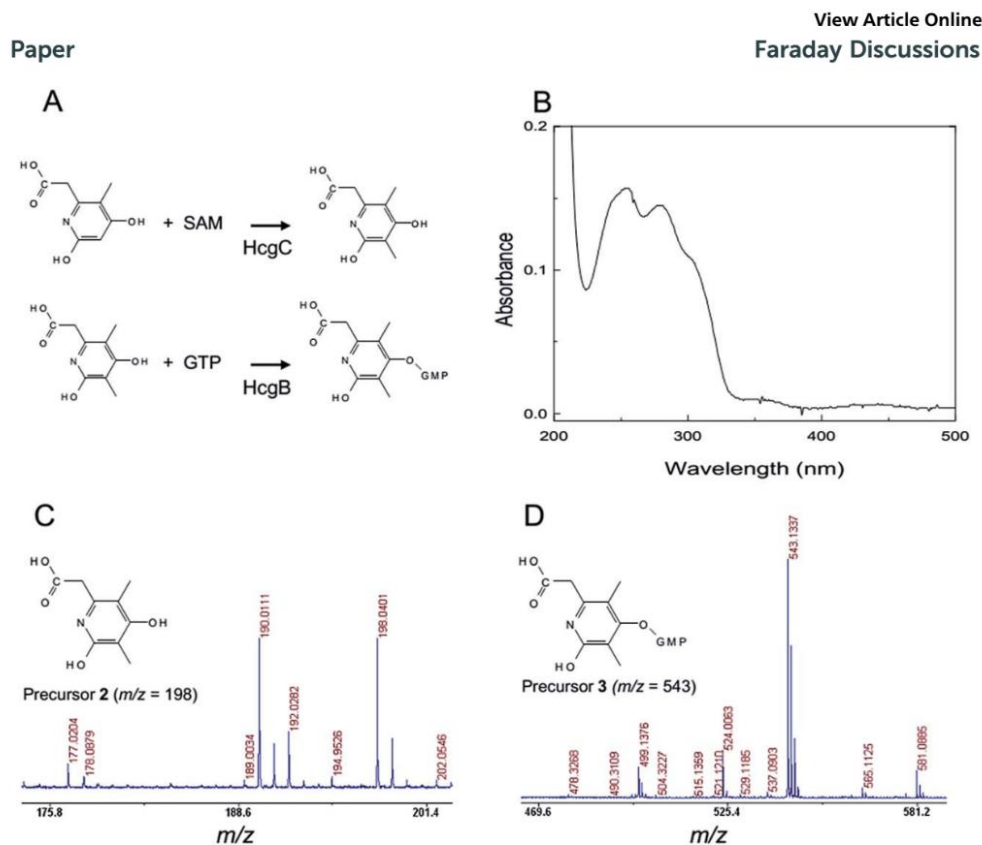


Fig. 10 Preparation of the guanylylpyridinol (precursor 3). Chemically synthesized precursor 1 (Fig. 5) was methylated by the HcgC reaction using *S*-adenosylmethionine (SAM) as the methyl-donor. Then precursor 2 was guanylated by HcgB. (A) The HcgC and HcgB catalyzed reactions. (B) UV-vis spectrum of the purified precursor 3 biosynthesized by the HcgC and HcgB reactions. (C) Chemical structure and mass spectrum of the methylated product of the HcgC reaction (precursor 2, $m/z = 198$). (D) Chemical structure and mass spectrum of the guanylated product of the HcgB reaction (precursor 3, $m/z = 543$).

methane-forming catalysts or semi-synthetic enzymes by mimicking the full enzymatic systems. However, we do not have to integrate all enzymes involved in the methanogenic pathway for an artificial system because the methanogenic

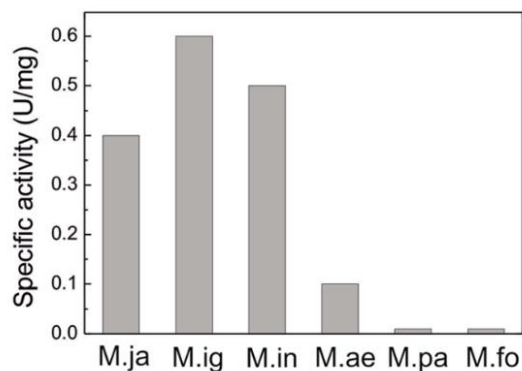


Fig. 11 Specific activity of the reconstituted semi-synthetic [Fe]-hydrogenase. (M.ja) *M. jannaschii*, (M.ig) *Methanotorris igneus*, (M.in) *Methanocaldococcus infernus*, (M.ae) *Methanococcus aeolicus*, (M.pa) *Methanolacinia paynteri*, (M.fo) *Methanoregula formica*.

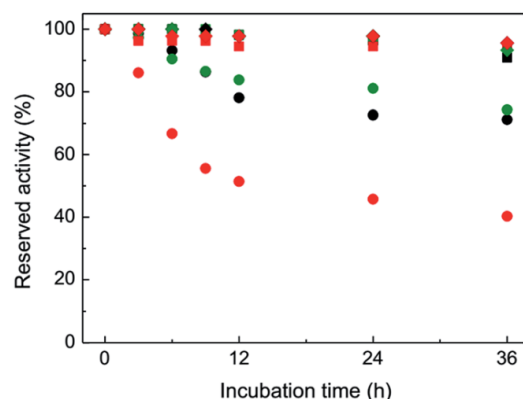


Fig. 12 Stability of the reconstituted semi-synthetic [Fe]-hydrogenase. (● circle) Reconstituted enzymes using the mimic compound. (■ square) Reconstituted enzymes using the FeGP cofactor. (♦ diamond) Native [Fe]-hydrogenase from *M. marburgensis*. The samples (1 mg ml^{-1}) in 10 mM MOPS/KOH pH 7.0 with 1 mM DTT were incubated at 8°C under 100% N₂ (black), 95% N₂/5% H₂ (green) and under air (red). 10 μl of the samples were withdrawn from the sample vial and tested for the [Fe]-hydrogenase activity at 40°C according to previous reports.^{45,46}

pathway was evolved for energy conservation rather than for methane formation. For example, the cobalamine containing membrane-spanning methyltransferase (MtrA-H) complex has the function to conserve energy by sodium-ion translocation. In artificial methanogenesis, this enzyme can be replaced by a simpler enzyme or catalyst which produces methane directly from methyl-H₄MPT. Although such an enzyme is not known in nature, some methylamine methyltransferases can cleave N-CH₃ bonds.⁷⁴ Their structure and mechanism may teach us how to design new catalysts, which produce methane from methyl-H₄MPT.

The terminal step of biological methane formation is catalyzed by Mcr, which contains the nickel porphyrinoid F₄₃₀. The heterodisulfide CoM-S-S-CoB, the physiologically highly important product of the Mcr reaction, is used as the strong electron-accepting substrate in the heterodisulfide reductase reaction in which ferredoxin is reduced *via* a flavin-based electron bifurcation reaction. The reduced ferredoxin is necessary for the first methanogenic CO₂ reduction-and-fixation reaction catalyzed by formyl-MFR dehydrogenase (Fwd or Fmd). If methyl-H₄MPT is the substrate for methane production, the original substrate methyl-S-CoM is not present and the important oxidant CoM-S-S-CoB cannot be produced by Mcr. However, if an electron donor with a redox potential lower than ferredoxin ($E^{\circ\prime} = \sim -500 \text{ mV}$), is available from artificial photosynthesis, the electron bifurcating enzyme becomes obsolete.

Conclusion

In the introductory part, we reviewed the biological methane formation from CO₂, [Fe]-hydrogenase and the biosynthesis of its cofactor, and finally the reconstitution of the semi-synthetic [Fe]-hydrogenase. In the experimental part, we analyzed possible enzymes for biosynthesis of the FeGP cofactor by comparative genomics and predicted two additional genes. The presence of the Hcg proteins in the cell

Paper

extract was determined by proteomics analysis using blue native polyacrylamide gel electrophoresis and mass-spectrometric sequencing. Moreover, we obtained further evidence regarding the reaction sequence of the biosynthetic pathway of the FeGP cofactor by an enzyme activity assay of HcgC and the crystal structure analysis of HcgB complexed with precursor 2 (Fig. 5). Finally, we tested the reconstitution efficiency of semi-synthetic [Fe]-hydrogenases using different [Fe]-hydrogenase apoenzymes and the stability of the semi-synthetic enzymes. On the basis of the enzymatic reactions involved in the methanogenic pathway, we came up with an idea how the methanogenic pathway could be simplified to develop an artificial methanogenesis system.

Acknowledgements

We thank R. Thauer for his discussions and helpful suggestions. This work was supported by grants from the Max Planck Society (to R. Thauer, S. Shima and U. Ermler), Deutsche Forschungsgemeinschaft-Priority Programme (Iron-Sulfur for Life, SH-87/1-1 to S.S.) the PRESTO program from the Japan Science and Technology Agency (to S. Shima) and the Swiss National Science Foundation (no. 200020_152850/1 to X. L. Hu). L. Bai and G. Huang were supported by the fellowship from China Scholarship Council (CSC). We are also grateful to H. Michel for continuous support, J. Kahnt for mass-spectrometry measurements and the staff of the SLS, Villigen for help in data collection.

References

- 1 R. K. Thauer, A. K. Kaster, H. Seedorf, W. Buckel and R. Hedderich, *Nat. Rev. Microbiol.*, 2008, **6**, 579–591.
- 2 R. K. Thauer, A. K. Kaster, M. Goenrich, M. Schick, T. Hiromoto and S. Shima, *Annu. Rev. Biochem.*, 2010, **79**, 507–536.
- 3 S. Shima and R. K. Thauer, *Hyperthermophilic Enzymes, part B*, 2001, vol. 331, pp. 317–353.
- 4 P. Schönheit, J. Moll and R. K. Thauer, *Arch. Microbiol.*, 1980, **127**, 59–65.
- 5 K. M. Schultz, D. Chen and X. Hu, *Chem.–Asian J.*, 2013, **8**, 1068–1075.
- 6 T. Xu, C. J. Yin, M. D. Wodrich, S. Mazza, K. M. Schultz, R. Scopelliti and X. Hu, *J. Am. Chem. Soc.*, 2016, **138**, 3270–3273.
- 7 T. Wagner, U. Ermler and S. Shima, *Science*, 2016, **354**, 114–117.
- 8 U. Ermler, M. C. Merckel, R. K. Thauer and S. Shima, *Structure*, 1997, **5**, 635–646.
- 9 S. Shima, R. K. Thauer, H. Michel and U. Ermler, *Proteins*, 1996, **26**, 118–120.
- 10 P. Acharya, E. Warkentin, U. Ermler, R. K. Thauer and S. Shima, *J. Mol. Biol.*, 2006, **357**, 870–879.
- 11 W. Grabarse, M. Vaupel, J. A. Vorholt, S. Shima, R. K. Thauer, A. Wittershagen, G. Bourenkov, H. D. Bartunik and U. Ermler, *Structure With Folding & Design*, 1999, **7**, 1257–1268.
- 12 K. Ceh, U. Demmer, E. Warkentin, J. Moll, R. K. Thauer, S. Shima and U. Ermler, *Biochemistry*, 2009, **48**, 10098–10105.
- 13 C. H. Hagemeyer, S. Shima, R. K. Thauer, G. Bourenkov, H. D. Bartunik and U. Ermler, *J. Mol. Biol.*, 2003, **332**, 1047–1057.

Faraday Discussions

- 14 S. W. Aufhammer, E. Warkentin, U. Ermler, C. H. Hagemeyer, R. K. Thauer and S. Shima, *Protein Sci.*, 2005, **14**, 1840–1849.
- 15 S. Shima, E. Warkentin, W. Grabarse, M. Sordel, M. Wicke, R. K. Thauer and U. Ermler, *J. Mol. Biol.*, 2000, **300**, 935–950.
- 16 R. K. Thauer, *Microbiology*, 1998, **144**, 2377–2406.
- 17 A. A. Dimarco, T. A. Bobik and R. S. Wolfe, *Annu. Rev. Biochem.*, 1990, **59**, 355–394.
- 18 T. Wagner, U. Ermler and S. Shima, *Sci. Rep.*, 2016, **6**, 28226.
- 19 G. Gottschalk and R. K. Thauer, *Biochim. Biophys. Acta*, 2001, **1505**, 28–36.
- 20 U. Ermler, W. Grabarse, S. Shima, M. Goubeaud and R. K. Thauer, *Science*, 1997, **278**, 1457–1462.
- 21 W. Grabarse, F. Mahler, E. C. Duin, M. Goubeaud, S. Shima, R. K. Thauer, V. Lamzin and U. Ermler, *J. Mol. Biol.*, 2001, **309**, 315–330.
- 22 S. Shima, M. Goubeaud, D. Vinzenz, R. K. Thauer and U. Ermler, *J. Biochem.*, 1997, **121**, 829–830.
- 23 E. C. Duin, T. Wagner, S. Shima, D. Prakash, B. Cronin, D. R. Yáñez-Ruiz, S. Duval, R. Ruembeli, R. T. Stemmler, R. K. Thauer and M. Kindermann, *Proc. Natl. Acad. Sci. U. S. A.*, 2016, **113**, 6172–6177.
- 24 T. Wagner, J. Kahnt, U. Ermler and S. Shima, *Angew. Chem., Int. Ed.*, 2016, **55**, 10630–10633.
- 25 T. Wongnate, D. Sliwa, B. Ginovska, D. Smith, M. W. Wolf, N. Lehnert, S. Rauei and S. W. Ragsdale, *Science*, 2016, **352**, 953–958.
- 26 R. Hedderich, A. Berkessel and R. K. Thauer, *Eur. J. Biochem.*, 1990, **193**, 255–261.
- 27 R. Hedderich, J. Koch, D. Linder and R. K. Thauer, *Eur. J. Biochem.*, 1994, **225**, 253–261.
- 28 E. Setzke, R. Hedderich, S. Heiden and R. K. Thauer, *Eur. J. Biochem.*, 1994, **220**, 139–148.
- 29 W. Buckel and R. K. Thauer, *Biochim. Biophys. Acta, Bioenerg.*, 2013, **1827**, 94–113.
- 30 A. K. Kaster, J. Moll, K. Parey and R. K. Thauer, *Proc. Natl. Acad. Sci. U. S. A.*, 2011, **108**, 2981–2986.
- 31 C. Afting, A. Hochheimer and R. K. Thauer, *Arch. Microbiol.*, 1998, **169**, 206–210.
- 32 D. J. Mills, S. Vitt, M. Strauss, S. Shima and J. Vonck, *eLife*, 2013, **2**, e00218.
- 33 S. Vitt, K. Ma, E. Warkentin, J. Moll, A. J. Pierik, S. Shima and U. Ermler, *J. Mol. Biol.*, 2014, **426**, 2813–2826.
- 34 S. W. Aufhammer, E. Warkentin, H. Berk, S. Shima, R. K. Thauer and U. Ermler, *Structure*, 2004, **12**, 361–370.
- 35 E. Warkentin, B. Mamat, M. Sordel-Klippert, M. Wicke, R. K. Thauer, M. Iwata, S. Iwata, U. Ermler and S. Shima, *EMBO J.*, 2001, **20**, 6561–6569.
- 36 S. Shima and U. Ermler, *Eur. J. Inorg. Chem.*, 2011, 963–972, DOI: 10.1002/ejic.201000955.
- 37 T. Hiromoto, K. Ataka, O. Pilak, S. Vogt, M. S. Stagni, W. Meyer-Klaucke, E. Warkentin, R. K. Thauer, S. Shima and U. Ermler, *FEBS Lett.*, 2009, **583**, 585–590.
- 38 S. Shima, O. Pilak, S. Vogt, M. Schick, M. S. Stagni, W. Meyer-Klaucke, E. Warkentin, R. K. Thauer and U. Ermler, *Science*, 2008, **321**, 572–575.

Paper

- 39 S. Shima, M. Schick, J. Kahnt, K. Ataka, K. Steinbach and U. Linne, *Dalton Trans.*, 2012, **41**, 767–771.
- 40 M. Korbas, S. Vogt, W. Meyer-Klaucke, E. Bill, E. J. Lyon, R. K. Thauer and S. Shima, *J. Biol. Chem.*, 2006, **281**, 30804–30813.
- 41 E. J. Lyon, S. Shima, R. Boecher, R. K. Thauer, F. W. Grevels, E. Bill, W. Roseboom and S. P. J. Albracht, *J. Am. Chem. Soc.*, 2004, **126**, 14239–14248.
- 42 E. J. Lyon, S. Shima, G. Buurman, S. Chowdhuri, A. Batschauer, K. Steinbach and R. K. Thauer, *Eur. J. Biochem.*, 2004, **271**, 195–204.
- 43 S. Shima, E. J. Lyon, M. S. Sordel-Klippert, M. Kauss, J. Kahnt, R. K. Thauer, K. Steinbach, X. L. Xie, L. Verdier and C. Griesinger, *Angew. Chem., Int. Ed.*, 2004, **43**, 2547–2551.
- 44 G. Buurman, S. Shima and R. K. Thauer, *FEBS Lett.*, 2000, **485**, 200–204.
- 45 S. Shima, M. Schick and H. Tamura, *Methods Enzymol.*, 2011, **494**, 119–137.
- 46 S. Shima, D. F. Chen, T. Xu, M. D. Wodrich, T. Fujishiro, K. M. Schultz, J. Kahnt, K. Ataka and X. L. Hu, *Nat. Chem.*, 2015, **7**, 995–1002.
- 47 M. Schick, X. L. Xie, K. Ataka, J. Kahnt, U. Linne and S. Shima, *J. Am. Chem. Soc.*, 2012, **134**, 3271–3280.
- 48 T. Fujishiro, L. Bai, T. Xu, X. Xie, M. Schick, J. Kahnt, M. Rother, X. Hu, U. Ermler and S. Shima, *Angew. Chem., Int. Ed.*, 2016, **55**, 9648–9651.
- 49 T. Fujishiro, U. Ermler and S. Shima, *FEBS Lett.*, 2014, **588**, 2789–2793.
- 50 T. Fujishiro, J. Kahnt, U. Ermler and S. Shima, *Nat. Commun.*, 2015, **6**, 6895.
- 51 T. Fujishiro, H. Tamura, M. Schick, J. Kahnt, X. L. Xie, U. Ermler and S. Shima, *Angew. Chem., Int. Ed.*, 2013, **52**, 12555–12558.
- 52 D. Chen, A. Ahrens-Botzong, V. Schunemann, R. Scopelliti and X. Hu, *Inorg. Chem.*, 2011, **50**, 5249–5257.
- 53 D. Chen, R. Scopelliti and X. Hu, *J. Am. Chem. Soc.*, 2010, **132**, 928–929.
- 54 D. Chen, R. Scopelliti and X. Hu, *Angew. Chem., Int. Ed.*, 2010, **49**, 7512–7515.
- 55 D. Chen, R. Scopelliti and X. Hu, *Angew. Chem., Int. Ed.*, 2011, **50**, 5671–5673.
- 56 D. Chen, R. Scopelliti and X. Hu, *Angew. Chem., Int. Ed.*, 2012, **51**, 1919–1921.
- 57 B. Hu, D. Chen and X. Hu, *Chem.–Eur. J.*, 2012, **18**, 11528–11530.
- 58 B. Hu, D. Chen and X. Hu, *Chem.–Eur. J.*, 2013, **19**, 6221–6224.
- 59 B. Hu, D. Chen and X. Hu, *Chem.–Eur. J.*, 2014, **20**, 1677–1682.
- 60 X. Hu, B. S. Brunshwig and J. C. Peters, *J. Am. Chem. Soc.*, 2007, **129**, 8988–8998.
- 61 K. A. Murray, M. D. Wodrich, X. Hu and C. Corminboeuf, *Chem.–Eur. J.*, 2014, **21**, 3978–3996.
- 62 B. V. Obrist, D. Chen, A. Ahrens, V. Schunemann, R. Scopelliti and X. Hu, *Inorg. Chem.*, 2009, **48**, 3514–3516.
- 63 P. Schönheit, J. Moll and R. K. Thauer, *Arch. Microbiol.*, 1979, **123**, 105–107.
- 64 A. Takabayashi, A. Niwata and A. Tanaka, *Sci. Rep.*, 2016, **6**, 29668.
- 65 W. Kabsch, *Acta Crystallogr., Sect. D: Biol. Crystallogr.*, 2010, **66**, 125–132.
- 66 A. J. McCoy, R. W. Grosse-Kunstleve, P. D. Adams, M. D. Winn, L. C. Storoni and R. J. Read, *J. Appl. Crystallogr.*, 2007, **40**, 658–674.
- 67 P. Emsley and K. Cowtan, *Acta Crystallogr., Sect. D: Biol. Crystallogr.*, 2004, **60**, 2126–2132.
- 68 G. N. Murshudov, A. A. Vagin and E. J. Dodson, *Acta Crystallogr., Sect. D: Biol. Crystallogr.*, 1997, **53**, 240–255.

Faraday Discussions

- 69 P. V. Afonine, R. W. Grosse-Kunstleve, V. B. Chen, J. J. Headd, N. W. Moriarty, J. S. Richardson, D. C. Richardson, A. Urzhumtsev, P. H. Zwart and P. D. Adams, *J. Appl. Crystallogr.*, 2010, **43**, 669–676.
- 70 A. W. Schuttelkopf and D. M. F. van Aalten, *Acta Crystallogr., Sect. D: Biol. Crystallogr.*, 2004, **60**, 1355–1363.
- 71 M. D. Winn, M. N. Isupov and G. N. Murshudov, *Acta Crystallogr., Sect. D: Biol. Crystallogr.*, 2001, **57**, 122–133.
- 72 V. B. Chen, W. B. Arendall, J. J. Headd, D. A. Keedy, R. M. Immormino, G. J. Kapral, L. W. Murray, J. S. Richardson and D. C. Richardson, *Acta Crystallogr., Sect. D: Biol. Crystallogr.*, 2010, **66**, 12–21.
- 73 H. Ito, M. Yokono, R. Tanaka and A. Tanaka, *J. Biol. Chem.*, 2008, **283**, 9002–9011.
- 74 B. Hao, W. Gong, T. K. Ferguson, C. M. James, J. A. Krzycki and M. K. Chan, *Science*, 2002, **296**, 1462–1466.

3. Water-bridged H-bonding network contributes to the catalysis of a SAM-dependent C-methyltransferase HcgC

Abstract

[Fe]-hydrogenase contains the iron-guanylylpyridinol (FeGP) cofactor, which is composed of a pyridinol ring substituted by GMP, two methyl groups and a methyl acyl ligated with the pyridinol-N, two CO and a cysteine thiol to the catalytically active low spin Fe^{II}. HcgC, an enzyme of FeGP biosynthesis, catalyzes the methyl transfer from S-adenosylmethionine (SAM) to C3 of 6-carboxymethyl-5-methyl-4-hydroxy-2-pyridinol. Here, we report on the structure of HcgC in complex with the demethylated product of SAM, S-adenosylhomocysteine (SAH) and the pyridinol substrate at 1.7 Å resolution. The proximity of C3 of pyridinol and S of SAH indicates a catalytically productive geometry. The 2- and 4-hydroxy and the carboxy groups of pyridinol are primarily fixed by a series of water-mediated hydrogen-bonds to polar and a few protonable groups including Glu209 and the ammonium group of SAH. These interactions stabilize the deprotonated state of the hydroxy group and a pyridone state of the pyridinol substrate by which the nucleophilicity of C3, attacking the SAM methyl group, is increased by resonance effects. Complemented by mutational analysis a structure-based catalytic mechanism was proposed.

SAM-dependent methyltransferases, found in all three domains of life, catalyze methyltransfer reactions to diverse substrates of all sizes, which are involved in secondary metabolism, transcriptional regulation, signal-transduction and modifications of the active sites of enzymes [117, 118]. They are classified into O, N, C and S-methyltransferases dependent on the methyl-accepting atom of the substrates. C-methyltransferases are further subdivided into canonical SAM dependent enzymes [119-123] and radical-SAM dependent enzymes [124, 125]. They catalyze the methyl transfer to a nucleophilic carbon via the S_N2 mechanism and to the electrophilic sp² hybridized carbon, respectively. Notably, SAM-dependent methyltransferase have attracted attention as synthetic tool for biotechnological applications [126].

RESULTS/PUBLICATIONS

[Fe]-hydrogenase is involved in the methanogenic pathway from H_2 and CO_2 and catalyzes the reversible hydride transfer from H_2 to methenyl-tetrahydromethanopterin [88, 91, 127]. The active site of [Fe]-hydrogenase hosts an iron-guanylylpyridinol (FeGP) cofactor. The low spin Fe^{II} is coordinated to two CO, one cysteine thiolate and furthermore, by the nitrogen and the methyl acyl substituent of the pyridinol ring (Figure 3-1A). The pyridinol ring is further substituted with one guanosine monophosphate (GMP) and two methyl groups [87, 92, 128].

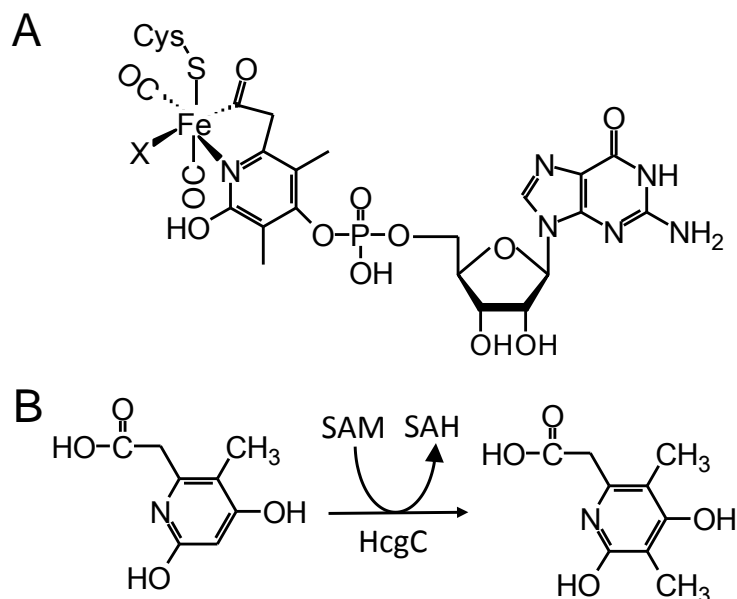


Figure 3-1. (A) Structure of the FeGP cofactor and (B) the HcgC catalyzed reaction.

According to isotope-labeling analysis, the 3-methyl group of pyridinol is originated from the methyl group of methionine, indicating the participation of a SAM dependent methyltransferase [93]. Recently, Fujishiro et al. have reported on the structure-based functional analysis of several biosynthetic enzymes for the FeGP cofactor, which are encoded in the *hcg* gene cluster [94, 98, 101]. They also determined the crystal structures of HcgC from *Methanocaldococcus jannaschii*. Structural comparison detected significant similarities between HcgC and the Rossmann-fold SAM-binding domain of methyltransferase RumA although the Blast search did not show any relationship. Biochemical experiments finally demonstrated that HcgC catalyzes the methyl transfer to C3 of 6-carboxymethyl-5-methyl-4-dihydroxy-2-pyridinol using SAM as a methyl donor (Figure 3-1B) [129]. In the reported HcgC-SAM complex structure, SAM binds in front of the C-terminal loop of the central parallel β -sheet of the N-terminal domain in line with group I SAM dependent methyltransferases characterized by a Rossmann-type $\alpha\beta$ fold. Docking simulation

RESULTS/PUBLICATIONS

convincingly suggested pyridinol binding in a pocket near the methyl group of SAM in HcgC. However, co-crystallization experiments between HcgC and the methylated pyridinol product were unsuccessful. Here, we report on the crystal structure of HcgC from *M. maripaludis* in complex with SAH and pyridinol substrate. Complemented with the kinetic analysis of several enzyme variants with site-specifically exchanged amino acids adjacent to the methyl acceptor, a catalytic mechanism for this methyltransferase was proposed.

His-tagged HcgC from *M. maripaludis* was heterologously produced in *E. coli*, purified using nickel-affinity chromatography and crystallized in the presence of the pyridinol substrate and SAH, as well as the pyridinol substrate and SAM. The HcgC-SAH-pyridinol structure determined at 1.7 Å resolution (Figure 3-2) reveals a dimer of homodimer architecture in analogy to the HcgC structure from *M. jannaschii*.

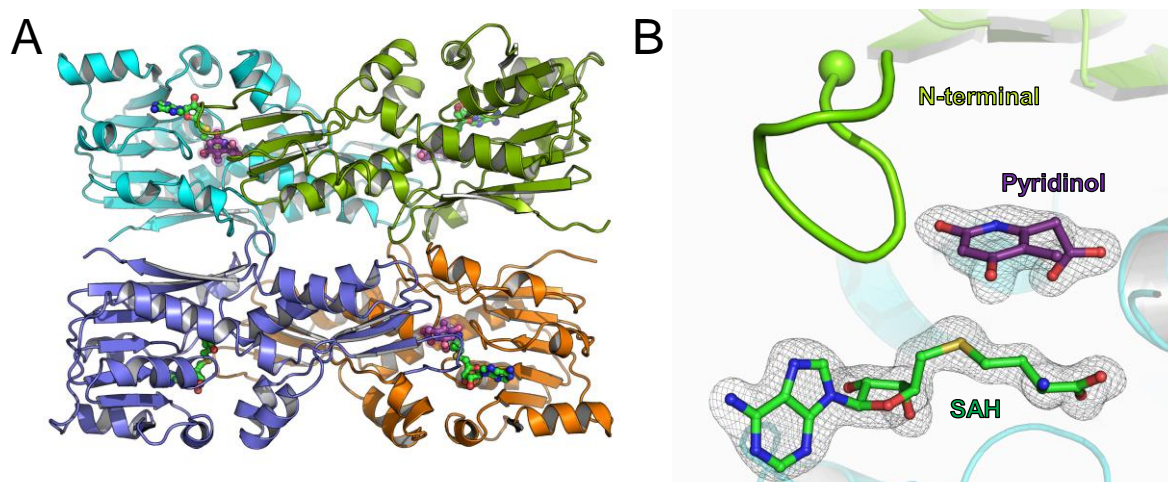


Figure. 3-2 The 1.7-Å crystal structure of HcgC complexed with SAH and the pyridinol substrate. The substrates are depicted with sticks. (A) Overall structure of the tetrameric form. (B) The active-site cleft with bound SAH (carbon in green) and pyridinol (carbon in purple). The $2F_o - F_c$ map was contoured at 1.0σ . Upon binding of pyridinol, the disordered N-terminal loop (highlighted without transparency) of the other monomer (green) is fixed to close the cleft from all sides. Pyridinol is bound to the predicted active-site pocket near SAH.

Each of the four active sites of the tetramer contains SAH and two of them contain pyridinol in the electron density (Figure 3-3). However, pyridinol in one of the active sites appears to be partly broken and is superimposed in the electron density with an unknown linear compound (Figure 3-4). The fourth monomer showed only electron density of SAH and water molecules.

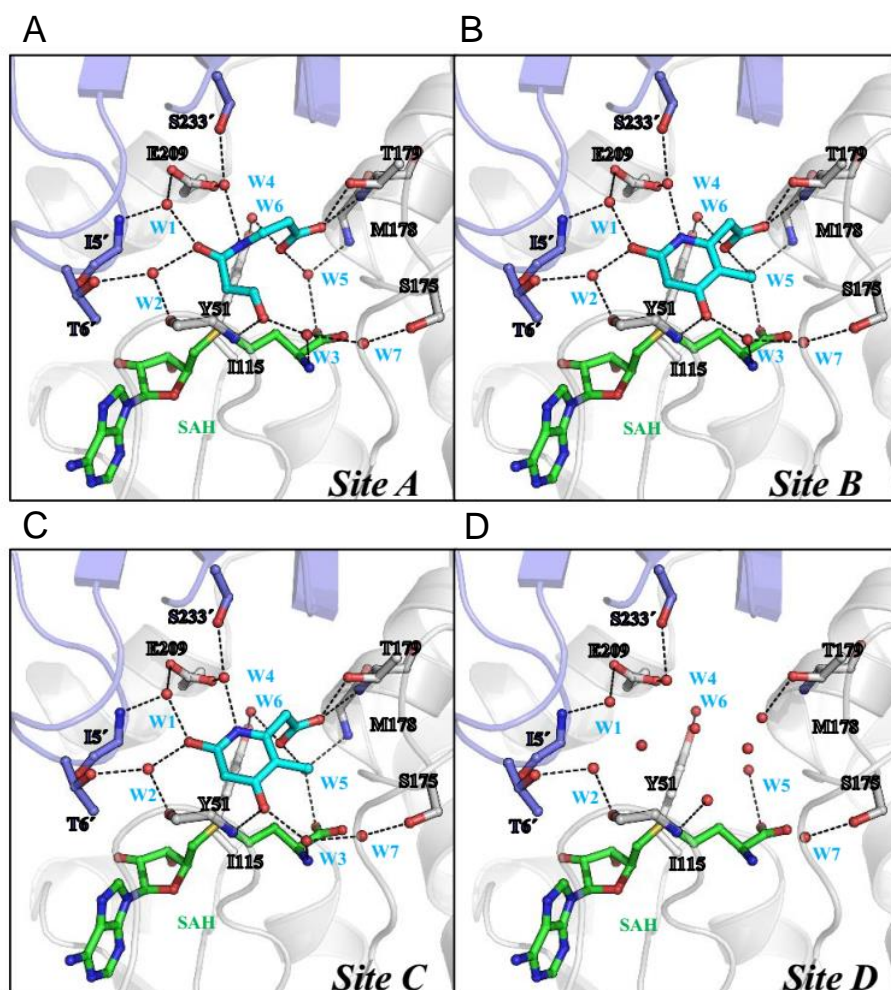


Figure 3-3. Active site of the four monomers in the HcgC homotetramer. (A) The active site binding SAH and a linear compound, (B) that binding SAH and pyridinol, (C) that binding SAH and a mixture of pyridinol and linear compound and (D) that binding only SAH.

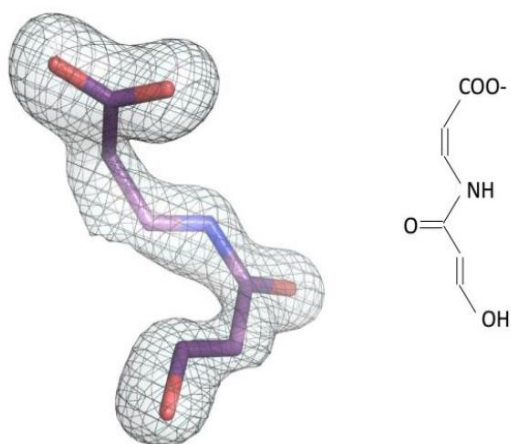


Figure 3-4. The linear compound found in one of the active site of the tetrameric HcgC. The chemical structure was estimated from the structure of pyridinol and the interactions with amino acids. The $2F_o - F_c$ map is contoured at 1.5σ .

RESULTS/PUBLICATIONS

To prevent the degradation of pyridinol during crystallization, we soaked crystals of the HcgC apoenzyme with pyridinol and SAH. In addition, HcgC was co-crystallized with SAH and pyridinol within less than two days. The X-ray structures based on rapidly grown and soaked crystals (2.0 and 2.05 Å resolution, respectively), revealed a full occupancy of the four active sites with SAH and the intact pyridinol substrate (Figure 3-5B and 3-5C). As their binding mode is identical to that of the 1.7 Å structure, the latter was consequently applied for further analysis.

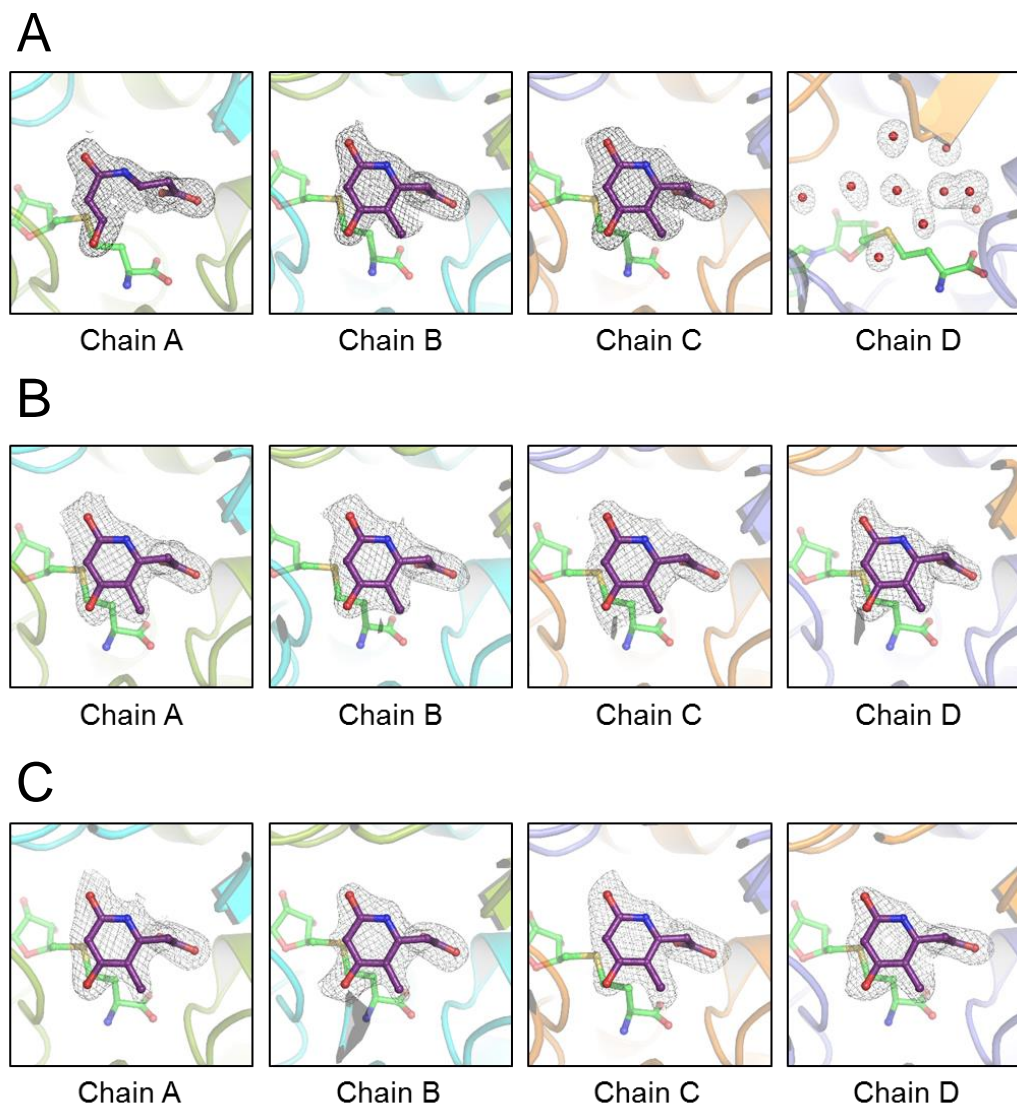


Figure 3-5. Active site structure of HcgC from *M. maripaludis* in complex with SAH and pyridinol. The four active sites of the dimer of homodimer (chain A-D) are shown in the panels. (A) Structure of the complex crystallized slowly (1.7 Å resolution). (B) Structure of the crystal rapidly-grown within less than two days (2.0 Å resolution). (C) Structure of HcgC crystal soaked with the substrates (2.05 Å resolution).

RESULTS/PUBLICATIONS

The binding of SAM or SAH was already described in detail in the previous report [129]. Pyridinol is bound to the predicted active-site pocket near SAH located between two subunits of the dimer. Comparison between the HcgC-SAH-pyridinol and the HcgC-SAM structures indicate a rigidification of residues 1-12 upon pyridinol binding which largely shields the substrate from bulk solvent and participate in its binding and in catalysis. The planar pyridinol ring is clamped between Ile115, Leu199 and Ile5', Val9' and SAH (amino acids of another monomer are shown with apostrophe) that adjusts the pyridinol-SAH orientation and the distance of 4.2 Å between their C3 and sulfur.

Pyridinol is primarily anchored to the polypeptide by its methylcarboxy group which is hydrogen-bonded to Thr179-N and –OG positioned at the positively charged N-terminal end of helix 178-194. In addition, W5 bridges the carboxymethyl group of pyridinol with Met178 NH and SAH-COO⁻ and W6 with Tyr51-OH, respectively. Except for Ile115-N, the 2-OH, 4-OH and 1-N groups are connected by a series of solvent mediated interactions (Figure 3-6). The 2-OH group of pyridinol is linked via W1 with Ile5'-NH and Glu209-COO⁻ and via W2 with Thr6'-OG and Ile115-CO and the 4-OH group via W3 itself coordinated via W7 with Thr175-OG, Glu134-COO⁻ and the SAM-NH₄⁺ group. W4 bridges the pyridinol-N with Ser233'-OH and Glu209-COO⁻. Note that two monomers and SAH are involved in binding the pyridinol and that the residues connecting the water molecules with pyridinol are fully conserved (Figure 3-7).

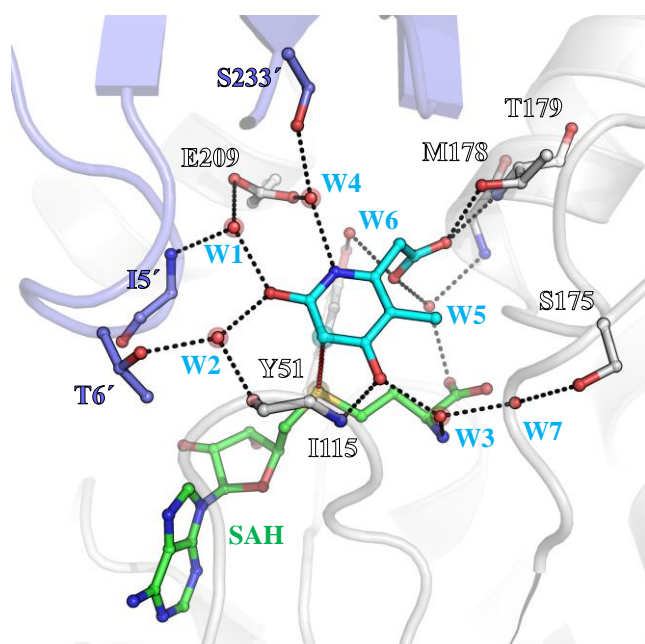


Figure 3-6. Water molecules that stabilize and activate the pyridinol. Pyridinol and SAH are shown in stick models with carbon in cyan and green, respectively.

RESULTS/PUBLICATIONS

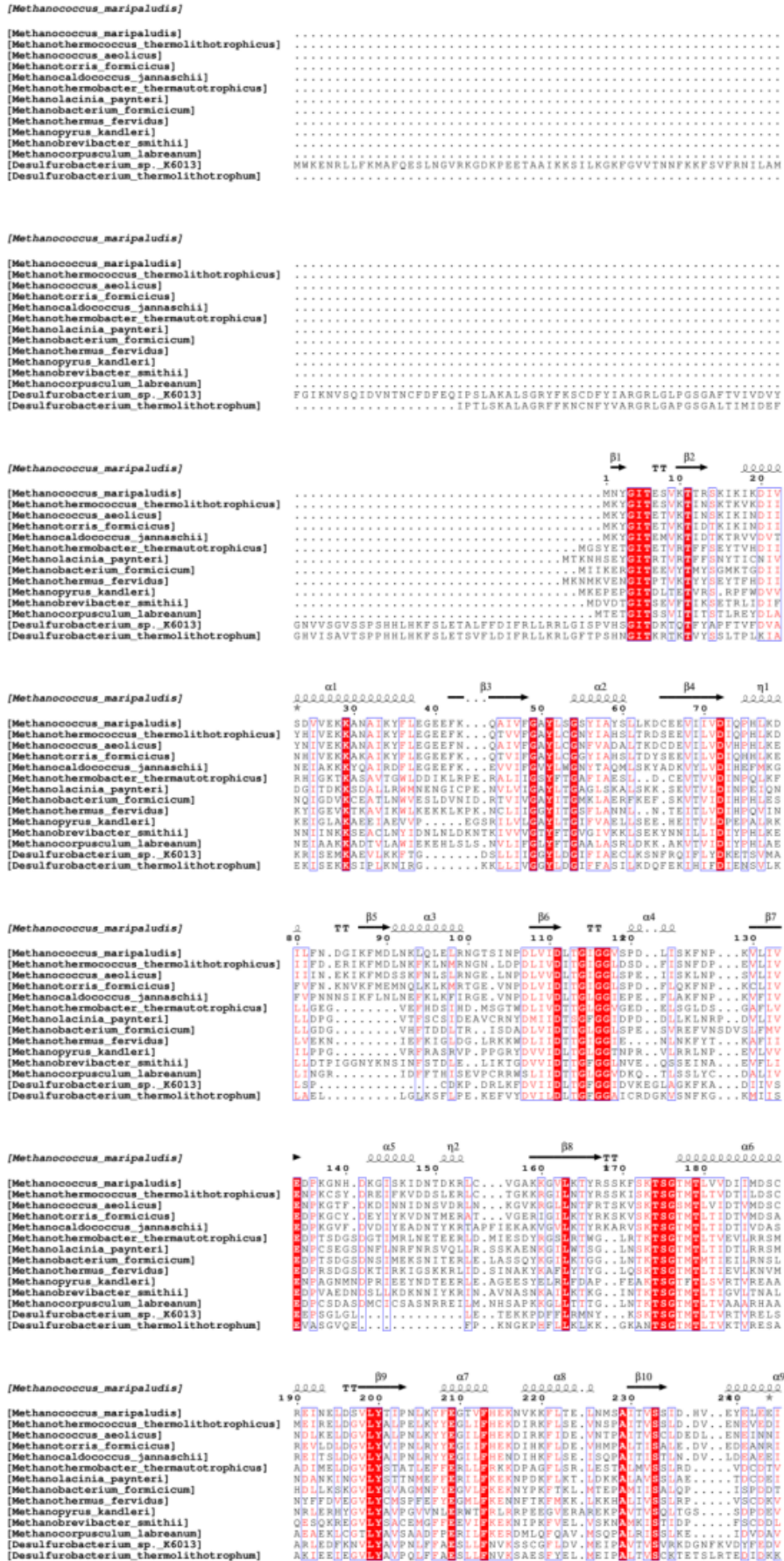


Figure 3-7. Comparison of primary structure of HcgC.

RESULTS/PUBLICATIONS

The X-ray structure at 1.8 Å resolution determined from crystals grown in the presence of HcgC, the pyridinol substrate and SAM only contains SAH in the four sites at the same position and conformation as in the HcgC-SAH-pyridinol complex but with a disordered N-terminal loop and thereby an open active-site pocket (data not shown). We assumed that under the crystallization conditions, pyridinol and SAM reacted to the methylated pyridinol and SAH, which was subsequently confirmed using MALDI-TOF-MS for identifying the methylated pyridinol product. This finding suggests a weaker binding of the HcgC-SAH complex to the methylated pyridinol product than to pyridinol, which is compatible with a collision between the 3-methyl group of pyridinol product in the planar pyridinol form and the main chain of Ile115.

To assess the role of the individual amino acids and indirectly of the water molecules on catalysis, mutational analysis were performed. Thr179 is the only amino acid, whose side-chain is directly coordinated with pyridinol. After its mutation to valine the enzyme variant exhibited no enzyme activity (Figure 3-8, Table 3-1), which emphasizes the crucial function of the carboxy group as anchor for substrate binding. Mutation of Thr6', Ser233 and Glu209, linked via one water molecules to pyridinol, to valine, alanine and glutamine resulted in drastic decrease of k_{cat}/K_M or the complete inactivity of the latter residue which demonstrated the importance of the water molecules W1, W2 and W4. In contrast, the exchange of Ser175 to alanine and Tyr51 to phenylalanine only show a minor effect perhaps because they do not form a hydrogen bond to water molecules directly involved in binding of the 2-OH and 4-OH groups.

The ternary HcgC-SAH-pyridinol structure and the kinetic characterization of enzyme variants allowed the postulation of a catalytic mechanism. In principle, SAM-dependent methyltransferase reactions are based on two catalytic strategies: 1) the proximity and desolvation mechanism to adjust an optimal geometry between the reaction groups and to avoid side reactions and 2) the general acid/base or the metal-based mechanism to increase the nucleophilicity of the methyl accepting atom. In HcgC, the two bulky compounds SAM and pyridinol are properly oriented for performing the S_N2 methyl transfer reaction. The distance below 2.7 Å between the methyl group of SAM and the C3 of pyridinol, based on the modeling of SAM into the HcgC-SAH-pyridinol complex and superposition of the HcgC-SAM onto the HcgC-SAH-pyridinol complex structure in the active site suggests a transiently strained conformation in the ternary complex. An energy-rich state prior to the methyl transfer

RESULTS/PUBLICATIONS

created by substrate binding energy would reduce the activation energy of the nucleophilic attack. Rigidification of residues 1-12 of the partner monomer enclosing the substrate from all sides might play an important role in this process, the active-site cleft is in majority closed and isolated from the solvent.

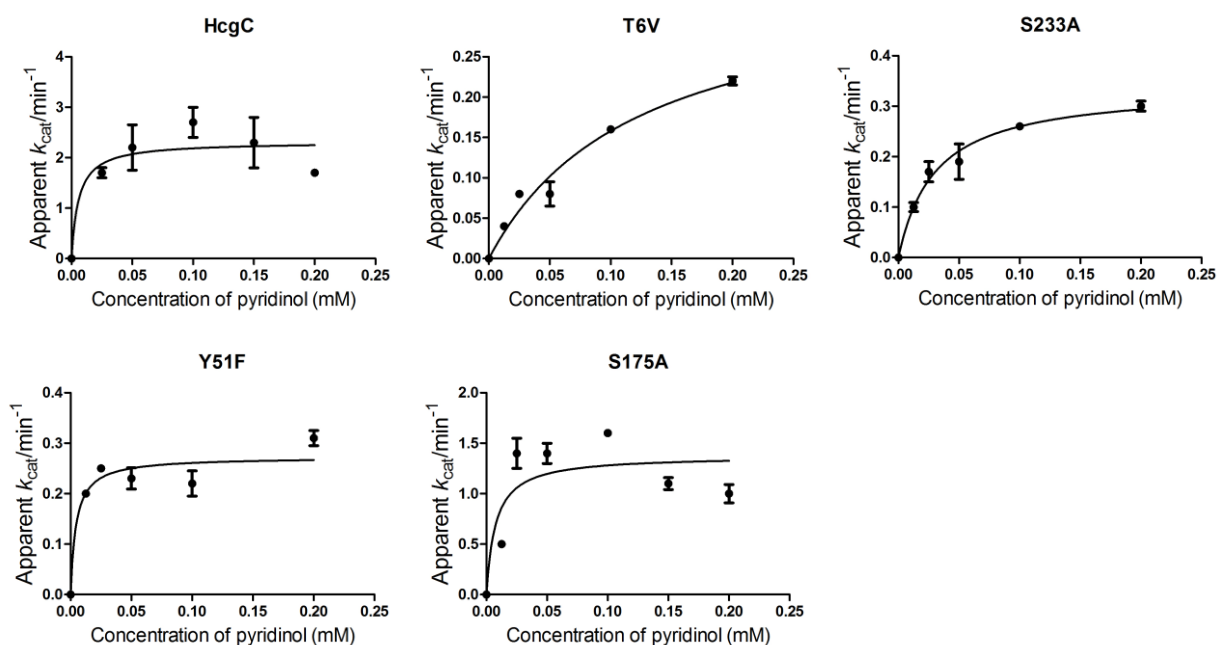


Figure 3-8. Kinetics data of the wild and mutated enzyme. Standard error of at least three measurements were calculated with the Standard Error Calculator. The assay mixture contained 1 mM SAM, the variable concentration of substrate pyridinol.

Table 3-1. Catalytic activity of the mutated enzymes.

Mutation ¹	Apparent k_{cat} (min ⁻¹) ²	Apparent K_M (μ M) ²	k_{cat}/K_M
Wild	2.3 ± 0.3	5.8 ± 8.7	0.40
T6V	0.35 ± 0.07	120 ± 45	0.0029
Y51F	0.27 ± 0.03	4.4 ± 3.4	0.061
S175A	1.4 ± 0.2	7.5 ± 8.4	0.19
T179V	— ³	—	—
E209Q	—	—	—
S233A	0.34 ± 0.02	30 ± 5.4	0.011

¹The mutated amino acid residues are fully conserved in HcgC (Figure 7).

²The concentration of SAM was 1 mM.

³The activity was too low to determine k_{cat} and K_M value.

RESULTS/PUBLICATIONS

In comparison to other SAM dependent methyltransferases HcgC contains neither a metal ion nor a protonable amino acid adjacent to the C3 of pyridinol, which excludes a metal-based and a catalytic acid/base mechanism (Figure 3-9). HcgC uses a special strategy thereby exploiting the chemical structure of pyridinol. Its 2-OH and 4-OH groups are ideally positioned for localizing formally an electron pair on C3 by resonance effects. Thus, the reaction starts from the pyridone form by a nucleophilic attack of the electron pair on C3 onto the positively charged methyl group of SAM. The subsequent pyridone/pyridinol tautomerization implicates a release of the acidic proton on C3. Proton at the C3 of the catalytic intermediate can be easily transferred out through the surrounding water molecules, perhaps to W2, which is 3.4 Å apart and adjacent to bulk solvent. The water molecules, W1, W2 and W3 might be ideally suited to exquisitely balance between deprotonation/protonation and pyridinol/pyridone mesomeric structures to maximize the probability electron density on C3.

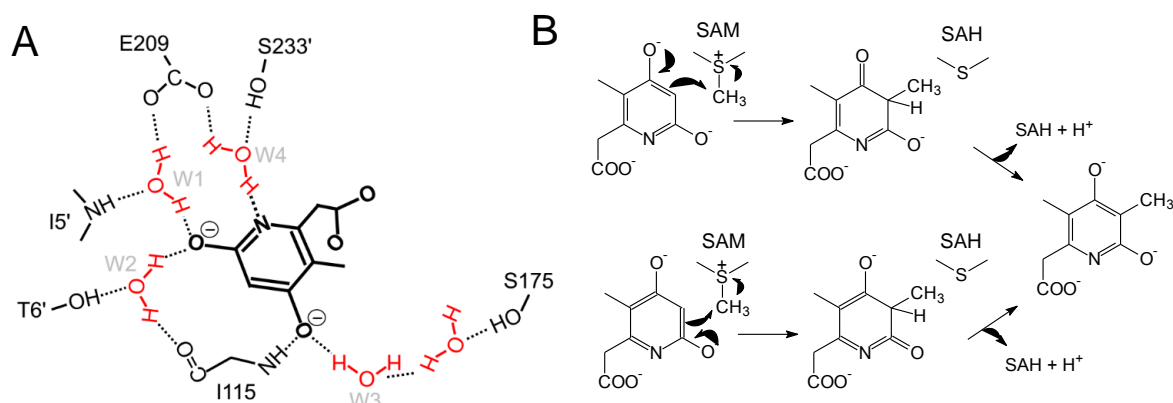


Figure 3-9. Water molecules that stabilize and activate the substrate pyridinol. (A) Schematic presentation of the water molecules for activation of C3 and resonance of deprotonate 2- and 4-hydroxy groups. For clarity, water molecules W5, W6 and their coordinating residue and SAH are not depicted in panel A. The 2- and 4-OH groups of the methyl acceptor pyridinol are mainly fixed with the polypeptide chain by a series of mostly water-mediated hydrogen-bonds. Solely, Thr179-O, Thr179-N and Ile115-N are directly hydrogen-bonded with the carboxy group and the 4-OH group of pyridinol, respectively. (B) Proposed catalytic mechanism of the SAM dependent methyltransfer reaction of HcgC.

Based on structural and mutational data we presented a unique water-assisted activation strategy of a methyl acceptor by which keto/enolate resonance effects activate the methyl acceptor C3. In addition, we learned from this study why nature

RESULTS/PUBLICATIONS

use the pyridinol substrate as precursor for 3-methylation in biosynthesis of the FeGP cofactor before conjugation with guanosine monophosphate catalyzed by HcgB. Methyl transfer to C3 of the 4-guanylyl-2-pyridinol is definitely more difficult than that of 4-hydroxy-2-pyridinol.

4. The growth phenotype of the Δhcg mutants of *M. maripaludis*

Abstract

M. maripaludis Mm901 $\Delta hmdjhmd$ strain has previously been made as the wild strain. In the wild strain, the endogenous *hmd* is deleted and *hmd* from hyperthermophilic *Methanocaldococcus jannaschii* was inserted (PhD thesis of M. Schick, 2012) [129]. No Hmd activity was detected in the cell extract of the *M. maripaludis* $\Delta hcgB$ and $\Delta hcgC$ mutants. These results revealed that *hcgB* and *hcgC* are crucial for production of active Hmd. In this section, the growth phenotype of the mutants are described.

Leigh et al. have reported the growth phenotype of the *hcg* mutants of *M. maripaludis* before our study [130]. They deleted each *hcg* gene and compared the growth phenotype with the Mm901 strain with the $\Delta frc\Delta fru$ background [130]. The Δhcg mutants has longer lag phase than that of the wild-type strain although the growth rate of the mutants were only slightly slower than that of the wild type. Similar lag phase was also observed in the case of the Δhmd mutant. From these findings, the authors concluded that the *hcg* genes are required for Hmd function. Unfortunately, their conclusion was not confirmed by the Hmd activity assay. To check the effects the $\Delta hcgB$ and $\Delta hcgC$ mutations, the Hmd activity of the mutants were measured in present work using the new *M. maripaludis* Mm901 strains with $\Delta hmdjhmd$ background.

Because the Hmd activity of the cell extract of *M. maripaludis* is unstable (Diploma thesis of Anne Kaster, 2011), in the Mm901 $\Delta hmdjhmd$ strain, the endogenous *hmd* gene was replaced by the *hmd* gene from *M. jannaschii*, which resulted in the strain Mm901 $\Delta hmdjhmd$. Based on this constructed wild type strain, the *hcgB* and *hcgC* genes were deleted for the analysis of the Hmd activity and the growth phenotype. All *M. maripaludis* strains have been prepared Mm901 by Michael Schick (Diploma thesis of Michael Schick, 2012).

At first, temperature dependency of the Hmd activity of the cell extract of *M. maripaludis* Mm901 $\Delta hmdjhmd$ was determined (Figure 4-1). The optimum temperature of the Hmd activity of this strain was 80 °C, which was consistent with the growth temperature optimum of the hyperthermophile *M. jannaschii* (85 °C). This result indicated that the Mm901 $\Delta hmdjhmd$ produced thermophilic Hmd from *M. jannaschii*.

RESULTS/PUBLICATIONS

In the presence of toluenesulfonylmethyl isocyanide (TosMIC), which is a specific inhibitor of Hmd, the Hmd activity was not observed at the temperature higher than 80 °C. However, at lower temperature (e.g. 40 °C), substantial Hmd-like activity was detected even in the presence of TosMIC. This observation indicated that at near the growth temperature of *M. maripaludis*, there are some Hmd-like activity in the cell extract. The enzyme responsible for this Hmd-like background activity is not investigated; however, it might be a coupled reaction catalyzed by F₄₂₀-dependent methylene-H₄MPT dehydrogenase (Mtd) and F₄₂₀-reducing hydrogenase (Frh). Frh and Mtd should be contained in the cell extract from mesophilic *Methanococcus* strains [131]. Due to relatively large amounts of the cell extract (7 µl) was injected into the assay solution (700 µl), which could support such coupled reactions. These data indicated that Mm901Δ*hmdjhmd* has an advantage to detect only real Hmd holoenzyme activity at 80 °C.

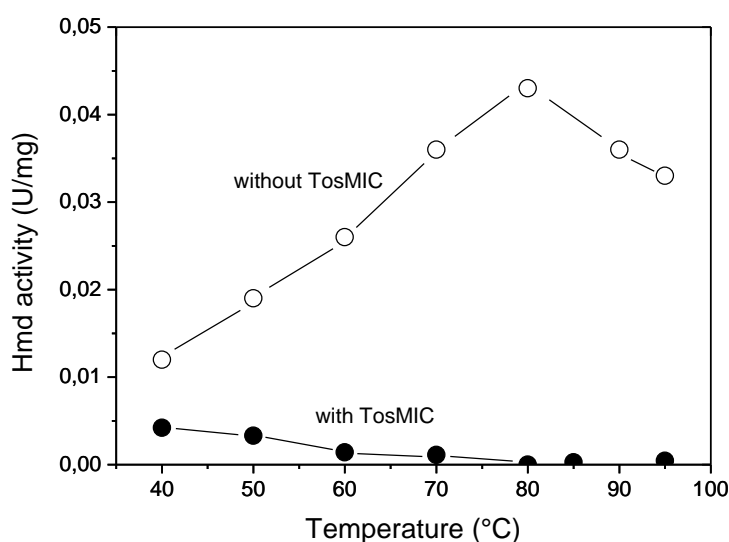


Figure 4-1. Hmd activity of the cell extract from *M. maripaludis*Δ*hmdjhmd*.

The Δ*hcgB* and Δ*hcgC* mutants revealed no activity at 80 °C, which confirmed that the *hcgB* and *hcgC* genes are crucial for production of active Hmd. The cell extract of *M. maripaludis* obtained from nickel-limiting condition revealed higher activity than that obtained from nickel-sufficient culture, which was in agreement with the previous studies (Diploma thesis of Anne Kaster, 2011) (Table 4-1) [30].

Table 4-1. Activity test of *M. maripaludis* and mutants

	Enzyme activity U/mg							
	Ni-sufficient condition				Ni-limiting condition			
	40 °C		80 °C		40 °C		80 °C	
	-TosMIC	+TosMIC	-TosMIC	+TosMIC	-TosMIC	+TosMIC	-TosMIC	+TosMIC
<i>jhmd</i>	0.15	-	0.28	-	1.2	-	3.6	-
Δhmd	0.16	0.17	-	-	0.12	0.08	-	-
$\Delta hcgB$	0.20	0.21	-	-	0.14	0.13	-	-
$\Delta hcgC$	0.22	0.19	-	-	0.14	0.08	-	-

The growth phenotype was studied using the media containing two different nickel concentrations (1 μ M or 50 nM) (Figure 4-2A). The growth rate of the strains are slightly higher in the nickel-sufficient (1 μ M nickel) than that of nickel-limiting conditions (50 nM nickel) but the difference is not so large that observed in the case of *Methanothermobacter marburgensis*. When the medium did not contain nickel, both the wild type and mutants did not grow. The wild type (Mm901 Δhmd *jhmd*), and the $\Delta hcgB$ and $\Delta hcgC$ mutants showed similar growth phenotype (Figure 4-2B,C) independent on the nickel concentrations. This finding contradicts with the observation of Leigh et al. [130]. The plausible reasons of the different growth properties could be attributed to the genetic background of the *M. maripaludis* strains. Leigh's group used Mm901 $\Delta frc\Delta fru$ background, in which two isoenzymes of F₄₂₀-reducing [NiFe]-hydrogenases (*frc* and *fru*) are deleted. As mentioned in the Introduction section, Hmd and Mtd together catalyze a coupled reaction, which is the same reaction that Frc and Fru catalyze. When the Hmd activity was deleted in the Mm901 $\Delta frc\Delta fru$ background, there is no known enzyme system for F₄₂₀H₂ regeneration in the mutated strains. In principle, such mutants are not able to grow on H₂ and CO₂. However, after relatively long lag-phase, the mutants started to grow with similar growth rate of the wild-type. This observation indicated that *M. maripaludis* Mm901 contains another H₂-dependent F₄₂₀-regenerating system other than Frc/Fru and Hmd-Mtd. Induction of the third F₄₂₀-regenerating enzyme might be observed as the lag-phase of the $\Delta hcgB$ and $\Delta hcgC$ strains of *M. maripaludis* strains with $\Delta frc\Delta fru$ background. In the case of our strain, Frc and Fru were not disrupted; therefore, we did not observe the lag-phase.

RESULTS/PUBLICATIONS

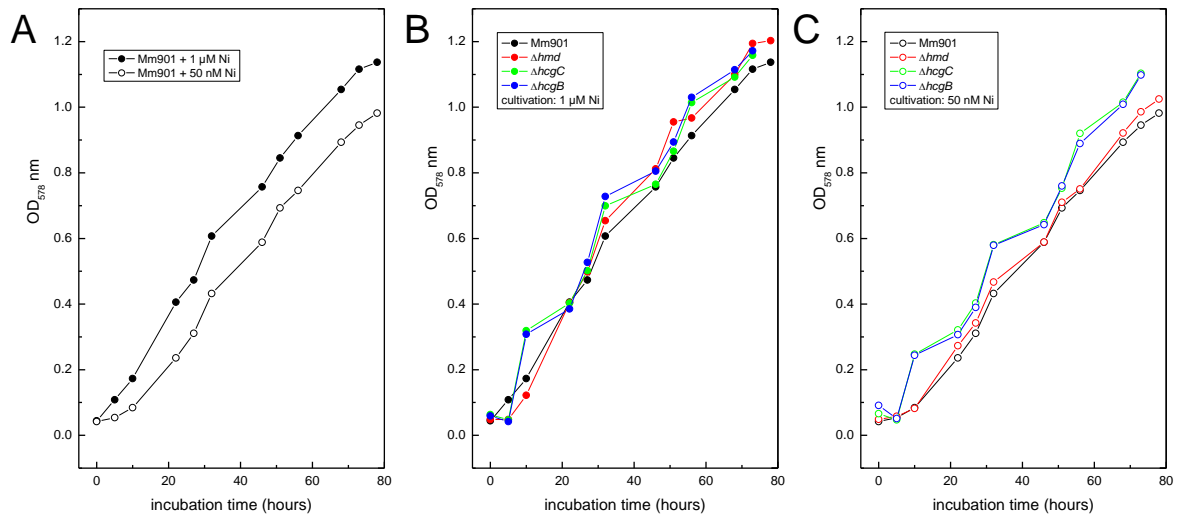


Figure 4-2. Growth curve of *M. maripaludis* wild type strain and mutants Δhmd , and $\Delta hcgB$ $\Delta hcgC$, which showed in black, red, blue and green, respectively. The cultivation medium used for this measurement was McA medium, which was described in the methods section. (A) Growth curve of Mm901 under different nickel concentration. (B) Growth curve of wild type strain and mutants cultivated under 1 μ M nickel. (C) Growth curve of wild type strain and mutants cultivated under 50 nM nickel.

5. Over-expression of HcgA and HcgG in *E. coli*

Abstract

The function of HcgA and HcgG are still unknown. To use the “structure to function” strategy like as the other Hcg proteins, we need to solve the crystal structure of the Hcg proteins. The *hcgA* gene from six methanogens were expressed in the *E. coli* and the over-produced proteins were purified. The purified HcgA proteins were soluble and showed a brown color of the iron-sulfur cluster bound to the protein. HcgA was tried to be crystallized without substrates and also in complex with SAM but no crystal was observed. HcgG from seventeen methanogens were expressed in *E. coli*, they formed inclusion body and no soluble protein was observed in the cell extract.

HcgA are a member of the radical SAM enzyme super-family, which includes biotin synthase (BioB), and [FeFe]-hydrogenase maturation proteins HydE and HydG. The *hcgA* gene from methanogens was synthesized by Genscript. The synthesized DNA was inserted into expression vector pET24b(+) and transformed into *E. coli*, which contained an iron-sulfur cluster plasmid pRKISC and charperon pCodonplus [106]. The over-produced HcgA proteins with His-tag were purified using nickel-affinity column. Determination of iron in the protein preparation indicated that 3.8 molecules of Fe was bound per protein. This Fe content was consistent with that HcgA contains a [4Fe-4S] cluster in the monomer. The buffer of purified HcgA was exchanged with 10 mM MOPS/KOH, and the protein was concentrated around 10 mg/mL for the crystallization. HcgA apoenzyme was crystallized using different screening kit (JBScreen series and QIAGEN JCSG series). Since HcgA is a possible radical SAM enzyme, crystallization of HcgA in complex with SAM was also tried. However, no crystal was observed. In the future, the crystallization condition must be optimized. As aggregation of protein was observed when it was concentrated, the protein concentration could be decreased to the half to avoid the aggregation. Changing temperature might be help for crystal growth. More crystal-screening kit should also be tried.

RESULTS/PUBLICATIONS

Table5-1. Methanogens used for heterologous expression of HcgA

No.	Methanogens	Optimum growth temperature (°C)
1	<i>Methanopyrus kandleri</i>	98
2	<i>Methanotorrus igneus</i>	70
3	<i>Methanocaldococcus fervens</i>	85
4	<i>Methanocaldococcus infernus</i>	85
5	<i>Desulfurobacterium thermolithotrophum</i>	70

Table5-2. Methanogens used for heterologous expression of HcgG

No.	Methanogens	Optimum growth temp. (°C)	No.	Methanogens	Optimum growth temp. (°C)
1	<i>Methanobrevibacter ruminantium</i>	37	10	<i>Methanococcus vannielii</i>	35
2	<i>Methanobrevibacter oralis</i>	35	11	<i>Methanococcus aeolicus</i>	37
3	<i>Methanobrevibacter wolinii</i>	-	12	<i>Methanobacterium formicicum</i>	37
4	<i>Methanocaldococcus fervens</i>	85	13	<i>Methanospirillum hungatei</i>	37
5	<i>Methanocaldococcus villosus</i>	80	14	<i>Methanolacinia petrolearia</i>	37
6	<i>Methanocaldococcus vulcanius</i>	80	15	<i>Methanoregula formicica</i>	30
7	<i>Methanocaldococcus infernus</i>	85	16	<i>Methanotorrus formicicus</i>	70
8	<i>Methanothermococcus thermolithotrophicus</i>	65	17	<i>Desulfurobacterium thermolithotrophum</i>	70
9	<i>Methanothermococcus okinawensis</i>	65			

RESULTS/PUBLICATIONS

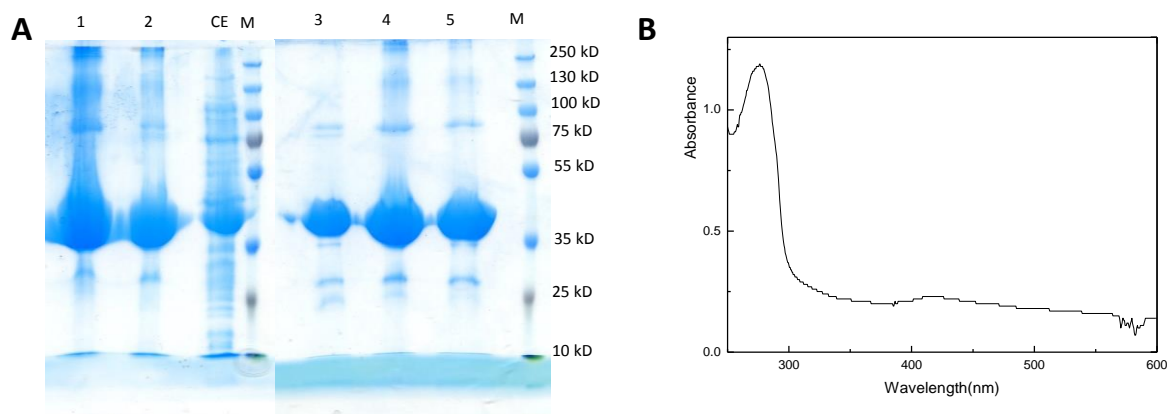


Figure 5-1. (A). Over-expression of HcgA. Line M: protein ladder marker. Line 1: HcgA from *Methanopyrus kandleri*. Line 2: HcgA from *Methanotorris igneus*. Line 3: HcgA from *Methanocaldococcus infernus*. Line 4: HcgA from *Methanocaldococcus fervens*. Line 5: HcgA from *Desulfurobacterium thermolithotrophum*. Line CE: cell extract of *E. coli*. (B) UV-Vis spectrum of the purified HcgA protein from *Methanopyrus kandleri*. The absorbance at 400-500 nm revealed the presence of iron-sulfur clusters. [74, 132].

The *hcgG* gene was synthesized and inserted into expression plasmid pET24b(+) and transformed into *E. coli* BL21(DE3). Over-production of HcgG was performed in LB medium. This 55 kD protein formed inclusion body in the cell under the normal cultivation condition (37 °C, 1 mM IPTG, 4-6 hours induction) (Figure 5-2). HcgG from 17 methanogens were tested. No protein was found in the soluble fraction. Lower temperature and different IPTG concentration were tested to optimize the expression but HcgG still formed inclusion body in the cell. The cell extract containing HcgG from the hyperthermophilic methanogen *Methanocaldococcus jannaschii*, which grows at 85 °C, was incubated at 65 °C for 20min and centrifuged to remove the *E. coli* proteins. Then the supernatant was concentrated but not visible in SDS-PAGE. To improve the solubility of HcgG, the expression system and host should be changed, for example, the yeast system. Additionally, as the primary structure analysis suggested that HcgG might contain an iron-sulfur cluster, co-expression with iron-sulfur chaperon might be another way to obtain the soluble protein (see the Discussion section).

RESULTS/PUBLICATIONS

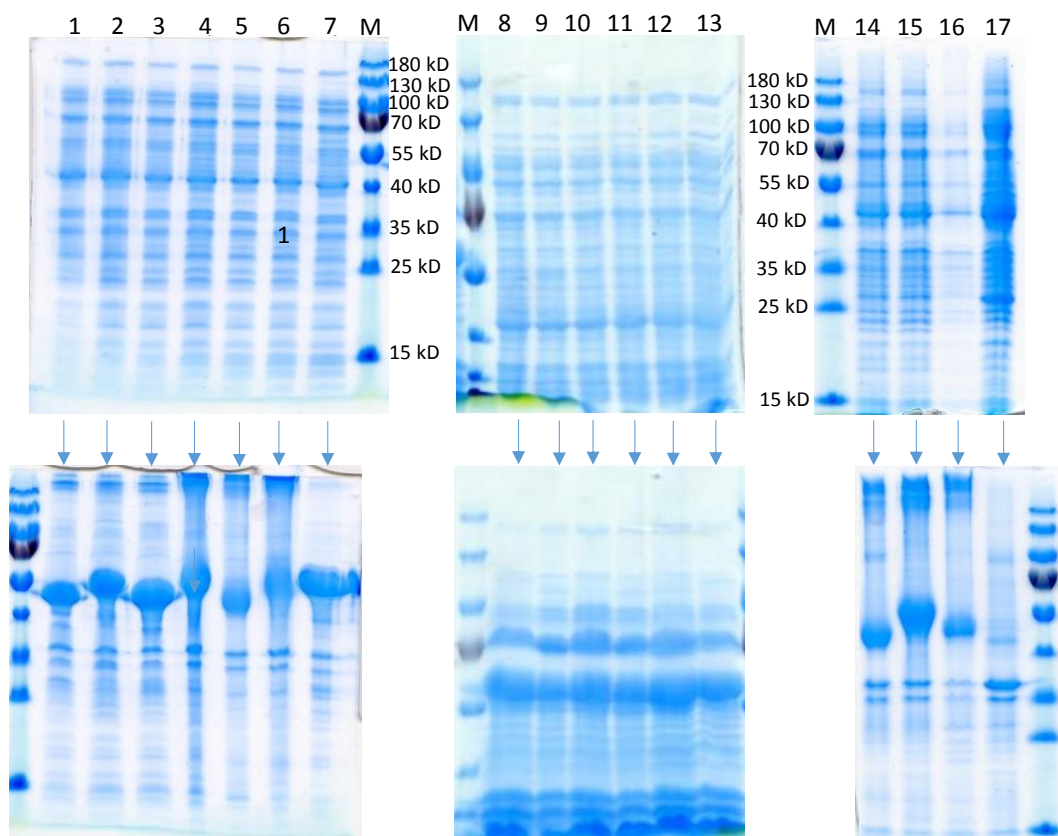


Figure 5-2. SDS-PAGE analysis of heterologously produced HcgG in *E. coli*. The samples in the top three gel pictures contained supernatant of the cell extracts, while the bottom three pictures showed the precipitated fractions. The arrow indicates the samples come from the same cell extracts. The numbers on the lanes in the top panels indicates the methanogenic archaea listed in the Table5-2. Inclusion body of HcgG proteins is visible between 40–55 kDa in SDS-PAGE of the precipitated fractions.

6. The FeGP cofactor from *M. maripaludis* and its precursors

Abstract

The structure and properties of the FeGP cofactor of Hmd from *M. marburgensis* has been extensively studied. Nevertheless, the FeGP cofactors from other methanogenic archaea were not well characterized yet. The model organism of the genetic experiments of hydrogenotrophic methanogenic archaea is *M. maripaludis*, which belongs to the family Methanococcales. To study the functions of the *hcg* genes using this methanogen, chemical structure of the FeGP cofactor from *M. maripaludis* should be demonstrated. Mass spectrometric analysis of the FeGP cofactor from Hmd, which was partially purified from *M. maripaludis*, did not exhibit the mass peaks of the guanylylpyridinol part of known FeGP cofactor. To obtain information of the FeGP cofactor in Methanococcales, the FeGP cofactor was isolated from Hmd from *M. jannaschii*. Mass spectroscopic analysis indicated that *M. jannaschii* contains the same guanylylpyridinol part with that from *M. marburgensis*. Three-dimensional structure of the enzyme-substrate complexes of HcgB and HcgC from *M. maripaludis* and the counterparts of *M. jannaschii* were compared. This analysis indicated that the binding site of guanylylpyridinol in HcgB and the pyridinol in HcgC are fully conserved in the enzymes. This finding suggested that the guanylylpyridinol part of the cofactor in *M. jannaschii* and *M. maripaludis* are identical. Metabolome analysis of *M. maripaludis* strains and of *M. marburgensis* were performed using liquid-chromatography-mass-spectrometry (LC-MS). The results suggested that there is a plausible precursor, which exists in both methanogens.

The structure and function of the FeGP cofactor have been elucidated by using that from *M. marburgensis*. Active Hmd can be reconstituted from the FeGP cofactor of Hmd from *M. marburgensis* and the apoenzymes from *M. maripaludis*, *M. jannaschii* and other methanogens and the reconstituted enzymes are fully active; therefore, the structure of the FeGP cofactor from the other methanogens is believed to be identical to that of the FeGP cofactor from *M. marburgensis*. However, it cannot be excluded that there are some variations of the structure of the FeGP cofactor. The iron complex structure appears to be crucial for activity but the organic part of the FeGP cofactor

RESULTS/PUBLICATIONS

might not be strictly restricted. For example, the GMP moiety could be exchanged with other nucleotides. The 3- and 5-methyl groups on the pyridinol affect the electronic properties of the pyridinol ring; however, at least one methyl group could be removed.

Here, we predicted the structure of the FeGP cofactor from the guanylylpyridinol structure of the FeGP cofactor from *M. jannaschii* and comparison of the enzyme-substrate complex structures of HcgB and HcgC from *M. jannaschii* and *M. maripaludis*. Moreover, to determine the structure of the precursors of the FeGP cofactor, LC-MS analysis was performed.

Hmd was partially purified from *M. maripaludis* Mm901 strain. The FeGP cofactor was extracted with the standard method using 60% methanol, 1 mM 2-mercaptoethanol and 1% ammonia and analyzed by MALDI-TOF-MS. Several mass peaks were observed but the typical peak of the guanylylpyridinol ($m/z = 543$) was not observed. The possible mass peaks [$m/z = 529$ (lacking one methyl), 527 (GMP was exchanged with AMP), 503 (with CMP), 501 (with TMP) and 504 (with UMP)] were also not detected.

We tried to isolate from the FeGP cofactor from Hmd, which was partially purified from *M. jannaschii* cell extract. MALDI-TOF-MS indicated the presence of the peak of the guanylylpyridinol ($m/z = 543$) and its Na^+ adduct ($m/z = 565$). In addition, the decarboxylated derivative ($m/z = 499$) and its Na^+ adduct ($m/z = 521$) was detected (Figure 6-1). This peak patterns were always observed when the FeGP cofactor of *M. marburgensis* was analyzed by MALDI-TOF-MS. This result indicated that the cofactor extracted from Hmd from *M. jannaschii* is identical with that of *M. marburgensis*.

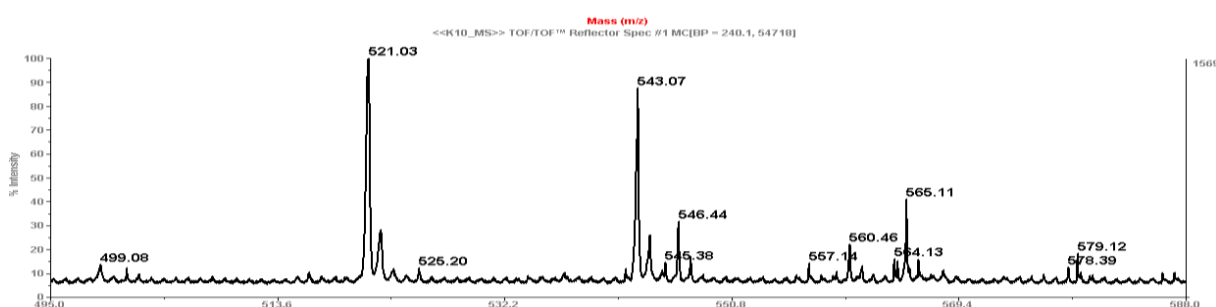


Figure 6-1. MALDI-TOF of FeGP cofactor extracted from *M. jannaschii*.

Crystal structure of HcgB and HcgC from *M. jannaschii* and *M. maripaludis* are solved. The HcgB-guanylylpyridinol complex and HcgC-SAH-pyridinol complex structure were solved using the enzymes from *M. jannaschii* and *M. maripaludis*, respectively. Structure comparison of these enzymes and enzyme complexes

RESULTS/PUBLICATIONS

indicated that the amino acid residues interacting with substrates in *M. jannaschii* and *M. maripaludis* were completely conserved (Figure 6-2). In the structure of HcgB-guanylylpyridinol complex using *M. jannaschii* enzyme, the amino group of the GMP moiety was bond to the protein via the peptide oxygen of Glu137. The carboxyl group of pyridinol ring bond to S132 and the pyridinol nitrogen, hydroxyl group, phosphate bond to residues Asp23, Arg20, Lys50, respectively. These amino acid residues are conserved in HcgB from the *M. maripaludis*. In the structure of the HcgC-SAH-pyridinol complex, the carboxyl group of the pyridinol was bond to Thr179. The pyridinol substrate was mainly connected via water molecules to the protein (not shown in Figure 6-2). The residues contacting to the water molecules were conserved in the *M. jannaschii* HcgC. This finding strongly suggested that the substrates of HcgB and HcgC reactions in two organisms were identical. In the two methanogenic archaea, the same pyridinol and guanylylpyridinol are involved in biosynthesis of the FeGP cofactor.

To investigate the biosynthetic precursors of the FeGP cofactor *M. maripaludis*, the metabolites was analyzed using LC-MS (Table 6-1). The metabolites were extracted from the cell extract in 60 % methanol. In the cell extract of *M. marburgensis*, the *m/z* values corresponding to the 3-methylated pyridinol (compound 2 in Table 1) and the guanylylpyridinol precursor (compound 5) were detected. The *m/z* peak at 198.0414 could be 3-hydroxy-pyridinol (compound 3). In the cell extract of *M. maripaludis* Mm901 Δ hmd Δ jhmd strain, the *m/z* peak of the guanylylpyridinol was not detected but those of 3-non-methylated pyridinols (compound 1), 3-methylated (compound 2) and 3-hydroxy-pyridinol (compound 3) were detected. The presence of the mass peak corresponding to the compound 3 in the cell extracts from *M. marburgensis* and *M. maripaludis* is of interest. The compound 3 could be a precursor of the FeGP cofactor (see Discussion section).

RESULTS/PUBLICATIONS

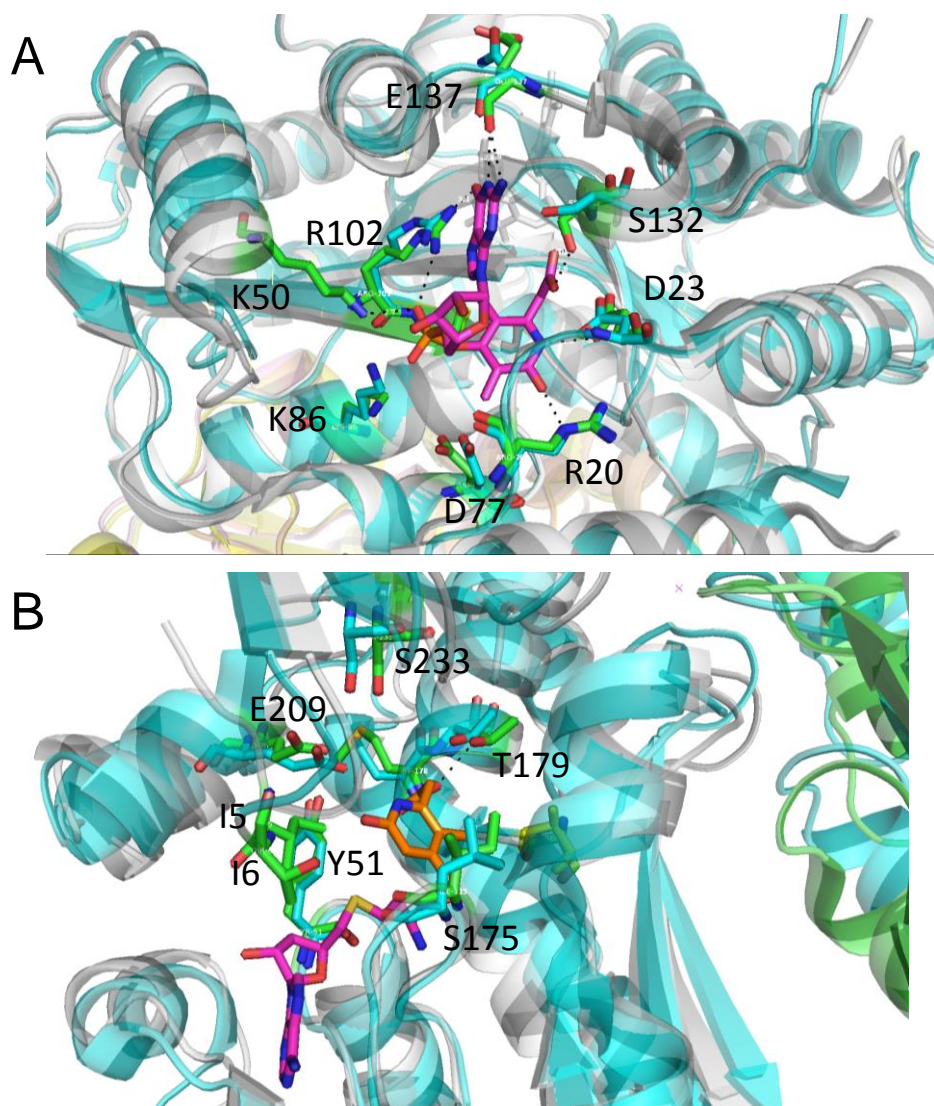
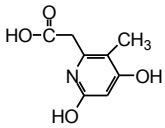
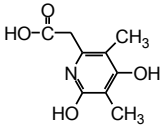
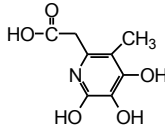
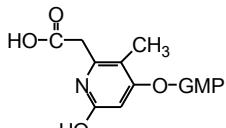
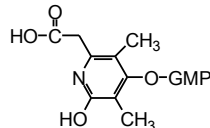


Figure 6-2. The active site structure of HcgB (A) and HcgC (B). The amino acids in the active site were conserved in the enzymes from *M. jannaschii* and *M. maripaludis*. (A) Superposition of the HcgB-guanylylpyridinol complex structure from *M. jannaschii* (green stick model of active-site residues and gray cartoon) and HcgB from *M. maripaludis* (light blue stick model of the active-site residues and light blue cartoon). Guanylylpyridinol is shown with magenta stick model. (B). Superposition of the HcgC-SAH-pyridinol structure from *M. maripaludis* (light blue stick model of the active-site residues and light blue cartoon) and HcgC from *M. jannaschii* (green stick model of active-site residues and gray cartoon). Pyridinol and SAH are shown with orange and magenta stick models.

RESULTS/PUBLICATIONS

Table 6-1. LC-MS analysis (negative mode) of possible precursors in methanogen's cell extract

	(1)	(2)	(3)	(4)	(5)
					
	$C_8H_9O_4N$	$C_9H_{11}O_4N$	$C_8H_9O_5N$	$C_{18}H_{21}N_6P_1O_{11}$	$C_{19}H_{23}N_6P_1O_{11}$
Calculated m/z	182.0453	196.0610	198.0402	527.0928	541.1084
Measured m/z	182.0464	196.0621	198.0414	-	541.1090
<i>M. marburgensis</i>	-	+	+	-	+
<i>M. maripaludis</i> Mm901 Δ hmdjhmd	+	+	+	-	-

DISCUSSION

DISCUSSION

Hydrogenases are important for the energy metabolism in numerous microorganisms. They catalyze the reversible activation of molecular hydrogen and reduction of electron/hydride carriers. Molecular hydrogen is not highly reactive because the covalent bond of H–H is very strong (+436 kJ/mol) [133]. Chemical cleavage of H–H bond needs high temperature and pressure even in the presence of platinum as catalyst. Hydrogenases are biological hydrogen-activating catalysts, which can work at room temperature under low pressure; therefore, attract attentions in industrial applications in the future. Among the three types of hydrogenases, [FeFe]-hydrogenase is considered to be applied for the H₂ production system due to its higher reaction turnover rate for H₂ production [134]. In contrast, most of [NiFe]-hydrogenases are better catalyst for reduction of substrates using electrons from H₂. Application of [NiFe]-hydrogenase on the bio-fuel cell is expected to be a high efficient use of H₂ as a new energy carrier [135]. [Fe]-hydrogenase catalyzes reversible activation of H₂ and hydride transfer to methenyl-H₄MPT⁺. Difference from the other two types of hydrogenases is that [Fe]-hydrogenase catalyzes hydrogenation reaction. Therefore, the [Fe]-hydrogenase model compounds are expected to be used for new types of hydrogenation catalysts [136]. All hydrogenases harbor metal centers in the active site. [NiFe]- and [FeFe]-hydrogenases contain the dinuclear metal center containing at least one iron-sulfur cluster. Current researches indicate that the metal centers are biologically synthesized by a complicated enzyme systems. Nature develops a smart pathway to synthesize these unique cofactors using toxic carbon monoxide and cyanide as precursors. The study on biosynthesis of the hydrogenase metal centers may stimulates the synthesis of H₂-activation hydrogenase mimic catalysts [137].

The maturation of [NiFe]-hydrogenase and [FeFe]-hydrogenase are studied extensively by many groups around the world. However, biosynthesis of [Fe]-hydrogenase cofactor has only been investigated in the last decade in Shima group in Max Planck Institute for Terrestrial Microbiology. The [Fe]-hydrogenase cofactor, namely the FeGP cofactor has two carbon monoxide ligands, an acyl-Fe and a highly substituted pyridinol ring. This unique cofactor is found only in [Fe]-hydrogenase of methanogens. Therefore, the study of the FeGP cofactor is scientifically interesting from the biological and inorganic chemistry viewpoints.

DISCUSSION

History of the [NiFe]- and [FeFe]-hydrogenases' maturation processes

In the case of [NiFe]-hydrogenase maturation, gene mutation analysis was initiated by the group of Böck [138]. They deleted the *hypA-F* operon, which resulted in inactivation of hydrogenase-3 in *E. coli*. Based on nickel-complementation studies using the *hypB* mutant, they obtained the first evidence of the specific function of HypB that incorporates nickel to the hydrogenase protein [139]. Subsequently, studies using sequence similarities, enzyme reactions, protein interactions, isotope-labeled compound incorporation and site-directed mutagenesis were performed by the groups of Böck, Friedrich and the others [59, 140, 141].

The study of the [FeFe]-hydrogenase maturation was also initiated by mutation analysis by the group of Seibert; gene deletion experiments of *Chlamydomonas reinhardtii* suggested that three genes, *hydEFG* are responsible for maturation of [FeFe]-hydrogenase [70]. The maturation functions of *hydEFG* were verified by production of active [FeFe]-hydrogenase in *E. coli*, which contains *hydEFG* and the *hydA* structural gene by the same group [70]. Further researches of the *hyd* genes were mainly performed based on sequence similarity search, enzymological characterization of the heterologously produced enzymes, *in vitro* biosynthesis experiments of the active center metal H-cluster and X-ray crystal structure analysis of [FeFe]-hydrogenase [77, 142, 143]. The overall functions of each maturation gene were described in the introduction section.

Structure to function strategy

The clue of the FeGP cofactor biosynthesis was the finding of the *hcg* gene cluster (*hcgA-G*), which was identified near the *hmd* gene of some methanogens. This finding led speculation that the *hcgA-G* genes could be the genes responsible for biosynthesis of the FeGP cofactor because the *hyp* genes in *E. coli* locate near the [NiFe]-hydrogenase structural genes [59]. According to the [NiFe]- and [FeFe]-hydrogenase maturation studies, knock-out mutation of the *hcg* genes appeared to be a promising methods to identify the function of the *hcg* genes. However, unfortunately, genetics experiments of methanogens without cytochromes are not straightforward due to instability of the vector; recombination of the vector with and without inserted DNA was often observed by unknown reasons. It is one of the reasons why we could prepare only the deletion mutants of *hcgB* and *hcgC* in *M. maripaludis* in relatively late stage of this project.

DISCUSSION

Function of proteins is defined by the three-dimensional structure of the protein. Therefore, from structure of the protein, we should be able to predict the function. This is one of the core idea of the structural genomics projects [144]. To analyze the function of the Hcg proteins, we used a “structure to function” strategy for the analysis of the Hcg proteins. In this method, proteins were firstly heterologously produced in *E. coli*, purified and crystallized. X-ray crystal structure of the protein was solved. Then the crystal structure was used as model for structural similarity search. The function of protein was predicted based on information from the similar proteins with known function. The function of the protein is tested by docking simulation, co-crystallization and enzyme reaction. By using this method, the functions of HcgB, HcgD, HcgE and HcgF were elucidated.

Generally, prediction of function from pure three-dimensional structure is very difficult. Only few proteins' function have been annotated by structural genomics projects [97]. The following reasons could explain why structure to function analysis of Hcg proteins was successful: (1) it was assumed that the *hcg* gene cluster are involved in the FeGP cofactor biosynthesis; (2) the possible substrates and the catalyzed reactions were predicted from the structure of the FeGP cofactor and the isotope-labeling analysis, and (3) commercially unavailable substrate was successfully synthesized.

Function of HcgC

The HcgC protein structure was solved and we found that the three-dimensional structure of HcgC was similar with NAD(P)-dependent dehydrogenase and SAM-dependent methyltransferase. This result suggested the possible function of HcgC. To find the ligand bound to HcgC, co-crystallization of HcgC with NAD(P) or SAM was performed. Only SAM bound to HcgC in the crystal structure. In addition, our previous stable-isotope labeling experiments have shown that the 3-methyl group of pyridinol ring is obtained by a SAM dependent methyltransfer reaction. The information strongly suggested that HcgC is a SAM-dependent methyltransferase. Docking simulation indicated the possible binding site of the pyridinol. In order to test the prediction of the HcgC catalyzed reaction, the substrate pyridinol was chemically synthesized in collaboration with Xile Hu (EPFL). Enzyme activity was tested using this substrate and SAM. As expected, the methylated product was observed by mass spectrometry and NMR spectroscopy. The NMR data indicated that the methylation was occurred on the

DISCUSSION

C3 of pyridinol, which was consistent with the isotope labeling experiment. This part of results was described in the Results section 1 [129].

Co-crystallization of HcgC with the pyridinol substrate and SAH showed that both substrates were bound to the cleft between N- and C-terminal domains. There were several water molecules near the pyridinol, which connect the pyridinol and protein residues. These water molecules stabilized the binding of substrate in active site. However, none of the water molecules appeared to work as a general base as observed in other SAM-dependent methyltransferases. The general-base mediated methylation is a common mechanism for many SAM-dependent methyltransferases, but this is not the case for HcgC. This contribution of water for methylation should be a new type of mechanism in the SAM-dependent methyltransferases. This part of results was described in the Results section 3.

Reaction sequence of HcgB and HcgC

The reaction of HcgC in the FeGP cofactor biosynthesis pathway was identified. However, the reaction sequence of HcgB and HcgC in the biosynthesis was not clear because HcgB is able to catalyze guanylation reaction using both 6-carboxymethyl-2,4-dihydroxy-5-methyl-pyridinol and 6-carboxymethyl-2,4-dihydroxy-3,5-dimethyl-pyridinols. Therefore, we could not draw conclusion whether pyridinol or guanylated pyridinol is the methyl acceptor of the HcgC reaction. We found that HcgC was not able to utilize the non-3-methylated guanylylpyridinol, which was made by HcgB. This experiment indicated that pyridinol was first 3-methylated and then HcgB conjugate GMP to the 3-methylated pyridinol. This part of results was described in the Results section 2 [145].

Proposed FeGP cofactor biosynthesis pathway.

Based on the results of the functions of Hcg proteins, the FeGP cofactor biosynthesis pathway was proposed [145]. HcgC catalyzes the methylation on C3 of pyridinol. HcgB catalyzes the conjugation of GMP and methylated pyridinol. HcgE catalyzes the adenylation of carboxy group of guanylylpyridinol (the HcgB product). Then HcgF catalyzes the formation of thioester bond of guanylylpyridinol and HcgF Cys9. HcgD was proposed to be an iron-trafficking protein, which transfer an iron for the iron center formation. Next, HcgA, HcgG or some unknown proteins catalyze the formation of acyl-

DISCUSSION

and CO-ligands. Once the iron center was formed, the intact cofactor is transferred to apoenzyme producing the active Hmd (Figure D-1).

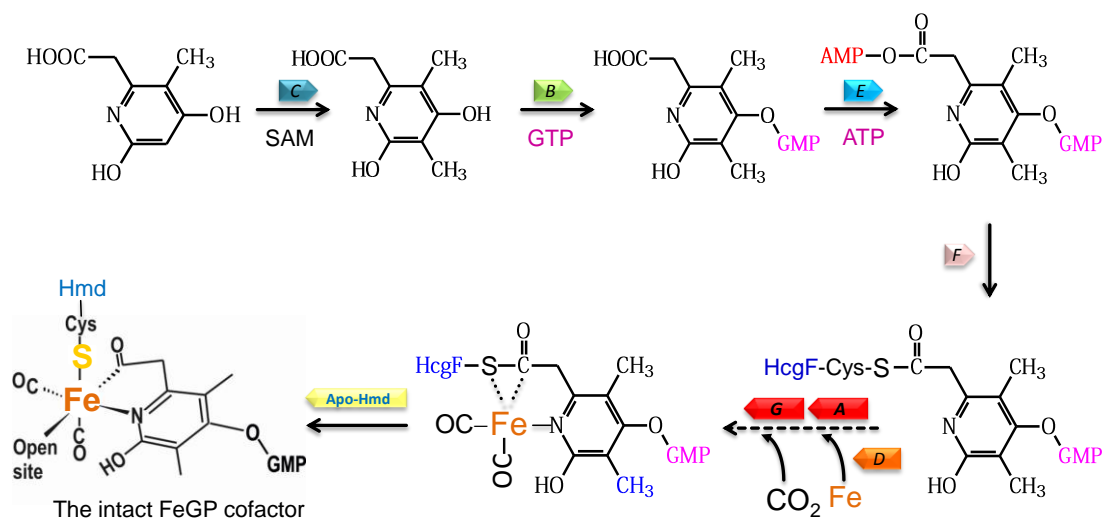


Figure D-1. Proposed FeGP cofactor biosynthesis pathway. The HcgA–G proteins are shown by arrows with different colors.

Analysis of HcgA and HcgG

To complete the pathway, the function research of HcgA and HcgG is required. I tried to solve the protein structures of these two proteins and find the functions by the same way used for the other Hcg proteins. HcgA can be expressed and purified from *E. coli*, but no crystal was obtained. HcgG always formed only inclusion body in the *E. coli* cell. Here, I discuss the potential functions of HcgA and HcgG.

The sequence similarity showed that HcgA belongs to the radical SAM superfamily. HcgA is similar with biotin synthase BioB, which was involved in the biotin biosynthesis, and [FeFe]-hydrogenase maturation protein HydE and HydG. HydG is responsible for synthesis of the CO and CN ligands of [FeFe]-hydrogenase and HcgE was proposed to catalyze the formation of dithiomethylamine bridge of the H cluster. HcgA has a CX₅CX₂C motif (Figure D-2), which is similar with the CX₃CX₂C motif for [4Fe-4S] cluster-binding found in radical SAM enzymes including HydE and HydG [103]. Because of the differentiation of the cysteine motif in HcgA, conservation of the [4Fe-4S] cluster in this protein should be verified. A homology model of HcgA from *M. jannaschii* was built using the structure of HydE (PDB: 3CIX) as template (Figure D-3). It indicated that HcgA is possible to harbor the [4Fe-4S] cluster using the three cysteine residues at the CX₅CX₂C motif.

DISCUSSION

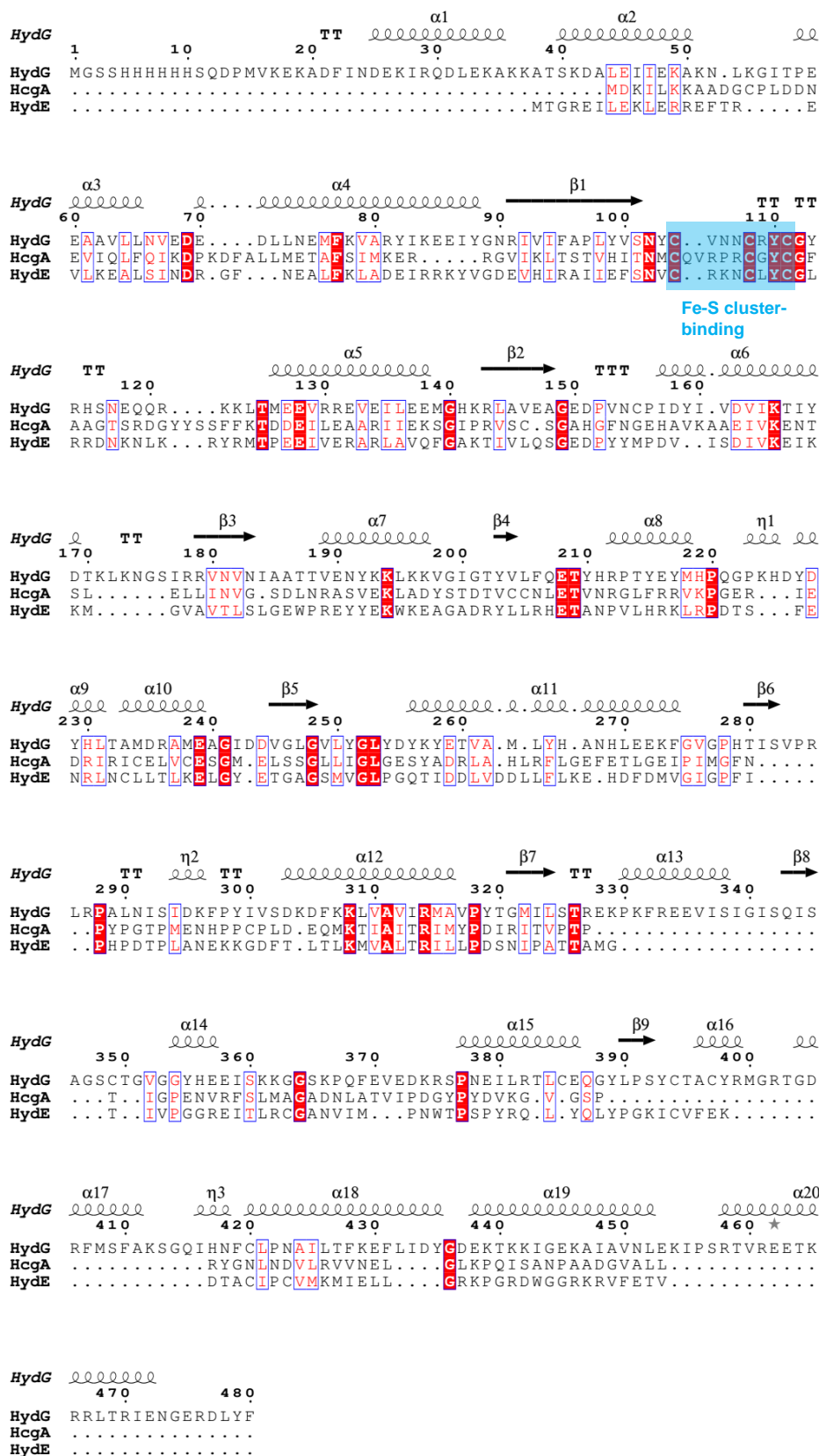


Figure D-2. Sequences alignment of HcgA, HydE and HydG. The conserved amino acids were marked with red color. The CX₅CX₂C motif in HcgA and the CX₃CX₂C motifs in HydG and HydE are shaded in blue.

DISCUSSION

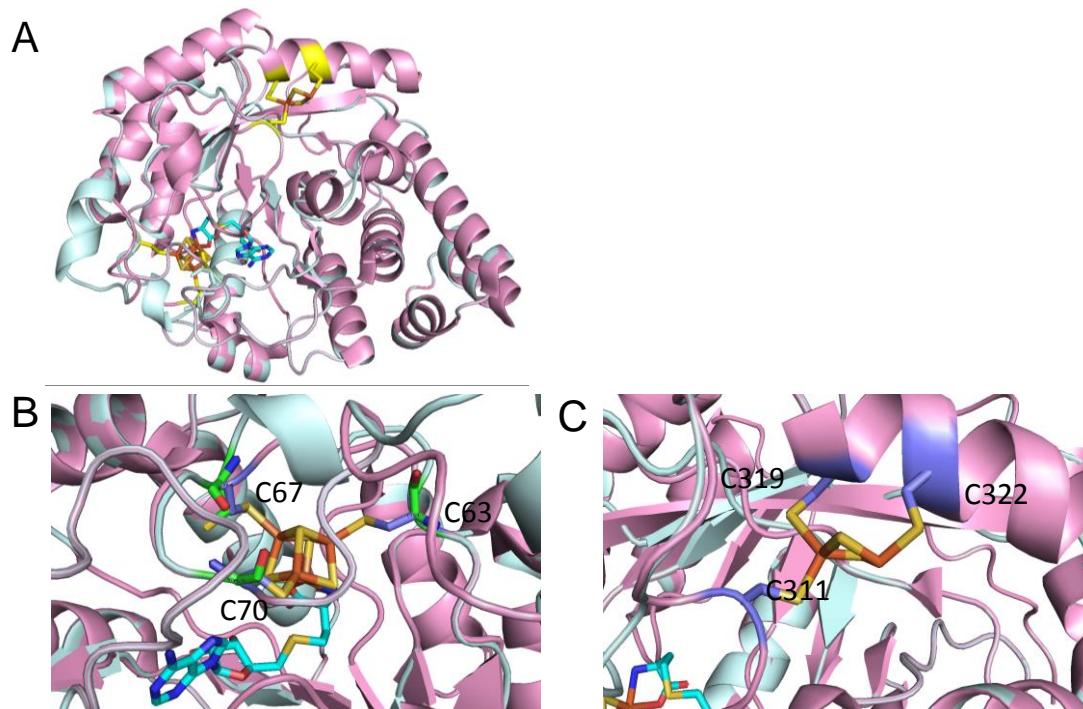


Figure D-3. Homology model of HcgA. HcgA was showed in cyan and HydE was showed in pink. (A) Comparison of overall structures of HcgA and the template protein HydE. (B) The [4Fe-4S] binding site in HcgA and HydE. The iron-sulfur cluster was showed in brown (Fe) and yellow (S) stick model. The conserved cysteines of the iron-sulfur binding site were showed in blue of HcgA and Green of HydE. Ehen the cysteine residues are fully overlapped, only blue color is shown. (C) [2Fe-2S] binding site in HydE. The cysteine was showed in blue. The cysteine residues were not conserved in HcgA. The homology model was made using SWISS MODEL.

Recently, Nicolet et al. reported that HydE could catalyze the cleavage of SAM to produce radical intermediate directly on the sulfur atom instead of abstracting a hydrogen atom to form aliphatic carbon-sulfur bond. Carbon-sulfur bond formation at aliphatic positions is a challenging reaction that is performed efficiently by radical S-adenosyl-L-methionine (SAM) enzymes. But function of the second [2Fe-2S] cluster was not reported. HydG synthesizes the CN and CO ligand for the H-cluster of [FeFe]-hydrogenase. The crystal structure of HydG indicated that HydG harbors two [4Fe4S] clusters at the N-terminal and C-terminal regions. The first N-terminal [4Fe4S] cluster was bound to SAM, which produces 5'-deoxyadenosyl radical by one electron reduction of SAM. The 5'-deoxyadenosyl radical abstracts one hydrogen atom from tyrosine, which results in the C α -C β bond cleavage of tyrosine to form dehydroglycine and *p*-cresol radical. Dehydroglycine is the precursor of CO and CN ligands. Recent

DISCUSSION

studies showed that an extra Fe coordinated with homocysteine is bound between His265 and the second C-terminal [4Fe4S] cluster [83]. The Fe(CO)CN unit is finally produced from this intermediate. BioB catalyzes the sulfur insertion in biotin biosynthesis [146, 147]. In this enzyme, the second iron-sulfur cluster is [2Fe-2S] type and one of the inorganic sulfur is inserted into the precursor desthiobiotin to produce biotin [148].

We could speculate that the function of HcgA could be similar with HydG because the iron center of FeGP cofactor also needs the coordination of CO ligands. However, isotope labeling experiments showed that the CO ligands in the FeGP cofactor was directly from CO₂ instead of tyrosine, which does not fit to the function of HydG. In addition, the second iron-sulfur cluster involved in HydG, HydE and BioB is not conserved in HcgA. In conclusion, HcgA could be a radical SAM enzyme even through it has unusual iron-sulfur binding motif (Figure D-2 and D-3) and HcgA might generate a radical for unknown substrate. However, it is difficult to speculate the function of HcgA in this moment. Further work is required to understand the function of HcgA.

I tried to heterologously produce seventeen distinct *hcgG* genes in *E. coli* as described in the result section. However, all formed inclusion body and even minor amount of soluble HcgG protein was not obtained. To solve this problem, I would change the expression system to such as yeast, which will be performed in collaboration with Professor Roland Lill (Philipps University Marburg). This yeast expression system could produce exogenous proteins using expression vector p426TDH with TDH promoter and high-level expression in yeast [149].

Sequence analysis showed that HcgG has a CX₃CX₉C motif at the N-terminal region (Figure D-4), which might be responsible for iron-sulfur cluster binding although this motif is not one of the "typical" iron-sulfur-binding motifs. Proline and glycine residues are conserved near the cysteine rich motif of HcgG, which is often observed in the iron-sulfur-binding motif. Thus, the CX₃CX₉C motif could accommodate a [4Fe-4S] cluster. The arginine or histidine residues near the cysteine-rich motif could be an additional ligand to the iron-sulfur cluster although the arginine ligand is rare. Therefore, it could be worth to produce the HcgG protein in the *E. coli* protein production system for iron-sulfur cluster proteins, which was used for heterologous expression of HcgA in *E. coli*.

DISCUSSION

compound ($m/z = 198.0414$ in the negative mode measurement) was found repeatedly in MS analysis. Interpretation of the exact mass is $C_8H_9NO_5$ (199.0481 Da), which could be a 6-carboxymethyl-2,3,4-trihydroxy-5-methyl pyridinol. From the previous isotope labeling experiment, the possible precursor of the pyridinol formation was predicted as alanine and 2,3-dihydroxy-4-oxo-pentanoate, which was derived from aspartate and 6-deoxy-5-ketoallulose-1-phosphate, respectively (Figure D-5). In the PhD thesis of Michael Schick, a proposed reaction mechanism of a hypothetical enzyme with pyridoxal-5'-phosphate (PLP) as a cofactor was proposed. In this proposed mechanism, aspartate and 2,3-dihydroxy-4-oxo-pentanoate (Figure D-6) are converted to a pyridinol with no hydroxyl group on C3. However, if dehydration reaction from compound 6 was omitted from the proposed reactions (see Figure D-6), the product 9 should have 3-OH group. Thus, this $m/z = 198.0414$ precursor might be an intermediate of the pyridinol formation enzyme system. In this case, dehydration enzyme is required to remove this hydroxyl group.

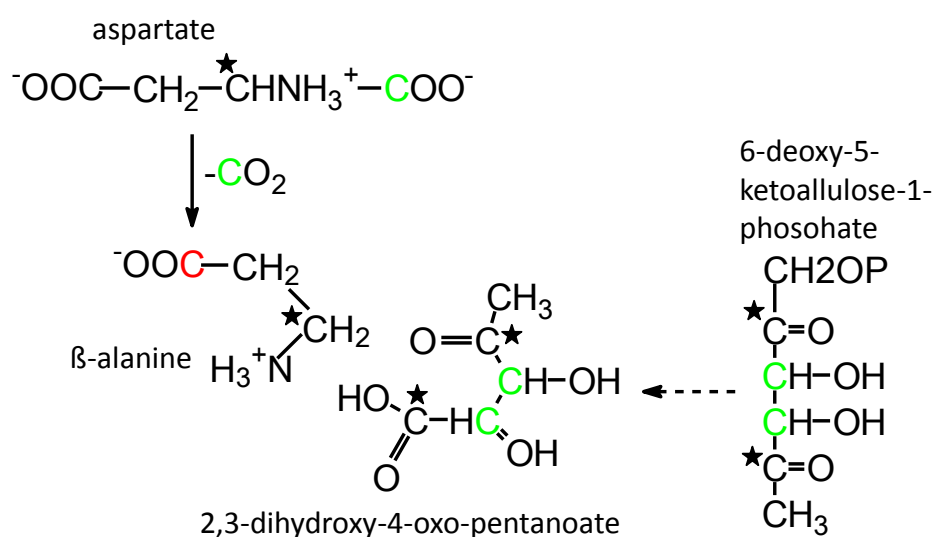


Figure D-5. Proposed reactions of pyridinol formation based on the isotope labeling experiment.

DISCUSSION

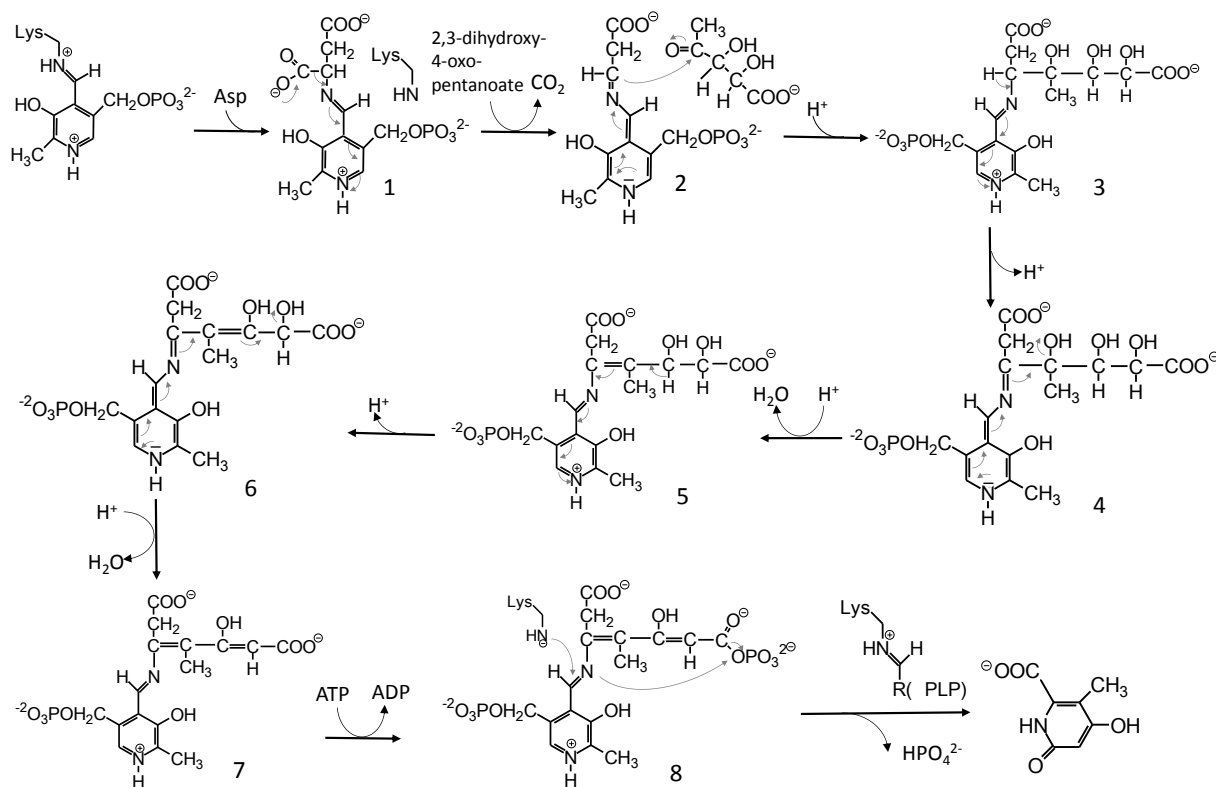


Figure D-6. Proposed reaction mechanism of pyridinol formation of FeGP cofactor (Michael Schick PhD thesis 2012). This hypothetical enzyme contains PLP as the prosthetic group at the active site.

Future work

Study of biosynthesis of the FeGP cofactor was not completed yet. HcgA crystal screening should be tested using more conditions. Since HcgA belongs to the SAM dependent radical enzyme family, characterization of HcgA using SAM and possible substrate, such as guanylylpyridinol and pyridinol is worth to try. If HcgA synthesizes the CO and CN ligands, what are the possible direct substrates for the CO ligands and how does HcgA react with the substrates? Further experiments is require to answer these questions. Heterologous production of soluble HcgG should be tried as described above.

HcgD was predicted as an iron-trafficking protein. This prediction also need to be confirmed. For instance, binding of CO and/or CO₂ to the Fe site of HcgD should be tested using UV-Vis- and infrared-spectroscopy and other methods. Additional mutation analysis of *M. maripaludis* is possible, which could test importance of HcgD in iron-insertion. This can be tested by similar experiments performed by Böck et al. for the HypB function study [139]; iron supplementation to the *M. maripaludis* Δ *hcgD* stain is worth to try.

DISCUSSION

To understand the formation of iron center of the FeGP cofactor, *in vitro* biosynthesis is alternative. Our finding of HcgB and HcgC functions and chemical synthesis of the pyridinol precursor made it possible to prepare a large amount of the guanylylpyridinol precursor, which is an important for the *in vitro* biosynthesis experiment. The *in vitro* system could contain Hcg proteins, Hmd apoenzyme, guanylylpyridinol, iron, magnesium, ATP, CO/CO₂ and reducing reagent. We can test the Hmd activity and the formation of some intermediates.

Besides the iron center formation, how the pyridinol ring formed is also need to be studied. Isotope-labeling experiment indicated the possible precursors for the pyridinol ring formation. If we could chemically synthesize the possible substrate (i.e. 2,3-dihydroxy-4-oxo-pentanoate), we can try to identify the pyridinol formation enzyme using cell extract or heterologously produced protein is possible.

Hcg protein function was studied *in vitro* using structure to function strategy. To complete biosynthesis of the FeGP cofactor, many more reactions appear to be required, for example: (1) CO ligand formation and insertion, (2) acyl-C ligand formation from the carboxy group, and (3) pyridinol ring formation. In addition, there is a question where biosynthesis of the FeGP cofactor takes place (scaffold proteins)? The FeGP cofactor biosynthesis might require more enzymes other than the Hcg proteins. In this case, comparative genomic analysis might help to answer this question. In the Results section 3, we performed comparative genomics analysis using several methanogenic archaea but now much more genomes are available. It is worthwhile to try again using more genomes. Expression of the *hcg* and *hmd* genes is regulated by nickel concentration in the medium. The unknown genes responsible for the FeGP cofactor biosynthesis could also be under regulation of nickel concentrations. Proteome and/or transcriptome analysis depend on the nickel-concentration could give a hint of such new enzymes.

REFERENCES

REFERENCES

- [1] Wahlen, M. (1993) The global methane cycle. *Annu. Rev. Earth Pl. Sci.*, 21: 407-426.
- [2] Ramanathan, V. (1988) The greenhouse theory of climate change: a test by an inadvertent global experiment. *Science* 240: 293-299.
- [3] Hasen, J., Fung, I., Lacis A., Rind, D., Lebedeff, S., Ruedy, R., Russell, G. (1988) Global climate changes as forest by goddard institute for space studies three-dimensional model. *J. Geophys. Res*, 93: 9431-9464.
- [4] Conrad, R. (2009) The global methane cycle: recent advances in understanding the microbial processes involved. *Environ. Microbiol. Rep.*, 1: 285-292.
- [5] Thauer, R. K., Kaster, A. K., Seedorf, H., Buckel, W., Hedderich, R. (2008) Methanogenic archaea: ecologically relevant differences in energy conservation. *Nat. Rev. Microbiol.*, 6: 579-591.
- [6] Thauer, R. K., Shima, S. (2008) Methane as fuel for anaerobic microorganisms. *Ann. N. Y. Acad. Sci.*, 1125: 158-170.
- [7] Thauer, R. K. (1998) Biochemistry of methanogenesis: a tribute to marjory stephenson. *Microbiology*, 144: 2377-2406.
- [8] Boetius, A., Ravenschlag, K., Schubert, C. J., Rickert, D., Widdel, F., Gieseke, A., Amann, R., Jorgensen, B. B., Witte, U., Pfannkuche, O. (2000) A marine microbial consortium apparently mediating anaerobic oxidation of methane. *Nature*, 407: 623-626.
- [9] Haroon, M. F., Hu, S., Shi, Y., Imelfort, M., Keller, J., Hugenholtz, P., Yuan, Z., Tyson, G. W. (2013) Anaerobic oxidation of methane coupled to nitrate reduction in a novel archaeal lineage. *Nature*, 500: 567-570.
- [10] Ettwig, K. F., Butler, M. K., Le Paslier, D., Pelletier, E., Mangenot, S., Kuypers, M. M., Schreiber, F., Dutilh, B. E., Zedelius, J., de Beer, D., Gloerich, J., Wessels, H. J., van Alen, T., Luesken, F., Wu, M. L., van de Pas-Schoonen, K. T., Op den Camp, H. J., Janssen-Megens, E. M., Francoijs, K. J., Stunnenberg, H., Weissenbach, J., Jetten, M. S., Strous, M. (2010) Nitrite-driven anaerobic methane oxidation by oxygenic bacteria. *Nature*, 464: 543-548.
- [11] Evans, P. N., Parks, D. H., Chadwick, G. L., Robbins, S. J., Orphan, V. J., Golding S. D., Tyson, G. W. (2015) Methane metabolism in the archaeal phylum Bathyarchaeota revealed by genome-centric metagenomics. *Science*, 1: 1-9.
- [12] Vanwonterghem, I., Evans, P. N., Parks, D. H., Jensen, P. D., Woodcroft, B. J., Hugenholtz, P., Tyson, G. W. (2016) Methylotrophic methanogenesis discovered in the archaeal phylum Verstraetearchaeota. *Nat. Microbiol.*, 1: 16170.
- [13] Bonne, D. R., Whitman, W. B., Rouviere, P., *Methanogenesis*, in *Diversity and taxonomy of methanogens*, J.G. Ferry, Editor. 1993: New York and London. p. 35.
- [14] Jussofie, A., Gottschalk, G. (1986) Further studies on the distribution of cytochromes in methanogens. *FEMS Microbiol. Lett.*, 37: 15-18.
- [15] Kühn, W., Fiebig, K., Hippe, H., Mah, R. A., Huster, B. A., Gottschalk, G. (1983) Distribution of cytochromes in methanogenic bacteria. *FEMS Microbiol. Lett.*, 20: 407-410.
- [16] Kühn, W., Gottschalk, G. (1983) Characterization of the cytochromes occurring in *Methanosarcina* species. *Eur. J. Biochem.*, 135: 89-94.
- [17] Welte, C., Deppenmeier, U. (2014) Bioenergetics and anaerobic respiratory chains of acetoclastic methanogens. *Biochim. Biophys. Acta*, 1837: 1130-1147.

REFERENCES

- [18] Johnes, W. J., Nagle, D. P., Whitman, W. B. (1987) Methanogens and the diversity of archaeobacteria. *Microbiol. Rev.*, 51: 135-177.
- [19] Boone, D. R., Johnson, R. L., Liu, Y. (1989) Diffusion of the interspecies electron carriers H₂ and formate in methanogenic ecosystems and its implications in the measurement of *K_m* for H₂ or formate uptake. *Appl. Environ. Microbiol.*, 55: 1735-1741.
- [20] Widdel, F. (1986) Growth of methanogenic bacteria in pure culture with 2-propanol and other alcohols as hydrogen donors. *Appl. Environ. Microbiol.*, 51: 1056-1062.
- [21] Vorholt, J. A., Thauer, R. K. (1997) The active species of 'CO₂' utilized by formylmethanofuran dehydrogenase from methanogenic Archaea. *Eur. J. Biochem.*, 248: 919-924.
- [22] Shima, S., Weiss, D. S., Thauer, R. K. (1995) Formylmethanofuran:tetrahydro-methanopterin formyltransferase (Ftr) from the hyperthermophilic *Methanopyrus kandleri* Cloning, sequencing and functional expression of the *ftr* gene and one-step purification of the enzyme overproduced in *Escherichia coli*. *Eur. J. Biochem.*, 230: 906-913.
- [23] Shima, S., Thauer, R. K., Michel, H., Ermler, U. (1996) Crystallization and preliminary X-ray diffraction studies of formylmethanofuran: tetrahydro-methanopterin formyltransferase from *Methanopyrus kandleri*. *Proteins*, 26: 118-120.
- [24] Klein, A. R., Breitung, J., Linder, D., Stetter, K. O., Thauer, R. K. (1993) N⁵,N¹⁰-methenyltetrahydromethanopterin cyclohydrolase from the extremely thermophilic sulfate reducing Archaeoglobus fulgidus: comparison of its properties with those of the cyclohydrolase from the extremely thermophilic *Methanopyrus kandleri*. *Arch. Microbiol.*, 159: 213-219.
- [25] Vaupel, M., Dietz, H., Linder, D., Thauer, R. K. (1996) Primary structure of cyclohydrolase (Mch) from *Methanobacterium thermoautotrophicum* (strain Marburg) and functional expression of the *mch* gene in *Escherichia coli*. *Eur. J. Biochem.*, 236: 294-300.
- [26] Vaupel, M., Vorholt, J. A., Thauer, R. K. (1998) Overproduction and one-step purification of the N⁵,N¹⁰-methenyltetrahydromethanopterin cyclohydrolase (Mch) from the hyperthermophilic *Methanopyrus kandleri*. *Extremophiles*, 2: 15-22.
- [27] Zirngibl, C., Van Dongen, W., Schworer, B., Von Bunau, R., Richter, M., Klein, A., Thauer, R. K. (1992) H₂-forming methylenetetrahydromethanopterin dehydrogenase, a novel type of hydrogenase without iron-sulfur clusters in methanogenic archaea. *Eur J Biochem*, 208: 511-520.
- [28] Ceh, K., Demmer, U., Warkentin, E., Moll, J., Thauer, R. K., Shima, S., Ermler, U. (2009) Structural basis of the hydride transfer mechanism in F₄₂₀-dependent methylenetetrahydromethanopterin dehydrogenase. *Biochemistry*, 48: 10098-10105.
- [29] Klein, A. R., Thauer, R. K. (1997) Overexpression of the coenzyme-F₄₂₀-dependent N⁵,N¹⁰-methylenetetrahydromethanopterin dehydrogenase gene from the hyperthermophilic *Methanopyrus kandleri*. *Eur. J. Biochem.*, 245: 386-391.
- [30] Afting, C., Hohheimer, A., Thauer, R. K. (1998) Function of H₂-forming methylenetetrahydromethanopterin dehydrogenase from *Methanobacterium thermoautotrophicum* in coenzyme F₄₂₀ reduction with H₂. *Arch. Microbiol.*, 169: 206-210.

REFERENCES

- [31] Vaupel, M., Thauer, R. K. (1995) Coenzyme F₄₂₀-dependent N⁶,N¹⁰-methylene tetrahydromethanopterin reductase (Mer) from *Methanobacterium thermoautotrophicum* strain Marburg. Cloning, sequencing, transcriptional analysis, and functional expression in *Escherichia coli* of the *mer* gene. *Eur. J. Biochem.*, 231: 773-778.
- [32] Shima, S., Goubeaud, M., Vinzenz, D., Thauer, R. K., Ermler, U. (1997) Crystallization and preliminary X-ray diffraction studies of methyl-coenzyme M reductase from *Methanobacterium thermoautotrophicum*. *J. Biochem.*, 121: 829-830.
- [33] Harms, U., Thauer, R. K. (1997) Identification of the active site histidine in the corrinoid protein MtrA of the energy-conserving methyltransferase complex from *Methanobacterium thermoautotrophicum*. *Eur. J. Biochem.*, 250: 783-788.
- [34] Gottschalk, G., Thauer, R. K. (2001) The Na⁺-translocating methyltransferase complex from methanogenic archaea. *Biochim. Biophys. Acta*, 1505: 28-36.
- [35] Becher, B., Müller, V., Gottschalk, G. (1992) N⁶-methyl-tetrahydromethanopterin: coenzyme M methyltransferase of *Methanosarcina* strain Gol is an Na⁺-translocating membrane protein. *J. Bacteriol.*, 174: 7656-7660.
- [36] Ermler, U., Grabarse, W., Shima, S., Goubeaud, M., Thauer, R. K. (1997) Crystal structure of methyl-coenzyme M reductase: the key enzyme of biological methane formation. *Science*, 278: 1457-1462.
- [37] Hedderich, R., Koch, J., Linder, D., Thauer, R. K. (1994) The heterodisulfide reductase from *Methanobacterium thermoautotrophicum* contains sequence motifs characteristic of pyridine-nucleotide-dependent thioredoxin reductases. *Eur. J. Biochem.*, 225: 253-261.
- [38] Thauer, R. K., Kaster, A. K., Goenrich, M., Schick, M., Hiromoto, T., Shima, S. (2010) Hydrogenases from methanogenic archaea, nickel, a novel cofactor, and H₂ storage. *Annu. Rev. Biochem.*, 79: 507-536.
- [39] Kaster, A. K., Moll, J., Parey, K., Thauer, R. K. (2011) Coupling of ferredoxin and heterodisulfide reduction via electron bifurcation in hydrogenotrophic methanogenic archaea. *Proc. Natl. Acad. Sci. USA*, 108: 2981-2986.
- [40] Ferry, J. G. (2011) Fundamentals of methanogenic pathways that are key to the biomethanation of complex biomass. *Curr. Opin. Biotechnol.*, 22: 351-357.
- [41] Ferry, J. G. (1997) Enzymology of the fermentation of acetate to methane by *Methanosarcina thermophila*. *BioFactors*, 6: 25-35.
- [42] Berger, S., Welte, C., Deppenmeier, U. (2012) Acetate activation in *Methanosaeta thermophila*: characterization of the key enzymes pyrophosphatase and acetyl-CoA synthetase. *Archaea*, 2012: 315-153.
- [43] Smith, K. S., Ingram-Smith, C. (2007) *Methanosaeta*, the forgotten methanogen? *Trends Microbiol.*, 15: 150-155.
- [44] Jetten, M. S., Fluit, T. J., Stams, A. J. M., Zehnder, A. J. B. (1992) A fluoride-insensitive inorganic pyrophosphatase isolated from *Methanotherix soehngenii*. *Arch. Microbiol.*, 157: 284-289.
- [45] Hagemeyer, C. H., Krer, M., Thauer, R. K., Warkentin, E., Ermler, U. (2006) Insight into the mechanism of biological methanol activation based on the crystal structure of the methanol-cobalamin methyltransferase complex. *Proc. Natl. Acad. Sci. USA*, 103: 18917-18922.
- [46] Naumann, E., Fahlbusch, K., Gottschalk, G. (1984) Presence of a trimethylamine HS-coenzyme M methyltransferase in *Methanosarcina barkeri*. *Arch. Microbiol.*, 138: 79-83.

REFERENCES

- [47] Oremland, R. S., Kiene, R. P., Mathrani, I., Whiticar, M. J., Bonne, D. (1989) Description of an estuarine methylotrophic Methanogen which grow on dimethyl sulfide. *Appl. Environ. Microbiol.*, 55: 994-1002.
- [48] Schönheit, P., Moll, J., Thauer, R. K. (1980) Growth parameters (K_s , μ_{max} , Y_s) of *Methanobacterium thermoautotrophium*. *Arch. Microbiol.*, 127: 59-65.
- [49] Pisa, K. Y., Weidner, C., Maischak, H., Kavermann, H., Muller, V. (2007) The coupling ion in the methanoarchaeal ATP synthases: H^+ vs. Na^+ in the A_1A_o ATP synthase from the archaeon *Methanosarcina mazei* Gö1. *FEMS Microbiol. Lett.*, 277: 56-63.
- [50] Murakami, E., Deppenmeier, U., Ragsdale, S. W. (2001) Characterization of the intramolecular electron transfer pathway from 2-hydroxyphenazine to the heterodisulfide reductase from *Methanosarcina thermophila*. *J. Biol. Chem.*, 276: 2432-2439.
- [51] Ide, T., Bäumer, S., Deppenmeier, U. (1999) Energy conservation by the H_2 :Heterodisulfide oxidoreductase from *Methanosarcina mazei* Gö1: identification of two Proton-translocating segments. *J. Bacteriol.*, 181: 4076-4080.
- [52] Wagner, T., Ermler, U., Shima, S. (2016) The methanogenic CO_2 reducing-and-fixing enzyme is bifunctional and contains 46 [4Fe-4S] clusters. *Science*, 354: 114-117.
- [53] Mitchell, P. (1975) The protomotive Q cycle: a Q general formulation. *FEBS Lett.*, 59: 137-139.
- [54] Osyczka, A., Moser, C. C., Dutton, P. L. (2005) Fixing the Q cycle. *Trends Biochem. Sci.*, 30: 176-182.
- [55] Buckel, W., Thauer, R. K. (2013) Energy conservation via electron bifurcating ferredoxin reduction and proton/ Na^+ translocating ferredoxin oxidation. *Biochim. Biophys. Acta*, 1827: 94-113.
- [56] Shima, S. (2014) Enzyme chemistry of methanogenesis and anaerobic oxidation of methane. *Kagakutoseibutsu*, 52: 307-312.
- [57] Vignais, P. M., Billoud, B. (2007) Occurrence classification and biological function of hydrogenases: an overview. *Chem. Rev.*, 107: 4206-4272.
- [58] Dai, Y. R., Reed, D. W., Millstein, J. H., Hartzall, P. L., Grahame, D. A., deMoll, E. (1998) Acetyl-CoA decarbonylase/synthase complex from *Archaeoglobus fulgidus*. *Arch Microbiol.*, 169: 525-529.
- [59] Böck, A., King, P. W., Blokesch, M., Posewitz, M. C. (2006) Maturation of hydrogenases. *Advan. Microb. Physiol.*, 51: 1-71.
- [60] Watanabe, S., Sasaki, D., Tominaga, T., Miki, K. (2012) Structural basis of [NiFe] hydrogenase maturation by Hyp proteins. *Biol. Chem.*, 393: 1089-1100.
- [61] Reissmann, S., Hochleitner, E. Wang, H., Paschos, A., Lottspeich, F., Glass, R. S., Böck, A. (2003) Taming of a poison: biosynthesis of the NiFe-hydrogenase cyanide ligands. *Science*, 299: 1067-1070.
- [62] Paschos, A., Glass, R. S., Böck, A. (2001) Carbamoylphosphate requirement for synthesis of the active center of [NiFe]-hydrogenase. *FEBS Lett.*, 488: 9-12.
- [63] Drapal, N., Böck, A. (1998) Interaction of the hydrogenase accessory protein HypC with HycE, the large subunit of *Escherichia coli* hydrogenase 3 during enzyme maturation. *Biochemistry*, 37: 2941-2948.
- [64] Bürstel, I., Siebert, E., Frielingsdorf, S., Zebger, I., Friedrich, B., Lenz, O. (2017) CO synthesized from the central one-carbon pool as source for the iron carbonyl in O_2 -tolerant [NiFe]-hydrogenase. *Proc. Natl. Acad. Sci. USA*, 113.
- [65] Blokesch, M., Albracht, S. P., Matzanke, B. F., Drapal, N. M., Jacobi, A., Bock, A. (2004) The complex between hydrogenase-maturation proteins HypC and

REFERENCES

- HypD is an intermediate in the supply of cyanide to the active site iron of [NiFe]-hydrogenases. *J. Mol. Biol.*, 344: 155-167.
- [66] Olson, J. W., Mehta, N. S., Maier, R. J. (2001) Requirement of nickel metabolism proteins HypA and HypB for full activity of both hydrogenase and urease in *Helicobacter pylori*. *Mol. Microbiol.*, 39: 176-182.
- [67] Leipe, D. D., Wolf, Y. I., Koonin, E. V., Aravind, L. (2002) Classification and evolution of P-loop GTPases and related ATPase. *J. Mol. Biol.*, 317: 41-72.
- [68] Theodorator, E., Huber, R., Böck, A. (2005) [NiFe]-Hydrogenase maturation endopeptidase: structure and function. *Biochem. Soc. Trans.*, 33: 108-111.
- [69] Peters, J. W., Schut, G. J., Boyd, E. S., Mulder, D. W., Shepard, E. M., Broderick, J. B., King, P. W., Adams, M. W. (2015) [FeFe]- and [NiFe]-hydrogenase diversity, mechanism, and maturation. *Biochim. Biophys. Acta*, 1853: 1350-1369.
- [70] Posewitz, M. C., King, P. W., Smolinski, S. L., Zhang, L., Seibert, M., Ghirardi, M. L. (2004) Discovery of two novel radical S-adenosylmethionine proteins required for the assembly of an active [Fe] hydrogenase. *J. Biol. Chem.*, 279: 25711-25720.
- [71] Brazzolotto, X., Rubach, J. K., Gaillard, J., Gambarelli, S., Atta, M., Fontecave, M. (2006) The [Fe-Fe]-hydrogenase maturation protein HydF from *Thermotoga maritima* is a GTPase with an iron-sulfur cluster. *J. Biol. Chem.*, 281: 769-774.
- [72] Berggren, G., Adamska, A., Lambertz, C., Simmons, T. R., Esselborn, J., Atta, M., Gambarelli, S., Mouesca, J. M., Reijerse, E., Lubitz, W., Happe, T., Artero, V., Fontecave, M. (2013) Biomimetic assembly and activation of [FeFe]-hydrogenases. *Nature*, 499: 66-70.
- [73] Kuchenreuther, J. M., Britt, R. D., Swartz, J. R. (2012) New insights into [FeFe] hydrogenase activation and maturase function. *PLoS One*, 7: e45850.
- [74] Betz, J. N., Boswell, N. W., Fugate, C. J., Holliday, G. L., Akiva, E., Scott, A. G., Babbitt, P. C., Peters, J. W., Shepard, E. M., Broderick, J. B. (2015) [FeFe]-hydrogenase maturation: insights into the role HydE plays in dithiomethylamine biosynthesis. *Biochemistry*, 54: 1807-1818.
- [75] Broderick, J. B., Duffus, B. R., Duschene, K. S., Shepard, E. M. (2014) Radical S-adenosylmethionine enzymes. *Chem. Rev.*, 114: 4229-4317.
- [76] Kriek, M., Martins, F., Challand, M. R., Croft, A., Roach, P. L. (2007) Thiamine biosynthesis in *Escherichia coli*: identification of the intermediate and by-product derived from tyrosine. *Angew. Chem., Int. Ed. Engl.*, 46: 9223-9226.
- [77] Pilet, E., Nicolet, Y., Mathevon, C., Douki, T., Fontecilla-Camps, J. C., Fontecave, M. (2009) The role of the maturase HydG in [FeFe]-hydrogenase active site synthesis and assembly. *FEBS Lett.*, 583: 506-511.
- [78] Kuchenreuther, J. M., Myers, W., Suess, D. L. M., Stich, T. A., Pelmentschikow, V., Schiigi, S. A., Cramer, S. P., Swartz, J. R., Britt, R. D., George, S. J. (2014) The HydG enzyme generates an Fe(CO)₂(CN) synthon in assembly of the FeFe hydrogenase H-cluster. *Science*, 343: 424-427.
- [79] Pagnier, A., Martin, L., Zeppleri, L., Nicolet, Y., Fontecilla-Camps, J. C. (2016) CO and CN⁻ syntheses by [FeFe]-hydrogenase maturase HydG are catalytically differentiated events. *Proc. Natl. Acad. Sci. USA*, 113: 104-109.
- [80] Dinis, P., Suess, D. L. M., Fox, S. J., Harmer, J. E., Driesener, R. C., Paz, L. D. L., Swartz, J. R., Essex, J. W., Britt, R. D., Roach, P. L. (2015) X-ray crystallographic and EPR spectroscopic analysis of HydG, a maturase in [FeFe]-hydrogenase. *Proc. Natl. Acad. Sci. USA*, 112: 1362-1367.

REFERENCES

- [81] Nicolet, Y., Martin, L., Tron, C., Fontecilla-Camps, J. C. (2010) A glycyI free radical as the precursor in the synthesis of carbon monoxide and cyanide by the [FeFe]-hydrogenase maturase HydG. *FEBS Lett.*, 584: 4197-202.
- [82] Driesener, R. C., Duffus, B. R., Shepard, E. M., Bruzas, I. R., Duschene, K. S., Coleman, N. J., Marrison, A. P., Salvadori, E., Kay, C. W., Peters, J. W., Broderick, J. B., Roach, P. L. (2013) Biochemical and kinetic characterization of radical S-adenosyl-L-methionine enzyme HydG. *Biochemistry*, 52: 8696-8707.
- [83] Suess, D. L., Burstel, I., De La Paz, L., Kuchenreuther, J. M., Pham, C. C., Cramer, S. P., Swartz, J. R., Britt, R. D. (2015) Cysteine as a ligand platform in the biosynthesis of the FeFe hydrogenase H cluster. *Proc. Natl. Acad. Sci. USA*, 112: 11455-11460.
- [84] Shepard, E. M., McGlynn, S. E., Bueling, A. L., Grady-Smith, C. S., George, S. J., Winslow, M. A., Cramer, S. P., Peters, J. W., Broderick, J. B. (2010) Synthesis of the 2Fe subcluster of the [FeFe]-hydrogenase H cluster on the HydF scaffold. *Proc. Natl. Acad. Sci. USA*, 107: 10448-10453.
- [85] Afting, C., Kremmer, E., Brucker, C., Hochheimer, A., Thauer, R. K. (2000) Regulation of the synthesis of H₂-forming methylenetetrahydromethanopterin dehydrogenase (Hmd) and of HmdII and HmdIII in *Methanothermobacter marburgensis*. *Arch. Microbiol.*, 174: 225-232.
- [86] Zhang, Y., Rodionov, D. A., Gelfand, M. S., Gladyshev, V. N. (2009) Comparative genomic analyses of nickel, cobalt and vitamin B₁₂ utilization. *BMC Genomics*, 10: 78.
- [87] Shima, S., Pilak, O., Vogt, S., Schick, M., Stagni, M. S., Meyer-Klaucke, W., Warkentin, E., Thauer, R. K., Ermler, U. (2008) The Crystal structure of [Fe]-hydrogenase reveals the geometry of the active site. *Science*, 321: 572-575.
- [88] Shima, S., Ermler, U. (2011) Structure and function of [Fe]-hydrogenase and its iron-guanylylpyridinol (FeGP) cofactor. *Eur. J. Inorg. Chem.*, 2011: 963-972.
- [89] Pilak, O., Mamat, B., Vogt, S., Hagemeyer, C. H., Thauer, R. K., Shima, S., Vonrhein, C., Warkentin, E., Ermler, U. (2006) The crystal structure of the apoenzyme of the iron-sulphur cluster-free hydrogenase. *J. Mol. Biol.*, 358: 798-809.
- [90] Hiromoto, T., Ataka, K., Pilak, O., Vogt, S., Stagni, M. S., Meyer-Klaucke, W., Warkentin, E., Thauer, R. K., Shima, S., Ermler, U. (2009) The crystal structure of C176A mutated [Fe]-hydrogenase suggests an acyl-iron ligation in the active site iron complex. *FEBS Lett.*, 583: 585-590.
- [91] Shima, S., Schick, M., Kahnt, J., Ataka, K., Steinbach, K., Linne, U. (2012) Evidence for acyl-iron ligation in the active site of [Fe]-hydrogenase provided by mass spectrometry and infrared spectroscopy. *Dalton Trans.*, 41: 767-771.
- [92] Shima, S., Lyon, E. J., Sordel-Klippert, M., Kauss, M., Kahnt, J., Thauer, R. K., Steinbach, K., Xie, X., Verdier, L., Griesinger, C. (2004) The cofactor of the iron-sulfur cluster free hydrogenase hmd: structure of the light-inactivation product. *Angew. Chem. Int. Ed.*, 43: 2547-2551.
- [93] Schick, M., Xie, X., Ataka, K., Kahnt, J., Linne, U., Shima, S. (2012) Biosynthesis of the iron-guanylylpyridinol cofactor of [Fe]-hydrogenase in methanogenic archaea as elucidated by stable-isotope labeling. *J. Am. Chem. Soc.*, 134: 3271-3280.
- [94] Fujishiro, T., Tamura, H., Schick, M., Kahnt, J., Xie, X., Ermler, U., Shima, S. (2013) Identification of the HcgB enzyme in [Fe]-hydrogenase-cofactor biosynthesis. *Angew. Chem. Int. Ed.*, 52: 12555-12558.

REFERENCES

- [95] Martens, J. A., Genereaux, J., Saleh, A., Brandi, C. J. (1996) Transcriptional activation by Yeast PDR1p Is inhibited by its association with NGG1p/ADA3p. *J. Biol. Chem.*, 271: 15884-15890.
- [96] Akiyama, H., Fujisawa, N., Tashiro, Y., Takanabe, N., Sugiyama, A., Tashiro, F. (2003) The role of transcriptional corepressor Nif3l1 in early stage of neural differentiation via cooperation with Trip15/CSN2. *J. Biol. Chem.*, 278: 10752-10762.
- [97] Galperin, M. Y., Koonin, E. V. (2004) 'Conserved hypothetical' proteins: prioritization of targets for experimental study. *Nucleic Acids Res.*, 32: 5452-5463.
- [98] Fujishiro, T., Ermler, U., Shima, S. (2014) A possible iron delivery function of the dinuclear iron center of HcgD in [Fe]-hydrogenase cofactor biosynthesis. *FEBS Lett.*, 588: 2789-2793.
- [99] Burroughs, A. M., Iyer, L. M., Aravind, L. (2009) Natural history of the E1-like superfamily: implication for adenylation, sulfur transfer, and ubiquitin conjugation. *Proteins*, 75: 895-910.
- [100] Schulman, B. A., Harper, J. W. (2009) Ubiquitin-like protein activation by E1 enzymes: the apex for downstream signalling pathways. *Nat. Rev. Mol. Cell. Biol.*, 10: 319-331.
- [101] Fujishiro, T., Kahnt, J., Ermler, U., Shima, S. (2015) Protein-pyridinol thioester precursor for biosynthesis of the organometallic acyl-iron ligand in [Fe]-hydrogenase cofactor. *Nat. Commun.*, 6: 6895.
- [102] Suess, D. L., Kuchenreuther, J. M., De La Paz, L., Swartz, J. R., Britt, R. D. (2016) Biosynthesis of the [FeFe] Hydrogenase H Cluster: a central role for the radical SAM enzyme HydG. *Inorg. Chem.*, 55: 478-487.
- [103] McGlynn, S. E., Boyd, E. S., Shepard, E. M., Lange, R. K., Gerlach, R., Broderick, J. B., Peters, J. W. (2010) Identification and characterization of a novel member of the radical AdoMet enzyme superfamily and implications for the biosynthesis of the Hmd hydrogenase active site cofactor. *J. Bacteriol.*, 192: 595-598.
- [104] Shima, S., Schick, M., Tamura, H. (2011) Methods in Enzymology. *Methods Enzymol*, 494: 119-137.
- [105] Takahashi, Y., Nakamura, M. (1999) Functional assignment of the ORF2-iseS-iscU-iscA-hscB-hscA-fdx-ORF3 gene cluster involved in the assembly of Fe-S clusters in *Escherichia coli*. *J. Bacteriol.*, 126: 917-926.
- [106] Huang, H., Hu, L., Yu, W., Li, H., Tao, F., Xie, H., Wang, S. (2016) Heterologous overproduction of 2[4Fe4S]- and [2Fe2S]-type clostridial ferredoxins and [2Fe2S]-type agrobacterial ferredoxin. *Protein Expr. Purif.*, 121: 1-8.
- [107] Tartof, K. D., Hobbs, C. A. (1987) Improved media for growing plasmid and cosmid clones. *Bethesda Res. Lab. Focus*: 9-12.
- [108] Bowen, T. L., Whitman, W. B. (1987) Incorporation of exogenous purines and pyrimidines by *Methanococcus voltae* and isolation of analog-resistant mutants. *Appl. Environ. Microbiol.*, 53: 1822-1826.
- [109] Moore, B. C., Leigh, J. A., (2005) Markerless mutagenesis in *Methanococcus maripaludis* demonstrates roles for alanine dehydrogenase, alanine racemase, and alanine permease. *J. Bacteriol.* 187: 972-979.
- [110] Brandford, M. M. (1976) A rapid and sensitive method for the quantitation of microgram quantities of protein utilizing the principle of protein-dye binding. *Anal. Biochem.*, 72: 248-254.
- [111] Hennessy, D. J., Reid, G.R., Smith, F.E., Thompson, S.L. (1984) Ferene-a new spectrophotometric reagent for iron. *Can. J. Chem.*, 62: 721-724.

REFERENCES

- [112] Kabsch, W. (2010) XDS. *Acta Crystallogr. D*, 66: 125-132.
- [113] Winn, M. D., Ballard, C. C., Cowtan, K. D., Dodson, E. J., Emsley, P., Evans, P. R., Keegan, R. M., Krissinel, E. B., Leslie, A. G., McCoy, A., McNicholas, S. J., Murshudov, G. N., Pannu, N. S., Potterton, E. A., Powell, H. R., Read, R. J., Vagin, A., Wilson, K. S. (2011) Overview of the CCP4 suite and current developments. *Acta Crystallogr D*, 67: 235-242.
- [114] Afonine, P. V., Grosse-Kunstleve, R. W., Chen, V. B., Headd, J. J., Moriarty, N. W., Richardson, J. S., Richardson, D. C., Urzhumtsev, A., Zwart, P. H., Adams, P. D. (2010) phenix.model_vs_data: a high-level tool for the calculation of crystallographic model and data statistics. *J. Appl. Crystallogr.*, 43: 669-676.
- [115] Emsley, P., Cowtan, K. (2004) Coot: model-building tools for molecular graphics. *Acta Crystallogr. D*, 60: 2126-2132.
- [116] Chen, V. B., Arendall, W. B., Headd, J. J., Keedy, D. A., Immormino, R. M., Kapral, G. J., Murray, L. W., Richardson, J. S., Richardson, D. C. (2010) MolProbity: all-atom structure validation for macromolecular crystallography. *Acta Crystallogr D*, 66: 12-21.
- [117] Dominissini, D., Nachtergaele, S., Moshitch-Moshkovitz, S., Peer, E., Kol, N., Ben-Haim, M. S., Dai, Q., Di Segni, A., Salmon-Divon, M., Clark, W. C., Zheng, G., Pan, T., Solomon, O., Eyal, E., Hershkovitz, V., Han, D., Dore, L. C., Amariglio, N., Rechavi, G., He, C. (2016) The dynamic N¹-methyladenosine methylome in eukaryotic messenger RNA. *Nature*, 530: 441-446.
- [118] Liscombe, D. K., Louie, G. V., Noel, J. P. (2012) Architectures, mechanisms and molecular evolution of natural product methyltransferases. *Nat. Prod. Rep.*, 29: 1238-1250.
- [119] Köksal, M., Chou, W. K., Cane, D. E., Christianson, D. W. (2012) Structure of geranyl diphosphate C-methyltransferase from *Streptomyces coelicolor* and implications for the mechanism of isoprenoid modification. *Biochemistry*, 51: 3003-3010.
- [120] Foster, P. G., Nunes, C. R., Greene, P., Moustakas, D., Stround, R. M. (2003) The first structure of an RNA m⁵C methyltransferase, Fmu, provides insight into catalytic mechanism and specific binding of RNA substrate. *Structure*, 11: 1609-1620.
- [121] Dai, Y. N., Zhou, K., Cao, D. D., Jiang, Y. L., Meng, F., Chi, C. B., Ren, Y. M., Chen, Y., Zhou, C. Z. (2014) Crystal structures and catalytic mechanism of the C-methyltransferase Coq5 provide insights into a key step of the yeast coenzyme Q synthesis pathway. *Acta Crystallogr D*, 70: 2085-2092.
- [122] Zou, X. W., Liu, Y. C., Hsu, N. S., Huang, C. J., Lyu, S. Y., Chan, H. C., Chang, C. Y., Yeh, H. W., Lin, K. H., Wu, C. J., Tsai, M. D., Li, T. L. (2014) Structure and mechanism of a nonhaem-iron SAM-dependent C-methyltransferase and its engineering to a hydratase and an O-methyltransferase. *Acta Crystallogr D*, 70: 1549-1560.
- [123] Chen, S. C., Huang, C. H., Lai, S. J., Liu, J. S., Fu, P. K., Tseng, S. T., Yang, C. S., Lai, M. C., Ko, T. P., Chen, Y. (2015) Structure and mechanism of an antibiotics-synthesizing 3-hydroxykynurenine C-methyltransferase. *Sci. Rep.*, 5: 10100.
- [124] Buckel, W., Thauer, R. K. (2011) Dual role of S-adenosylmethionine (SAM⁺) in the methylation of sp²-hybridized electrophilic carbons. *Angew. Chem., Int. Ed.*, 50: 10492-10494.
- [125] Grove, T. L., Benner, J. S., Radle, M. I., Ahlum, J. H., Landgraf, B. J., Kerbs, C., Booker, S. J. (2011) A radically different mechanism for S-adenosylmethionine-dependent methyltransferase. *Science*, 332: 604-607.

REFERENCES

- [126] Struck, A. W., Thompson, M. L., Wong, L. S., Micklefield, J. (2012) S-adenosyl-methionine-dependent methyltransferases: highly versatile enzymes in biocatalysis, biosynthesis and other biotechnological applications. *Chembiochem*, 13: 2642-2655.
- [127] Shima, S., Chen, D., Xu, T., Wodrich, M. D., Fujishiro, T., Schultz, K. M., Kahnt, J., Ataka, K., Hu, X. (2015) Reconstitution of [Fe]-hydrogenase using model complexes. *Nat. Chem.*, 7: 995-1002.
- [128] Shima, S., Lyon, E. J., Thauer, R. K., Mienert, B., Bill, E. (2005) Mössbauer studies of the iron-sulfur cluster-free hydrogenase: the electronic state of the mononuclear Fe active site. *J. Am. Chem. Soc.*, 127: 10430-10435.
- [129] Fujishiro, T., Bai, L., Xu, T., Xie, X., Schick, M., Kahnt, J., Rother, M., Hu, X., Ermler, U., Shima, S. (2016) Identification of HcgC as a SAM-dependent pyridinol methyltransferase in [Fe]-hydrogenase cofactor biosynthesis. *Angew. Chem., Int. Ed.*, 55: 9648-9651.
- [130] Lie, T. J., Costa, K. C., Pak, D., Sakesan, V., Leigh, J. A. (2013) Phenotypic evidence that the function of the [Fe]-hydrogenase Hmd in *Methanococcus maripaludis* requires seven *hcg* (*hmd* co-occurring genes) but not *hmdII*. *FEMS Microbiol. Lett.*, 343: 156-160.
- [131] Schwörer, B., Thauer, R. K. (1991) Activities of formylmethanofuran dehydrogenase, methylenetetrahydromethanopterin dehydrogenase, methylenetetrahydro-methanopterin reductase, and heterodisulfide reductase in methanogenic bacteria. *Arch. Microbiol.*, 155: 459-465.
- [132] McGlynn, S. E., Boyd, E. S., Shepard, E. M., Lange, R. K., Gerlach, R., Broderick, J. B., Peters, J. W. (2010) Identification and characterization of a novel member of the radical AdoMet enzyme superfamily and implications for the biosynthesis of the Hmd hydrogenase active site cofactor. *J. Bacteriol.*, 192: 595-598.
- [133] Shima, S., Thauer, R. K. (2007) A third type of hydrogenase catalyzing H₂ activation. *Chem. Rec.*, 7: 37-46.
- [134] Burgdorf, T., Lenz, O., Buhrke, T., Linden, E., Jones, A. K., Albracht, S. P., Friedrich, B. (2005) [NiFe]-hydrogenases of *Ralstonia eutropha* H16: modular enzymes for oxygen-tolerant biological hydrogen oxidation. *J. Mol. Microbiol. Biotechnol.*, 10: 181-96.
- [135] Lubitz, W., Ogata, H., Rudiger, O., Reijerse, E. (2014) Hydrogenases. *Chem. Rev.*, 114: 4081-4148.
- [136] Xu, T., Yin, C. J., Wodrich, M. D., Mazza, S., Schultz, K. M., Scopelliti, R., Hu, X. (2016) A functional model of [Fe]-hydrogenase. *J. Am. Chem. Soc.*, 138: 3270-3273.
- [137] Schwartz, L., Eilers, G., Eriksson, L., Gogoll, A., Lomoth, R., Ott, S. (2006) Iron hydrogenase active site mimic holding a proton and a hydride. *Chem. Commun.*: 520-522.
- [138] Sauer, M., Böhm, R., Böck, A. (1992) Mutational analysis of the operon (*hyc*) determining hydrogenase 3 formation in *Escherichia coli*. *Mol. Microbiol.*, 6: 1523-1532.
- [139] Maier, T., Jacobi, A., Sauter, M., Böck (1993) The product of the *hypB* gene, which is required for nickel incorporation into hydrogenase, is a novel guanine nucleotide-binding protein. *J. Bacteriol.*, 175: 630-635.
- [140] Hube, M., Blokesch, M., Böck, A. (2002) Network of hydrogenase maturation in *Escherichia coli*: role of accessory proteins HypA and HypF. *J. Bacteriol.*, 184: 3879-3885.

REFERENCES

- [141] Magalon, A., Böck, A. (2000) Analysis of the HypC-HycE complex, a key intermediate in the assembly of the metal center of the *Escherichia coli* hydrogenase 3. *J. Biol. Chem.*, 275: 21114-21120.
- [142] Kuchenreuther, J. M., Stapleton, J. A., Swartz, J. R. (2009) Tyrosine, cysteine, and S-adenosyl methionine stimulate *in vitro* [FeFe] hydrogenase activation. *PLoS One*, 4: e7565.
- [143] King, P. W., Posewitz, M. C., Ghirardi, M. L., Seibert, M. (2006) Functional Studies of [FeFe] Hydrogenase Maturation in an *Escherichia coli* Biosynthetic System. *J. Bacteriol.*, 188: 2163-2172.
- [144] Chandonia, J., Brenner, S. (2006) The impact of structural genomics: expectations and outcomes. *Science*, 311: 347-351.
- [145] Bai, L., Fujishiro, T., Huang, G., Koch, J., Takabayashi, A., Yokono, M., Tanaka, A., Xu, T., Hu, X., Ermler, U., Shima, S. (2017) Towards artificial methanogenesis: biosynthesis of the [Fe]-hydrogenase cofactor and characterization of the semi-synthetic hydrogenase. *Faraday Discuss.*, doi: 10.1039/c6fd00209a. [Epub ahead of print]
- [146] Jarrett, J. T. (2005) The novel structure and chemistry of iron-sulfur clusters in the adenosylmethionine-dependent radical enzyme biotin synthase. *Arch. Biochem. Biophys.*, 433: 312-321.
- [147] Reyda, M. R., Fugate, C. J., Jarrett, J. T. (2009) A complex between biotin synthase and the iron-sulfur cluster assembly chaperone HscA that enhances *in vivo* cluster assembly. *Biochemistry*, 48: 10782-10792.
- [148] Fugate, C. J., Jarrett, J. T. (2012) Biotin synthase: insights into radical-mediated carbon-sulfur bond formation. *Biochim. Biophys. Acta*, 1824: 1213-1222.
- [149] Biederbick, A., Stehling, O., Rosser, R., Niggemeyer, B., Nakai, Y., Elsasser, H. P., Lill, R. (2006) Role of human mitochondrial Nfs1 in cytosolic iron-sulfur protein biogenesis and iron regulation. *Mol. Cell Biol.*, 26: 5675-5687.

APPENDIX

APPENDIX

Table 1. Codon optimized sequence of *hcgB*, *hcgC*, *hcgA* and *hcgG*

<i>hcgB</i> from <i>M. maripaludis</i>
5'CATATGAACATTGAAAATACCATTAAATCCGCATACGAAGAATCGCTGAATAACGCTCGCTTTGGTGATAAAATCGAAGAAATTGACGCAATTCAGAGTACCATCAAATCCGCGAAAAACGTCACCGTGGCCACGTCAAATGAGAAAAAATCAAAGTGTTTTAGATATCATCTCGCGTATTACGACGCGAACATCAGCATGCTGGAAATCCGACCAATTCTGCGGATCTGACCGCATGCCGGCCCTGAACAAAGGCCTGATCGCAGTTGACAGCTCTGATGCTGACCTGATTATCACCCGTGGCCGCTGGGTATTCGGGCTCAGGTTCTGCTGCTGATGGATAAAAAAGCCGATTCTGACGGGTAGCGTCTCCGAGTTCATTATCCATAAAAATCCGATCGATAAAACGGTTGAACTGGAACGATTACGGCACTGGAACGCATCGGTATTGTGGTGA AAAACTCGAG3'
<i>hcgC</i> from <i>M. maripaludis</i>
5'CATATGAACTACGGCATTACCGAAAGCGTGAAAACGACCCGACGCAAAAATCAAATCAAAGATATTGTGTCCGATGTGTGAAAAAGAAAGCGAACGCCATCAAATATTTTCTGGAAGGCGAAGAATTTAAACAGGCAATTGTGTTGGCGCTTACCTGTCAGGTTCTGATATCGCGTACTCACTGCTGAAAGATTGCGAAGAAGTCATTATCGTGGACATTAGCCGCATCTGAAAGATATTCTGTTCAACGACGGTATCAAATTCATGGATCTGAACAAACTGCAACTGGAACGCGTAACGGCACCCAGCATCAATCCGGATCTGGTGATTGACCTGACGGGTATCGGCGGTGTTAGTCCGGATCTGATTTCAAATTCATCCGAAAGTTCTGATCGTGAAGATCCGAAAGGCAACCACGACAAAGGTATCTCTAAAATCGATAACACCCGACAAACGCTGTGCGTGGGCGCGAAAAAGGTGTTCTGAAAACCTATCGCAGCTCTAAAATTTAGCAAAACGCTCTGGCACCATGACCCTGGTGGTGGATATTATCATGGACTCATGTGCGGAAATTAACGAACTGGATTGCGTTCTGTATACCATCCCGAATCTGAAATACTTTGAGGGTACGGTCTCCATGAGAAAAACGTGAAAAAATTCCTGACCGAAGTGAATATGTCCGCCATTACCGTTAGTCCATCGATCAGTCGAATACGAACTGGAAGAAATCCTGTCAAAAAACATCAGCCGTGTGGACTCGTTCGTGAAAGAATTTGTCGAC3'
<i>hcgC</i> from <i>M. jannaschii</i>
5'CATATGAACTACGGCATTACCGAAAGCGTGAAAACGACCCGACGCAAAAATCAAATCAAAGATATTGTGTCCGATGTGTGAAAAAGAAAGCGAACGCCATCAAATATTTTCTGGAAGGCGAAGAATTTAAACAGGCAATTGTGTTGGCGCTTACCTGTCAGGTTCTGATATCGCGTACTCACTGCTGAAAGATTGCGAAGAAGTCATTATCGTGGACATTAGCCGCATCTGAAAGATATTCTGTTCAACGACGGTATCAAATTCATGGATCTGAACAAACTGCAACTGGAACGCGTAACGGCACCCAGCATCAATCCGGATCTGGTGATTGACCTGACGGGTATCGGCGGTGTTAGTCCGGATCTGATTTCAAATTCATCCGAAAGTTCTGATCGTGAAGATCCGAAAGGCAACCACGACAAAGGTATCTCTAAAATCGATAACACCCGACAAACGCTGTGCGTGGGCGCGAAAAAGGTGTTCTGAAAACCTATCGCAGCTCTAAAATTTAGCAAAACGCTCTGGCACCATGACCCTGGTGGTGGATATTATCATGGACTCATGTGCGGAAATTAACGAACTGGATTGCGTTCTGTATACCATCCCGAATCTGAAATACTTTGAGGGTACGGTCTCCATGAGAAAAACGTGAAAAAATTCCTGACCGAAGTGAATATGTCCGCCATTACCGTTAGTCCATCGATCAGTCGAATACGAACTGGAAGAAATCCTGTCAAAAAACATCAGCCGTGTGGACTCGTTCGTGAAAGAATTTGTCGAC3'
T6V mutant of HcgC from <i>M. maripaludis</i>
CATATGAACTACGGCATTGTGAAAAGCGTGAAAACGACCCGACGCAAAAATCAAATCAAAGATATTGTGTCCGATGTGTGAAAAAGAAAGCGAACGCCATCAAATATTTTCTGGAAGGCGAAGAATTTAAACAGGCAATTGTGTTGGCGCTTACCTGTCAGGTTCTGATATCGCGTACTCACTGCTGAAAGATTGCGAAGAAGTCATTATCGTGGACATTAGCCGCATCTGAAAGATATTCTGTTCAACGACGGTATCAAATTCATGGATCTGAACAAACTGCAACTGGAACGCGTAACGGCACCCAGCATCAATCCGGATCTGGTGATTGACCTGACGGGTATCGGCGGTGTTAGTCCGGATCTGATTTCAAATTCATCCGAAAGTTCTGATCGTGAAGATCCGAAAGGCAACCACGACAAAGGTATCTCTAAAATCGATAACACCCGACAAACGCTGTGCGTGGGCGCGAAAAAGGTGTTCTGAAAACCTATCGCAGCTCTAAAATTTAGCAAAACGCTCTGGCACCATGACCCTGGTGGTGGATATTATCATGGACTCATGTGCGGAAATTAACGAACTGGATTGCGTTCTGTATACCATCCCGAATCTGAAATACTTTGAGGGTACGGTCTCCATGAGAAAAACGTGAAAAAATTCCTGACCGAAGTGAATATGTCCGCCATTACCGTTAGTCCATCGATCAGTCGAATACGAACTGGAAGAAATCCTGTCAAAAAACATCAGCCGTGTGGACTCGTTCGTGAAAGAATTTGTCGAC
Y51F mutant of HcgC from <i>M. maripaludis</i>
CATATGAACTACGGCATTACCGAAAGCGTGAAAACGACCCGACGCAAAAATCAAATCAAAGATATTGTGTCCGATGTGGTGGAAAAAGAAAGCGAACGCCATCAAATATTTTCTGGAAGGCGAAGAATTTAAACAGGCAATTGTGTTGGCGCTTTTCTGTGTCAGGTTCTGATATCGCGTACTCACTGCTGAAAGATTGCGAAGAAGTCATTATCGTGGACATTAGCCGCATCTGAAAGATATTCTGTTCAACGACGGTATCAAATTCATGGATCTGAACAAACTGCAACTGGAACGCGTAACGGCACCCAGCATCAATCCGGATCTGGTGATTGACCTGACGGGTATCGGCGGTGTTAGTCCGGATCTGATTTCAAATTCATCCGAAAGTTCTGATCGTGAAGATCCGAAAGGCAACCACGACAAAGGTATCTCTAAAATCGATAACACCCGACAAACGCTGTGCGTGGGCGCGAAAAAGGTGTTCTGAAAACCTATCGCAGCTCTAAAATTTAGCAAAACGCTCTGGCACCATGACCCTGGTGGTGGATATTATCATGGACTCATGTGCGGAAATTAACGAACTGGATTGCGTTCTGTATACCATCCCGAATCTGAAATACTTTGAGGGTACGGTCTCCATGAGAAAAACGTGAAAAAATTCCTGACCGAAGTGAATATGTCCGCCATTACCGTTAGTCCATCGATCAGTCGAATACGAACTGGAAGAAATCCTGTCAAAAAACATCAGCCGTGTGGACTCGTTCGTGAAAGAATTTGTCGAC
S175A mutant of HcgC from <i>M. maripaludis</i>
CATATGAACTACGGCATTACCGAAAGCGTGAAAACGACCCGACGCAAAAATCAAATCAAAGATATTGTGTCCGATGTGGTGGAAAAAGAAAGCGAACGCCATCAAATATTTTCTGGAAGGCGAAGAATTTAAACAGGCAATTGTGTTGGCGCTTACCTGTGTCAGGTTCTGATATCGCGTACTCACTGCTGAAAGATTGCGAAGAAGTCATTATCGTGGACATTAGCCGCATCTGAAAGATATTCTGTTCAACGACGGTATCAAATTCATGGATCTGAACAAACTGCAACTGGAACGCGTAACGGCACCCAGCATCAATCCGGATCTGGTGATTGACCTGACGGGTATCGGCGGTGTTAGTCCGGATCTGATTTCAAATTCATCCGAAAGTTCTGATCGTGAAGATCCGAAAGGCAACCACGACAAAGGTATCTCTAAAATCGATAACACCCGACAAACGCTGTGCGTGGGCGCGAAAAAGGTGTTCTGAAAACCTATCGCAGCTCTAAAATTTAGCAAAACGCTCTGGCACCATGACCCTGGTGGTGGATATTATCATGGACTCATGTGCGGAAATTAACGAACTGGATTGCGTTCTGTATACCATCCCGAATCTGAAATACTTTGAGGGTACGGTCTCCATGAGAAAAACGTGAAAAAATTCCTGACCGAAGTGAATATGTCCGCCATTACCGTTAGTCCATCGATCAGTCGAATACGAACTGGAAGAAATCCTGTCAAAAAACATCAGCCGTGTGGACTCGTTCGTGAAAGAATTTGTCGAC

APPENDIX

CATGGACTCATGTGCGGAAATTAACGAAGCTGGATTTCGGTTCTGTATACCATCCCGAATCTGAAATACTTTGAGGGTACGGTCTTCCATGAGAAAAACGTGAAAAAATCCTGACCGAAGTGAATATGTCCGCCATTACCGTTAGTCCATCGATCACGTCGAATACGAAGTGAAGAAAATCCTGTCAAAAAACATCAGCCGTGTGGACTCGTTCGTGAAAGAATTTGTCCGAC
T179V mutant of HcgC from <i>M. maripaludis</i>
CATATGAACTACGGCATTACCGAAAGCGTGAAAAAGACCCGACGCAAAAATCAAATCAAAGATATTGTGTCCGATGTGGTGGAAAAGAAAGCGAAGCCCATCAAATATTTTCTGGAAGGCGAAGAATTTAAACAGGCAATTGTGTTGGCGCTTACCTGT CAGGTTTCGTATATCGCGTACTCACTGCTGAAAGATTGCGAAGAAGTCATTATCGTGGACATTACGCCGCATCTGAAAGAT ATTCTGTTCAACGACGGTATCAAATTCATGGATCTGAACAAACTGCAACTGGAAGTGCCTAACGGCACCAGCATCAATCC GGATCTGGTGATTGACCTGACGGGTATCGGCGGTGTTAGTCCGGATCTGATTTCAAATTCATCCGAAAGTTCTGATC GTCGAAGATCCGAAAGGCAACCACGACAAAGGTATCTCTAAAATCGATAACACCGACAAACGTCTGTGCGTGGGCGCG AAAAAAGGTGTTCTGAAAACCTATCGCAGCTCAAATTTAGCAAACGTCTGGCACCATGGTCTGGTGGTGGATATTAT CATGGACTCATGTGCGGAAATTAACGAAGCTGGATTTCGGTTCTGTATACCATCCCGAATCTGAAATACTTTGAGGGTACGG TCTTCCATGAGAAAAACGTGAAAAAATCCTGACCGAAGTGAATATGTCCGCCATTACCGTTAGTCCATCGATCACGTC GAATACGAAGTGAAGAAAATCCTGTCAAAAAACATCAGCCGTGTGGACTCGTTCGTGAAAGAATTTGTCCGAC
E209Q mutant of HcgC from <i>M. maripaludis</i>
CATATGAACTACGGCATTACCGAAAGCGTGAAAAAGACCCGACGCAAAAATCAAATCAAAGATATTGTGTCCGATGTGGTGGAAAAGAAAGCGAAGCCCATCAAATATTTTCTGGAAGGCGAAGAATTTAAACAGGCAATTGTGTTGGCGCTTACCTGT CAGGTTTCGTATATCGCGTACTCACTGCTGAAAGATTGCGAAGAAGTCATTATCGTGGACATTACGCCGCATCTGAAAGAT ATTCTGTTCAACGACGGTATCAAATTCATGGATCTGAACAAACTGCAACTGGAAGTGCCTAACGGCACCAGCATCAATCC GGATCTGGTGATTGACCTGACGGGTATCGGCGGTGTTAGTCCGGATCTGATTTCAAATTCATCCGAAAGTTCTGATC GTCGAAGATCCGAAAGGCAACCACGACAAAGGTATCTCTAAAATCGATAACACCGACAAACGTCTGTGCGTGGGCGCG AAAAAAGGTGTTCTGAAAACCTATCGCAGCTCAAATTTAGCAAACGTCTGGCACCATGACCCTGGTGGTGGATATTAT CATGGACTCATGTGCGGAAATTAACGAAGCTGGATTTCGGTTCTGTATACCATCCCGAATCTGAAATACTTTGAGGGTACGG TCTTCCATGAGAAAAACGTGAAAAAATCCTGACCGAAGTGAATATGTCCGCCATTACCGTTAGTCCATCGATCACGTC GAATACGAAGTGAAGAAAATCCTGTCAAAAAACATCAGCCGTGTGGACTCGTTCGTGAAAGAATTTGTCCGAC
S233A mutant of HcgC from <i>M. maripaludis</i>
CATATGAACTACGGCATTACCGAAAGCGTGAAAAAGACCCGACGCAAAAATCAAATCAAAGATATTGTGTCCGATGTGGTGGAAAAGAAAGCGAAGCCCATCAAATATTTTCTGGAAGGCGAAGAATTTAAACAGGCAATTGTGTTGGCGCTTACCTGT CAGGTTTCGTATATCGCGTACTCACTGCTGAAAGATTGCGAAGAAGTCATTATCGTGGACATTACGCCGCATCTGAAAGAT ATTCTGTTCAACGACGGTATCAAATTCATGGATCTGAACAAACTGCAACTGGAAGTGCCTAACGGCACCAGCATCAATCC GGATCTGGTGATTGACCTGACGGGTATCGGCGGTGTTAGTCCGGATCTGATTTCAAATTCATCCGAAAGTTCTGATC GTCGAAGATCCGAAAGGCAACCACGACAAAGGTATCTCTAAAATCGATAACACCGACAAACGTCTGTGCGTGGGCGCG AAAAAAGGTGTTCTGAAAACCTATCGCAGCTCAAATTTAGCAAACGTCTGGCACCATGACCCTGGTGGTGGATATTAT CATGGACTCATGTGCGGAAATTAACGAAGCTGGATTTCGGTTCTGTATACCATCCCGAATCTGAAATACTTTGAGGGTACGG TCTTCCATGAGAAAAACGTGAAAAAATCCTGACCGAAGTGAATATGTCCGCCATTACCGTTAGTCCATCGATCACGTC GAATACGAAGTGAAGAAAATCCTGTCAAAAAACATCAGCCGTGTGGACTCGTTCGTGAAAGAATTTGTCCGAC
<i>hcgA</i> from <i>Methanopyrus kandleri</i>
5'CATATGCGTTTTCAAGGATGCGCTGCGTGAAGTGCCTACCGACCGTAAACTGGCGGATACCGAAGCGACGTGCGTCTG CTGAGCGCGAAGAGCGTGCCTGTTCCAGACCTGTTCCGTGCGGCGCTGAGCGAGAAGCTGCACCACCGTGGTGAAGT GGTGAAACTGACCAGCACCATCCACGTTACCAACGAATGCCGTATTCGTCCGCGTTGCGCGTACTGCGGTTTTGCGGC GGGTGCAGCCCGGAGGGTTACTTCAAGGCTTACCCGTAGCTATGAGGAAATTGCGGAGGCGGCGAAGGCGATCG AGGAAAGCGGTATTCCGCGTGTGAGCTGCAGCGGTGCGTATCGTGGCGACGGTGGCAAGCTGGCGGTGACCGCGGC GCGTGCCTTAAAGAGAACACCGACCTGGAAGTGCCTGATCAACTTCGGTACGATCTGAGCGAGGAAACCATTGCGGA GCTGGCGCGTCTGGATGTTGAAACCATCTGCTGCAACCTGGAGACCACCAACCGTGAGCTGTTGCAACGTCTGAAACC GGGCGACAGCTTTGAGGAACGTGTGCGTGTGCGGAAACCGTGTGCCGTTACGGTATCGATCTGAGCAGCGGCCTGCT GTTGGATTGGCGAAGACTATCGTATCGTGGCGGACCGTGAAGTTTCTGGCGCGTTTTGAGACCCTGGCGGAAAT CCCGATTATGGGTTTCAACCCGATCCGGGTACCCTGATGGAACATGTGCCGCTTGCCCGCTGCTGGAGCAGGCGAA AGTGATGGCGGTGCGCGTCTGATGTATCCGGATCTGATGATCACCGCGCCGACCCCGACCGTGGGTCCGGAGGAAG TGGAAGTTGCGCTGATGGCGGGTGCAGCAACCTGGCGACCGTTATTCGGGATAACACCCGACGAGGTGAAGGGT GTTGGCAACCCGCTACCGGTAACCTGGACCGTGTGGTTGAGCTGATCGAAGGTTTTGGCTGAAACCGGAGCTGCGT GCGATCGCGCGTGCAGCACCAACTGTTAATCGTAGCACCAACCGTAGCAGCTAACTCGAG3'
<i>hcgA</i> from <i>Methanotorris igneus</i>
5'CATATGGTTTTTAAAGAAGATTGAGGAGAATTTGAGGAACTGAAGAAGGGTAACGAAGAATTTATTAAGTACGGTCTGA TTGACAAAGAGGACGCGCTGAAGCTGTTTCGAGATCAACCACTGGAGCGATTACCTGCGTCTGTTCAACATTGCGAGCAA AGTGCCTGACTACTTCAAGAAAGAGATCGAAATCACCAGCACCATCCACATTACCAACATCTGCAAGGTTAAACCGAAAT GCCACTATTGCGGTTTTGCGGCGGGTACCAGCCGTGAGGGTTACTATAAGCCGTTTCGTATCAGCGACGAAGATATTAA GAAAAGCGCGATCGCGATTGAGGAAAGCGGTATCTGCCGTGTGAGCTGCAGCAGCGCGCATGTTATGGTGGCCGTG AAGTGTGCGTGCCTGAAGATTGTTAAAGAGAACAACCAACCTGGAAGTGTGGTTAACGCGGGTGCAGACCTGACCG AGGAAACCATCAAAGAGATGAAGAAATATGCCATCGATCAACATTTGCTGCAACCTGGAACCCACCAACGAACTGTT TAACAAGGTTAAACCGGGCGAGAAGCTGGAAGACCGTATCAAGGTGTGCAAACTGGTTCGTAAATACGATATTGAGCTG AGCAGCGGCCTGCTGATCGGTATTGGCGAGAGCTACGAAGACCGTGTGGAACACCTGTTCTATCTGAAGGAGCTGGGT GTTGGCGAAATCCCGATTATGGGTTTTAACCCGTACAAAGATACCCCGATGGAGAACCACCCGAAGTGCAGCGCGCTG GAACAGGCGAAAACCATCGCGATTACCCGTCTGATCTCCCGACATCCGATTAACAGCCCGACCCGACCCATTGGTG CGGAGCTGGTGCATTTGCGCTGCTGGGTGGCGCGAGCAACCTGGCGACCGTTATCCCGGATAACCCCGATGAACA TTAAGGGTGTGGCAACCCGCTACCGGCAACCTGAACGAAGTTATCAAATGATTAGCGAACTGGGTCTGAAACCGAA ACTGAACCTGAGCAAAATCAATAGCAAGAATTAACCTCGAG3'
<i>hcgA</i> from <i>Methanocaldococcus fervens</i>
5'CATATGGTTTTTAAAGAAGATCGAAGAGAATTTCAAGGAACTGAAGGACGGTAACAAGGAGTTTATTAAGAACGGTCTGA TTGACAAGGATGAGACCCTGAAGCTGTTCAAATCGACAAGTGAAGAAGATTACCTGCAGCTGTTTCGTCTGGCGAGCGA

APPENDIX

<p>AGTGCGTGACTTCTTTAAGAAAGAGATCGAAATTACCAGCACCATCCACATTACCAACATTTGCAAGGTTACCCGAAATGCCTGTATTGCGGTTTCGCGGGCCACCAGCAAGAGGGTTACTATAAACCGTTTCGCTGACCGGATGAGGAAATCAAAGAAAGCGCATCGCGATTGAGGAAAGCGGCATTTCGCTGTGAGCTGCAGCAGCGGCACCGTTACGGTGGCAAGGAAAGTATCCGTGCGCTGAAGATTGTTAAAGAGAACACCAACCTGGAAGTGCTGGTTAACGCGGGTGGGACCTGACCGAGGAAGCGGTGAAGGAGCTGAAGAAATATGAAATCGATACCATTTGCTGCAACCTGGAGACCATCAACGAGGAACTGTTCAAGAAAGTTAAACCGGGCGAGGAACTGGAGGACCGTATCCGTGTGTGCAAGCTGGTTAACAAATACGGTATTGAACTGAGCAGCGGCTGTGATCGGTATTGGCGAGAGCTACGAAGATCGTGTGGAGCACCTGTTCTATCTGAAGAACGAGCTGAAGTTGGTGAATCCCGATTATGGGCTTTAACCCGTATAAAGGTACCCCGATGGAGAACCACCCGAAAGTGCAGCGGCTGGAACAGCGGAAAACCATCGCGATTACCCGTCTGCTGTTCCGAACATCCGTATTACCAGCCCGACCCGACCATTTGTCGGAACTGGTTCAATTCGCGCTGTTTTCGGGGTGGCAGCAACATCGCGACCGTATTCCGAAAGAACCCCGATCAACATTAAGGGTGTGGCAGCCCGAAAACCGGTAACCTGGAGGAAGTGGTTAAAATGATCATGGACCTGGGTCTGAAACCAGAACTGGACTGGGAGAAATTTGAGAACTACCTGAAAACCTACTAACTCGAG3'</p>
<p><i>hcgA</i> from <i>Methanocaldococcus infernus</i></p>
<p>5'CATATGATTGACGAGATCTACCGTCGCCTGGAGGATAAATACTTTCTGGAGAAGGGTCTGATTGACCGTGAAGAAGCGCTGAAAACCTGTTACGATCGACAAAGTGCCTGATTACCTGGAGCTGTTCAAGATTAGCAGCCTGGTTTCGTGACAAGTTTAAAGAGAATCGAAATTACCAGCACCATCCACATTACCAACATCTGCAAAATTAGCCCGAAGTGCCTGTATTGCGGTTTTGCGGCGGTACCAGCGAGGAAGTTACTATAAAGGCTTTTCGCTGAGCGATGAGGAAATCAAGCGTTGCGCGCTGGCGATCGAGGAAAGCGGCATTTCGCTGTGAGTGCAGCAGCGCGCACACCGAGCGTGGTGAAGTGGTTTCGTGCGCGCGCTATCGTTAAAGAAAACCAACCTGGAAGTGCTGGTTAACGCGGGCAGCGACCTGACCGAGGAACACATTAAGGAACTAAGAAACTGCGTGTGGAGACCGTTTGTGCAACCTGGAACCAACGAGGAAATTTCAAACCTGTGAAGCCGGCAGGAACTGGAGGATCGTATCAAAGTGTGCAAGCTGGTTAACAAATACGGTATTGAACTGAGCAGCGGCCTGCTGATCGGTATTGGCGAGAGCTATGAAGACCGTGTGATCACCTGTTCTTTCTGAAAGAGAATTCGAAATCGGCGAGATCCCGATATATGGGCTTTAACCCGTACAAGGGTACCCCGATGGAACACTTCGAGAAATGCCACCCGCTGGAGCAGGGCAAGACCATCCGATACCCGCTGATTTTCCGAAGATCCGATCACCAAGCCGAGCCCGACCATTTGGTCCGGAACATTTACCTGCCGTGATGGCGGGTGCAGCAACATCGCGACCGTATTCCGAAAACCTATCCGCTGCTGGTGAAGGGTGGCAACCCGAGACCGGAACTGGAGGAAGTGGTTAAGACCATCGAAATGCTGAACCTGAACCGAAGCTGGACCTGGAACGCTTCCGTCGCTACTATGACCGCTACAATCGTGTGCAACGCTACTGGTAACTCGAG3'</p>
<p><i>hcgA</i> from <i>Desulfurobacterium thermolithotrophum</i></p>
<p>5'CATATGATTGAGATTACCAGCACCATCCACGTTAGCAACTATTGCAGCTTTGAGCGTAAATGCGCGTATTGCGGCTTTGCGGTTGGCACCAGCACCGAGGGTACTTCTTTCTGACCGAAAAGAAAGAGAAAGAAATCATTACCGCGGCGAAGATCATTGAGGAAAGCGGCATCCGTCGTGTGAGCATTAGCGCGGGTACGGCAACTTCTATAAGGTGCTGAAAGCGCTGGAGCTGGTTAAGAAAAGCACCGCTGAAAGTGCCTGATCAACATTTGGTGGCGACCTGAACCGTGAGCGTATCCGTATGCTGAAGAAAGCGGGTGTGATACCATTTGTGCAACCTGGAACCAACGAAGAACTGTTCAAAGAACTGAAGCCGAGCAGACGCTTTAAACACCGTCTGCACGTGTGCTATCTGGTTAAAGAGGAAGGTATCGAGCTGAGCAGCGGCATCCTGGTTGGTATGGCGAGACCGAAAAGGATCGTGAGCAGCACATCGAAATTCGAAAGAACTGGAACCGGAGGAAATCCCGGTGATGCGTTTTATGCCGTACAAGAGACCCCGATGGAAGCGTTCGCGCGGCGAGCCTGAAGCTGCTGATCTACGTGATTAAGAAAAGTTAAGAAAGAGATGAGAGCCCTGAAACGCTGACCGTGCCGTTTCCGACCATTAGCAAAGAAAGACCTGATCAGCGTTAATAACCGGGTGCAGCAACATCGCGACCGTGGTTCCGCAAAAGTACCCGCTGCTGATTAAGGGTGGGCAACCCGAGAGGTTGGCATCCTGGAGGAAATTCGGAGATTCTGAAACGTCATGGCATCGAAACCAATGTGCGTCTGAAAGTGCCTACTTCTAACTCGAG3'</p>
<p><i>hcgG</i> from <i>Methanobrevibacter ruminantium</i></p>
<p>5'CATATGTACGAACATAAAAAGAAAGTATAAACTCAGATGAAAGTGCTCTAGAAGTAGCGAAGAGCAAGAAGGACGTGATTAGCGTGGTGGACGCGATCAGCGATCTGAGCTTCGAGGACACCATGAAGCTGGGCACCCGTTTCAAAGAAATTTCCGATGGTTGCGATCTGACCGAGGTGGTTGTGGGTACCTGCGCGAGCGACCTGGAAAAATGGACCTGTTCCGTAACCTGCATGCTGGCGAACATGATCGGCGCGCCGATTACATCTGCGCGTACGCGTTTAGCGACATTGCGGAGAAGTATGGTCAACGTGGCTGGAATCATGGAGGAAGTTACAACATTCAGGATGTCGCTGGACCTGGATCACTCGGCAAGTATGGCGCGATGCGTTTTCCGAAACACATCGTTGGTTGCGGTGGCGACTGCTACAACCAAGTCCGAGCTTTACCGAGTGCCCGCGTGGTCTGATTACCGAACGTCGCTGATAAGGAGAAAGCGGAACTGGACGATAAAGAGACCTGGGTTACGCTGAGCAGCAGCGTGGCGATCAACCTGAGCAGCGAACATGCAACGATGGTCTATGCGCGCCCGCTGGAGGAAGCGCAGGACCTGGCAGCTGGGAAGAAATACCGCAAGGGCCTGGAGGCGATTATGTTTCGTGGTGACGGCTATGAACTGATCACCGGCTTTACAAAAGCGATTGAGATGGGTGTTGACGTGTTCTGTTATCGAAAGTGGCCCGTTTAAACCGTTGCGAGAACACCAACGAAAGCTTCGCGAAGACCATTCGATGAGCCGTGTTCTGTGCCGGCAAAGTTGTGGCGACCAACCGTGGTACCGAGAGCGAATGCCGTGCGGGTCTGCGTAGCGGTCTGAACGTGATCATTACCGTTTTCCGAAAGAACACCGTTATATGTCCGTTTTGAACCGGTACCAGCGCTCGTGGCAAGTTTGGCCTGCCGCGTGTATTAATAATCATGAACGAGGAAATAGCGCGGGTCCGACCCGTGTGCCGTTCAACGTGAGGAACTGCTGGCGCTGACCCATGCGGTGAAGCTGGCGGGTCCGGAGAACATTTACGAAAACCATCGGCAGCTTCGCGATTGGTGACGCGCACTGGGCGACCATCCAGAACAGCAAGATGTACAAAGAAATGATCTGCCGAAAACCCCTGGAGGAAATTCGGATAGCGTGAACGGAACAGCGTTAGCCTGCACGGTGGCCGTTTTGTGAGCTGGCTGGTTGCGAAGGAGCTGGACAAGAAAGGTATCGATGAAATCATTATCACCGACAGCAACCCGTGGTTGAGAAAGTGAAGCGTTGATAACCTGCAAGAGGAACTGAACGCGACCATTTCCGTTGCTACGCGGACGATAAGGGTGGCGGCATGATCGCGAAAGAAAGCATTGTGACCACCACCATCCGAAAATCCACAATGCGATCAAGAGCAAAATCCCGCACGCGTTAATATCATCTAAGTCGAG3'</p>
<p><i>hcgG</i> from <i>Methanobrevibacter oralis</i></p>
<p>5'CATATGTTGAACTAATAAAAAGAAAGTATAACAGATGATACTGTAGCATTGCAATTGAGCAAGATGGATAAGGACGTGGTTGAAGTGGTTGATGCGATCAGCGAACTGAGCCTGGAGGAAACCATGGCGCTGGGTATGAAATTCAGAAATTTCCGCTGGGCTGCGACCTGACCGAAGTGGTTGCGGGTACCTGCGCGAGCGACCTGGAGCTGAAGGATCTGATCGGCAACTGCCGTCTGAGCGATGATTGGTGCGCCGATCCACATTTGCGCGTACGCGTTACGCGACATCGCGGAACACTTTGGCATGCTGGTATCGAATGAAAATGGTTTATGACGCGGTGGATGTTCCGCTGGACCTGGATCACTTCGCGATCAACGGTCCGATGCGTTTTCCGAAAACATTAGCGGCTGCGGTGGCGAGTGCCTACAACAAAGGTTCCGGCGTTACCGAGTCCCGCGTGAACGTATCCAGAGCGTCTGATTGATAAGGAAATGCTGGGCACCCCGGACAAAGAGGACTGGATCAAACCTGAGCAGCAGCGTGGCGTTAACCTGACCAGCGAACAGACCGGTGATGGTTCATGCGCGCCGTACGAGGAAGCGAAAAACATTCGGAACCTGGCGAAGAAATAAGAAAGGTCTGGAGCGCATCATGTTTCGTTGGCGACGGTTATGATGAGCTGATTACCGGTTTTGAAAAGAGCCTGGAGCTGGGTGCGGATGTGTTTGGTGGTGGCGGTCCGTTTAAACCGTGGCGAAAACCGCA</p>

APPENDIX

CCGAAGCGTACGCGAAAGCGATTGCGGCGAGCCGATTCTGGCGCCGGCAAGGTGGTTGCGACCAACGGCGCGTAT
 GAGCACGAATGCCGTGTTGGCCTGCGTAGCGGTCTGAACATGATCATTACCGGTTCCCGGAAAAACCACCGGCTACA
 TGTGCGGTTATGAGCCGGTACCAGCGAAGCGTGGCCGTTTCGGTCTGCCGCGTGTGATCGAGATCATTAAACGAGGAAT
 TTCCGAACCGTGGCCTGCCGTTAGAAAACATGACCTGCTGGCGATTGCGACCGCGGTGAAAATTGCGGGTCCGGATT
 ACATCTATCCGCGTAAGATTGGTAGCTATCATGTTGGTGTATGCGCACTGGGCGACCCTGACCCACAGCAAGATGTATAA
 AAACCTGCAACTGAAACACACCCTGAACGATATCATTGAAAGCGTTAACGGTAACAGCGTGAACCTGCACGGCGGTGCT
 TTTATCAGCTGGGTTATTGCGAACGAACTGGACAAGCAGCTGGATGAGATCTACATTAGCGACGTTGATCCGTGGGTGC
 TGAACGCGACCGTGGACAACCTGCAGGAAGAGCTGAACGCGACCATCATTGCGAGCAACAGCGACAAAAAGCTGCAGCA
 GCCAAGCGGATAGCAGCATCATTAGCACCACCATGATCCAAGTAAAAATAACATCCTGAAAAAGTTCCGAATGCGCT
 GACCCTGGTTAAGTCGAC3'

hcgG from Methanobrevibacter wolinii

5'CATATGTACGATCTAGTTAAAGAAGCTGTAACGATATGGATGCTGCACTAGAATTGAGCAAGGCGAAGAAGGACGCTG
 ACCGGCGTGGTGGACGCGATCAGCCAGCTGCCGCTGGACGATGTTCTGAAACTGGGCGACCACTTCAAGAAATTTCCG
 CTGGGTTGCGATATCACCAGGCGGTGGTTGGTACCTGCGCGAGCGACCTGGAGGAAATTGATCTGCTGGGTAACCTGC
 TACCTGGCGAAACAACTGGGCACCCCGATCCACATTTGCGCGTATGCGTTCGCGGACATCGGTGAACGTTTTGGCAAG
 ACCGGCCTGGAAGTGATGCAAGAAGTGTACGACCGGTGGATGTTCCGCTGGACCTGGATCACTTCGGTATCAACGCG
 GCGATGCGTTTTCCGCGTCCGATTACCGCGTGGCGTGGCGATTGCTATAACGAGGGTCCGGGCTTCAAAGAATGCCCC
 CGTGGTCTGATCCACGAGCGTCTGATTGACAAGGAAGTGGCGCAGGCGGGCGATAAAGAGGAGTGGGTGAAACTGAG
 CAGCAGCGTGGCGGTTAACGTGAGCATGCAACAACCGGCGAGGCGCATGCGGCGCCGATCAGCGAAGCGCAAGACA
 CCGGAAACTGGCGAAGAATACGGCAAGGGCCTGGAGACCATGTTCTGTTGGTGACGCTATGACGATGTGATTA
 CCGGTTTTGAGGCGGCGATGGGTCTGGGCACCGATGTTTTCTGATCGAAGGTGGCCCGTTTAAACCGTGCGAAGGACA
 CCACCGATGCGTACGCGCGTACCATTGCGGCGGCGCTATTCTGACCCCGGGTGGCGTGGTTCGACCAACGGTGGC
 TATGAGCAGCAATGCCGATTTGGTCTGCGTGGCGGCTGAACATGATCATTACCGGCTTCCCGAAAAACCACCGAGTT
 ACATGTCGGTATGAGCCGGTACCAGCGCTGCTGGCAAGTTGGCCTGCCGCTATCTCTGAAGATCATTAAAGG
 AAGTTCCGAGGATACGACCTGCCGATTTGGTCTGAACGAAATGCTGAGCATCGCGCGTGGGTTAAAAATTGGGGCC
 CGGATAAGATCTACCCGAACAAAATTGGCGACTCAAGCTGGGTGATGCGCACTGGGCGACCATGGTTAACGCGAAGA
 TGTATAAAACCTGAAGATCAAAGACGATGTGGAAGGTATTGCGAGCAAGGTTAACGGTAGCAACGTGGGTCTGCTGGG
 TGCCCGTTTTGTTAGCTGGGCGTGGCGCAGGAGCTGGACAACAAGGCATCGATGAAATCACCATTAGCGACATCGA
 TCCGTGGATTGAGAAAGTTAGCGTGGACAACCTGCAGAGCTGCCGTAACGCGAACATTCTGCCGCGCACGGTAACGA
 CAAAGCGATGGCGGAAAAGGTGGATACCAGCATCATTACCAGCACCATGCGCCCCGATTACGATGCGATGCTGCGTAG
 CGTTCGGATGCGATTACCCTGTTCTAAGTCGAC3'

hcgG from Methanocaldococcus fervens

5'CATATGAGGGATCTAATAAAAGAAGCAGTAAACAACCTAGATGCTGCACTAGAACTACGTAAGATTGTGCTGAAGAAGA
 TCAACGAGAAAAAGCTGAAAGAAAGCGATATCGTTGAGGTGGTTGACGCGTTGACGATCTGAGCCTGGAGGAAATTC
 GAAACTGGGCGACCAACTGCGTAAGTCCCGATGGGTTGCGATCTGATCGAAATTGGTGTGGTCCGTGCAGCAGCAG
 CTTGACCCGTACCAATTCATCGAGAAGTGCATTTGACCGATTACATGGGCTTTCCGATCCACATTTGCGACTATGCG
 GTTGGCGACATCCGCGAAGAAGTCTGAACCCGATTGATGCTGCTGAAGATGTTCTGAAACCTGGACCTGGTTCGG
 ATCGACATTGATCACTTCGTTAAATACGGCCCGATGCGTTTTCCGAAGGATCACCCTGCTACGGTATTGCTATTT
 CAAAGTCCGCCGTTAAGGGTTGCCGCGTACCGTATCCACAACGCTCTGATTGAGAAGAAAAAGAGCACGCGAA
 CGAATTTGAGGACTGGGTGCGTCTGGCGAGCACCGTTTGCATCAACGTGGTTGAGGAACAGGGTGGCGAGGAACATGC
 GGGCCGCTGGATGAAATGGAAGTGGTTCGGAAGCGGCGAAGAATAACGGTAAAGGCCTGGAGGCGATCTTCCACA
 TTGGTGACGGCCACGACGATCTGATCACCAGTTAAGGGCTGCATCGACCTGGATGTTGGACGTTTTCCGTGGTTGAAG
 GTGCGCCGTTAACCCTGCGAAGGATCGTCTGAAAGTGGTTCGGAAGGCGGTGGCGGTTAGCCGTTATTCTGGTTAAGG
 GTGGCGTGGTTGCGACCAACGGCGCTATGAAGACGAGTGGCGTATCGGTTGCGTAGCGGCCTGAACACCATTCTGA
 CCGTTTTCCCGTGAACACCACGGTTACATGTGCGGCTATAGCCCGGTACCGCGAAACGTGGTAACTTTGGCCTGC
 CTCGTGTGATGCGTATTCGTGAGGAAATCAAGGGCGGTTAACGTTAACGCGAGCTTCATCGATAAAGACGTTGTTAA
 GGCGATTGCGCTGGCAACCGTTTTCTGAACGGTAACATCTACCCTATAGCATTGGTGGCTTTTACCTGGGCGATGCG
 CACTGGGCGTGCATCAAAGAAAGCAACCTGTGCAAGAACTGAACGTGAACAAAAACCATCGACGATATTAGCGCGGAGA
 AGGTTGGTCTGATTGGTGGCCGTTACATCAGCTGGCGATTGCGGAAAAAGCGGAGGAAGCGTATATCAGCGATATTG
 ACAGCTGGGTGGAGGTCGACCATCAAGATTCTGAACGACAACGGCATCAACGCTACCCGTGCACCGTGCAGGATA
 AGAAAGCGGTTGAAAACAGCGAGAAGGCGTATATCACCACCTTTATTCCGAACATCGCGCTGAAGATTCTGGACCGTAT
 CCGTGACAAAAAGGTTGAACTGCTGATTTAAGTCGAC3'

hcgG from Methanocaldococcus villosus

5'CATATGAGGGATCTAATAAAAGGAATCAATAAACAACCTAGATGCTGCACTAGAACTACGTAAGATCGTGCTGAATAAGA
 TTCGTAACCGTAAGCTGAAAGAGAGCGACATCATTGAAATCCTGGATGCGATTGACGATCTGAGCCTGGAGGAAATCAT
 TAAGCTGGGCGACCACTTCCGTAATTTCCGCTGGGTTGCGACCTGGTTGATATCGCGATTGGCCCGTGCAGGAGCAA
 CCTGAGCATGCTGGAGCTGCTGAAAACTGCATCCTGGCGGACTACATTGGTTATCCGATCCACATTTGCGCGTATGCG
 ATCGCGGATATTGCGGAGAAGGAAGGCATCGAGACCATGAACTGTTCAAGAAAAATCATTGAGAACGTGGAAGTTCCGA
 TCGACATTGATCACTTCGGCCAGTACGGCCCGATGCGTTTTCCGAAGGAGATCACCCTGCTACCGTGAATGCTATTT
 CAAAGTTACTTTCTGGCTGCCCGGTAACGATCCACAAGCGTCTGATTGAGAAAGAAAAGAAAGAGCGTTTTGTG
 GAAGACTACATCCGCTGGCGAGCACCGTGTGCGTTAACGTTGTTGAAGAACAGGGTGGCGGAGGAACATGCGGCGCC
 GATTGAGGAAATGGAGATTGTTGCAACCTGGCGAAGAATAATGGAAGGGCCTGGAAGGTATCTTCCACGTGGGTGA
 CCGCTACGACGATCTGACGAGGGCATTAAACCGTGCCTGAAACTGGACGTGGATGTTTTCTGATTGAGGGTGCCTG
 CTTTAAACCGTGCAGGATAAACTGAAGGCGTTTGCAGGCGGTTGCGATCAGCCGATTCTGGTGAAGGTGGCGT
 GGTTGCGACCAACGGCGCGTATGAGAAGCAATGCCGATCGCGCTGCGTGGGGCCTGAACACCATCATTACCGGTTT
 CCCGTACAACCACCGGTTATATGTGCGGTTACAGCCCGGTTACCGGAAAGCGTGGTAACTTTGGCCTGCGTGTGT
 TATGCTGATCATTAAAGGAAATCAAGGACCTGAACCTGAACTGGCGGATAAGAACATCAACAAGCGATTGCGATG
 GGTAACAACCTTCTGAAAGACAAGATTTACCCGTAACCCCTGGGCGACTTCTTTCTGGGTGATCGCGACTGGCGTGC
 TAAAGAAAGCAAGCTGATGAAATATAAGCCGAGAAAGACCATCGACGATATTAAAGAAGACAAGCTGGGTCTGATCGGT
 GGCCGTTATATCGCGTGGGCGATTGCGGAGAAAGCGGAGGAAGTTTACATTAGCGACCGTATCCGTGGGTGGAGAAG
 GCGACCGTTAAAGTGTGCTGAACGAAAACGGCATCAACGCTACCCGTGCAACGGTGAACGCTGACGATCGTAAGCGCTGCGTTAC
 AAAGGTTATATCACCACCTTTATTCCGGAGCTGGCGCTGAAGATTACAAAAAAGTGAAGAATAATAACATTGAAGT
 CTGATTTAAGTCGAC3'

APPENDIX

<i>hcgG</i> from <i>Methanocaldococcus vulcanius</i>
5'CATATGAGGGATCTAATAAAAAGAAGCAGTAAACAGTCTAGATTACAGCTCTAGAACTACGTAAGCTGATCATCAAGAAAC TGAACGAAGGTAAGCTGAAAGAGAGCGATATCATTGAAGTGGTTGACGCGGTGGACGATCTGCCGCTGGAGGAAATCC AGAAACTGGGTAGCAACCTGCGTACCTTCCCGATGGGCTGCGATCTGGTGGAGATTGCGGTTGGTCCGTGCAGCAGCA GCCTGACCCTGACCCAATTCATCGAAAACCTGCATTCTGACCGATTACATGGGCTTCCGATCCACATTTGCAGCTATGCC GTTGCGGACATCGCGGAGCGTGAAGGTCTGAAACCGATTGAGGTGCTGAAGATGGTTCTGAACGAAGTGAGCGTTCCG ATCGACATTGATCACTTCGGCATGTACGGCGGATGCGTTTCCGAAGGAGATCACCCTGCTACGGTGAATTGCTATT TCAAAGGTCCGCCGTTTAAAGGGTCCGCCGCTGACCGTATCCACAAACGTTGATTGAGAAGGAAAAAGAGCACGAAG ATGAGTTTGAAGACTGGATCAAGCTGGCGAGCACCCTGTGCGTTAACGTGGTTGAGGAACAGGTTGGCGAGGAACATG CGGCGCCGCTGGAGGAAATGAAAATTGTGGCGGAGACCAGCAAGAAATACGGCAAGGGCCTGGAAGGCATCTTCCAC ATTGGTAGCGGCCACGATCTGATCAGCGGTATTAAGCGTGCATCGACCTGGATGTGACGTTTTCGTGGTTGAAG GCGCGCCGTTTAAACCGTGAAGGATCGTCTGAAAAGCGTTTCCGAAGAGCATCGCTGTGAGCCGTTTCTGGTTAAG GTGGCGTGGTTGCGACCAACGGCGGTATGAGGACGAATGCCGTGTGGTCTGCGTAGCGCCCTGAACACCATCCTG ACCGTTTTCCCGCTGAACCACCAGGTTACATGTGCGGTATAGCCCGAAGACCGCGAAACGTTGTAACCTTTGGCCTG CGTCTGTTATGCGTATCATTAAAGAGGAGATTGCTGCGGTAACGTGAACGCGAGCTTCTGTTGATAAAGACATCATTAA GGCGATCGCGCTGGTAAACAAGTTCCTGAAAAGCAACATTTACCCGCACAACGTTGGTGGCTTTTATCTGGCGCATGC GCACTGGCGGCGATCAAAGAGAGCAACCTGTGCCGCAAGCTGAAAGTGAACAAAACCATCGACGATATTAGCGCGGA AAAGTTGGTCTGATCGGTGGCCGTTACATCAGCTGGGCGATTGCGGAGAAGGCGGAGGAAGTGTATATTAGCGATGC GGACAGCTGGTTGAAAAGCGACCATCAAGATTGAAACGATGCGGACATCAACGCGTACCCGTGCAACGGTGACGA TCTAAAAGCTGGAGGCGGACAAGCGTATACCACCTTTATCCGAACATCGCGCTGAAAATTCTGAACAAAACG CGTGACGGCAAGGTTGAACTGCTGATCTAAGTCGAC3'
<i>hcgG</i> from <i>Methanocaldococcus infernus</i>
5'CATATGGAAGATCTAATAAAGGAAACAGTAAAGAACAAGTTTGTCTGGACTAGAATTACGTAAGATCATCCTGGATAAGA TTGAGAAGGCAAGCTGAAAGAGGAAGATATCATTAAAGTGGTTGATACCGTTGACAGCCTGAGCCTGGAGGAAATCAT TAACTGGGCAACAACCTGCGTACCTTCCCGCTGGGTTGCGATCTGGTGGACCTGGCGATTGGTCCGTGCAGCAGCAG CCTGAGCCTGATTGAGCTGCTGAAAACTGCATCCTGAGCGATTACATTGGCTTCCGATCCACATTTGCGGTTATGCG ATCGCGGACATTGCGGAAAAGGAGAACCCTGACCCCGCTGGAAGTGTCAAGAAAAGTTTACGATACCGTTGAGGTGCCG ATCGACATTGATCACTTTGGCAAGTATGGCCCGATGCGTTTCCGAAAGAAATCGTGTGTTGCGGTGGCGACTGCTACA ACCTGGGCTTGGCGGTGAATGCCCGCGTGAGCGTATCCACAACGTTCTGATTGAAAAGGAGAAAGAATATGAGGAAG AGTTCCTGGACTGGATCCGCTGTGGCGAGCACCCTGTGCGTTAACGTGGTTGAAGAACAAGGTCGTGAAGAGCATGGTG CGCCGATCGATGAGATGCGTGAAGTTGCGGAGGCGGCGAAGCGTTTCCGTAAGGCGTGGAAAGGTATCTTTCACATTG GTGACGGCTACGACGATCTATCGAGGGCATTCTGGCGTGCATCGACCTGGATGTGGACGTTTTCTGGTTGAGGGTGG TCCGTTTTAACCTGAAGGATCGTGTGAAAACCTTCGCGAAGCGGTTGCGATCAGCCGTTTCTGGTGAAGGGTGGCGT GGTTGCGACCACGGTGCATGAGGACGAATGCGTATCGGTCTGCGTGGCGGCTGAACACCGTGATTACCGTTTTT CCGCTGAACCACCACGGTTACATGTGCGGTTATAGCCCGGTACCGCGCGTCTGTTGTAACCTTCGGCTGCGTCTGTT ATGCGTATCATTAAAGGAAGGGCTTAAACTGATGGGCAAGGAAATCGCGAAAAGCGATTGCGATGAGCGGCAACTTCC TGAAGGCGGAGATCTACCCGAGCCGCTGGGCAAGCTTTTATATCGGTGACGCGCACTGGCCTGCGATTTACGAAAGCA AACTGAGCAACCTGAAGCCGAGCAAAAAGCATCGAGGATATTGACGAAGAGAAGGTTGGTCTGCTGGGTGGCCGTTACA TCAGCTGAAAATTGCGGAACGTGCGGAAGAGGCGTATATCAGCGATAAGGACGAATTCGTGGAGCGTGGCACCATCC GTATTCTGAACGAGAACAACATTAACGCGTACCCGTGCAACGGTGACGATAAGAAAAGCGATCAGCGTTGGCAAAGCGTA TATTACCAGCTTTATCCCGAAAATCGCGCTGAAACTGCTGAATAAATACAAAACCTGGAACCCTGTTCTAAGTCGAC3'
<i>hcgG</i> from <i>Methanothermococcus thermolithotrophicus</i>
5'CATATGGAAGATCTAATAAAGAACGCAATAAAGGATCTAGATTGTGCTCTAGAACTACGTAAGCTGATTGTGAAGAAAC TGAATAAGGGTAGCCTGAAGGAAAAAGATATCATTAAACATCGTGGATACCGTTGACAGCCTGAGCATCGAGGACATTCA GACCCTGGGTAGCAACCTGCGTAAATCCCGCTGGGCTGCGATCTGATCGAAGTGGGTATTGGTCCGTGCGCGAGCAG CCTGAGCCTGAGCAATTCATCGAGAACTGCATGCTGACCGATTATGGGTTTTCCGATTCACGTTTCCGCTACCGC CTGGCGGACATCGCGGAGAAGGAAGGCATTAGCCCGTGGAAAGTTATGAAGAAAAGTGTATGAAAACACCGAGGTTCCG CTGGACCTGGATCACTTCGGTAAATACGGCCGATGCGTTTTCCGAAGGAGATCACCCTGCGTGGGTGATTGCTACT ATAACGGTCCCGGTATAAGGGTTGCCGAAAAGCCGCTATCCACAACGTTCTGATTGAGAAGGAAAAAGAGTACAGCAA GCAATTTGAGGATGGATCAAGCTGAGCAGCACCCTTGTACATCAAGTGGTTGAGGAACAGGGTGGCGATGAACACGG TGCGCCGCTGGACGAAATGAAAGTGGTTGCGGAGGCGGCGAAGAAATATGGCAAGGGCCTGGAAGGTATCTTCCACAT TGGTGTGGCTACGAGGACCTGATCACCGCCTGAAAAGCTGCATTGACTTTGATGTGGACGTTCTGGTGGTTGAGGG TGGCCCGTTCAACCGTGCGAAGGACAACCTGAAAAGCGTTTCCGAAGGCGATCGCTGTGAGCCGATTCTGGTTAAGGG TGCGTGGTTGCGACCAACCGTGCATGAAAACGAGTCCGATCGGTTCTGCGTAGCGCCCTGAACGTTGATTCTGAC CGTTTTACGCGGCAACCACCAGGTTACATGTGCGGCTATAGCCCGAAAAGATGCGCGCTGTTGTTAACTTTGGCCTGCC GCGTGTCTGCGTATCATTAAAGAGGAAATCATGAACAACCCGGGTGCGCACATCATTGACAAGAGCCAACCTGATTACC CTGACCCGTAGCTGCAAAATCCTGAACTACAAGAACGAAAGCCTGATCTATCCGAAGACCTTTGGTGAATTACCTGATTGG CGACGCGACTGGGTGAGCGTTTCGTAACAGCAAACGTGTAACCGTCTGAACTGGGCAAGACCCCTGGACGATATCGA GCGTGATTGACTGCAAGAAACTGGGCTGCTGGTGGCCGTTACATCAGCTGGGGCCTGGTGGATGTTCTGAAAACC GGAGGAAGTGTATATTAGCGACGCGAACAGCTGGGTGGAGGAAAGCACCGTTAAGATCCTGAACGAAAACGGTATTAA CGCGTACCGTTGCAACGGCAACGACAAAAGAGCGGTTAAGAACGCGGAGACCAGCTTACACCACCATGATGCCGGA ACTGATTCTGAAAATTAATAAAGGTTGACGCGGAGAGCCTGATCTAAGTCGAC3'
<i>hcgG</i> from <i>Methanothermococcus okinawensis</i>
5'CATATGAAGGATATAATAAAGAACGCTGTAACGATCTAGATATATGTCTAGAATTACGCAAGGACGTTGATCGAGAAGA TTACCAAGAACAAGCTGAGCGAGAAAGAAATCATTGAGATTGTGGATGCGGTTGACGATCTGAGCATCGAGGAAATTC GAAGCTGGGTAGCAACTCCGTAATTTCCCGTGGGCTGCGACCTGGTGGAAATGGGTATTGGTCCGTGCGAGCAGCAG CCTGACCCTGACCGACTGATCGAAAACCTGCATTCGAGCATATTGTTTCCCGATCCACATTTGCGCGTATGCC CTGGGTGACATCGCGGAGAAGGAAGGCATGACCCCGTGGAAAGTGTAAAACCATCCACAACCGATTGAAGTTCCG ATCGACCTGGATCACTTCGGCAAGTACGGCGGATGCGTTTTCCGAAGAGATCACCCTGATGGGTGACTGCTACT ATAACGGTCCCGCTTCAAGGGCTGCCGAAAAGATCGTATTCACAAGCGTCTGATCGACAAAAGAGAAGAAATACAGCTA TGAATTTGACGATTGGATCAAGCTGAGCAGCACCCTGTGCGTTAACGTGGTTCTGTAACAAGGTGGCGAGGAACATGC GGCGCCGCTGGATGAGATGGAATTTGGCGGAGGCGGCGAAGAAATACGGCAAGGGCCTGGAAGGTATCTTCTACG

APPENDIX

<p>TTGGTGACGGCTATGACGATCTGATTACCGGCCTGAAAAGCTGCATCGACCTGGATGTGGACGTTTTCTGGTTGAGGG TGGCCGTTTAAACCGTGCAGAGGATCGTCTGAAAGCGTTTGCAGGCGGTGGCGGTTAGCCGTATCCTGGTAAAGG TGGCGTGGTTGCGACCAACCGGTGCGTATGAGGACGAATGCCGATTGGTCTGCGTAGCGGCCTGAACGTTATCCTGAG CGGTTTCCGTGGCAACCACCGGTTACATGTGCGGCTATAGCCCGAAGACCGCGAAACGTGGTAACTTTGGCGTGCC GCGTGTCTGCGTATCATCAAAGAGGAGATCAAGAAACAACAACTGGATACCCACATCCTGAACCGTAAACATTCTGAAAG CGATCGCGCTGGGTAGCAAGTTCCTGAACTACAAAAACGAGAGCCTGATTTATCCGAACAGCCTGGGTGGCCACTTTAT CGCGGATGCGCACTGGGTTGCGGCGAAGAACAGCAACCTGTACAACAACATCAACAACATCAACAACAGACCATCGA CGATATTGACAACCTGCAGCAAACCTGGGTCTGCTGGGTGGCCGTTACATTGCGTGGGGCATCGCGAAGGCGCTGAAACC GGATGAGGTGTATATCAGCGACGCGAACAATGGGTGGAAGGCGACCGTTAAAATTCTGAACGACGCGAAGATCAA CGCGTACGGTTGCAACGGCAACGATAAGAAAATTATGGAAAACGCGGACAAAAGCATATTACCAGCTTCATCCCGGAA ATCGTTCTGCGTATTAACAAACAAATTTGACGCGGAGAGCCTGATCTAAGTTCGAC3'</p>
<p><i>hcgG from Methanococcus vannielii</i></p>
<p>5'CATATGAAGGAACTAATAAAGTCAAGTCTAAACGATTTGATTGAGCTATGGAACACGTGAGATTGTGGTGA AAAAAGA TCAACGATAAGAAACTGACCGAGAGCGACATCATTGATATTGTGGACAGCGTTGACGATCTGAGCTTCGAGGAAATCCA GAACTGGGCAGCAACTTCCGTAAGTTTCCGCTGGGTTGCGACCTGCTGGAGATCGGCGTGGTCCGTGCAGCAGCA GCCTGAACCTGAGCCAATTTATTGAAAACCTGCATCCTGACGATGCGATGGGCTACCCGATTACCTGTGCACCTATCGC CTGGCGGAATCGCGGAGAAAAGAAGGTATCAACCCGATTGAGGTGATGAAGCAGGTTACGAGAACGTGGAAGTTCCGC TGGACATTGATCACTTCGCGCGTTTTGGTCCGATGCGTTTTCCCGAAAAGAAATCACCCACTGCATGGCGATTGCTACTA TAACGGTCCGCGTATAAGGGTTGCCCGCGTGACCGTATTCACAAACGTCTGATACCAAGGAGCGTGAACACTTCCA GGAATTTAGCGACTGGATTAACCTGAGCAGCACCGTGTGCGTTAACCGTGGTTGAGGAACAGGTTGGCGGTGATCAGCG TGCGGACATCAGCGAGATGGA AACCTGAGCAAGGCGGCGCAAAAATATGGCAAGGGTATCGAGGGCATTTCACAT CGGCGATGGTTACGACGATCTGATTAGCGGTCTGCGTGCCTGCAGCGAGCTGAACGTGGACGCGCTGGTTATCGAAG GCGGTCCGTTCAACCGTAGCAAGAACAACTGAGGATTTTGCAGAAAGCGGTGGCGGTTAGCCGTTATTCTGGTTAAGG GCGGTGTGGTTGCGAACACCGTCCGTACGAGGATGAATGCCGTGTGGCCCTGCGTAGCGGTCTGACCTTTATCCTGA GCGGCTTACGCGTGAACACACCGCTACATGTGCGGTTATAGCCCGAAAAGAAAGCGCTCGTAACAACTTTGCCCTGC CGCGTGTGCTGAAAATTATGAAGGAAGAGCGGAGCAACATGGGTATCTGCATTGCGAACCGTGAGCTGCTGAAAATCCT GGTTAAGAGCAGCCGTTTCCCTGAACTACAACGGCAAGCAGCATGATTTATCCGGAAATGATCGGCAACTACTTTATGGT GACGCGCACTGGGTGAGCGTTAGCAACAGCAAAATGTACAACGCGCGTATTTCCGCAAGACCCTGGATAGCCTGAGC GAGGAACCTGAGCAAGAAAATCGCGGTTCTGGGTGCGGTTATATTAGCTGGGGATTGCGAGCGCGCTGAACCCG GAGGAACTGTATGTGAGCGACGTGGACCCGCTGGTTGAGTACGCGACCGTTAAAATTCTGAACGATAACGGCATCAAC GCGTACGCGTGCAGCGTAGCGATCGTAAAGCGCTGGAACAAGCGGACAAGAGCATATTACCACCATGATCCCGGAG ATTGCGCTGCGTATCAAAAACAAGTTCAATGCGATTAGCCTGATTTAAGTTCGAC3'</p>
<p><i>hcgG from Methanococcus aeolicus</i></p>
<p>5'CATATGCACGATATAATAAAGAGTGCAGTAAACGATCTAGATGCTTGTCTAGAACTACGTGGCCTGATTACCAATAAAC TGACCAATAACAACTGACCGAGGGCGACATCATTAGCGTGGTTGATGCGGTGGCGGAGCTGCCGATCGAAGACATTC AGAAAATCGGCAGCACTGCGTAAGTTCCCGCTGGGTTGCGATCTGGTGGAGATCGGTATTGGTCCGTGCAGCAGCA GCCTGACCATGCCGCAACTGTTGAAAACAGCATCCCGCTGCTGAGCGATTACATGGGCTTCCCGATCCACATTTGCGGATGC GCTGGGTGATATTGCGGAGCGTGAAGGCATCACCCGCTGGAAGTGTTTAAGACCATTAGCGAGAGCGTGAACGTTCC GATCGACCTGGATCACTTCGTAATAACGGCGCGATGCGTTTTCCGAAGGAGATCACCCACTGCGGTGGCGACTGCTA TCGTATGGGTGCGCCGAGCGAAGGTTGCCCGCGTGGCCGTTATTCACAAACGTCTGATCGACAAGGAGAAGGAATACAG CTATGAATCAACGATTGGATCAAGCTGAGCAGCACCGTGTGCATCAACGTGGTTGAGGAACAGGGTGGCGAGGAACA TGGTGGCGCGCTGGAGGAAATGAAAATTTGTTGCGAACGAGGCGCAACAAGCACCGTAAAGGCTGGAAGGTTATTTCCA CATCGGTGATGGCTACGACGATCTGATCACCGGTCTGAAGAGCTGCGTGGACCTGGGCGTTGATGCGTTCTGGTTGA AGGTGCGCCGTTAACCCTGCGAAGGACCGTCTGAAAACCTTTGCGAAGGCGATTGCTGTGAGCCGATCCTGGTTAAA GGTGGCGTGGTTGCGACCAACGGTGCCTACGAGGATGAATGCCGTTGGTCTGCGTAGCGGCCTGAACATGATCCTG AGCGGTTTACAGCGGCAACCACCGGTTACATGTGCGGCTATAGCCCGACACCGCGAAGCCTGGAACCTTTGGCGG CCGCGTGTGCTGCGTATCATCAAAGAGGAAATCGAGTACAACAAGCTGGATACCTGCCTGCTGACCAACCGGTTCTGC GTGCGCTGACCAAGAGCGCGAAATTCCTGAACTACGGTGGCAACAGCCTGATTTATCCGAACAAGATCGGTGACTTCTT TACCGCGATGCGCACTGGGTGGCGGTTAACAACAGCAACCTGGCGAACAACCTGCACACCAAAACCATTGACGAT CGAAAAGGTGCGCAAAATTTGGTGGCTGGGTGGCGGTTACGTTGCGTGGGGTCTGATTGACGCGCTGAACCGGAGG AAGTGTACATCAGCGATGCGAACAAATGGGTTGAGTATGCGACCATCAAGATTCTGAACGACGCGGGTATTAACGCGTA TGGTACCGACGGCAACGATAAGAAAAGTATCGAACAAGCGGATAAAAAGCTTCATTACCAGCTTTATCCCGGAAATTAAC CTGAAAATCAAAAATCGCTACAATAAGGACGTTGAGAGCCTGATCTAAGTTCGAC3'</p>
<p><i>hcgG from Methanobacterium formicum</i></p>
<p>5'CATATGTACGATATAGTAAAAGAAGCAGTTAACGATATGGATAGTGCCTAGAACTAAGCAAGGCGAATAAGAACGTGA ACGACGTGGTTGATGCTGTGAGCGAACTGAGCACCGCGGAAGCGACCCAGCTGGGCATGAACCTCAAGAAAATTTCCGA TTGGTTGCGATCTGACCGAGATCGTTGTTGGTACCCTGCGCGAGCGACCTGGGTGCTGATGAACTGATGGGTAACGTGA TGCTGAGCAACATGCTGGGTGCGAGCATTACGTTTGGCGGTACGCGTTTGGCGACATTGCGGAGGCGAACAACATGC TGCCGATTGACACTTGCCTGAGGTGCGCGAAGCGACCGATGTTCCGCTGGACCTGGATCACTTCGGTCTGTTTTGGCG CGATGCGTTTTCCCGCTGAGATTGTGAAGTCCCCGGGCCAGTGCTATAACCAAGTCCGCCGTTTCAGGAATGCCCGC GTGATCGTATCCACGCGCGTCTGGTTGACAAGGAAGAGGCGGCGCAAGATGAGCGTGAGGAATGGATTAATGCAGCA GCAGCGTGGCGATCAACGTTACCAGCGCGCAGGGTGGCGAAGGTCATGCGGCGCCGCTGGAGGAAGCGGAGGAAAT TGCCAGCCTGGCGCAAGAGTACGGCAAGGGCGTGAAGCGATTATGTTTCATCGGTGACGCTATGACGATCTGGTTAC CGGCTTAGCAAAGCGCTGGAGCTGGGTGCGGACATCTTCTGCTGGAAGGTGGCCCGTTTAAACCAAAGCAGCAACCG TCTGGATAGCTTTGCGAAGGCGGTTGCGATGGCGCGTATTCTGGTGCCGGGCAAAAATCGTTGCGACCAACGGTGCCTA CGAGGATGAATGCGGTGCGGTCTGCGTGGCGGTTGAAACCGCATATTACCAGGTTTCCCGAGCAACCACCAAGGTTA CATGTGCGGCTATAGCCCGGTTACCGCAAGAAAGTGAACCTGCGGCTGCCGCTGAGCAAGATCATAAAGGTA ACTGAAGCCGCTGACCAACGTTCCGATTCAACGTGGCGAGCTGGAAGCGCTGGCGAGCAGCATCAAGGTGGTTG GTCCGGAGAACGTGATCCCGCAAAAATTTGGCGAATTTACCCTGGGTGATGCGCACTGGGCGGTGGTTCCGAACAGCC CGATCTATGAGAAGGTGGAAGTTTCAGCGTACCATTCAAAGCATTATGAAAAGCCTGACCGGTAGCAGCGCGGCGCTGA TCGGTGGCCGTTTTGTTAGCTGGGCGCTGGCGCGTGAAGTGAACAAAGACATGGATGAAATCATTATCAGCGACAAG ATCCGTGGGTGGAGAAAAGTACCCTGACATTGAAACCTGAACTGCCGAGCACCGTTATCCGCTGGCGAGCAGCGACG</p>

APPENDIX

ATAAACTGGCGAGCCAGAACGCGGATCACACCATTATACCAGCACCATTCCGGGTCTGGTTCGTCGTATTAGCGGCAA CCTGGATGGCGGATTACCCTGATTTAAGTCGAC3'
<i>hcgG from Methanospirillum hungatei</i>
5'CATATGCACGATCTAATAAGAAAGGCTATAAACGATCCCGATGCTGCATGGGAATTGAGCAAGATTGAGAAAGGCCCG CGTGACGTGATTGATGCGGTGACCAGCCTGAACCGTGAGGAAGCGATCAAGCTGGGCAACACCTTCAAACGTTTTCCG CTGGGTTGCGACCTGACCGAAATTTCTGGTGGTACCTGCGCGAGCGACCTGGAGAAGACCGATATTTCTGGGTAACGTC ATGCTGGCGGATAGCATTGGCGCGAGCATCCACGTTTGCGCTACGCGTTTCGCGGATATTGCGGAAGCGCACGGTATG AAGGGCATCGACCTGCTGAAAGAGGTGCGCAAATTAACGAGGTTCCGCTGGACCTGGATCACTTTGGTCTGATCGGT CCGATGCGTCTGCCGCGCAGATCATTGGTTGCAACGGCCAATGCTATAACGAGGGTCCGCCGTTTACGCGTTGCCCG CGTGATCGTATCCACAGCCGTCTGCTGGACGTGGAACAGGATGCGCTGAGCGACCGTGATGAGTGGGTTAAGATTAGC AGCAGCGTGGCGGTTAACCTGACCTGCGTGCAGGGTGCAGGATGGTGCATGCGGCGCCGCTGGATGAAGCGCAAGAGGT TGCGGACCTGGCGCGTAAAGTACGGTAAAGGCATTGAAGCGATCATGTTTCGTTGGGTGACGGCTATGACGATCTGATCAA AGGCTTTACC GCGCGCTGGACATGGGTGTGGATGTTTTCTGCTGGAGGGTGGCCCGTTTAACTGCAGCACCGATCG TCTGACCGGTTTTGCGCGTGCAGTTGCGATTGCGCGTATCCTGGTGCCGGGCAAAAATCGTTGCGACCAACCGGTGCGTA CGAGGACGAATGCCGATTGGTCTGCGTGCAGGGCTGAACGCGATCATTACCGGTTTCCCGAAGAACCACCAGCGTTA CATGCGCCTATAGCCCGGCAAGATCAAACCGTGGTGTATTTTTGGCTGCGCGTATTCTGCGACCTTAAAGAGGAA GTTCTGACCGTTGGACCCACACCCCGATCCAAAAGGCGAGCTGGAAGCGCTGGCGCGTGCAGTGAAGTGGTTGG CATTGATACCGTTTACC GCGAAAAGATCCGTTACACCTATGTTGGTGATGCGCACTGGGCGTGCCTGCCGACACCCCG GGTTTTAGCGGATCCACGTTCTGAAGACCGTGCAGGATATCGTTAGCATGGCGCTGGACGGTCAAATTTGGTGATAC GTGGCGCTGATGCGGTTGGCGTTTTGTTAGCTGGGCGATCGCAAGAACTGGACGGTGTGGTGTGACGATCATTA AGCGACGTGGATCCGTGGATTGAACACGTTACCATCGACAACCTGCGTAGCGAACTGCACACCGAGATTAGCCCGGCG AAAAGCAGCGATACCTATGCGCACGAGCACGCGGACACCAGCATTATCTGCAGCACCATGCCGGAAGTGGTTCGTAAG ATGAGCTGGAATGCGCGATGCGATTACCCTGATTTAAGTCGAC3'
<i>hcgG from Methanolacinia petrolearia</i>
5'CATATGTACGATCTAGTTAAGAAAGCAGTACTAGATCCCTATGCTGCATGGGAATAAGCAAGATGGATAAGAGCCCG GCGGAGATCGTGGAGCGGTTAGCCGTCTGGACCGTGATGAAGCGATGAAGCTGGGCATGAACCTCAAACGTTTTCCG CTGGGTTGCGACCTGACCGAGATCCTGGTTGGCACCTGCGCGAGCGACCTGGATAAGATCGACATTTCTGGGTAACAGC ATTCTGAGCGATAGCATCGGCGCGAGCATTACGTTGCGCGTACGCGTTTCGCGGACATCGCGGAAGCGAACGGTATG CGTGGCATTGACCTGTTCCCGTGAAGTTCTGTAAGAACACCGAGGTTGCCGCTGGACCTGGATCACTTCGGCAAGTTTTGC CCGATGCGTTTTCCCGAAGATATCACCGGTTGCTGGGGCCAGTCTATAACGAGGGTCCGCCGTTTATGTTGGTTGCCCG CGTGATCGTATCCACAGCCGTCTGATTGACAAAGAGGAAGATGCGCTGGGTGAAAAGGACGAGTGGATCAAACCTGAGC AGCAGCGTGGCGATCAACCTGACCTGCATTCAAGGCGCGGAAGGTGCATGCGGCGCCGCTGGATGAAGCGATTGAGGT TGCGCAACTGGGTAAAGAAATACGGCAAGGGCATCGAGGCGATTATGTTTCGTTGGGTGACGGCTATGAAGATCTGATCAA AGGCTTTACCACCGCGATTGACATGGGTGTGGATGTTTTCTGATCGAGGGTGGCCCGTTTAACTGGCGGAAAACCG TCTGGATGCGTTTTGCGCGTGCAGTTGCGATGGCGCGTATTCTGGTTCCGGGCAAGATCGTGGTTACCAACCGGTGCGTA CGAGGATGAATGCCGTTGGGTTCTGCGTGCAGGGTCTGAACGGCATCATTACCGGTTTCCCGAAGAACACCACCGGTTAC ATGTGCGTTATAGCCCGGTTACC GCGCGTCTGGCAAGTTGGCTGCCGCTATCATTCTGATCAATTAAGAGGAA GTTACGGAAGACTGACCAAGGCCCGGATCCAAAAGATGAGCTGGAAGCCTGGCGCTGCGGTGAAGGTGGTTGA CCCGTTAAGCTGTACCCGCGTAAAATTGGCTTCGCGCCGTTGGTGATGCGCATTGGGTGTGCTGCCGAGCACCCCG GATCTATGAACGTGTTACCGTGAAGCGTACCGTTACGACATTCGTAAGATGGCGGAGGAAGGTAATAATCGGCGATAGC ATTGCGCTGCTGGGTGGCGTTTTGCGAGCTGGGTTACGCGAAAGAGCTGGAAGGTTATGTGGACCAGATCACCAT AGCGACCTGATCCGTGGGTTGAAAAGATTAGCGTGGAGAACCTGCAAAGCGAACTGAAAGCGAACATCTACACCGGT AACAGCGACGATAACGCGGCGTATAAGAACAGCGAGACCGCGATTGTGTCACCACCATCCCGAGCATTAGCAATAAG ATTAGCAAAAACCTGAACGACCGGATTACCCTGATTTAAGTCGAC3'
<i>hcgG from Methanoregula formicica</i>
5'CATATGTCAGATATAGTAAGAGAAGCTGCAAGGAATGCTGATGCTGCATGGGAATAAGCCGATGAAGAAGGACCCG GCGGAGATCGTGGAGCGGTTAGCGAGCTGCACCGTGAGGAAGCGATTGCGCTGGGCAACAACCTCAAACGTTTTCCG CTGGGTTGCGACCTGACCGAAATCTTCTGGTTGGCACCTGCGCGAGCGATATGGAGAAGATTGACATCCTGGGTAACGTC CAGCTGAGCGATGCGATTGTTGCGAGCATCCATGTTGCGCGTACGCGTTTTCGCGACATTGCGGAAGCGCACGGTATG AAAGGCATCGATCGTATGAGTTGAGTTCTGTAACCTGACCGAGGTGCCGCTGGACCTGGATCACTTCGGTACCTTTGGC CCGATGCGTCTGCCGAAGGACATCATTGGTTGCCAGGGCCAATGCTACAACACCGGTCCGCCGTTTACGCGGTTGCCCG CGTGATGTATCCACAGCCGTCTGCTGGACAAGGAGAAAAGAGCGATTGCGGATCGTGGGAATGGGTTAAAATCAGCA GCAGCGTGGCGGTTAACGTGAGCTGCGTGCAGGGTGCAGAGGTGCATGCGGCGCCGCTGGAGGAAGCGCGTGAATTT GCGGAGCTGGCGATCAAGTTGCGTAAAGTGGTTGAAGCGATTCTGTTTGTGGTGACGGCGATGAAGACCTGCTGCGT GGCTTACC GCGCGCTGGAACCTGGGTGCGGACGTTTTCTGATCGAGGGTGGCCCGTTTAACTGCGCGAAAACCGT CTGGATGCGTTTTGCGCGTGCAGTTGGCGGCGGCGGATTTCTGGCGCCGGCAAGGTGGTTGCGACCAACCGGTGCGTA TGAGGACGAATGCCGATCGGTCTGCGTGCAGGGCTGAACGCGATCATTACCGGTTTCCCGAAGAACACCACCGGTTA TATGTGCGGTTATGCCCGGGTACC GCGCGTCTGGTAACTTGGCCTGCCGCGTGTCTGCGTATCATTCTGAGGAG AGTGCCTGATGGTCAGACCCGTCGCGGATCATGAAGGAAGAGGTGGAAGCGCTGGCGCGTGCAGTTAAAATTGTGG GCCCGGAACACGTGATCCCGGAGAAGACGGCGATTGCGCGGTTGGTGATGCGCACTGGGTGTGCTGCAAAGCACCC CGCTGTATCACCGTGTGGCATTAGCAAGACCGCGCGGATATCAGCAGCATGGCGAAAAGAGGGTCTGCTGGGTGACA CCGTGGCGCTGCTGGGTGGCGTTTTGTTAGCTGGGTGTGGCGCGTGCAGTGGAAAGTTACGTTGATCGTATCATT TCAGCGATACCGACCGCTGTGGAAAACGTTACCGTGGAGAACCTGCGTGTGCGCTGCGTATGACATTGAACAAGG TGGCAGCGACGATCGTCTGAGCGGAGCCGTAGCGATGCGGCGATCGTGTGACGACCATCCCGAGCATTAAACCGTA AGATTAGCCTGGGCGTTCTGAACCGATTAGCCTGCTGTAAGTCGAC3'
<i>hcgG from Methanotorris formicicus</i>
5'CATATGAGGGAATAATAAAGGATGCTATAAACGATCTAAATGCTGCACTAGAATTACGTAAGCTGATTATCAAGAAAC TGAACGAGAATAAGATCAAAGAGAGCAACATCATTGAAATTGTTGATGCGGTGGACGATCTGACGATCGAGGAAATTC GAACTGGGCAGCAACCTGCGTAAGTTCCCGATGGGTTGCGACCTGGTTGAGGTGGTTGTTGGTCCGTGCGCGAGCAG CCTGACCCGTAACCAATTCGTGGAAGAACTGCATCCTGACCGATTACATGGGTTTTACCATTCATGCGTGCAGGATGCG CTGGCGGACATCGCGAGAAAAGGCATCCCGCCGCTGGAAGTATGAAGATGGTGTACGAAAACGTTGATGTGCCG CTGGACCTGGATCACTTCGGCCAGTATGGCGCGATGCGTTTTCCGAAAAGAGATCACCCACTGCATGGGTGAATGCTACT

APPENDIX

ATAAAGTCCGCCGTACAAGGGTTGCCCGCGTAAGCGTATCCACAAACGTCTGATTGATAAGGAGAAAGAATATGCGCA
 CGAGTTTGAAGACTGGATCAAGCTGGCGAGCACCGTTTGCATTAACGTTGTGGAGGAACAAGGTGGCGAGGAACATGC
 GGCGCCGCTGGAGGAAATGGCGGTTGTGGCGAAAACCGCGAAGAAATACGGCAAGGGCCTGGAGGGTATCTTCCACG
 TGGGTGACGGCTATGACGATCTGATCACCGGCTGAAAAGCTGCATTGACTTTGATGTTGACGTGCTGGTTGTGGAAGG
 TGCGCCGTTCAACCGTGCGAAGGATCGTCTGAAAGCGTTTGCGAAGCGATCGGTGTTAGCCGTATTCTGGTGAAGGG
 TGGCGTTGTGGCGACCAACGGCGCGTACGAGGACGAATGCCGTATCGGTCTGCGTAGCGGCTGAACGTTATCATTAG
 CGGTTTCAGCGGCAACCACCACGGTTACATGTGCGGCTATAGCCCGGGTACCGCGAAACGTGGTAACTTTGGCCTGCC
 GCGTGTGATGCGTATCATCAAAGAGGAAATCAAGAACATGGATGTTACCCTGGTTAGCCGTCACGACCTGATCGCGATT
 GCGCGTAGCAGCAAGTTTCTGGGTAACGTTGTGTACCCGGAGACCCTGGGTGGCATGTTTATCGCGCATGCGCACTGG
 GTTGCGATTAAGAACAGCAAACCTGCACGATAAAGTTGGTATCCGTAAAGACCCTGGAGGACGTGGAGAACGAATACAACG
 CGAAAAAACTGGGTTTCTGGGTGGCCGTTATATCGCGTGGGGCATTGCGAAGAAACTGATCCCGAGGAAGTTTATG
 TGAGCGACGCGAACAAATGGGTTGAGGAAGCGACCCTGAAGATCCTGAACGAAGTGGGCATTAACGCGTACAAGTGCA
 ACGGTAACGATGAGGAAGTTGTAAAAACGCGGACAAGACCTATATCTGCAGCATGATCCCGGAGATTATTCTGAAGAT
 TAAAAACAAAGTTGAGCGGAGACCTGATGTAAGTCGAC3'

hcgG from *Desulfurobacterium thermolithotrophum*

5'CATATGAAAGAAGCTAATATATAGAACAAATACAAGGAGATATAAACAGTCAATACATACTGTATAAGAAGGCCGAAAGAAG
 AGATCCAGAAGCTGTTTCGAGAACATTAAGAACTGAGCGACGGTGAAGTATGCGCTGGGCCAGCGTTTTAAAGAGTT
 CCCGTTTGGTTGCGACCTGAACGAAATTATGGTGGATGTGGTTAGCCTGAAGCAAGAGATCGACGAAATTCGTGGTGGC
 TTCCGCTCTGGTGGATCGTCTGGGTTTTCCGATCCACGTTTGCAGCTACGTGGTTGCGGAGCTGGCGGAGCGTGAAGGC
 AAAACCCCGCTGGAGCTGATGAAGGAACTGCGTGCGCTGACCAGCATGCCGATCGACATTGATCACTTCGGCCAGTTT
 GGCCCGATGCGTTATCCGGAGGAAATCGCGAAATGCCCGGCTACTGCTATCGTAGCGGCAAGCCGTTTAAACGTTGCG
 CCGCGTGGCCGTTTACAAACGCTCTGATCGAGAAGGAACGTTGCTTCGCGAAAGAGAAGGAAGGCTGGAGCGAACTG
 GTGCAGAGCATTAGCGTTAGCCTGATGGCGTTTTCAGAAAGAACACCGTGCATGCGGCGAGCCCGGAGGAAACCCCTGAAA
 GTTATCGATTTTCGCGAAGAGCAAGAAAAAGGGTGTGGCGCGATCATTGCGTTGGTAACGGCAAGGACGAGCTGCTG
 CGTGGTCTGAAAGCGTGCATCAAGCACAGCATTGATGAGATCGTGATTGAAGGTGGCCCGTACAACACCCGCGCGAAC
 CGTGTTCGTGCGTTTGGCGAAACCGTGGTTATGGCGCGTATCATTGCGCCGGTAAAATCGTGGCGACCAACGGCCAG
 TATGAGGACGAACTGCGTTTTCCGTCTGAAGTGCAGGCTGAACAGCGTTATTAGCGGTTTTCCGGGCAACCACCGCG
 TACATGAGCGGTTATAAACCGGAGAAGGCGACCATCGATCGTTTTCGGCCTGCCGAAAATCATTGAGCTGATGGCGCAA
 GAACTGAAGGACAGCCCGTTTTCCGATTCCGCGGATCGTGAGAGCGCGATCGTGATTGCGAAAAGCGCGAAGTTCTG
 GGTAAGAAAACCATCTACCCGAACGGCAAGCTGGGCGACATCTATATTGGTGTGCGCACTGGTTCTGCTGCTGAACA
 GCCCGCTGGCGCAAGGCAATCAACATTAATGGAGCCTGGAGCTGCTGACCGAATTCATCCGTAAGAACAAGTTCAAAAA
 GGTTGGTCTGCTGGGTGGCCGTTTTCATCGCGTGGGGCATTGCGAAAGCGATCGACCCGTTTGTGAAGGAGATTCTGGT
 TAGCGACAAAAGATAAGCGTATCGAGAACACCCTGAAAGTTTTTAAGGAATACCTGAGCAGCAAAATCACCCGTTGC
 AACGGTAACGACGATATGTGCATTAAGAACAGCGAAATCACCGTTCTGTGCAGCTTCATCCCGAGCTTCATCCGTAAGTT
 CAAAGGTATTCAAAGGTTATCACCCCTGGAGAGCTAAGTCGAC3'

ACKNOWLEDGEMENTS

ACKNOWLEDGEMENTS

Many thanks to my supervisor Dr. Seigo Shima for providing the opportunity of studying in the project, nice education, suggestion and discussion.

I would like to thank Professor Dr. Rudolf. K. Thauer for suggestion and discussion on the project.

I would like to thank Professor Johann Heider for suggestion and discussion on the project as the second referee of my thesis.

I would like to thank Professor Lars-O. Essen and Professor Hans-Ulrich Mösch for suggestion and discussion on the project as the referee of my thesis.

I would like to thank all committee member Prof. R. K. Thauer, Prof. J. Heider and Prof. Martin Thanbichler for the thesis guidance in the past four years.

I would like to thank Prof. Xile Hu and Dr. Tao Xu for the chemical synthesis of substrate; Dr. Xiulan Xie for the NMR determination; Dr. Uwe Linne and Jörg Kahnt for the mass spectroscopic measurements; Professor Dr. Michael Rother and Dr. Michael Schick for the mutation of *M. maripaludis*; Gangfeng Huang for reconstitution experiments of Hmd; Makio Yokono, Atsushi Takabayashi, and Ayumi Tanaka for blue native PAGE-MS analysis and the comparative genomics calculation.

I would like to thank Professor Dr. Takashi Fujishiro, Dr. Tristan Wagner and Dr. Ulrich Ermler for the crystal structure analysis.

I would like to thank Professor Roland Lill for giving me the information of the conserved sequence of HcgG for possible iron-sulfur cluster-binding.

I would like to thank Jürgen Koch for the technical support and all members in the group of Seigo Shima for the kind support and friendly atmosphere.

I would like to thank Dr. Jan Zarzycki for translating title and abstract to German.

CURRICULUM VITAE

CURRICULUM VITAE**Personal information:**

Name: Liping Bai

Birthday: 25.09.1987

Gender: Female

Place of birth: Sichuan (China)

Contact: +4906421178110

E-mail: liping.bai@mpi-marburg.mpg.de

Education:

09, 2013 - 09, 2017 PhD candidate of Max-Planck Institute for Terrestrial

Microbiology

09, 2010 - 06, 2013 Master student in Life sciences School, Xiamen University,

Xiamen, China

09, 2006 – 06, 2010 Bachelor student in Guizhou University, Guizhou, China